N 70 36360 NASA CR-72727
TWR-4037

Vol II

FINAL REPORT

THRUST VECTOR CONTROL (TVC) SYSTEM STUDY PROGRAM

Thiokol
CHEMICAL CORPORATION
WASATCH DIVISION
BRIGHAM CITY, UTAH
84302

PREPARED FOR

National Aeronautics and Space Administration

CLEVELAND, OHIO 44135

NASA Lewis Research Center

CONTRACT NAS-3-12040

JAMES PELOUCH, PROJECT MANAGER

NASA CR-72727
TWR-4037

FINAL REPORT

THRUST VECTOR CONTROL (TVC) SYSTEM STUDY PROGRAM

THIOKOL CHEMICAL CORPORATION
WASATCH DIVISION
Brigham City, Utah 84302

Prepared for

NATIONAL AERONAUTICS AND SPACE ADMINISTRATION
15 June 1970

Contract NAS 3-12040

NASA LEWIS RESEARCH CENTER
Cleveland, Ohio 44135

James Pelouch, Project Manager
Solid Rocket Technology Branch
Chemical Rocket Division

Publications No. 0770-28976

NASA CR-72727
TWR-4037

FINAL REPORT

THRUST VECTOR CONTROL (TVC) SYSTEM STUDY PROGRAM

Stephen G. Goddard 27 July 70
Project Engineer

for Kenneth A. Northness
Program Manager

THIOKOL CHEMICAL CORPORATION
WASATCH DIVISION
Brigham City, Utah

Publications No. 0770-28976

FOREWORD

The Thrust Vector Control Study Program described herein was conducted by Thiokol Chemical Corporation, Wasatch Division under NASA Contract NAS3-12040. Mr. James Pelouch, Solid Rocket Technology Branch, Chemical Rocket Division, NASA Lewis Research Center, was the project manager.

ABSTRACT

During the period 3 Jun 1969 to 15 Jun 1970, a program was conducted to study various techniques that could be used for thrust vector control (TVC) on the 260 in. solid rocket booster of a MLV-SAT-1B-5A two stage launch vehicle. This study was structured such that three major categories of TVC were considered: liquid injection thrust vector control, movable nozzle flexible seal, and mechanical exhaust jet interference systems.

Of all the techniques considered, two were selected as the most promising and were subjected to a detailed design and cost analysis with the object of developing a low cost, high reliability system.

One of these two systems was a cold gas blowdown nitrogen tetroxide liquid injection TVC system with 16 electromechanical injector valves. The other technique selected was a passive cold gas blowdown movable nozzle flexible seal system with hydraulic actuators.

On the basis of cost, weight, and relative simplicity, the movable nozzle flexible seal system is the superior approach.

TABLE OF CONTENTS

1.0 Summary

TVC STUDY PROGRAM INDICATES THAT MOVABLE NOZZLE FLEXIBLE SEAL SYSTEM IS BEST APPROACH

This report is the final report for NASA contract NAS3-12040 "Contract for Thrust Vector Control (TVC) Study." The objective of this contract was to make a design comparison of several booster TVC systems for use on the 260 in. (6.6m) solid rocket motor similar to the First Stage of the MLV-SAT-1B-5A two stage vehicle. Techniques considered for thrust vector control included liquid injection TVC, movable nozzle flexible seal, and mechanical exhaust jet interference methods.

The technical effort consisted of the following three primary tasks.

Preliminary Design (Task 1)

Within each of the above mentioned TVC categories, several design variations were screened in order to select the most promising designs for more detailed effort. In the liquid injection TVC (LITVC) category, eight different configurations were selected for additional preliminary design work. Of these, a cold gas blowdown, nitrogen tetroxide injectant system with 16 electromechanical injector valves was chosen as the design to be optimized in the detailed design task. Similarly, several movable nozzle flexible seal design variations were analyzed in the preliminary design task, and as the result of extensive screening, a cold gas passive blowdown system with hydraulic actuators was selected for design optimization in the detailed design task. Mechanical exhaust jet interference designs considered in this task included mechanical probes, jetavators, jet tabs, supersonic splitline, flexible exit cone (Flex-X) and jet vanes. A jet tab design was chosen as the best design in this category, but further detailed design effort was cancelled because of its obvious inferiority to the designs chosen in the other two categories.

Detailed Design (Task 2)

The selected LITVC design and movable nozzle was subjected to design optimization in such detail that accurate sizing of components could be made. From the detailed layout drawings, planning documents were prepared in order to define reasonable manufacturing, inspection, and test requirements to develop and produce the designs.

Cost Analysis (Task 3)

The planning and designs prepared in task (2) were used to prepare cost estimates for the development and production of the two TVC systems. The results of this analysis indicate that the movable nozzle flexible seal system is less expensive on a production unit cost basis and from a long term system development and production standpoint.

Although a complete system tradeoff study was not conducted, it is concluded that the movable nozzle flexible seal TVC system is superior from a cost, weight, and relative simplicity point of view.

2.0 Introduction

TVC OPTIMIZATION FOR LARGE SOLID PROPELLANT BOOSTERS

The purpose of this program was to study various TVC systems using the NASA-furnished reduced steering requirements. The study included three major TVC categories: (1) liquid injection, (2) movable nozzle flexible seal, and (3) mechanical exhaust jet interference.

Large solid propellant booster studies funded by the National Aeronautics and Space Administration have shown that as the size of the solid motor booster increases, the steering requirement generally decreases. The magnitude of the thrust vector deflection angle (percent of side thrust required for steering) and its time rate of change required to maintain vehicle control during booster operation could therefore be decreased to reduce cost and complexity and improve reliability of the system.

This program was conducted during the period of June 1969 to June 1970 to study various thrust vector control (TVC) systems using the NASA-furnished reduced steering requirements for the 260 in. motor booster (MLV-SAT-1B-5A two stage vehicle). Emphasis was placed on low cost, simplicity, and increased reliability for optimization of each TVC system.

Three major TVC categories were studied: liquid injection, movable nozzle flexible seal, and mechanical exhaust jet interference methods. Selection of the two most promising, namely, liquid injection and movable nozzle, were subjected to a detailed design and cost analysis with the objective being development of a low cost, highly reliable system.

CONTENTS
SECTION 3.0

3.0 Baseline Nozzle Designs

3.1 Baseline Fixed Nozzle

BASELINE FIXED NOZZLE DESIGN ESTABLISHED

The baseline fixed nozzle design, provided by NASA LeRC, was a fixed, external, convergent-divergent nozzle with an initial expansion ratio of 8.515, an initial throat diameter of 89.10 in. (226.31 cm), a half angle of 17.5° (0.305 RAD), and an exit diameter of 260.0 in. Weight of the basic nozzle was 47,901 lb (21,728 kg).

The nozzle used as a baseline for all liquid injection and mechanical interference TVC designs is indicated in Figure 3-1 .

As part of the general groundrules established for this study, NASA LeRC provided Thiokol with two basic nozzle designs. A fixed, external, convergent-divergent nozzle as shown in Figure 3-1 was used for the LITVC and mechanical interference designs.

The fixed, convergent-divergent nozzle incorporated all required design parameters listed in the RFP, proposal, and drawings submitted to Thiokol by NASA LeRC. These requirements included:

Expansion ratio, initial	8.515	
Throat diameter, initial (in.)	89.10	226.31 cm
Half angle (deg)	17.5	0.305 RAD
Exit diameter (in.)	260.0	6.6 m

In addition, the nozzle was required to interface with the aft closure on a 180 in. (3.3 m) diameter mounting circle located 55.10 in. (139.95 cm) forward of the nozzle throat. A downstream external throat radius equal to the throat radius, as well as materials and material thickness taken from the envelope drawings submitted by NASA LeRC, were incorporated in the design of not only the convergent-divergent nozzle, but in the movable concepts as well.

For the fixed nozzle, the materials were: V-44 (silica and asbestos filled Buna rubber) as the entrance structural shell insulation from the aft closure mounting flange (55.10 in. (139.95 cm) forward of the throat), to a point 42 in. (106.68 cm) forward of the throat; carbon cloth phenolic as the remaining length of entrance structural shell insulation and throat liner.

In both the fixed and movable nozzles, the exit cone was identical. Carbon cloth phenolic liner, 3.10 in. (7.87 cm) thick, extended 90 in. (228.60 cm) aft of the throat. Canvas, 3.10 in. thick, formed the liner from the 90 in. (228.60 cm) dimension to the

aft end of the exit cone (277.866 in. (705.780 cm) aft of the throat). Silica cloth phenolic, 0.42 in. (1.07 cm) thick, was used as a backup to both carbon cloth and canvas. The exit cone was overwrapped with fiberglass, 0.70 in. (1.78 cm) thick at the forward end tapering to 0.25 in. (0.64 cm) thick at the aft end. Weight of the basic nozzle was 47,901 lb (21,747 kg) 38,117 lb (17,305 kg) insulation and 9.784 lb (4.442 kg) structure.

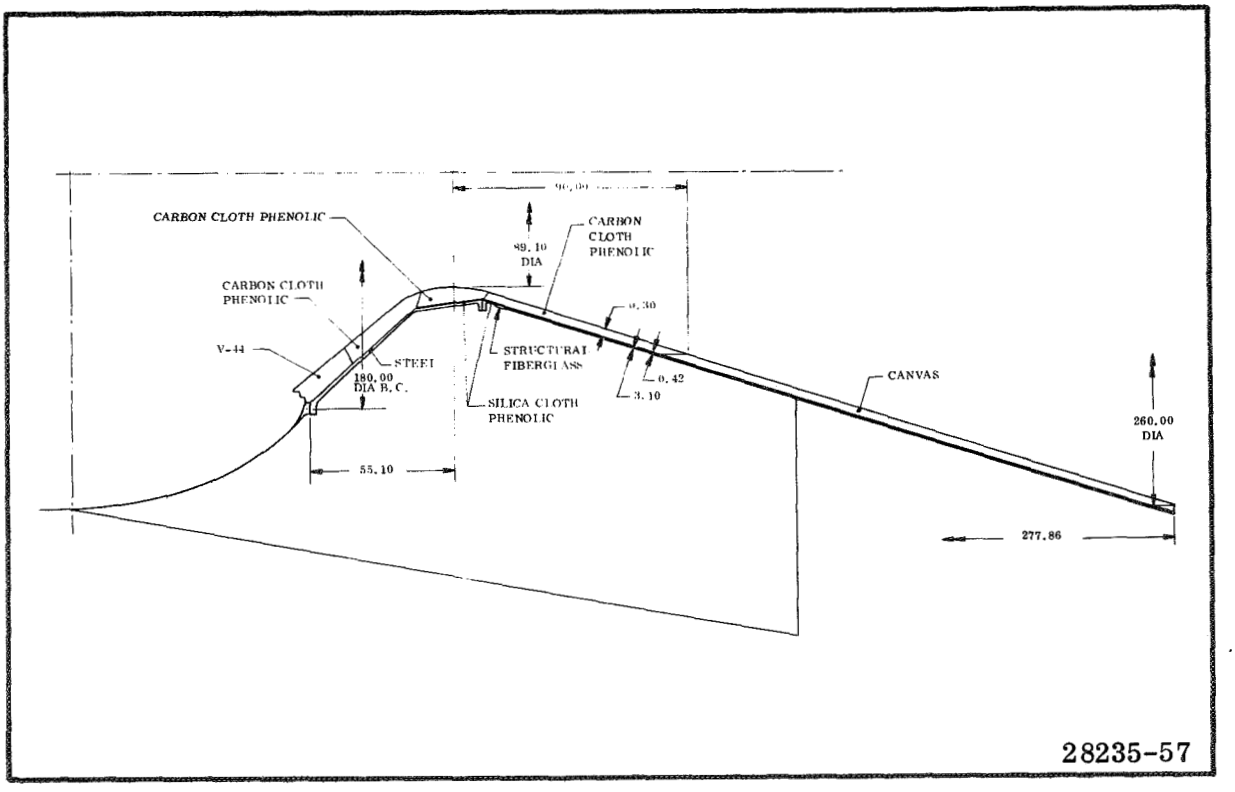

Figure 3-1. Baseline Fixed Nozzle

3.2 Baseline Flexible Seal Nozzles

3.2.1 Thiokol Baseline Flexible Seal Nozzle

THIOKOL BASELINE FLEXIBLE SEAL NOZZLE DESIGN ESTABLISHED

The Thiokol baseline movable nozzles had the same design constraints as the fixed nozzles except that the distance between the aft closure interface and the nozzle throat was 27.00 in. (68.58 cm) instead of 55.10 in. (39.95 cm). Materials and material thicknesses closely approximated the Aerojet design to establish a valid basis for comparison. Nozzle assembly weight was 54,025 lb (24,527 kg). Actuation torque was 16.27 million in.-lb (1.86×10^5 kg-m) including gravity torque, which is the torque resulting from the product of the movable nozzle weight times the distance from the nozzle c.g. to the pivot point (applicable only for horizontal static test.

During the preliminary design phase, the nozzle shown in Figure 3-2 was used on the movable nozzle-flexible seal designs.

The movable nozzles had the same design constraints as the fixed nozzle with the exception of the distance between aft closure interface and nozzle throat which was 27 in. (68.58 cm) instead of 55.10 in. (139.95 cm).

In addition, the leading edge location of 32.768 in. (83.230 cm) forward of the throat at the 63.003 in. (160.03 cm) radius was specified. The nozzle contour equation for the elliptical cross-section between the nose and throat was specified as:

$$R = 66.825 - \sqrt{496.1756 - \frac{496.1756}{1116.39} x^2}$$

To establish a valid basis for comparison between Thiokol Chemical Corporation's designs and those by Aerojet-General Corporation, it was decided to follow Aerojet's design except where changes were necessary to interface with the Thiokol flex seal. Therefore, materials and material thicknesses were much the same on the Thiokol nozzle designs as they were on Aerojet's.

For the movable nozzles this included: rubber mastic as the entrance structural shell insulation, 5.70 in. (14.48 cm) thick at the aft closure mounting flange, decreasing to 3.5 in. (8.9 cm) thick at the splitline; canvas cloth phenolic as the chamber side insulation of the submerged portion of the nozzle, 3.20 in. (8.12 cm) thick; and carbon cloth phenolic as the nose cap, entrance ring and throat section insulation. Silica cloth phenolic, 0.42 in. (1.07 cm) thick, was used to back up all insulation except the rubber mastic in the entrance structural shell.

The Thiokol movable nozzle incorporated a forward pivoted, near-conical flexible seal with folding protective boot. The flex seal consisted of 36 stainless steel spherical shims 0.071 in. (0.180 cm) thick and 37 elastomer layers 0.021 in. (0.053 cm) thick. The pivot point was located 53.90 in. (36.91 cm) forward of the nozzle throat. The flex seal was optimized for minimum "system" (the combination of nozzle and actuator weights) weight by means of Thiokol's Advanced TVC Computer Program. Aerodynamic analysis of this optimum design showed that the seal was subject to a tensile, rather than a compressive load. While this condition would not necessarily result in seal failure, all past experience with flex seal nozzles is based on compressive seal loading. The seal radius, therefore, was changed to 53.5 in. (135.9 cm), an increase of 2.1 in. over the optimum. This increase subjected the seal to a compressive load.

Weight of the nozzle assembly was 54,025 lb (25,886 kg), including 37,107 lb (16,847 kg) insulation and 16,918 lb (7,681 kg) structure. The fixed section weight was 8,359 lb (3,795 kg); while the movable section weight was 45,666 lb (20,732 kg). Preliminary actuation system torque requirements were 16.27 million in.-lb (1.86 x 10^5 N-m), including gravity torque.

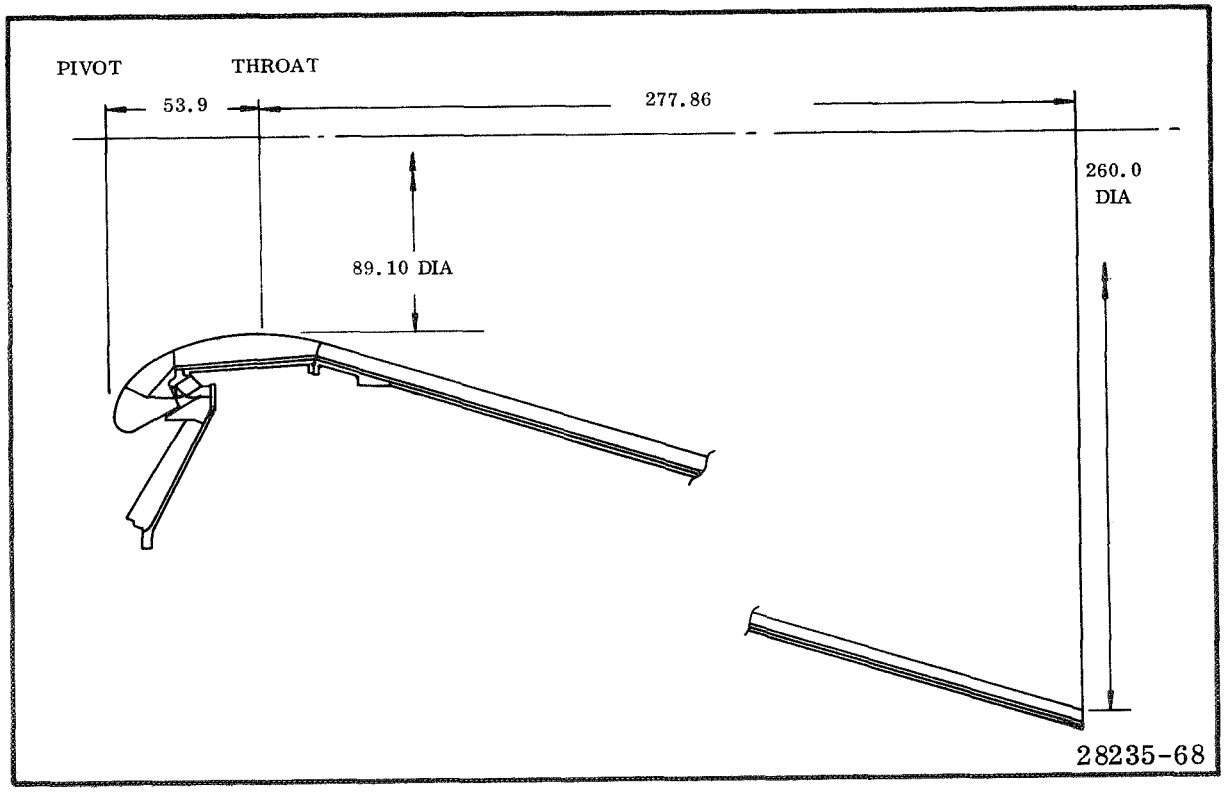

Figure 3-2. Thiokol Baseline Flexible Seal Nozzle

3.2 Baseline Flexible Seal Nozzles

3.2.2 Aerojet Baseline Flexible Seal Nozzle

AEROJET BASELINE FLEXIBLE SEAL NOZZLE DESIGN ESTABLISHED

The Aerojet baseline movable nozzles had the same design constraints as the fixed nozzles. Using the computer program, the Aerojet design was duplicated to obtain weight and torque estimates. Nozzle assembly weight was 56,298 lb (25,559 kg). Actuation torque was 17.88 million in.-lb (2.06 x 10^5 kg-m) including gravity torque.

The nozzle indicated in Figure 3-3 was provided by NASA LeRC and was used throughout the movable nozzle flexible seal design studies.

From a nozzle design standpoint, this portion of the study entailed duplicating the flexible seal nozzle as designed by Aerojet-General Corporation in the computer to obtain weight and torque estimates. The Advanced Thrust Vector Control Computer Program was again utilized.

The AGC nozzle and seal design provided by NASA LeRC incorporated a forward pivoted cylindrical flex seal with folding protective boot. The seal core consists of four alloy steel conical shims, each 0.70 in. (1.78 cm) thick and five layers of elastomer, each 0.30 in. (0.76 cm) thick. The pivot point location was 60.5 in. (153.67 cm) forward of the throat.

As in the Thiokol flexible bearing nozzle, an I-shaped steel exit ring was employed to distribute the hydraulic actuator's forces around the nozzle's movable section. Aft of the exit ring, fiberglass was used for the support structure material. The interface between the steel and fiberglass support structures was joined by an overwrap of fiberglass.

The total Aerojet nozzle assembly weight was calculated to be 56,298 lb (25,559 kg). This was comprised of 36,262 lb (16,463 kg) insulation, and 20,036 lb (9,096 kg) structure; 47,398 lb (21,519 kg) for the movable section and 8,899 lb (4,040 kg) for the fixed section. Total actuation system torque requirements were 17.88 million in.-lb (2.06 x 10^5 N-m) which includes gravity torque.

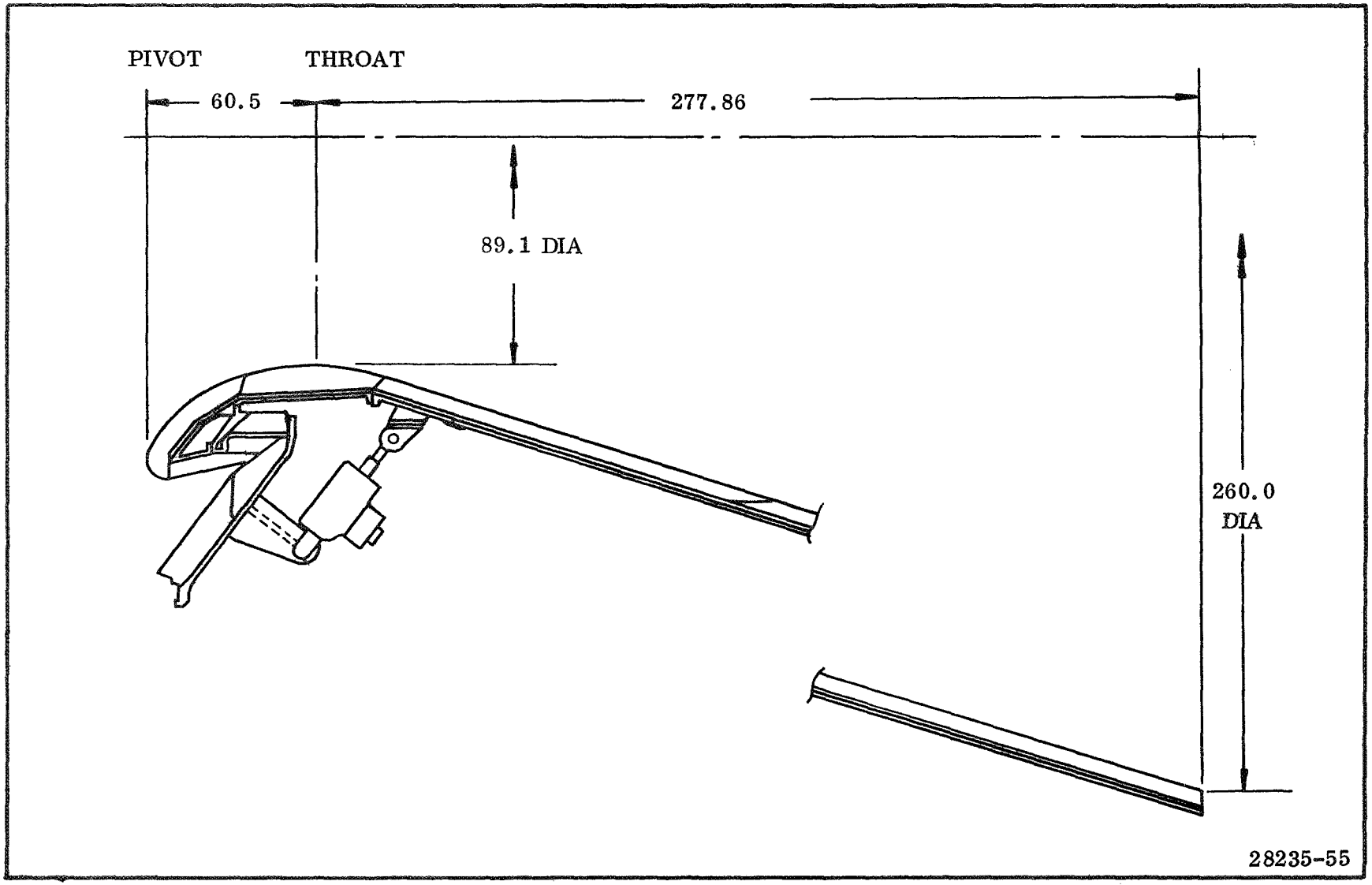

Figure 3-3. Aerojet Baseline Flexible Seal Nozzle

CONTENTS
SECTION 4.0

4.0 LITVC System Studies

4.1 Introduction

LITVC SYSTEM OBJECTIVES STATED

The objectives of the LITVC system design studies for application to a 260 in. solid rocket motor of a MLV-SAT-1B-5A vehicle were to (1) investigate liquid injection parameters and system components, (2) compare potential design approaches, (3) select candidate designs, and (4) select the design approach for a detailed design analysis.

The liquid injection thrust vector control (LITVC) scheme implements vehicle guidance commands by injection of a secondary liquid into the nozzle supersonic exhaust stream. A side force to provide pitch and yaw control results primarily from the induced pressure unbalance acting over a portion of the internal nozzle surface area, and secondarily from the reaction force of the injected liquid.

The general objectives of the LITVC system design studies for application on a 260 in. solid rocket motor (SRM) of a MLV-SAT-1B-5A type vehicle were as follows. (1) Investigate liquid injection parameters and LITVC system components, (2) compare potential LITVC system design approaches, (3) select candidate LITVC system designs which would best meet the study goals, and (4) in collaboration with NASA LeRC, select the better design approach for a detailed design and analysis of a LITVC system for use on the 260 in. SRM.

The LITVC system design requirements used in this study are presented in Table 4-1 ; the LITVC duty cycle is illustrated in Figure 4-1 . The selected 260 in. SRM and nozzle parameters are presented in Table 4-2 .

The following discussions include (1) a summary of the mechanics of LITVC, (2) a summary of the LITVC literature search, (3) design analyses (parametric and component) performed, (4) candidate LITVC system evaluation tradeoff, (5) selection of the best LITVC system design approach, and (6) a description of the final LITVC system design.

TABLE 4-1

LITVC SYSTEM DESIGN REQUIREMENTS

Total injection impulse (deg-sec)	60 (1,047 RAD-sec)
Pitch and yaw; assumes a 0.25° (0.00436 RAD) thrust misalignment throughout the entire flight	
Total injection impulse (lbf-sec)	6.287×10^6 (27,965,000 N-sec)
Maximum required equivalent thrust vector angle each - pitch and yaw (deg)	1.2 (0.021 RAD)
Maximum required equivalent slew rate (deg/sec)	3 (0.0524 RAD/sec)
Average thrust deflection angle of duty cycle, 60°-sec 143 sec (deg)	0.42 (0.0073 RAD)
Average side force (lbf)	43,965 (196,000 N)
Ratio of control thrust impulse to total vehicle vacuum thrust impulse (%)	0.727 (0.727%)

The amount of injectant required for duty cycle operation must provide a minimum side impulse of 60°-sec (1.047 RAD-sec) (pitch and yaw total) between motor ignition signal and the end of motor action time (143 sec).

The total amount of injectant carried on board was to include the duty cycle injectant and allow for expulsion efficiency errors, motor and LITVC performance tolerances, injector valve leakage, and extra injectant to fill ducting and manifolds.

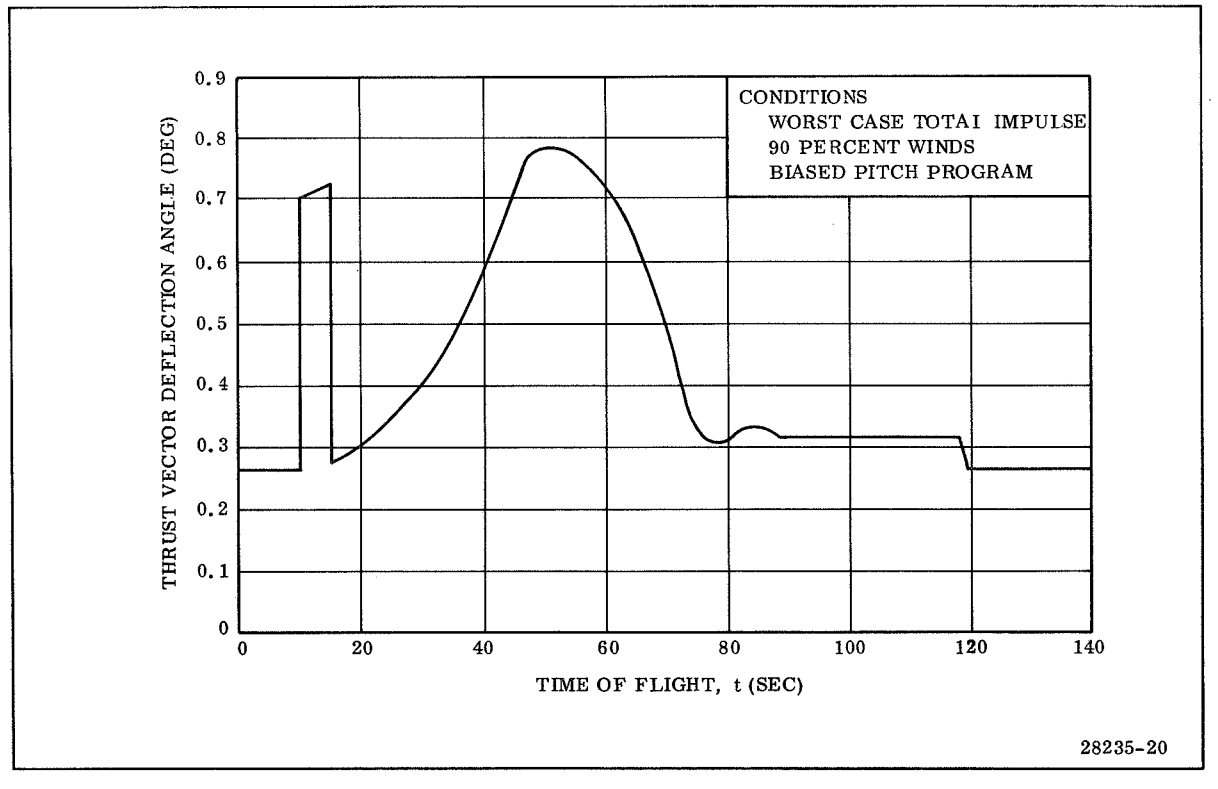

Figure 4-1. LITVC Duty Cycle

TABLE 4-2

260-IN. MOTOR AND NOZZLE PARAMETERS

Motor

Propellant load (lbm)	3.4×10^6 (1,542,000 kg)
Action time duration (sec)	143 (143 sec)
Average flow rate of motor (lbm/sec)	23,776 (10,800 kg/sec)
Maximum flow rate of motor (lbm/sec)	29,880 (13,600 kg/sec)
Vacuum total impulse (lbf-sec)	864,776,960 (3,846,528,000 N-sec)
Delivered total impulse (lbf-sec)	819,297,792 (3,644,237,000 N-sec)
Vacuum specific impulse (lbf-sec/lbm)	254.353
Average vacuum thrust (lbf)	6,047,391 (26,899,000 N)
Maximum vacuum thrust (lbf)	7,600,000 (33,805,000 N)
Average chamber pressure (psia)	587.00 (4,047,000 N/m^2)
Maximum expected operating pressure (MEOP) (psia)	764.00 (5,268,000 N/m^2)

Nozzle

Initial throat diameter (in.)	89.10 (226 cm)
Initial throat area (sq in.)	6,235.121 (40,200 cm^2)
Average throat diameter (in.)	90.269 (229 cm)
Average throat area (sq in.)	6,399.762 (41,300 cm^2)
Exit diameter (in.)	260.00 (660 cm)
Initial expansion ratio	8.515 (8.515)
Average expansion ratio	8.367 (8.367)
Ideal vacuum C_F at average expansion ratio	1.6934 (1.6934)
Length, throat to exit (in.)	277.86 (706 cm)
Nozzle exit half angle (deg)	17.50 (0.305 RAD)
Divergence correction (lambda)	0.9769 (0.9769)

4.0 LITVC System Studies

4.2 Mechanics of LITVC

ROCKET MOTOR TVC ACHIEVED BY CONTROLLED INJECTION OF SECONDARY LIQUID INTO GAS STREAM

TVC of rocket motors can be achieved by controlled injection of a secondary liquid into the primary gas stream from a port or ports located in the wall of the divergent section of the nozzle. The resulting total side force (FS) is a result of the reaction force from the injected fluid and the induced pressure unbalance acting over an area of the internal nozzle surface. With the injection of liquids, the induced, or interference, side force produced by the altered pressure profile within the nozzle accounts for 80 to 90 percent of the total lateral side force.

In an LITVC system, the liquid is generally injected at high pressure producing a high velocity jet which breaks up into droplets in the main gas stream. These droplets are rapidly accelerated in the direction of the gas flow by the high drag forces to which they are subjected. The secondary stream acts as an obstruction to the primary flow causing an adverse pressure gradient in the subsonic region of the boundary layer ahead of the injection port. This gradient is usually sufficient to cause the flow to separate. A shock wave forms in the supersonic flow ahead of the port as shown in Figure 4-2 . This wave appears as a bow wave about the separated region in a plan view of the injection port and as a three dimensional oblique shock when viewed in elevation. The radial dispersion of the separated zone, and thus the shape of the bow shock, is a function of the penetration of the injectant. After the primary flow is turned through the initial bow shock it proceeds until it is again deflected by a second shock produced by the expanding gases resulting from vaporization of the injected liquid. The strength of this shock is a function of the rate of vaporization and/or chemical reaction of the injectant in the primary gas stream.

The disturbance system described above produces an asymmetric pressure distribution which creates an unbalanced side force on the nozzle exit cone in a direction opposite that of the injected liquid. The magnitude of this force is a function of the strength of the shock system generated which in turn is a function of the geometry of the effective obstruction formed by the injectant.

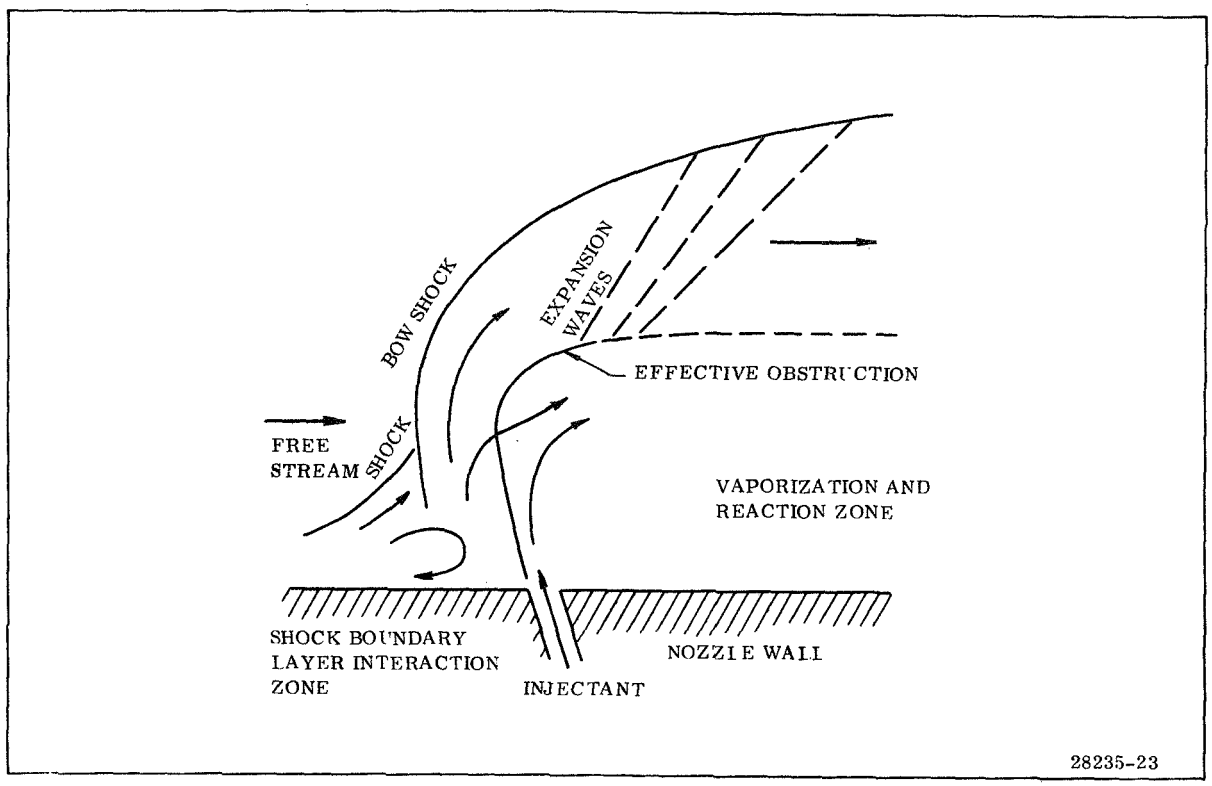

Figure 4-2. Liquid Injection Flow Model

4.0 LITVC System Studies

4.3 LITVC Literature Search

LITERATURE SEARCH REVEALS DESIGNS COMPARABLE TO DESIGN OF THIS STUDY PROGRAM

The literature search revealed that although previous 260 in. LITVC studies were conducted with different design requirements (higher vector angle, lower injection impulse), the system designs were comparable to the design finalized in this study program.

A significant portion of the effort in the first phase of the Contract NAS3-12040 LITVC study was devoted to a literature search to ferret information on work done by other companies and agencies in the field of LITVC. A bibliography of the LITVC literature search is presented in Appendices A and B. Where LITVC data, analytical methods, design information, etc, were used in the subject study, the respective report or paper is referenced as a footnote in that particular portion of the technical discussion.

The 260 in. SRM LITVC system studies conducted by Douglas Missile and Space Systems Division under Contracts NAS8-20242 and NAS8-21051 were reviewed in depth. Table 4-3 gives a summary of the Douglas 260 in. LITVC system weights.

TABLE 4-3

DOUGLAS LITVC SYSTEM WEIGHTS

Component	Phase II LITVC Weight (lbm)	(kg)	Revised[1] Phase II LITVC Weight (lbm)	(kg)	Simplified LITVC Weight (lbm)	(kg)
Injectant tanks	3,280	1,488	2,404[2]	1,090	3,560	1,614
N_2O_4	25,850[3]	11,730	25,850[3]	11,730	28,367	12,867
Helium gas	147	66.7	147	66.7	183	83.0
Tank mounts	202	91.6	202	91.6	202	91.6
Manifold	1,650	748.4	852[2]	386.5	852	386.5
Injectant valves	1,020	462.7	1,020	462.7	876	397.4
Fill and vent modules	15	6.8	15	6.8	15	6.8
Lines and fittings	197	89.4	197	89.4	197	89.4
Contingencies	636[4]	288.5	469[4]	212.7	570[4]	258.6
Electronics	204[5]	92.5	204[5]	92.5	190[5]	86.2
Totals	33,201	15,060	31,360	14,225	35,012	15,922

(1) Revised weight figures used for performance calculations and in the TVC comparison.
(2) Design safety factor revised.
(3) N_2O_4 weight represents allowables for trapped N_2O_4, reserves, and the actual calculated injectant necessary to meet the control side force impulse requirements.
(4) A 10 percent contingency weight was included to compensate for incidental hardware.
(5) Strictly TVC system-oriented electronic weight estimates for the control package, N_2O_4 dump system, batteries, signal conditioners, transducers, and associated wiring.

4.0 LITVC System Studies

4.4 LITVC System Design Analysis

STANDARDIZED LITVC ANALYTICAL PROCEDURE HAS NOT BEEN DEVELOPED

The approach used to establish LITVC design parameters was to acquire data on various injectants, injection parameters, and system components from previous test and study programs. Other limiting factors included weight, cost, development effort, and simplicity.

The practical aspect of thrust vector control of a rocket motor by liquid injection into the supersonic stream of a rocket motor is well established. As pointed out in the previous discussion and Appendices A and B, numerous investigations have been made in an attempt to arrive at an analytical solution which could accurately predict LITVC performance. The results of these works are inconclusive, and to date, a standard LITVC analytical procedure has not been developed. The main approach in establishing LITVC system design parameters has been to acquire experimental data and available information of various injectants, injection parameters, and LITVC system components from previously conducted test and study programs. This procedure was utilized extensively throughout the 260 in. SRM LITVC system tradeoff studies. Other basic ground rules included minimum weight, cost, development effort and simplicity.

The following subsections discuss the LITVC design analysis efforts listed on the facing page.

- Liquid injectant selection procedure.
- Investigation of injection parameters.
- Evaluation of LITVC system components.
- Summary of design analysis.

4.4 LITVC System Design Analysis

4.4.1 Liquid Injectant Selection Procedure

N_2O_4 AND Sr $(ClO_4)_2$ + H_2O SELECTED AS BETTER INJECTANTS

N_2O_4, Sr $(ClO_4)_2$ + H_2O, Pb $(ClO_4)_2$ + H_2O, Freon 114B2 and 113, and N_2H_4 were investigated as candidate injectants for this study. N_2O_4 and Sr $(ClO_4)_2$ + H_2O were chosen as the better injectants on the basis of weight and performance and were used in sizing the preliminary designs.

The most obvious feature of LITVC performance is its strong dependence on the liquid injected into the primary nozzle's exhaust stream; therefore, the choice of the liquid injectant is of primary importance.

Preliminary LITVC system weight tradeoff comparisons were made to select the more promising liquid injectants for further detailed LITVC system design analyses. The tradeoff studies relied heavily on data from previous programs for prediction of injectant effectiveness. Performance curves for the candidate injectants were established by empirical correlations of existing LITVC data. Weight trade studies were performed per the design requirements of Table 4-1 to establish total LITVC system comparisons incorporating each candidate injectant.

Of the liquid injectants experimentally inspected, only three (Freon 114B2, aqueous strontium perchlorate, and nitrogen tetroxide) have been thoroughly tested and developed as operational LITVC systems. A Freon 114B2 LITVC system is employed in the second stage of both the Polaris and Advanced Minuteman missiles and is in developmental status for the HiBex and Sprint missiles. Nitrogen tetroxide is used as the secondary injectant in the Titan III 120 in. (304.8 cm) diameter motors. Strontium perchlorate injection is under development for the Stage III Realigned Minuteman. Therefore, these three liquid injectants, plus aqueous lead perchlorate, Freon 113, and hydrazine (sufficient performance data were available for these injectants from miscellaneous sources), were selected for evaluation as potential 260 in. SRM LITVC system candidates.

Thiokol's IBM Computer Program for Design of a LITVC System was used to establish preliminary design data of the size and weight of LITVC systems using each of the candidate injectants for the established system requirements. The computer program calculated the amount of duty cycle injectant, total amount of onboard injectant required, and the maximum required injectant flow rate. The computer program also was used to calculate the size and weight of actuation and pressurization subsystems, tankage, injector valves, power supply components, liquid and gas lines, plus the weights of hydraulic fluid, disconnects, filters, electrical cabling, brackets, and fittings.

For the determination of the amount of duty cycle injectant required, the side specific impulse (ISP_S) for each injectant corresponding to 0.42° (0.0073 RAD) thrust vector was utilized (Figure 4-3). The ISP_S for each injectant corresponding to 1.2° (0.021 RAD) thrust vector (Figure 4-4) was used to calculate the maximum injectant flow rate required per injector port. Due to the higher performance (more side force generated per unit of injectant), the maximum injectant flow rate required per injection port and number of ports per quadrant (Figure 4-5) was considerably less with N_2O_4 than with the other injectants.

For this weight study, a representative injectant tankage and pressurization system consisting of two toroidal tanks was selected. One tank contained the injectant; the other contained nitrogen gas initially charged at 3,000 psi (20,684,400 N/m^2) and then regulated to maintain a constant injectant tank pressure of 600 psi (4,136,880 N/m^2). An electrohydraulic actuation system and 20 equally spaced single pintle-type injectors also were selected. For these weight tradeoff studies, it was felt that representative LITVC system weight comparisons could be made.

Using the N_2O_4 LITVC system weight (35,180 lbm) (15,958 kg) as a baseline factor, the computer program results of the initial LITVC system launch weights (nozzle excluded) are compared below.

LITVC System	Weight Factor
Nitrogen tetroxide, N_2O_4	1.00
Aqueous strontium perchlorate, $Sr\ (ClO_4)_2 + H_2O$	1.35
Aqueous lead perchlorate, $Pb\ (ClO_4)_2 + H_2O$	1.55
Freon 114B2	2.01
Freon 113	2.03
Hydrazine, N_2H_4	2.13

Each LITVC system was similar in all respects except for the type of liquid injectant used. As a result of the initial LITVC system weight tradeoffs, nitrogen tetroxide (N_2O_4) and aqueous strontium perchlorate $\left[Sr\ (ClO_4)_2 + H_2O\right]$ injectants were selected for more detailed LITVC system design work.

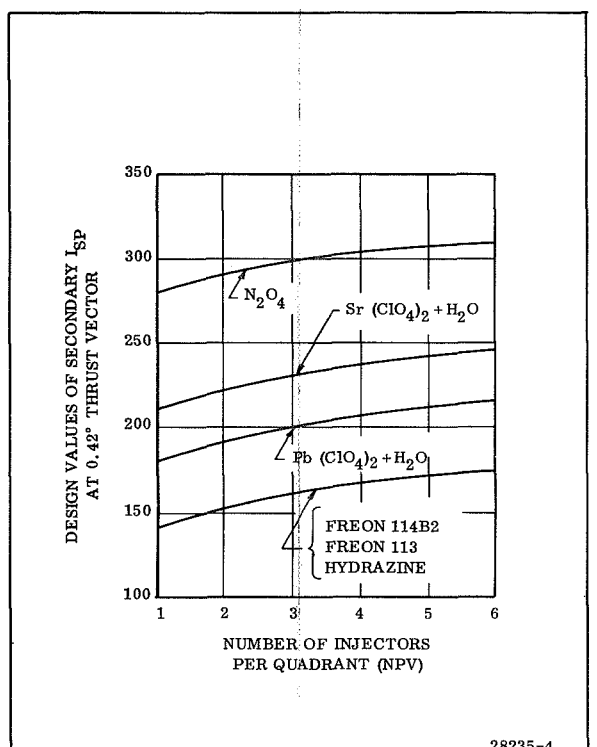

Figure 4-3. Injectant Performance at Avg Thrust Vector Angle

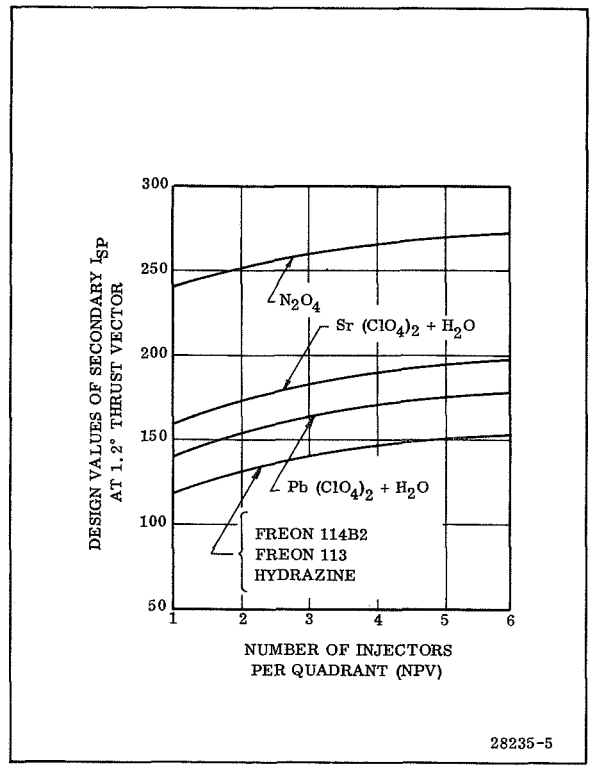

Figure 4-4. Injectant Performance at Max Thrust Vector Angle

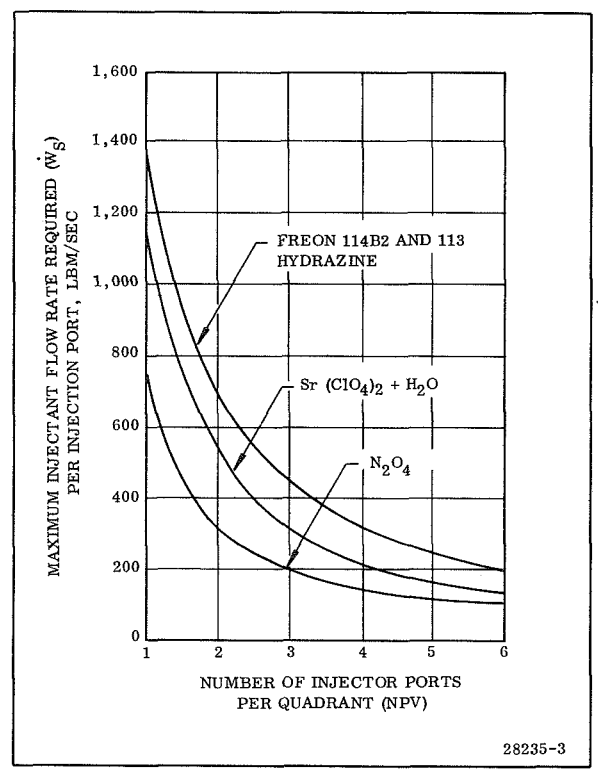

Figure 4-5. Max Injectant $\dot{W}_S$ per Injector Port vs No. of Ports per Quadrant

4.4.2 Investigation of Injection Parameters

4.4.2.1 Effective Point of Side Force Reaction

EFFECTIVE POINT OF REACTION ASSUMED TO BE AT POINT OF INJECTION

Insufficient nozzle wall pressure data are available to make an accurate analysis of the effective point of side force reaction on an LITVC system. Therefore, for this study it was conservatively assumed that the point of reaction is at the point of injection.

The effective point of side force reaction on the nozzle wall during liquid injection has not been investigated by the industry to any great extent. A limited amount of work is presented by Newton and Spaid.[1] In this paper, an average centroid of the induced pressure buildup during secondary injection may be established through integration of pressure profiles.

The induced pressure buildup accounts for approximately 80 percent of the generated side force. The remaining 20 percent of the side force is due to the momentum of the injectant and the separated region upstream of the injector. The breakdown of the 20 percent, due to the momentum of the injectant and the separated region, was estimated to be 12 percent due to the separated region upstream of the injector and 8 percent due to the momentum of the injectant. Using this breakdown, and assuming that the separated region force acts through the injector, a location was computed for the point through which the resultant side force acts, which was slightly downstream of the injector. However, the effective reaction point was suspected of varying with the secondary-to-primary flow rate ratio; but, insufficient data prohibited such an analysis. Most data in the industry do not reflect sufficient nozzle wall pressure data to result in an adequate analysis on this subject.

Since the reaction point is somewhere downstream of the injector, probably within a matter of inches, it was felt that a conservative, simplifying, assumption could be made; ie, the reaction point is at the point of injection. The assumption is conservative in that if the point of application of the thrust vector is further aft on

---

[1] J. F. Newton, Jr., and F. W. Spaid: "Interaction of Secondary Injectants and Rocket Exhaust for Thrust Vector Control," ARS Journal, August 1962.

the nozzle, greater moments would be applied to the vehicle. The above assumes that the reaction point is at the point of injection for all secondary-to-primary weight flow ratios; ie, for all jet deflection angles.

4.4.2 Investigation of Injection Parameters

4.4.2.2 Vehicle Turning Moment

LITVC TURNING MOMENT EQUATED WITH GIMBALED NOZZLE TURNING MOMENT TO OBTAIN EQUIVALENT LITVC THRUST VECTOR ANGLE

An equivalent thrust vector angle for LITVC can be obtained by considering the actual vehicle turning moment obtained through LITVC and by equating this turning moment to that which would be obtained with the same primary nozzle and chamber pressure by gimbaling the primary nozzle at its throat (center of nozzle rotation in the throat plane).

The turning moment for the gimbaled nozzle may be determined with the aid of Figure 4-6a. Assuming that the thrust vector angle for the gimbaled nozzle is equal to the nozzle vector angle, θ, then turning moment = $M_t = F_s (L^* + L \cos \theta) - F_a L \sin \theta$.

Since $F_s = F_p \sin \theta$, and $F_a = F_p \cos \theta$,

then $M_t = F_p \sin \theta \, L^* + F_p \sin \theta \, L \cos \theta - F_p \sin \theta \, L \cos \theta$

$$M_t = F_p L^* \sin \theta = F_p L^* \sin \theta \text{ eff} \qquad (1)$$

where θ eff = θ in this case.

The turning moment for a vehicle employing LITVC may be determined from the sketch in Figure 4-6b. Assuming that the LITVC forces (F_s and ΔF_p) act at the intersection of the secondary injection port with the primary nozzle wall, the rocket motor turning moment is

$$M_t = F_s (L^* + x) + \Delta F_p (r). \qquad (2)$$

Equating the LITVC turning moment to that of the gimbal nozzle results in a definition of an effective thrust vector angle for a vehicle employing LITVC.

$$F_p L^* \sin \theta \text{ eff} = F_s (L^* + x) + \Delta F_p (r)$$

$$\sin \theta \text{ eff} = \frac{F_s (L^* + x) + \Delta F_p (r)}{F_p L^*} \qquad (3)$$

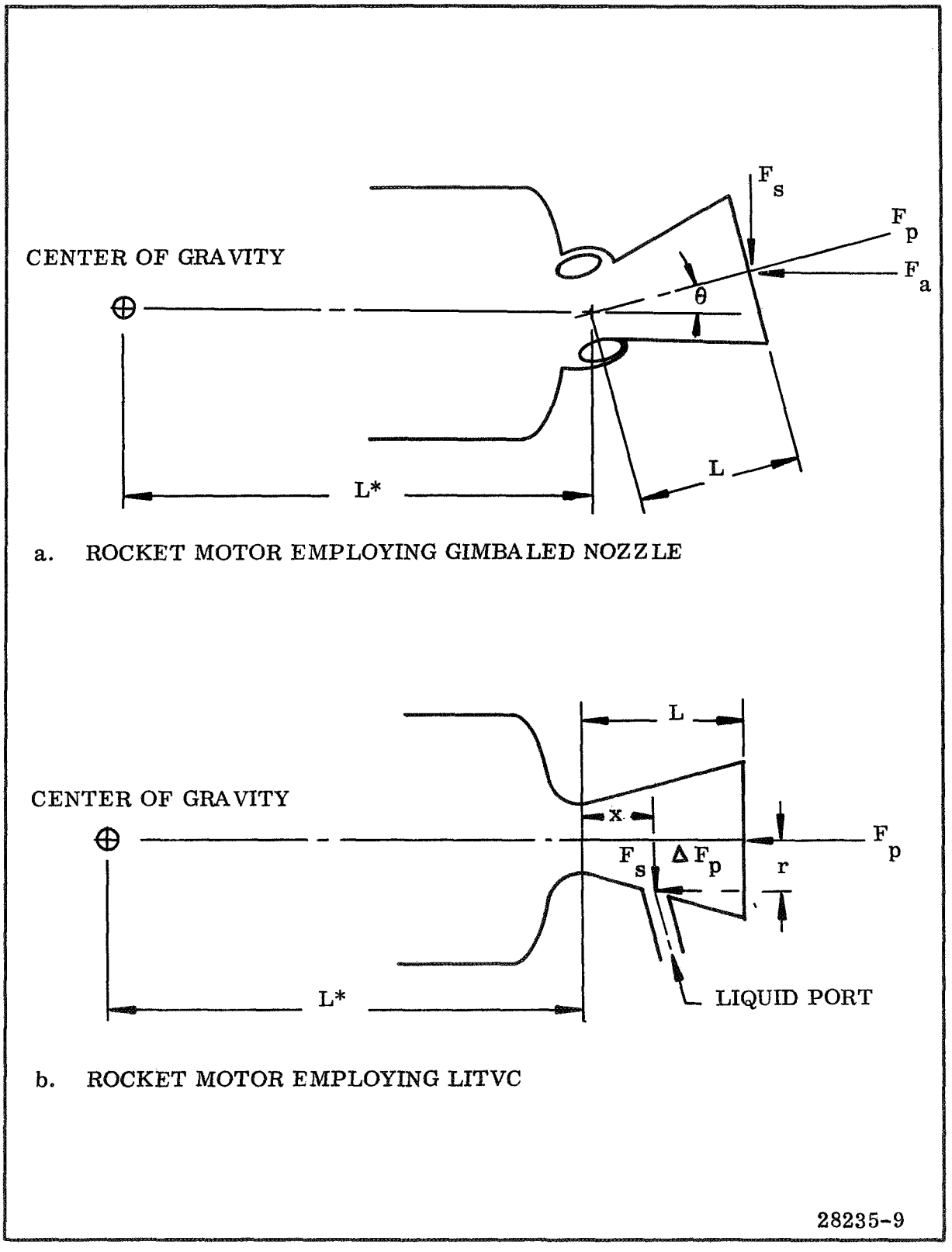

Figure 4-6. Sketches of Vehicle Turning Moments

4.4.2 INVESTIGATION OF INJECTION PARAMETERS

4.4.2.3 Injection Location and Angle

EMPIRICAL DATA INDICATE OPTIMUM INJECTION LOCATION AND ANGLE

Empirical data indicate that a nominal injection location exists on any nozzle that gives a high level of side force efficiency during liquid injection. This optimum injection location seems to be dependent primarily upon the x/L ratio, ie, the axial distance from the nozzle throat to the injection plane (x) divided by the axial distance from the nozzle throat to the nozzle exit plane (L). An x/L ratio of 0.35 and an injection angle of 15° (0.26175 RAD) were used for the designs in this study.

Figures 4-7 and 4-8 show the change in injectant side specific impulse (ISP_S), as the x/L ratio and the effective thrust vector angle are varied.

Figure 4-7 is a plot of nitrogen tetroxide performance; Figure 4-8 is a performance plot of Freon 114B2. These data were acquired from a survey made during the HiBex studies.* Similar trends of the effects of x/L on aqueous strontium perchlorate injection performance also were indicated during the Lockheed Polaris research studies.

These curves indicate that, as the thrust vector angle increases from 1° (0.01745 RAD) to 4° (0.0698 RAD), the point of injection for optimum performance moves from approximately an x/L location of 0.34 to 0.45.

It has been determined in rocket motor LITVC tests that changing the injection angle from a downstream direction to an upstream direction (with respect to injection perpendicular to that nozzle centerline) increases the control force. It was determined in a Lockheed analytical study** that control force is dependent on the size and shape of the vapor body formed by the injectant. As the injection angle changes to an upstream direction, the vapor body assumes the shape of a blunt nose cone. The cone shape maintains an overpressure along the full length of the cone, and the magnitude of the pressure depends upon the cone angle. At downstream angles, the vapor body is more cylindrical in shape. A cylindrical shape allows the gas flow and pressure to return to normal along the cylinder length. This means that a cone shape induces an overpressure over a larger nozzle area than the cylindrical shape.

*Barret, E. H., et al., HiBex Liquid TVC System Development and Test.

**LeCount, R., et al., An Analysis of the Physical and Chemical Aspects of Liquid Injection, LMSC 55-12-6, September 1964.

Therefore, from the results of the above studies, it was determined that the injectors would be located at an x/L of 0.35 and that injection would be oriented in an upstream direction of +15° (0.26175 RAD).

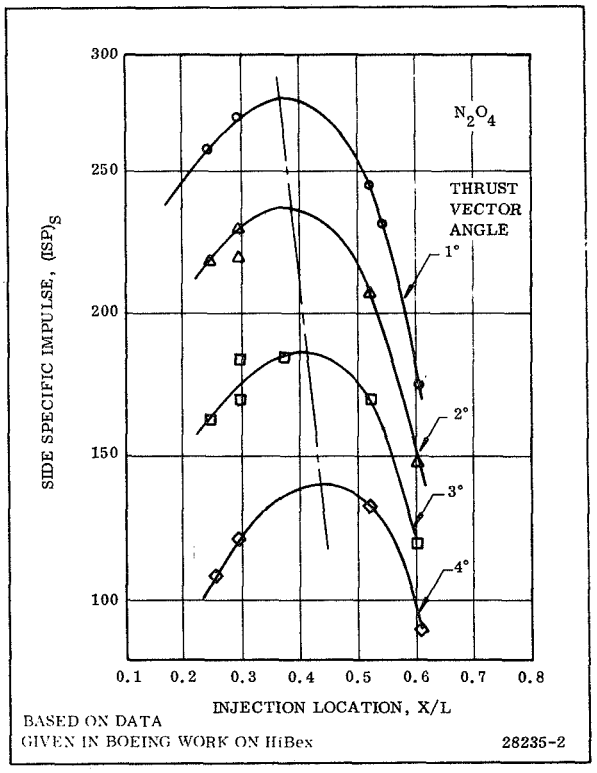

Figure 4-7. Effect of Injector Location on N_2O_4 LITVC Performance

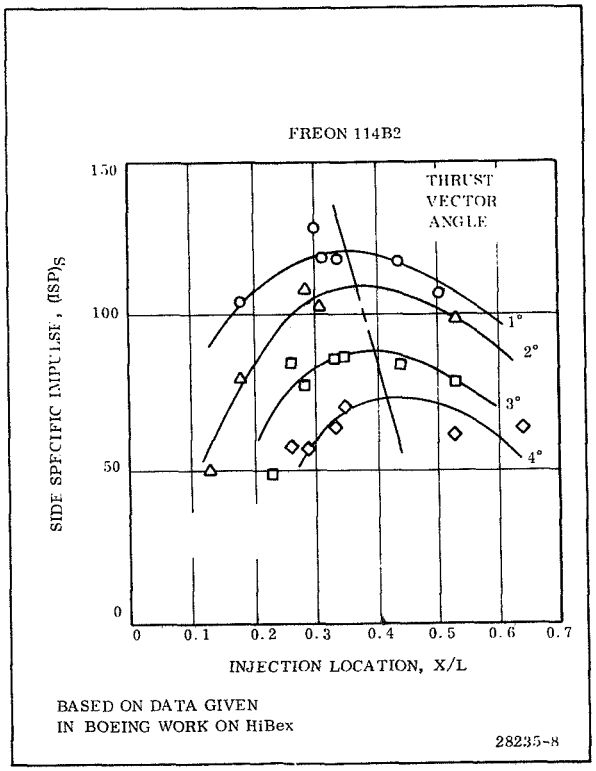

Figure 4-8. Effect of Injector Location on Freon 114B2 LITVC Performance

4.4 LITVC System Design Studies

4.4.3 Evaluation of LITVC System Components

LITVC SYSTEM COMPONENTS STUDIED

LITVC system components were studied to provide configuration data for use in detailed design studies of N_2O_4 and $Sr(ClO_4)_2 + H_2O$ LITVC systems for the 260 in. motor.

A study was conducted to provide configuration information for use in the detailed design studies of N_2O_4 and $Sr(ClO_4)_2 + H_2O$ LITVC systems for the 260 in. motor. Several typical LITVC system techniques are illustrated in Figure 4-9 . The most significant components investigated included the type of injection valve, pressurization concepts, tank configurations, and LITVC control system schemes.

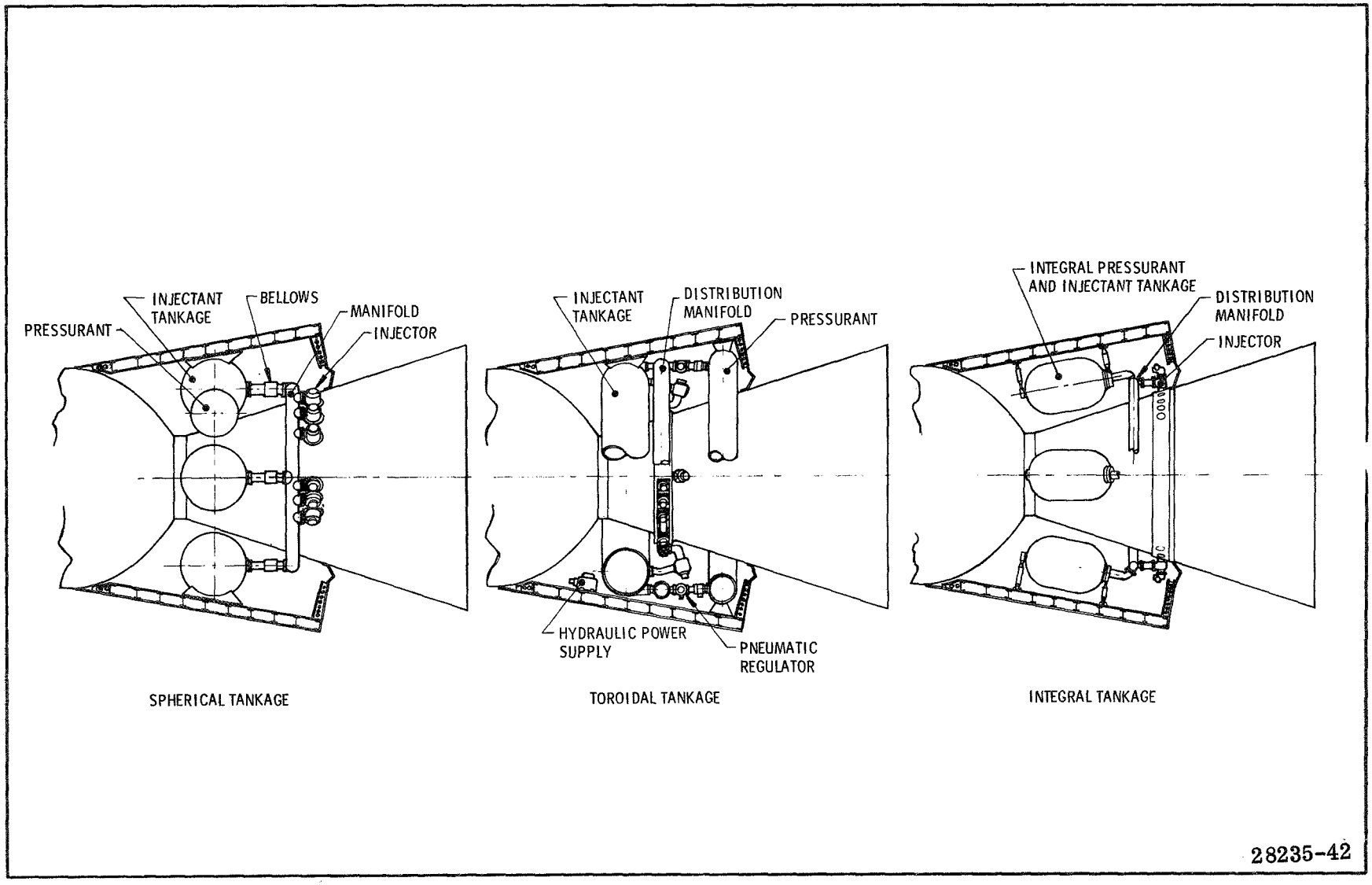

Figure 4-9. Typical LITVC System Techniques

4.4.3 Evaluation of LITVC System Components

4.4.3.1 Liquid Injector Valves and Actuation Methods

VARIABLE AREA (PINTLE-TYPE) INJECTORS SELECTED AND BOTH ELECTROHYDRAULIC AND ELECTROMECHANICAL ACTUATION INVESTIGATED

The basic types of liquid injector valves investigated included the constant area injector and the variable area injector. As the result of its demonstrated reliability, the variable area (pintle-type) injector was selected for use in the LITVC system designs. Consideration was given to both electrohydraulic and electromechanical actuation of the injector valves.

The constant area injector uses a fixed flow orifice; flow variations are accomplished by modulating the pressure across the injection orifice. This type of injector has not been developed on an operational LITVC system.

The variable area injector produces injectant flow changes by varying the size of the injector orifice (accomplished by use of a movable pintle in the orifice) while the injectant pressure remains constant. The pintle injector type is being used in all operational LITVC systems, therefore, the pintle injector was selected for use in the subject LITVC system design.

The pintle injector valve is a proportional positioning unit that modulates the flow of injectant fluid in proportion to an electrical command. A control servo device converts an electrical signal from the guidance system into a proportional displacement of a mechanical actuator. The motion of the mechanical actuator is used to position a metering pintle relative to the pintle seat, thus controlling the liquid injectant flow into the motor nozzle.

A tri-pintle injector scheme has been successfully demonstrated on a smaller scale, and several design approaches have been pursued far enough to insure the feasibility of implementing tri-pintle injector configurations for this large scale application. For design simplicity in a LITVC system that requires a maximum deflection angle of only 1.20° (0.021 RAD), the Thiokol studies indicated that the single injector scheme was the easiest to implement. Therefore, the single injector approach (equally spaced about the circumference of the nozzle) was selected for the Thiokol 260 in. motor LITVC system studies.

Both electromechanical and electrohydraulic injector schemes were investigated. The Ling-Temco-Vought (LTV) Titan III designs, illustrated in Figure 4-10, were selected for this study.

Typical injector valve actuation and pressurization schematics are shown in Figure 4-11. Three types of injector actuation systems were selected for incorporation into the candidate LITVC system design evaluations. (Refer to Table 4-4 .)

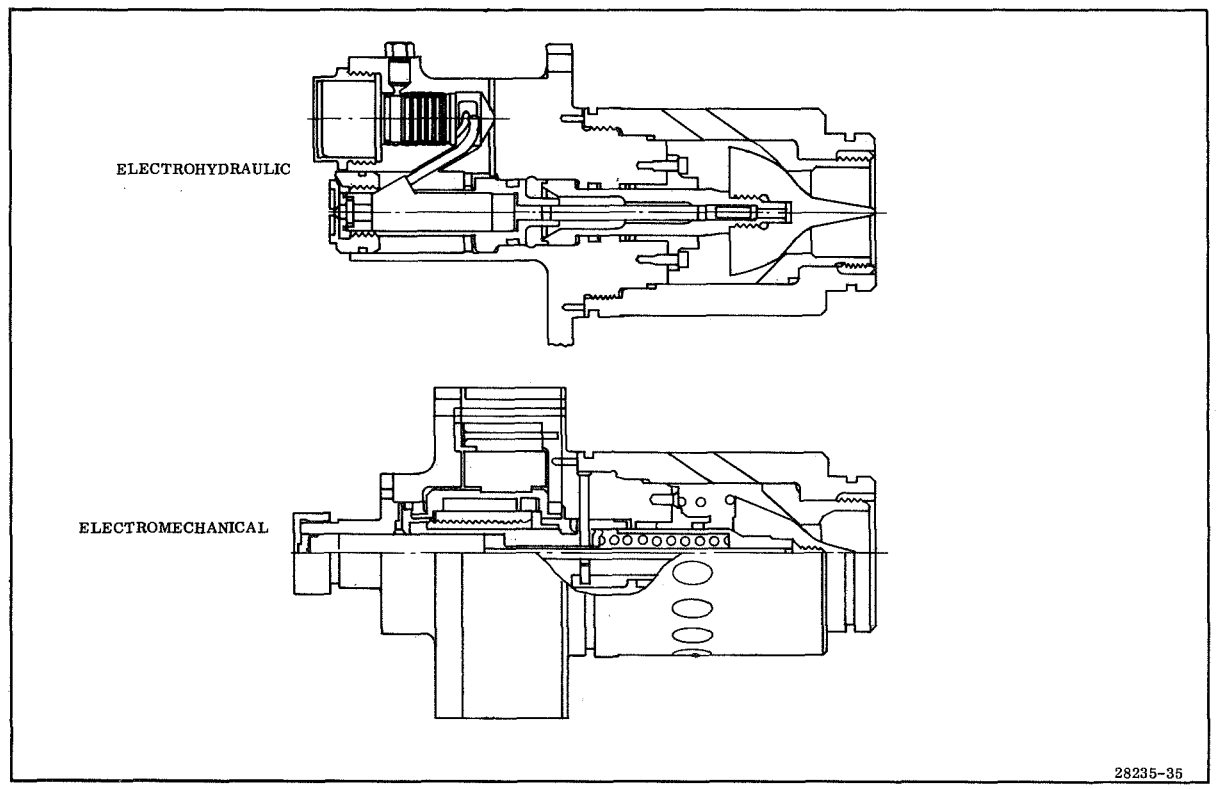

Figure 4-10. LTV Titan III Injector Configurations

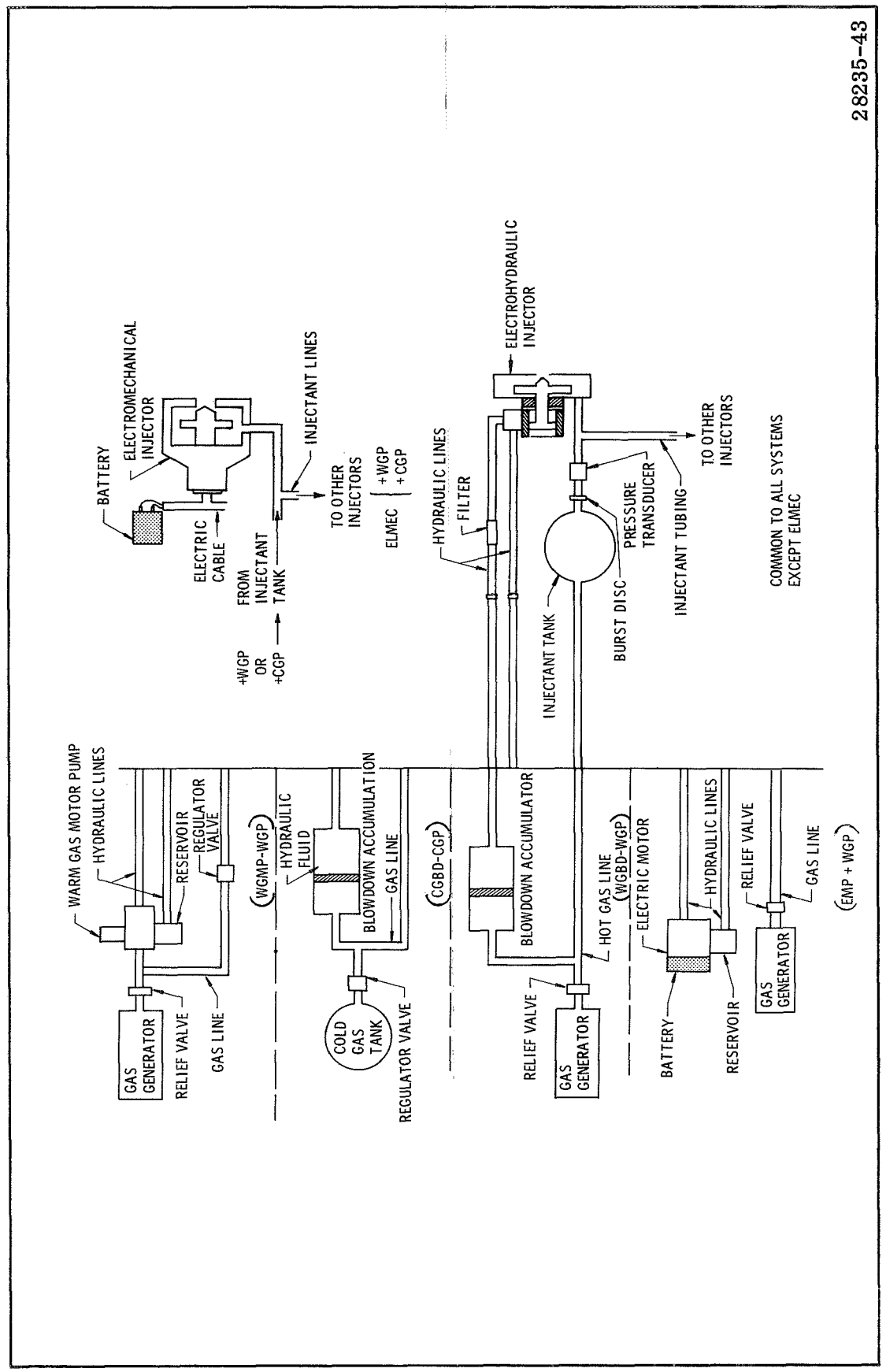

Figure 4-11. Liquid Injector Valve Actuation and Pressurization Schematics

4.4.3 Evaluation of LITVC System Components

4.4.3.2 Pressurization Concepts

COLD GAS BLOWDOWN SYSTEM SELECTED FOR LITVC PRESSURIZATION

Three basic types of pressurization techniques were considered for the 260 in. motor LITVC system. These were: (1) warm gas using a solid propellant gas generator, (2) cold gas pressure regulated, and (3) cold gas pressure blowdown. A cold gas blowdown system was selected as the most promising concept.

Several potential problems were encountered with a warm gas pressurant system, including the compatibility interface between the 2,200°F (1,200°C) gas and the selected injectants (would require design and development of an expulsion bladder), and the requirement of an auxiliary warm gas overboard dump system. This pressurant system was not chosen because the expected problem areas, although solvable, would have resulted in too long a development program.

For the cold gas pressurant systems (Figure 4-11, see CGBD-CGP), nitrogen and helium were considered. In comparing the two cold gas media, the helium system was lighter than the nitrogen system, but the high diffusibility of helium presented a more demanding problem in the tank design. The nitrogen gas (GN_2) pressurization system was selected for the 260 in. motor LITVC application as the more conservative approach.

A comparison was made between GN_2 pressure regulated and GN_2 pressure blowdown systems. The single main advantage of the regulated system, namely, constant injectant fluid pressure, was found to be more than offset by several important advantages of the blowdown system. The blowdown system eliminated the need for a regulator, leading to a less complex system of higher intrinsic reliability. It also allowed either separate or common tankage for the pressurant and injectant, whereas common tankage is unfeasible in the regulated system. As a result of this comparison, the blowdown system was selected for further analysis.

A blowdown system using separate tanks for GN_2 and N_2O_4 was compared with a blowdown system consisting of common GN_2 and N_2O_4 tankage. A weight breakdown showed about a 600 lbm (272.2 kg) weight increase using the separate tankage system as opposed to the common GN_2 and N_2O_4 tankage.

The use of common tankage presented significant savings in manufacturing and qualification testing (both time and costs). Common tankage means storage of injectant fluid in the same tank with the pressurant required to expel that injectant fluid. This allows every tank built to have identical volume, fittings, outlets, support, etc. Therefore, only one tank, rather than a pressurant tank plus an injectant tank, has to be qualified. Also, logistics problems are eased because spare tanks are interchangeable with every tank in the system. Another advantage of common tankage is the design of less complex tank supports. Separate injectant and pressurant tankage would require two sets of tank supports.

The above comparisons resulted in the selection of a GN_2 pressure blowdown system using common tankage for the pressurant injectant.

4.4.3 Evaluation of LITVC System Components

4.4.3.3 Tank Configurations

SINGLE COMMON TOROIDAL TANK AND FOUR COMMON CYLINDRICAL TANKS SELECTED FOR DETAILED DESIGN TRADEOFFS

Several storage tank configurations were evaluated for the pressurant (GN_2) and injectant (N_2O_4). The use of multiple spheres yielded a space limitation problem, and the most complex and heaviest tankage system investigated. Also, access for assembly and servicing was poor with a multiple sphere tankage configuration. The double toroidal tank configuration (one tank for gas storage and another for the injectant) was used in the general preliminary LITVC system weight tradeoffs for reasons explained previously. Further tank studies revealed that various dual tank (one for GN_2; one for N_2O_4) arrangements were considerably heavier than single common tank configurations for the pressurant and injectant.

Typical common tank configurations studied are shown in Figure 4-12. The advantages found with the single common toroidal tank were lighter weight, savings in tank manufacturing and qualification testing, lessening of logistic problems, and less complex tank supports. Cylindrical tank configurations, located within the aft section, also were considered; each tank contained both the pressurant and injectant. This type of tankage was utilized in the Douglas* second evolution 260 in. motor LITVC studies.

The single common toroidal tank and an arrangement of four common cylindrical tanks were considered for incorporation into more detailed design tradeoffs.

*Use of Large Solid Motors in Booster Applications, Thrust Vector Control Systems Comparison: Detailed Technical Report. DAC-58038, Volume III. Douglas Missile and Space Systems Division. Prepared under Contract No. NAS 8-21051: 30 Aug 1967.

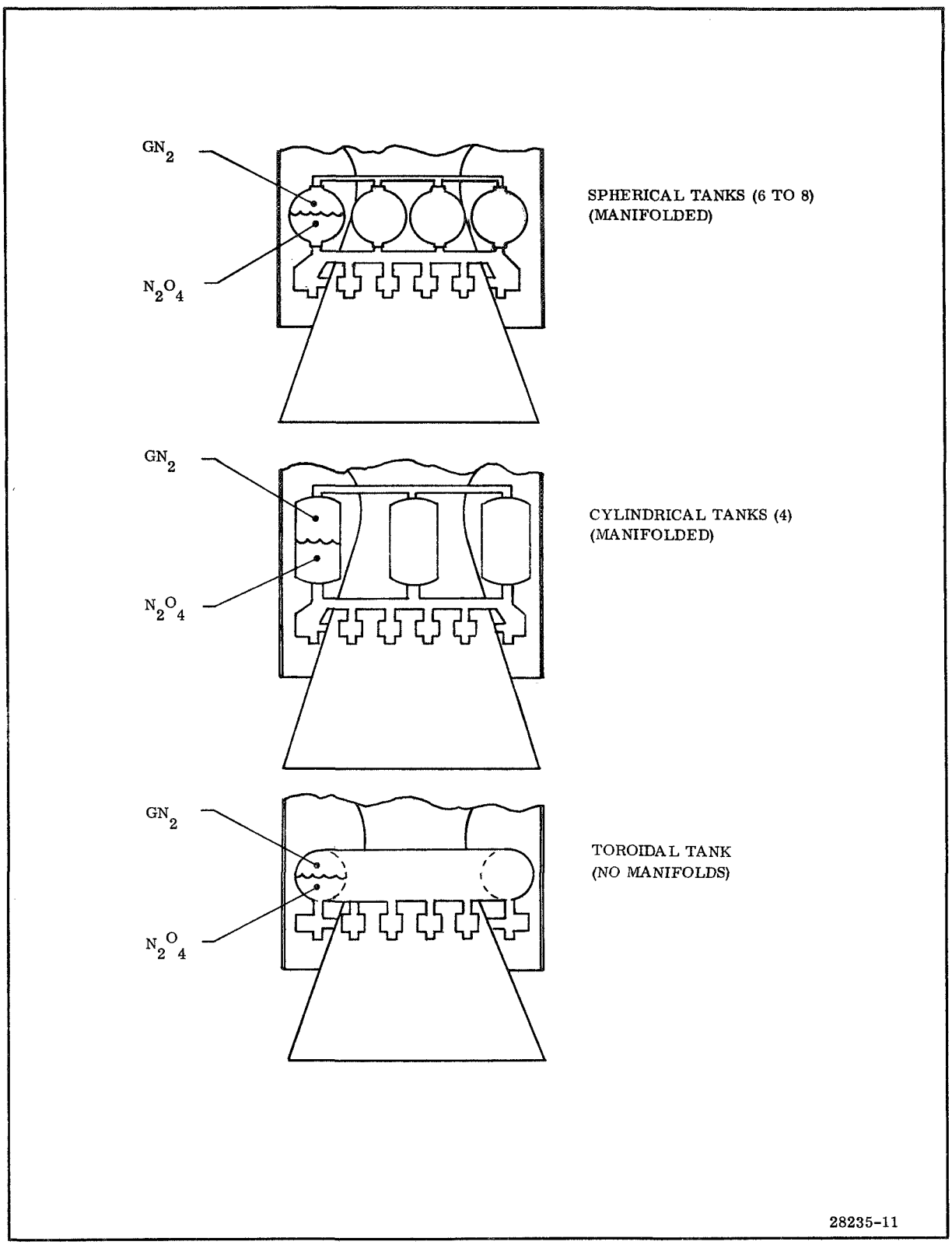

Figure 4-12. Typical LITVC Common Tank Configurations Studied

4.4.3 Evaluation of LITVC System Components

4.4.3.4 LITVC Control System Schemes

PITCH-YAW CONTROL SYSTEM SELECTED FOR LITVC SYSTEM

Several different LITVC control system schemes were investigated during the preliminary design phase. Basically, there are two methods to resolve the guidance system steering commands into injector valve positions. These two methods are pitch-yaw and omniaxis control. Because of its simplicity, a pitch-yaw controller was the selected concept.

In the pitch-yaw control system, the steering commands are used directly to drive the nozzle mounted injector valves within a specified nozzle quadrant. Figure 4-13 shows a typical 24 injector system. Pitch-yaw commands are applied to phase splitters to separate negative and positive commands. For the system shown, injectors are opened equally. Thus, for a 50 percent pitch command, six injectors (1 thru 6) are all opened to 50 percent flow. For an oblique command of 50 percent, 12 injectors (1 thru 12) are opened at 36 percent.

In the omniaxis control, the steering commands from the guidance system are resolved in the direction of the required thrust vector to favor a quadrant of injectors. Several methods are available to implement omniaxis control. Figure 4-14 shows one method successfully tested by Ling-Temco-Vought. In LTV's method, fixed gain summing amplifiers are used to vectorially resolve the steering command to align a single quadrant of injector valves in the direction of the required thrust vector. Figure 4-15 shows the injector positions as a function of steering commands when the thrust vector is aligned between injectors. Thus, for a 50 percent pitch command, injectors No. 3 and 4 are 78 percent open, injectors No. 2 and 5 are 54 percent open, and injectors No. 1 and 6 are 10 percent open. It can be seen that those injectors closest to the thrust vector have increased gain. For a 50 percent command in an oblique plane, injectors No. 4 thru 9 would be opened similarly.

It was found that a substantial reduction in electronic complexity and cost could be realized if the pitch-yaw control scheme was selected over the omniaxis control scheme. The pitch-yaw scheme is the simplest to implement and has been used on all of the first generation LITVC systems, including the Polaris, Minuteman, and Titan IIIC. Based upon the primary system design objective (simplicity), the pitch-yaw control scheme was selected for incorporation in the subject LITVC system studies.

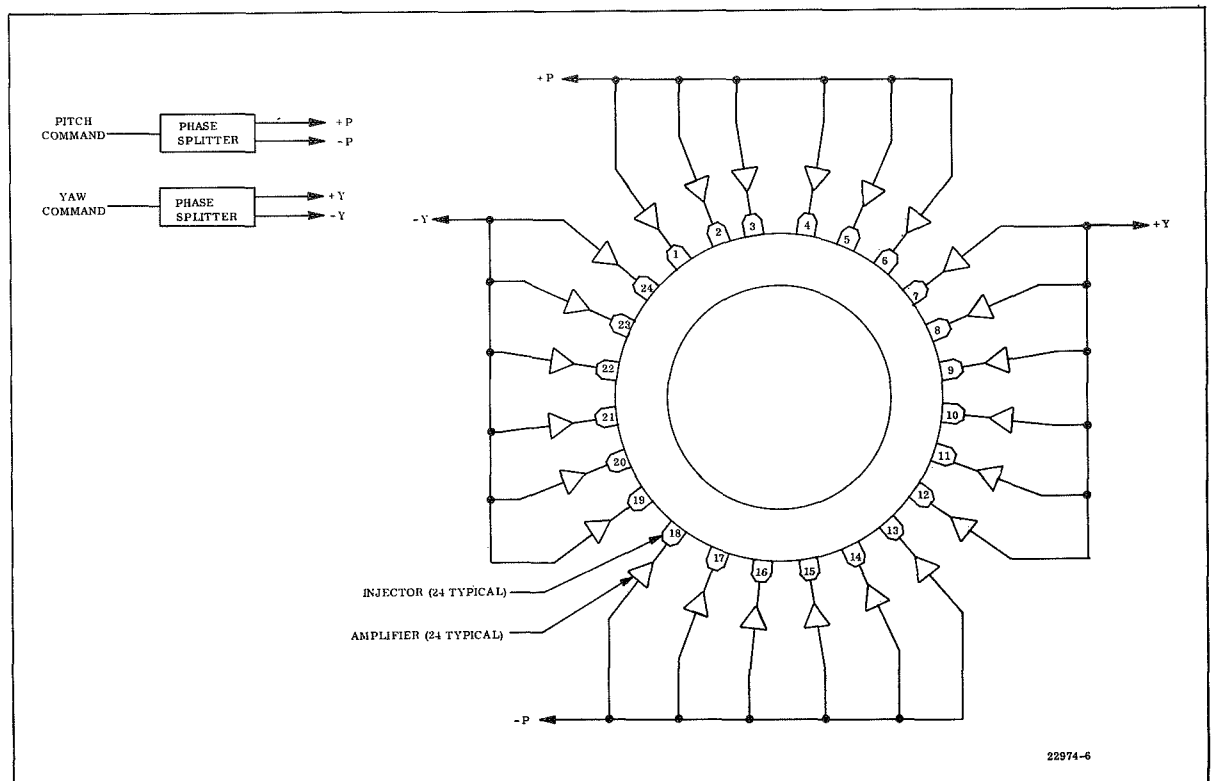

Figure 4-13. LITVC Pitch-Yaw Control System

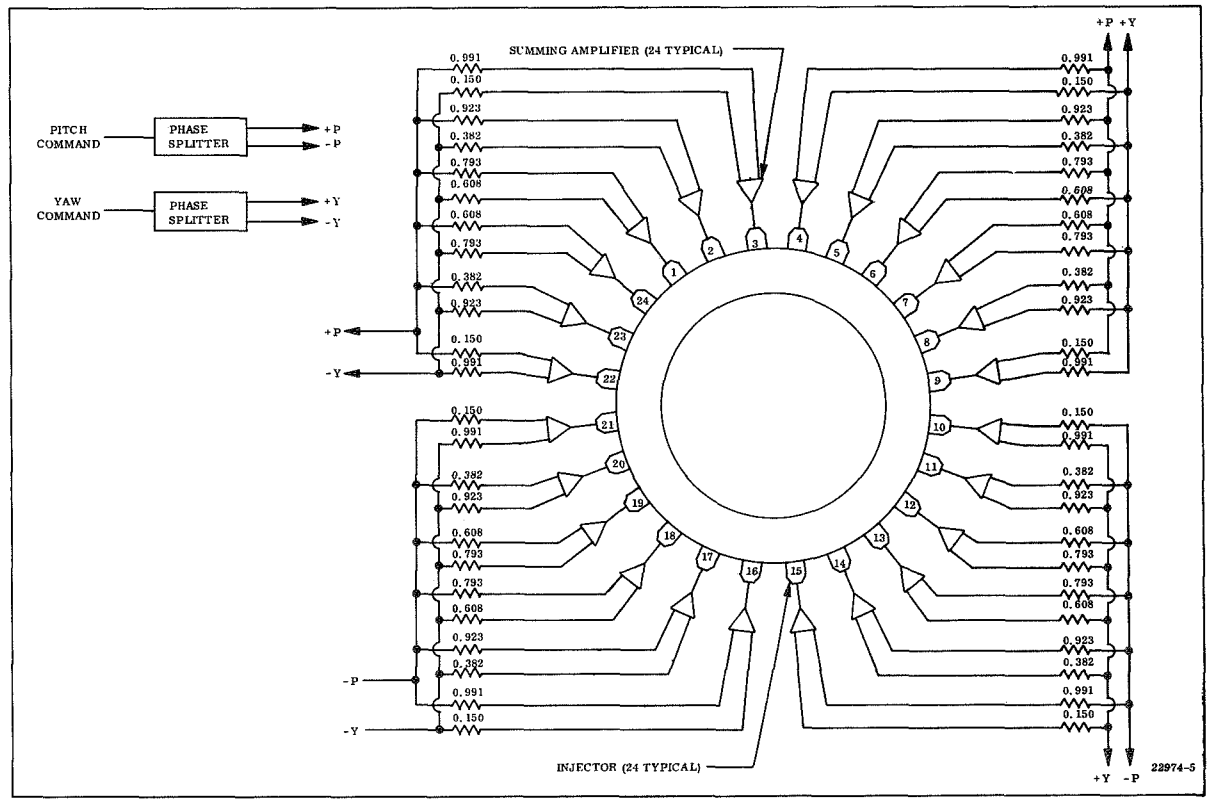

Figure 4-14. LITVC Omniaxis Control System

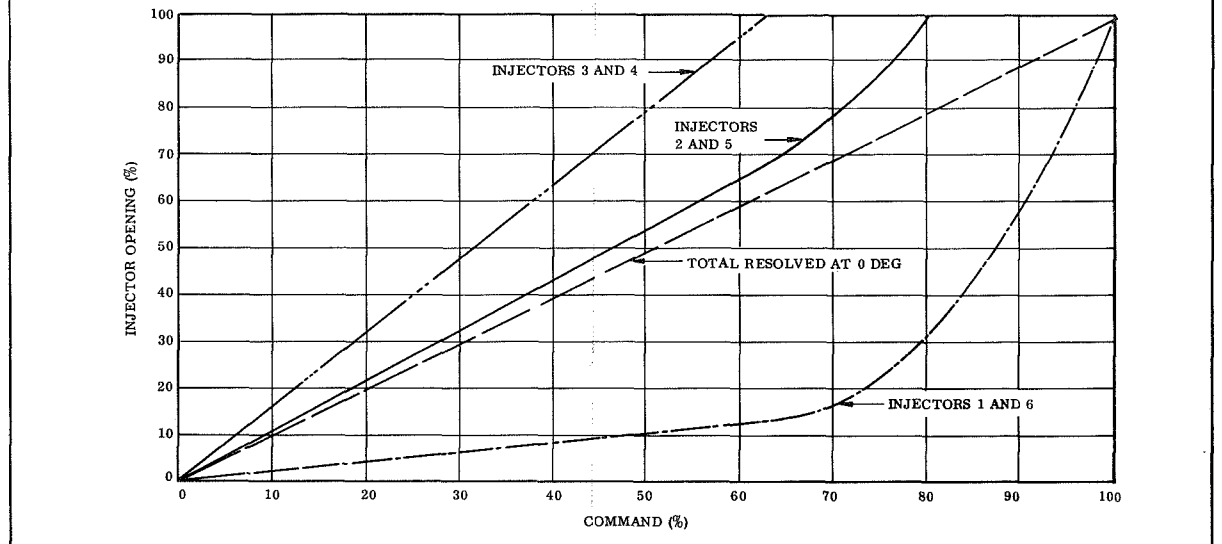

Figure 4-15. Omniaxis Injector Opening Profile

4.4 LITVC SYSTEM DESIGN ANALYSIS

4.4.4 Summary of Design Analysis

SELECTED LITVC INJECTION PARAMETERS, COMPONENTS, AND SUBSYSTEMS SUMMARIZED

Investigations were conducted to provide configuration data and tradeoff curves for use in the candidate and final LITVC system design for the 260 in. Solid Rocket Motor.

The selected injection parameters, components and subsystems are summarized in Table 4-4.

TABLE 4-4

SELECTED LITVC SYSTEM DESIGN CHARACTERISTICS

Type of injectants	1. N_2O_4 2. Aqueous Sr $(ClO_4)_2$ solution
Injector position	35 to 40 percent of nozzle length
Injection angle	+15° (0.26175 RAD) upstream of a perpendicular to the nozzle centerline
Type of injection valve	Single pintle-type injectors
No. of valves per nozzle quadrant	4 and 5
Type of injector actuation system	1. Electromechanical actuators/ battery power source 2. Hydraulic actuators/electric motor pump power source 3. Hydraulic actuators/passive blowdown power source
Type of injectant pressurization	Nitrogen gas (GN_2) blowdown
Type of tank configuration	1. Single common toroidal tank* 2. Four common cylindrical tanks*
Injection pressure	800 psia (5.516×10^6 N/m^2) initially; blows down to 400 psia (2.758×10^6 N/m^2)
LITVC control system scheme	Pitch-yaw controller

*No bladder required between pressurant and injectant because the vehicle acceleration forces parallel to the longitudinal axis of the vehicle maintain the liquid injectant in the aft end of the tank (location of injectant outlet ports).

4.0 LITVC System Studies

4.5 Candidate LITVC System Evaluation Tradeoff

EIGHT CANDIDATE LITVC SYSTEMS EVALUATED - SYSTEM 3B SELECTED

Eight candidate LITVC system designs are discussed in the following subsections. System 3B design approach was selected.

The earlier tradeoff studies affected the choice of the candidate LITVC systems to be evaluated for 260 in. SRM application. A cursory component breakdown of each of the candidate LITVC system configurations is presented in Table 4-5 .

Each of the eight candidate designs are discussed in the following subsections. LITVC system No. 1 is described in detail to aid the reader in visualizing the general equipment, then the differences of each of the other LITVC system designs are briefly explained. The final subsection concludes with a comparative discussion of the estimated weights and costs of each candidate design, and the selection of the LITVC system for further detailed design and analysis.

TABLE 4-5

COMPONENT BREAKDOWN OF CANDIDATE LITVC SYSTEM DESIGNS

LITVC System Component	LITVC System Designation							
	1	2	3A	3B	4A	4B	5A	5B
N_2O_4 injectant	X	X	X	X	X	X		
Sr $(ClO_4)_2$ injectant							X	X
GN_2 pressurant	X	X	X	X	X	X	X	X
Cylindrical tanks (4)	X							
Toroidal tank (1)		X	X	X	X	X	X	X
Injectant distribution manifold	X	X						
Injectant ducts - tank to manifold	X	X						
Injectant ducts - manifold to injectors	X	X						
Injectant ducts - tank to injectors			X	X	X	X	X	X
Electrohydraulic injector valves	X	X			X	X	X	X
Electromechanical injector valves			X	X				
5 injectors/quadrant	X	X	X				X	X
4 injectors/quadrant				X	X	X		
Battery assembly	X	X	X	X	X		X	
Power transfer switch	X	X	X	X	X		X	
Hydraulic power supply system (electric motor pumps)	X	X	X	X	X		X	
Passive blowdown hydraulic power system						X		X

4.5 Candidate LITVC System Evaluation Tradeoff

4.5.1 LITVC System No. 1

LITVC SYSTEM NO. 1 DESCRIBED

LITVC system No. 1 is schematically depicted in Figure 4-16. A preliminary component weight and cost breakdown of this system is presented in Table 4-6 (the nozzle weight is not included).

The tankage for this LITVC system design consists of four identical cylindrical tanks (nominal storage volume of 173 cu ft (4.90 m^3) per tank). Each tank contains both the GN_2 pressurant (105.5 cu ft) (2.99 m^3) and the N_2O_4 injectant (67.5 cu ft) (1.91 m^3), has provisions for filling and venting of the GN_2, emergency venting of N_2O_4 injectant vapors, distribution of N_2O_4 injectant to a common manifold, and measurement of unexpended N_2O_4.

The GN_2 blowdown system pressure is initially 800 psia (5,515,840 N/m^2) minimum with the vehicle fully loaded and ready for launching. The system blows down to 400 psia (2,757,920 N/m^2) during the course of the flight. Experimental data indicate satisfactory LITVC vectoring performance at injectant pressures down to 400 psia (2,757,920 N/m^2) within the duty cycle requirements specified for this study.

The pressurant is distributed equally among the four tanks during loading, and each tank has an identical pneumatic charge disconnect which fits pressurant distribution manifold that ties all four tanks together. The relief valve vents are designed to handle N_2O_4 vapor as well as nitrogen gas. The burst disc provides automatic pressure relief in the event of an excessive unexpected pressure rise.

A single feed line transfers the injectant from each tank to the nozzle distribution manifold. The inlet of each 6 in. (15.24 cm) flexible stainless steel feed line is attached to the injectant tank, and the outlet is attached to the toroidal distribution manifold. The manifold receives the N_2O_4 delivered by the feed lines and distributes the N_2O_4 to each of the 20 injector valve ducts. The manifold also contains a balanced quick disconnect coupling (compatible with N_2O_4) for filling of the injectant tanks. Twenty injector valve housings are attached to the nozzle and provide support for the distribution manifold and the 20 equally spaced injector valve assemblies.

The injectors are electrohydraulically actuated pintle-type valves which vary the flow rate by changing the effective flow area. These servo-controlled assemblies are capable of modulating N_2O_4 flow from 0 to 169 lbm/sec (76.7 kg/sec) at 800 psi (5,515,840 N/m^2), and from 0 to 120 lbm/sec (54.4 kg/sec) at 400 psi (2,757,920 N/m^2). The injector valves use developed servovalves to obtain valve opening and closing time capabilities to achieve the required slew rate of 3 deg/sec (0.0524 RAD/sec).

The LITVC system has the capability of providing correction for all transient and steady-state perturbations in the pitch and yaw axes. The pitch and yaw control subsystem provides (1) servodrive amplifiers and coupling between the input autopilot command signals and the injection valves, (2) a linearization of the side force-voltage relation, (3) controller integration of the liquid dump commands with the TVC requirements, and (4) compensation for quadrant interaction.

The dual electric motor pump hydraulic power supply (schematically illustrated in Figure 4-16) provides 3,000 psi (20,684,400 N/m^2) hydraulic fluid to the injector valve actuators. The power supply package is attached to the aft skirt. Hydraulic manifolds are connected to each of the 20 injector valve assemblies by supply and return lines. An electrical distribution box is mounted on the nozzle as an electrical power and command interchange for the TVC and flight instrumentation system. The battery assembly provides the electrical power required by theLITVC system components during flight. The battery assembly and a power transfer switch are mounted on supports attached to the vehicle aft skirt. The electric power transfer switch is provided to permit checkout operation of the LITVC.

TABLE 4-6

LITVC SYSTEM NO. 1 PRELIMINARY WEIGHTS AND COSTS

Component	Weight (lbm)	Weight (kg)	Cost ($)
Injectant: nitrogen tetroxide (N_2O_4) Duty cycle injectant = 20,956 lbm (9,506 kg) Allowance* injectant = 3,353 lbm (1,521 kg) (Expended injectant) = (23,681 lbm) (10,742 kg)	24,309	11,027	1,580
Nitrogen gas (GN_2)	1,650	748	270
N_2O_4 - GN_2 cylindrical tanks (4 at 2,100 lbm (953 kg) and $25,000 each)	8,400	3,810	100,000
N_2O_4 - Distribution manifold	500	227	25,900
Tank-to-manifold transfer ducts (4 at 20 lbm) (9.1 kg) and $3,000 each)	80	36.3	12,000
Manifold-to-injector ducts (20 at 12 lbm (5.4 kg) and $500 each)	240	109	10,000
Injector valves (20 at 20 lbm (9.1 kg) and $3,800 each)	400	181	76,000
Injector housings (20 at 12 lbm (5.4 kg) and $200 each)	240	109	4,000
Tank attach mounts	400	181	46,000
Wiring harness and conduit	80	36.3	13,400
Tankage miscellaneous (4 relief vent valves, 4 pneumatic charge disconnects, 4 fluid level transmitters, 4 operational pressure transducers, 4 burst discs, 1 fill/drain disconnect, pressurant manifold)	123	55.8	33,800
Pitch and yaw control	40	18.1	20,000
Hydraulic power supply	105	47.6	55,500
Electrical harness assemblies	200	90.7	24,000
Battery assembly	77	34.9	1,400
Power transfer switch	8	3.6	1,700
Hydraulic manifold and plumbing	70	31.8	7,700
Mounting supports	183	83	19,700
Total initial weight (lbm)	37,105	16,831	--
Total burnout weight (lbm)	13,424	6,089	--
Total cost ($)			452,950

*Allowances for expulsion efficiency system errors, motor and LITVC performance tolerances, ullage, manifolds, and injector leakage.

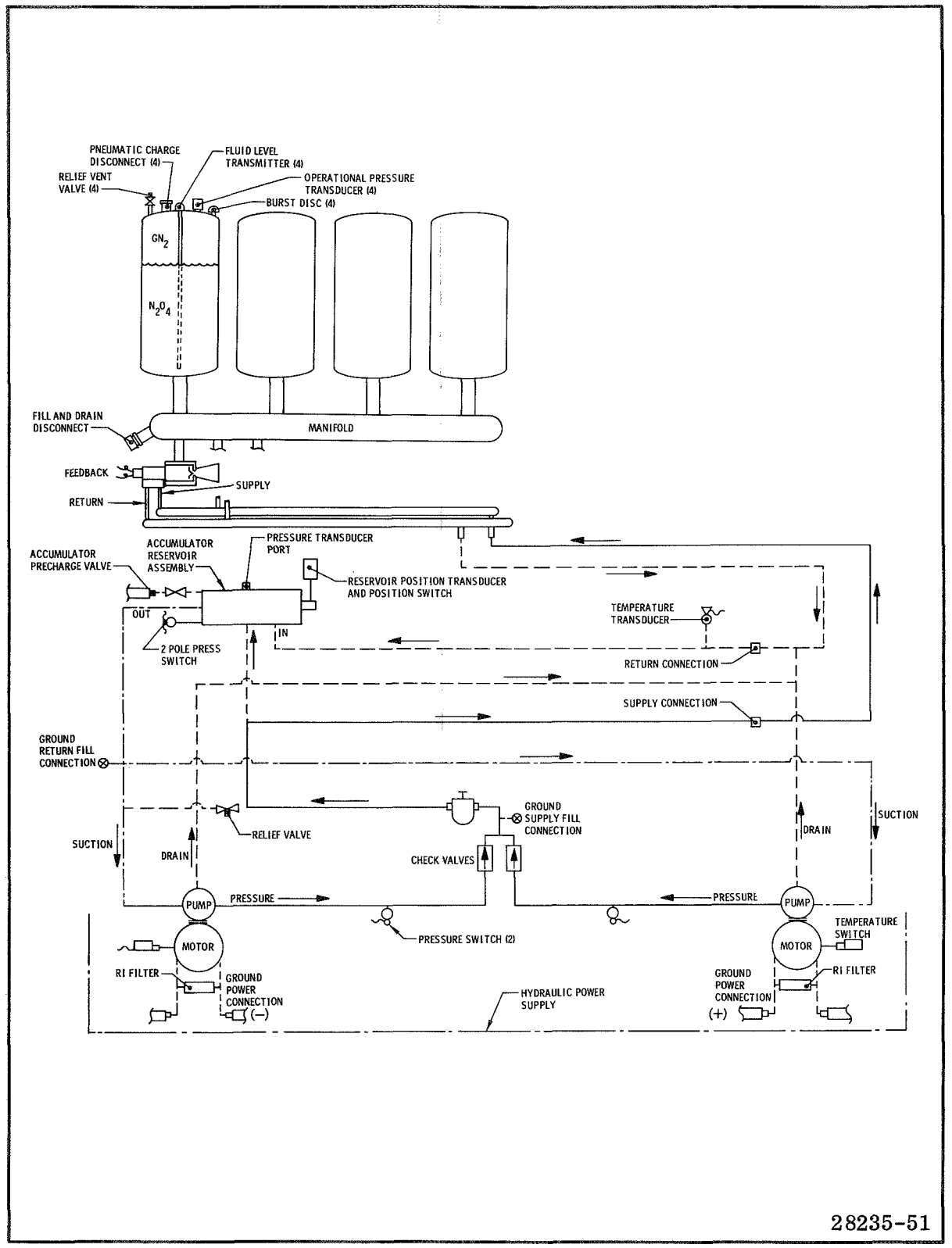

Figure 4-16. Schematic for LITVC System No. 1

4.5 Candidate LITVC System Evaluation Tradeoff

4.5.2 LITVC System No. 2

LITVC SYSTEM NO. 2 DESCRIBED

LITVC system No. 2 uses a single toroidal injectant-pressurant tank which simplifies supporting hardware requirements.

The LITVC system No. 2 schematic is illustrated in Figure 4-17. Presented in Table 4-7 are preliminary component weights and cost of this system (nozzle excluded).

The major difference between system No. 2 and system No. 1 (previously discussed) is that system No. 2 uses a single toroidal injectant-pressurant tank in place of the four cylindrical tanks. Therefore, LITVC system No. 2 requires only a single relief vent valve, pneumatic charge disconnect, fluid level transmitter, operational pressure transducer, and burst disc.

TABLE 4-7

LITVC SYSTEM NO. 2 PRELIMINARY WEIGHTS AND COSTS

Components	Weight (lbm)	Weight (kg)	Cost ($)
Injectant: nitrogen tetroxide (N_2O_4) Duty cycle injectant = 20,956 lbm (9,506 kg) Allowance* injectant = 3,353 lbm (1,521 kg) (Expended injectant) = (23,681 lbm) (10,742 kg)	24,309	11,027	1,580
Nitrogen gas (GN_2)	1,650	748	270
Toroidal N_2O_4 - GN_2 tank	5,250	2,381	50,000
N_2O_4 distribution manifold	500	227	25,900
Tank-to-manifold transfer ducts (4 at 20 lbm (9.1 kg) and $3,000 each)	80	36.3	12,000
Manifold-to-injector ducts (20 at 12 lbm (5.4 kg) and $500 each)	240	109	10,000
Injector valves (20 at 20 lbm (9.1 kg) and $3,800 each)	400	181	76,000
Injector housings (20 at 12 lbm (5.4 kg) and $200 each)	240	109	4,000
Tank attach mounts	300	136	40,000
Wiring harness and conduit	80	36.3	13,400
Tankage miscellaneous (1 relief vent valve, 1 pneumatic charge disconnect, 1 fluid level transmitter, 1 operational pressure transducer, 1 burst disc, 1 fill/drain disconnect)	26	11.8	8,500
Pitch and yaw control	40	18.1	20,000
Hydraulic power supply	105	47.6	55,500
Electrical harness assemblies	200	90.7	24,000
Battery assembly	77	34.9	5,000
Power transfer switch	8	3.6	1,700
Hydraulic manifold and plumbing	70	31.8	7,700
Mounting supports	183	83	19,700
Total initial weight (lbm)	33,758	15,313	--
Total burnout weight (lbm)	10,077	4,571	--
Total cost ($)			375,250

*Allowances for expulsion efficiency, system errors, motor and LITVC performance tolerances, ullage, manifolds, and injector leakage.

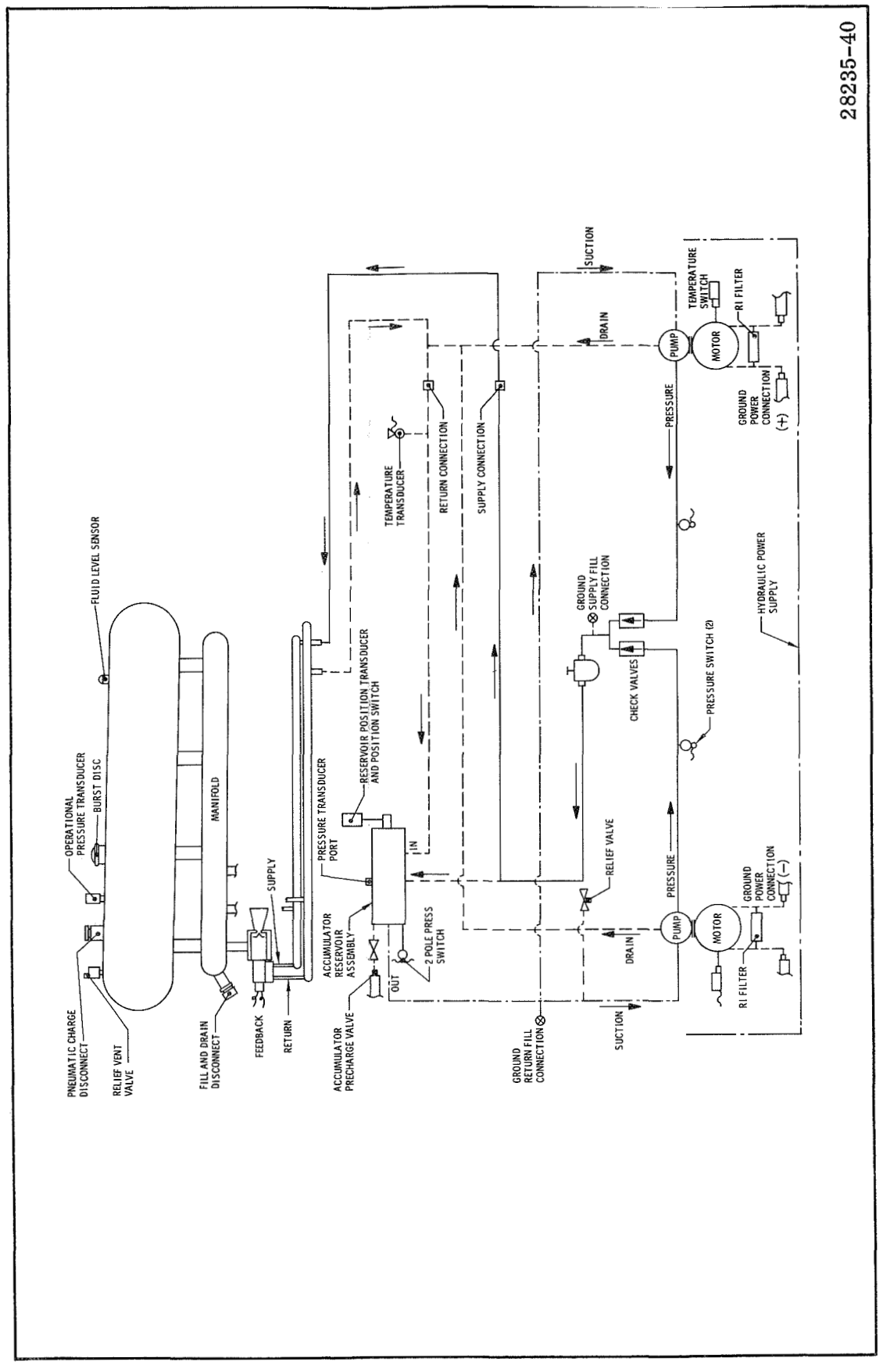

Figure 4-17. Schematic for LITVC System No. 2

4.5 Candidate LITVC System Evaluation Tradeoff

4.5.3 LITVC Systems No. 3A and 3B

LITVC SYSTEMS NO. 3A AND 3B DESCRIBED

LITVC systems No. 3A and 3B are both similar to system 2. Exceptions are the absence of a distribution manifold, and the use of electromechanical injector valves.

LITVC systems No. 3A and 3B are schematically illustrated in Figure 4-18. System No. 3A is similar to system No. 2; the exceptions being no distribution manifold and the use of electromechanical (EM) injector valves instead of electro-hydraulic (EH) injector valves. A preliminary component weight and cost breakdown of system No. 3A is displayed in Table 4-8.

LITVC system No. 3B is identical to LITVC system No. 3A except that five injectors per quadrant have been decreased to four injectors per quadrant (the minimum number of N_2O_4 injectors per quadrant necessary to achieve the 260 in. SRM TVC requirements). The preliminary component weights and costs for system No. 3B are shown in Table 4-9.

TABLE 4-8

LITVC SYSTEM NO. 3A PRELIMINARY WEIGHTS AND COSTS

Component	Weight (lbm)	Weight (kg)	Cost ($)
Injectant: nitrogen tetroxide (N_2O_4) Duty cycle injectant = 20,956 lbm (9,506 kg) Allowance* injectant = 3,353 lbm (1,521 kg) (Expended injectant) = (23,681 lbm) (10,742 kg)	24,309	11,027	1,580
Nitrogen gas (GN_2)	1,650	748	270
Toroidal N_2O_4 - GN_2 tank	5,250	2,381	50,000
Tank-to-injector ducts (20 at 15 lbm (6.8 kg) and $600 each)	300	136	12,000
Injector valves (20 at 20 lbm (9.1 kg) and $3,800 each)	400	181	76,000
Injector housings (20 at 12 lbm (5.4 kg) and $200 each)	240	109	4,000
Wiring harness and conduit	80	36.3	13,400
Tank attach mounts	300	136	40,000
Tankage miscellaneous (See LITVC No. 2)	26	11.8	8,500
Pitch and yaw control	35	15.9	20,000
Battery assembly	40	18.1	4,000
Electrical harness assembly	200	90.7	24,000
Power transfer switch	8	3.6	1,700
Mounting supports	100	45.4	13,500
Total initial weight (lbm)	32,938	14,941	--
Total burnout weight (lbm)	9,257	4,199	--
Total cost ($)			268,950

*Allowances for expulsion efficiency, system errors, motor and LITVC performance tolerances, ullage, manifolds, and injector leakage.

TABLE 4-9

LITVC SYSTEM NO. 3B PRELIMINARY WEIGHTS AND COSTS

Component	Weight (lbm)	Weight (kg)	Cost ($)
Injectant: nitrogen tetroxide (N_2O_4) Duty cycle injectant = 21,236 lbm (9,633 kg) Allowance* injectant = 3,398 lbm (1,541 kg) (Expended injectant) = (23,997 lbm) (10,885 kg)	24,634	11,174	1,600
Nitrogen gas (GN_2)	1,690	767	280
Toroidal N_2O_4 - GN_2 tank	5,290	2,400	50,000
Tank-to-injector ducts (16 at 15 lbm (6.8 kg) and $600 each)	240	109	9,600
Injector valves (16 at 20 lbm (9.1 kg) and $3,800 each)	320	145	60,800
Injector housings (16 at 12 lbm (5.4 kg) and $200 each)	192	87.1	3,200
Wiring harness and conduit	64	29.0	11,000
Tank attach mounts	305	138.3	41,000
Tankage miscellaneous (See LITVC No. 2)	26	11.8	8,500
Pitch and yaw control	35	15.9	20,000
Battery assembly	40	18.1	4,000
Electrical harness assembly	160	78.6	20,000
Power transfer switch	8	3.6	1,700
Mounting supports*	100	45.4	13,500
Total initial weight (lbm)	33,104	15,016	--
Total burnout weight (lbm)	9,107	4,131	--
Total cost ($)			245,180

*Allowances for expulsion efficiency, system errors, motor and LITVC performance tolerances, ullage, manifolds, and injector leakage.

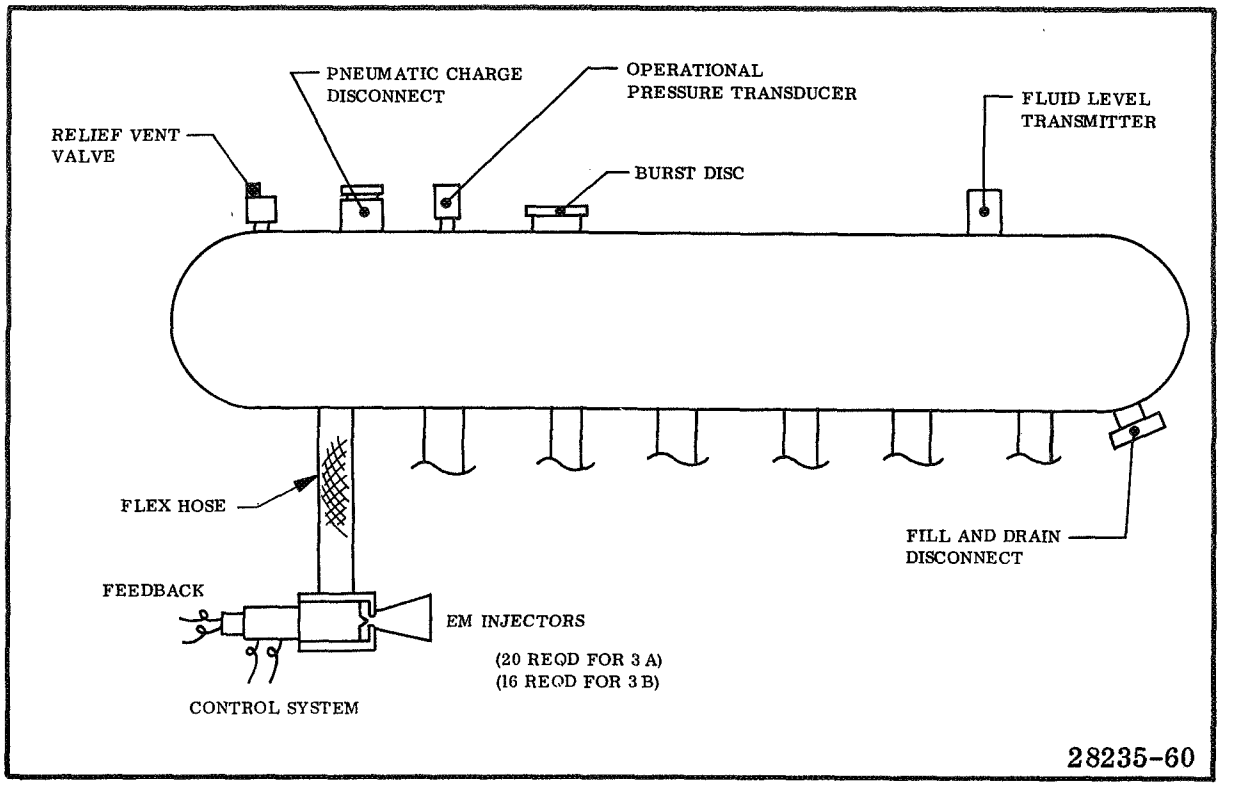

Figure 4-18. Schematic for LITVC Systems No. 3A and 3B

4.5 Candidate LITVC System Evaluation Tradeoff

4.5.4 LITVC Systems 4A and 4B

LITVC SYSTEMS 4A AND 4B DESCRIBED

LITVC systems 4A and 4B are similar to system 3B. Exceptions are in the injection system and the hydraulic power system.

LITVC system No. 4A is identical to LITVC system No. 3B except that the electromechanical injection system has been replaced with an electrohydraulic injection system (four injectors per quadrant).

LITVC system No. 4B is a modification of No. 4A; the conventional hydraulic power system utilizing electric-motor driven pumps has been replaced with a passive blowdown power system. The schematic of the LITVC No. 4B passive blowdown power system is presented in Figure 17. The preliminary component weights and costs for systems, No. 4A and 4B are displayed in Tables 4-10 and 4-11.

TABLE 4-10

LITVC SYSTEM NO. 4A PRELIMINARY WEIGHTS AND COSTS

Component	Weight (lbm)	Weight (kg)	Cost ($)
Injectant: nitrogen tetroxide (N_2O_4) Duty cycle injectant = 21,236 lbm (9,633 kg) Allowance* injectant = 3,389 lbm (1,541 kg) (Expended injectant) = (23,997 lbm) (10,885 kg)	24,634	11,174	1,600
Nitrogen gas (GN_2)	1,690	767	280
Toroidal N_2O_4 - GN_2 tank	5,290	2,400	50,000
Tank-to-injector ducts (16 at 15 lbm (6.8 kg) and $600 each)	240	109	9,600
Injector valves (16 at 20 lbm (9.1 kg) and $3,800 each)	320	145	60,800
Injector housings (16 at 12 lbm (5.4 kg) and $200 each)	192	87	3,200
Wiring harness and conduit	64	29	11,000
Tank attach mounts	305	138.3	41,000
Tankage miscellaneous (1 relief vent valve, 1 pneumatic charge disconnect, 1 fluid level transmitter, 1 operational pressure transducer, 1 burst disc, 1 fill/drain disconnect)	26	11.8	8,500
Pitch and yaw control	40	18.1	20,000
Hydraulic power supply	105	47.6	55,500
Electrical harness assemblies	160	72.6	20,000
Battery assembly	77	34.9	5,000
Power transfer switch	8	3.6	1,700
Hydraulic manifold and plumbing	56	25.4	6,200
Mounting supports	146	66.2	17,000
Total initial weight (lbm)	33,353	15,129	--
Total burnout weight (lbm)	9,356	4,244	--
Total cost ($)			311,380

*Allowances for expulsion efficiency, system errors, motor and LITVC performance tolerances, ullage, manifolds, and injector leakage.

TABLE 4-11

LITVC SYSTEM NO. 4B PRELIMINARY WEIGHTS AND COSTS

Component	Weight (lbm)	Weight (kg)	Cost ($)
Injectant: nitrogen tetroxide (N_2O_4) Duty cycle injectant = 21,236 lbm (9,633 kg) Allowance* injectant = 3,398 lbm (1,541 kg) (Expended injectant) = (23,997 lbm) (10,885 kg)	24,634	11,174	1,600
Nitrogen gas (GN_2) to pressure injectant	1,690	767	280
Nitrogen gas (GN_2) for hydraulic blowdown	7	3.2	
Toroidal N_2O_4 - GN_2 tank	5,300	2,404	50,000
Tank-to-injector ducts (16 at 15 lbm (6.8 kg) and $600 each)	240	109	9,600
Injector valves (16 at 20 lbm (9.1 kg) and $3,800 each)	320	145	60,800
Injector housings (16 at 12 lbm (5.4 kg) and $200 each)	192	87	3,200
Wiring harness and conduit (4 lbm (1.8 kg)/injector)	64	29	11,000
Tank attach mounts	306	138.8	41,000
Tankage miscellaneous (See LITVC No. 4A)	26	11.8	8,500
Tank-to-hydraulic oil reservoir manifold	5	138.8	500
Hydraulic oil reservoir (includes brackets)	100	45.4	1,500
Hydraulic oil (14 gal at 7 lbm/gal) (Expended oil = 91 lbm (41.3 kg)	98	44.5	
Shuttle valve	4	1.8	500
Fill valve and ground checkout disconnect (pressure)	3	1.4	500
Solenoid valve and ground checkout disconnect (return)	5	2.3	
Pitch and yaw control	40	18.1	20,000
Electrical harness assemblies	100	45.4	20,000
Hydraulic manifold and plumbing	60	27.2	7,000
Mounting supports	146	66.2	17,000
Total initial weight (lbm)	33,340	15,123	--
Total burnout weight (lbm)	9,252	4,197	--
Total cost ($)			252,980

*Allowances for expulsion efficiency system errors, motor and LITVC performance tolerances, ullage, manifolds, and injector leakage.

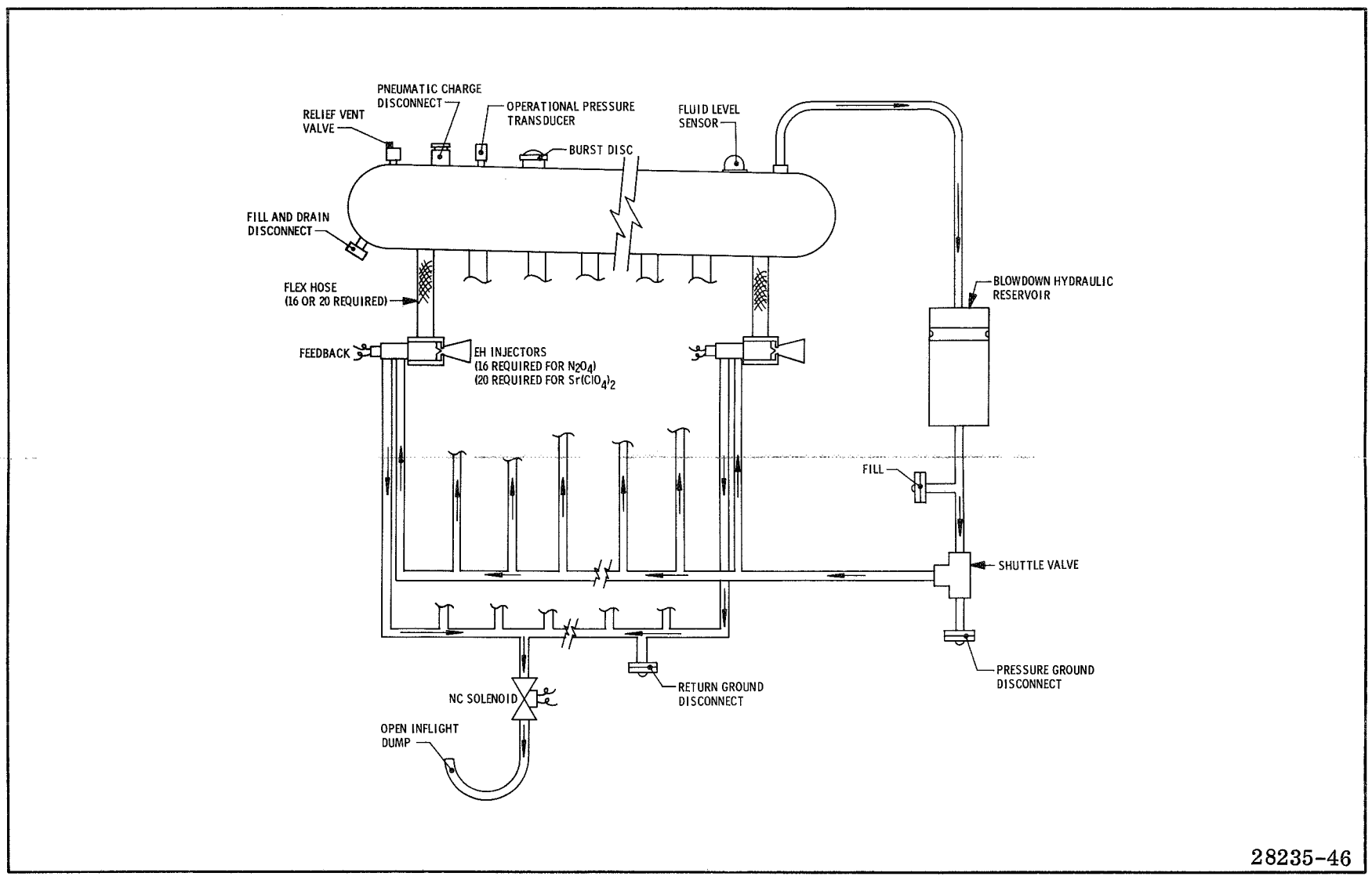

Figure 4-19. Schematic for LITVC Systems No. 4B and 5B

4.5 Candidate System Evaluation Tradeoff

4.5.5 LITVC Systems No. 5A and 5B

LITVC SYSTEMS 5A AND 5B DESCRIBED

LITVC systems 5A and 5B are similar to LITVC systems 4A and 4B except for injectant subsystem.

LITVC systems No. 5A and No. 5B are identical to LITVC systems No. 4A and No. 4B except that (1) the nitrogen tetroxide (N_2O_4) injectant has been replaced with an aqueous solution of strontium perchlorate, Sr $(ClO_4)_2$, and (2) five injectors per quadrant are required with aqueous Sr $(ClO_4)_2$ injectant. The LITVC system No. 5B schematic is shown in Figure 4-19. Preliminary component weight and cost breakdowns of systems No. 5A and No. 5B are presented in Tables 4-12 and 4-13, respectively.

TABLE 4-12

LITVC SYSTEM NO. 5A PRELIMINARY WEIGHTS AND COSTS

Component	Weight (lbm)	Weight (kg)	Cost ($)
Injectant: aqueous strontium perchlorate Duty cycle injectant = 26,196 lbm (11,883 kg) Allowance* injectant = 4,191 lbm (1,901 kg) (Expended injectant) = (29,601 lbm) (13,427 kg)	30,387	13,784	4,260
Nitrogen gas (GN_2)	1,560	708	260
Toroidal N_2O_4 - GN_2 tank	5,120	2,322	50,000
Tank-to-injector ducts (20 to 15 lbm (6.8 kg) and $600 each)	300	136	12,000
Injector valves (20 at 20 lbm (9.1 kg) and $3,800 each)	320	145	60,800
Injector housings (20 at 12 lbm (5.4 kg) and $200 each)	240	109	4,000
Wiring harness and conduit	80	36.3	13,400
Tank attach mounts	290	132	41,000
Tankage miscellaneous (1 relief vent valve, 1 pneumatic charge disconnect, 1 fluid level transmitter, 1 operational pressure transducer, 1 burst disc, 1 fill/drain disconnect)	26	11.8	8,500
Pitch and yaw control	40	18.1	20,000
Hydraulic power supply	105	47.6	55,500
Electrical harness assemblies	200	90.7	24,000
Battery assembly	77	34.9	5,000
Power transfer switch	8	3.6	1,700
Hydraulic manifold and plumbing	70	31.8	7,700
Mounting supports	183	83.0	19,700
Total initial weight (lbm)	39,006	17,693	--
Total burnout weight (lbm)	9,405	4,266	--
Total cost ($)			327,820

*Allowances for expulsion efficiency system errors, motor and LITVC performance tolerances, ullage, manifolds, and injector leakage.

TABLE 4-13

LITVC SYSTEM NO. 5B PRELIMINARY WEIGHTS AND COSTS

Component	Weight (lbm)	Weight (kg)	Cost ($)
Injectant: aqueous strontium perchlorate Duty cycle injectant = 26,196 lbm (11,883 kg) Allowance* injectant = 4,191 lbm (1,901 kg) (Expended injectant) = (29,601 lbm) (13,427 kg)	30,387	13,784	4,260
Nitrogen gas (GN_2)-to-pressurized injectant	1,560	708	260
Nitrogen gas (GN_2) for hydraulic blowdown	10	4.5	
Toroidal N_2O_4 - GN_2 tank	5,125	2,325	50,000
Tank-to-injector ducts (20 at 15 lbm (6.8 kg) and $600 each)	300	136	12,000
Injector valves (20 at 20 lbm (9.1 kg) and $3,800 each)	400	181	60,800
Injector housings (20 at 12 lbm (5.4 kg) and $200 each)	240	109	4,000
Wiring harness and conduit	80	36.3	13,400
Tank attach mounts	290	132	41,000
Tankage miscellaneous (See LITVC No. 5A)	26	11.8	8,500
Tank-to-hydraulic oil reservoir manifold	5	2.3	500
Hydraulic oil reservoir (includes brackets)	120	54.4	1,600
Hydraulic oil (18 gal at 7 lbm/gal) (expended oil = 119 lbm) (54.0 kg)	126	57.2	
Shuttle valve	4	1.8	500
Fill valve and ground checkout disconnect (pressure)	3	1.4	500
Solenoid valve and ground checkout disconnect (return)	5	2.3	
Pitch and yaw control	40	18.1	20,000
Electrical harness assemblies	200	90.7	24,000
Hydraulic manifold and plumbing	70	31.8	7,700
Mounting supports	183	83.0	19,700
Total initial weight (lbm)	39,174	17,769	--
Total burnout weight (lbm)	9,454	4,288	--
Total cost ($)			268,720

*Allowance for explusion efficiency, system errors, motor and LITVC performance tolerances, ullage, manifolds, and injector leakage.

4.5 CANDIDATE LITVC SYSTEM EVALUATION TRADEOFF

4.5.6 Selection of LITVC System Design Approach

LITVC SYSTEM 3B SELECTED AS MOST PROMISING DESIGN APPROACH

Thiokol and NASA LeRC jointly determined that LITVC system 3B offered the most design potential and therefore should be pursued further in the detailed LITVC system design task. The decision was based on system weight, cost effectiveness, and simplicity.

A comparison of the injectant and pressurant requirements, the estimated total launch and burnout weights (nozzle weight excluded), and estimated cost of each candidate LITVC system design are shown in Table 4-14.

Referring to the total (wet) launch weights in Table 4-14, the two aqueous Sr $(ClO_4)_2$ LITVC systems (No. 5A and 5B) exceeded the launch weights of their N_2O_4 counterpart designs (No. 4A and 4B) by 17 percent. The heavier aqueous Sr $(ClO_4)_2$ system launch weights resulted primarily from the increase in injectant weight (due to lower ISP_S capabilities than N_2O_4) and the requirement for a minimum of five injectors per quadrant (instead of four per quadrant with N_2O_4).

Within the six N_2O_4 LITVC systems evaluated (systems No. 1 thru 4B), system No. 1, which used four cylindrical N_2O_4-GN_2 tanks, was estimated to be the most costly system, and also the heaviest at launch and burnout. LITVC system No. 3B was the second lightest N_2O_4 design at launch, had the lightest burnout weight, and was the least costly.

TABLE 4-14

NASA 260 IN. SRM WEIGHT AND COST COMPARISON OF CANDIDATE LITVC SYSTEM DESIGNS

	LITVC No. 1	LITVC No. 2	LITVC No. 3A	LITVC No. 3B	LITVC No. 4A	LITVC No. 4B	LITVC No. 5A	LITVC No. 5B
Injectant	N_2O_4	N_2O_4	N_2O_4	N_2O_4	N_2O_4	N_2O_4	$Sr(ClO_4)_2 + H_2O$	
Injectant volume (total initial) (cu in.)	466,000	466,000	466,000	473,470	473,470	473,470	437,600	437,600
Injectant weight (total initial) (lbm)	24,309	24,309	24,309	24,634	24,634	24,634	30,387	30,387
Pressurant	GN_2	GN_2	GN_2	GN_2	GN_2	GN_2	GN_2	GN_2
Pressurant volume (total initial) (cu in.)	728,000	728,000	728,000	739,800	739,800	739,800	683,700	683,700
Pressurant weight (total initial) (lbm)	1,650	1,650	1,650	1,690	1,690	1,690	1,560	1,560
LITVC system								
Estimated total launch weight* (lbm)	37,105	33,758	32,938	33,104	33,353	33,340	39,006	39,174
Estimated total burnout weight* (lbm)	13,424	10,077	9,257	9,107	9,356	9,252	9,405	9,454
Estimated LITVC system unit cost**	$452,950	$375,250	$268,950	$245,180	$311,380	$252,980	$327,820	$268,720

*Nozzle weight excluded.

**Nozzle cost excluded; unit cost based on thirty 260 in. motors and LITVC systems.

4.0 LITVC System Studies

4.6 Final LITVC System Design

OVERALL DESIGN OF FINAL LITVC SYSTEM PRESENTED

The overall design of the final LITVC system is presented in this subsection. The following subsections discuss the major selected components.

The LITVC system design developed for application on the 260 in. SRM is schematically presented in Figure 4-20, and pictorially illustrated in Figure 4-21. Thiokol Drawing No. TUL-13085 shows additional detail design features of the system components. The addition of an aft skirt access door was the only modification required to the basic vehicle design.

The NASA 260 in. final LITVC system design consisted of the following components.

- Fixed nozzle.
- N_2O_4 injectant.
- GN_2 pressurant.
- Toroidal GN_2-N_2O_4 tank.
- Tank to injector ducts (16 required).
- Tank supports and mounting brackets.
- Electromechanical injectors (16 single pintle-type required).
- Injector housings (16 required).
- Injector drainage manifold.
- Tankage miscellaneous.
    - Solenoid vent valve.
    - Pneumatic charge disconnect.
    - Fluid level sensor.
    - Operational pressure transducer.
    - Burst disc assembly.
    - Relief valve.
    - Fill and drain valve.
- Pitch and yaw controller.
- Control system battery
- Power transfer switch.
- Electrical control harness assembly.
- Burst disk, relief and vent valve tubing assemblies.

Discussions of the major selected components for the final LITVC system design follow. The final design characteristics are summarized in Section 4.6.7.

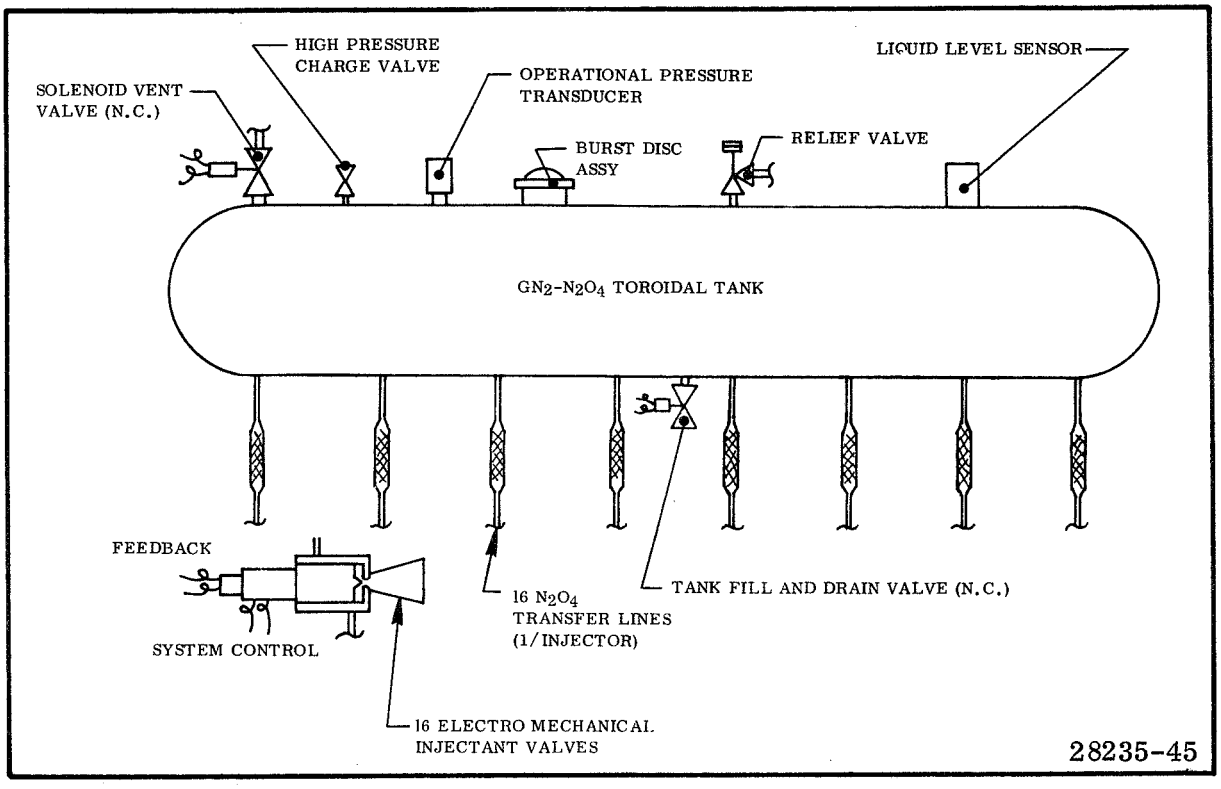

Figure 4-20. Schematic of NASA 260 In. SRM Final LITVC System Design

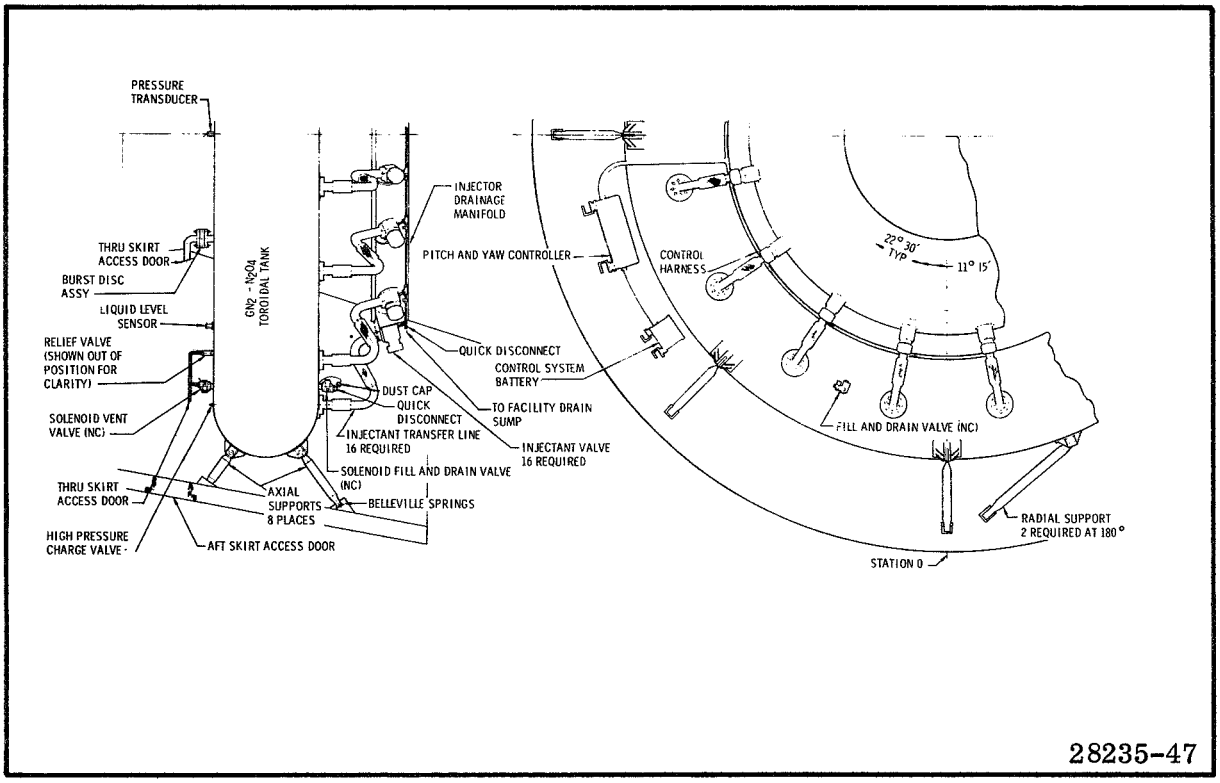

Figure 4-21. NASA 260 In. SRM Final LITVC System Design

4.6 FINAL LITVC SYSTEM DESIGN

4.6.1 LITVC Fixed Nozzle Design

BASELINE FIXED NOZZLE DESIGN MODIFIED FOR LITVC NOZZLE DESIGN

The LITVC nozzle design consisted of the baseline fixed nozzle design with the following modifications: (1) replacing the exit cone fiberglass with steel to support the liquid injectors, (2) mounting the injectors on an integral steel support ring, and (3) inserting silica cloth phenolic ports (one per injector) into the exit cone liner.

The same basic convergent-divergent nozzle (with appropriate modifications) was used for the LITVC and mechanical interference concepts (Figure 3-1). The nozzle had an initial throat diameter of 89.1 in. (226.3 cm), an initial expansion ratio of 8.515, exit cone half-angle of 17.5° (0.3054 RAD), and exit diameter of 260 in. The aft closure mounting flange, whose upstream face is 55.10 in. (140.0 cm) forward of the nozzle throat, incorporates a 180 in. (457.2 cm) mounting circle; the exit plane is 277.86 in. (705.8 cm) aft of the nozzle throat. The throat contour radius is equal to the throat radius. The above basic fixed nozzle dimensions, with the exception of the aft mounting flange location, also applied to the movable nozzle designs.

Low cost ablative materials were used to line the nozzle wherever possible: silica and asbestos filled Buna rubber (V-44) from the aft closure mounting flange to a point 42 in. (106.7 cm) forward of the throat; and canvas, from 90 in. (228.6 cm) aft of the throat to the exit plane. Carbon cloth, backed with 0.42 in. (1.067 cm) thick silica cloth, lined the nozzle in the throat region.

Alloy steel (4130) was used as the structural support between the aft closure and exit cone mounting flanges. The exit cone structure was fiberglass, filament wound to a steel nozzle mounting flange.

The modification necessary to adapt the basic nozzle (see Subsection 3.1) to the LITVC system consisted of replacing the structural fiberglass in the exit cone from the nozzle exit cone interface to a distance 20 in. (5.08 cm) aft of the liquid injectors with a steel shell in order to support these injectors and react the side load. Upon termination of this steel shell, structural fiberglass formed the exit cone shell to the end of the nozzle, as it does in the unmodified nozzle design. An overwrap of fiberglass was used for joining the steel and fiberglass shells at their interface.

The liquid injectors were mounted on a steel support ring which is an integral part of the steel structure. A silica cloth phenolic port (one per injector) was inserted into the exit cone liner to take advantage of silica cloth's ability to better withstand the thermal gradients associated with the injectant ports. Construction details within the injector port area of the nozzle are shown in Thiokol Drawing No. TUL-13085.

The initial total weight of the LITVC nozzle, exclusive of any liquid injectant components, was 53,947 lb (24,470 kg) (38,562 lb (17,492 kg) insulation and 15,385 lb (6,979 kg) structure). This total is 6,046 lb (2,742 kg) greater than the initial weight of the fixed baseline nozzle. The total expended LITVC nozzle weight during flight was calculated to be 5,772 lbm (2,618 kg).

4.6 FINAL LITVC SYSTEM DESIGN

4.6.2 GN_2-N_2O_4 Tank Assembly

GN_2-N_2O_4 TOROIDAL TANK ASSEMBLY DESCRIBED

The LITVC tank assembly is a single toroidal tank (volume, 702 cu ft) (19.88 m^3) which contains both the GN_2 pressurant and the N_2O_4 injectant fluid. The tank has provisions for loading and unloading N_2O_4, filling and venting GN_2, emergency venting of N_2O_4 vapors, nonvortex distribution of N_2O_4 to each of 16 injectors, and measurement of unexpended N_2O_4. The GN_2 blowdown system pressure is 800 psia (5.516 x 10^6 N/m^2) (minimum) at launch and blows down to 400 psia (2.758 x 10^6 N/m^2) at the end of all duty cycle requirements.

A single toroidal tank (nominal volume, 702 cu ft) (19.88 m^3), which is shown in Figure 4-22, contains both the GN_2 pressurant and the N_2O_4 injectant fluid. Thiokol Drawing No. TUL-13107 displays additional detail design features of the GN_2-N_2O_4 tank assembly.

A N_2O_4 liquid and nitrogen gas separator is not necessary since g forces will keep the N_2O_4 outlets covered in any anticipated flight attitude. G loading (maximum of 7.2) aids in maintaining the N_2O_4 level perpendicular to the axis of the motor. Anti-vortexing devices were designed and are located within the tank at each of the 16 N_2O_4 outlets.

The GN_2-N_2O_4 tank is supported by a tubular system attached to the internal structural members of the vehicle aft flare. The tank support structure design has features to allow for misalignment, asymmetric loads from various sources and possibilities for future support design structure modification and/or growth. The tank has provisions for loading and unloading the N_2O_4, filling and venting the GN_2, emergency venting of N_2O_4 vapors, nonvortex distribution of the N_2O_4 from the tank to each of 16 injectors, and measurement of the unexpended N_2O_4. A weight breakdown of the tank assembly components is presented in Table 4-15.

The toroidal reservoir will be constructed from four 90° (1.57 RAD) stainless steel 17-4 PH CRES (175,000 psi (1.2066 x 10^9 N/m^2) minimum yield) elbows welded together. Since almost all of the major components of the LITVC system are existing hardware, the only area that structural analysis was conducted on was the toroidal tank and its support structure. This analysis is included in Appendix D.

At launch, the N_2O_4 liquid injectant occupies 473,470 cu in. (7.97 m^3); and the GN_2 pressurant, 739,800 cu in. (12.46 m^3). The total N_2O_4 launch weight is 24,634 lbm (11,174 kg) (including the required duty cycle fluid plus allowances for expulsion efficiency, system errors, motor and LITVC performance tolerances, ullage, manifolds, and injector leakage). The total minimum required GN_2 pressurant by weight is 1,690 lbm (767 kg).

The GN_2 blowdown system pressure is initially 800 psia (5.516 x 10^6 N/m^2) minimum with the vehicle fully loaded and ready for launching. The system blows down to 400 psia (2.758 x 10^6 N/m^2) during the course of the flight; experimental data indicate satisfactory N_2O_4 LITVC system performance at injectant pressures down to 400 psia (2.758 x 10^6 N/m^2) within the thrust vector range and duty cycle requirements specified for this study.

TABLE 4-15

NASA 260 IN. SRM LITVC SYSTEM
INJECTANT-PRESSURANT TANK ASSEMBLY

	Weight (lbm)	Weight (kg)
Torus (less port openings)	8,884.60	4,030
Antivortex device and port (16)	937.60	425
Burst disc holder port		
Solenoid fill and drain valve port		
Solenoid vent valve port		
Relief valve port	14.68	6.7
Pressure transducer port		
Liquid level indicator port		
GN_2 pressure charge valve port		
Tank support mounting brackets (18)	632.88	287
	10,469.76	4,748.7

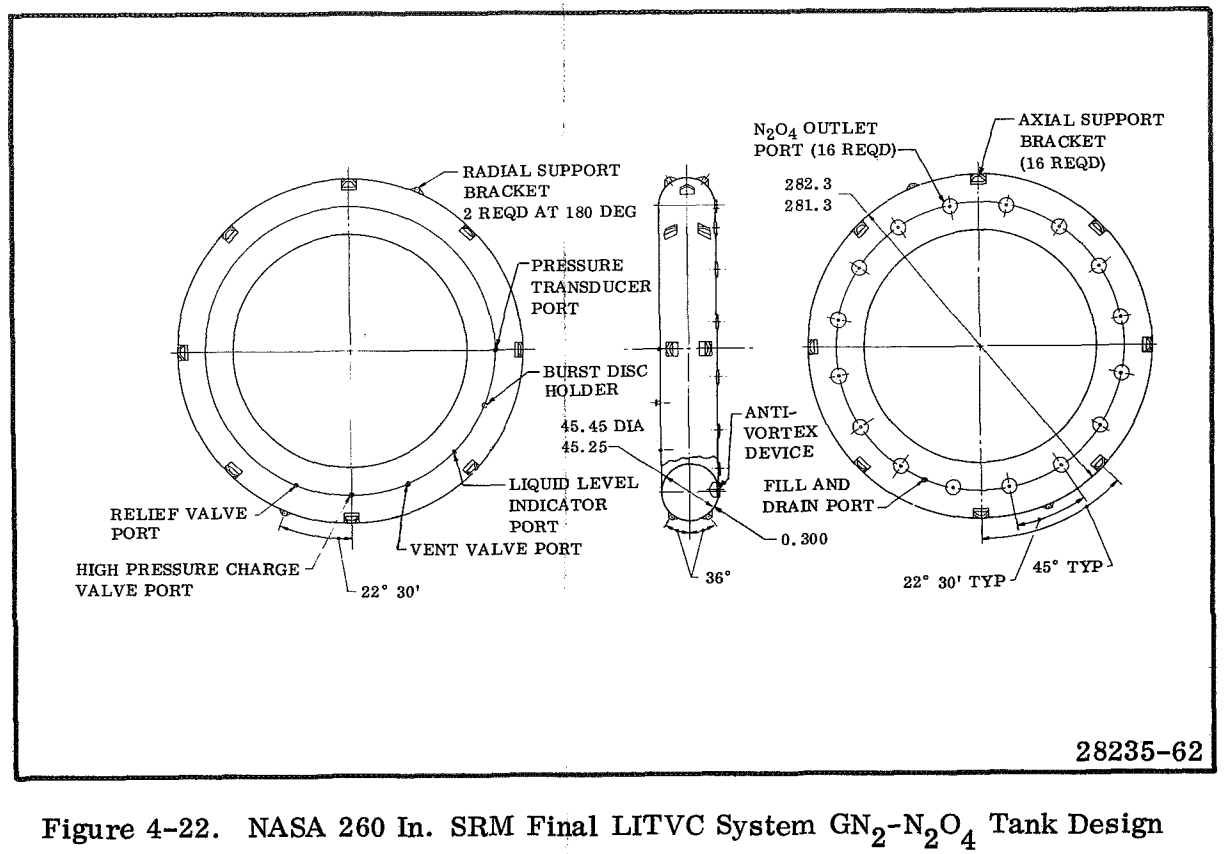

Figure 4-22. NASA 260 In. SRM Final LITVC System GN_2-N_2O_4 Tank Design

4.6 Final LITVC System Studies

4.6.3 N_2O_4 Transfer Ducts

FLEXIBLE TRANSFER DUCTS DISTRIBUTE INJECTANT

Flexible expansion ducts are used to distribute N_2O_4 to each of 16 injectors.

The N_2O_4 injectant is distributed from the toroidal tank to each of the 16 injectors through flexible expansion ducts (Figure 4-23). Details of the transfer duct design are shown in Thiokol Drawing TUL-13115.

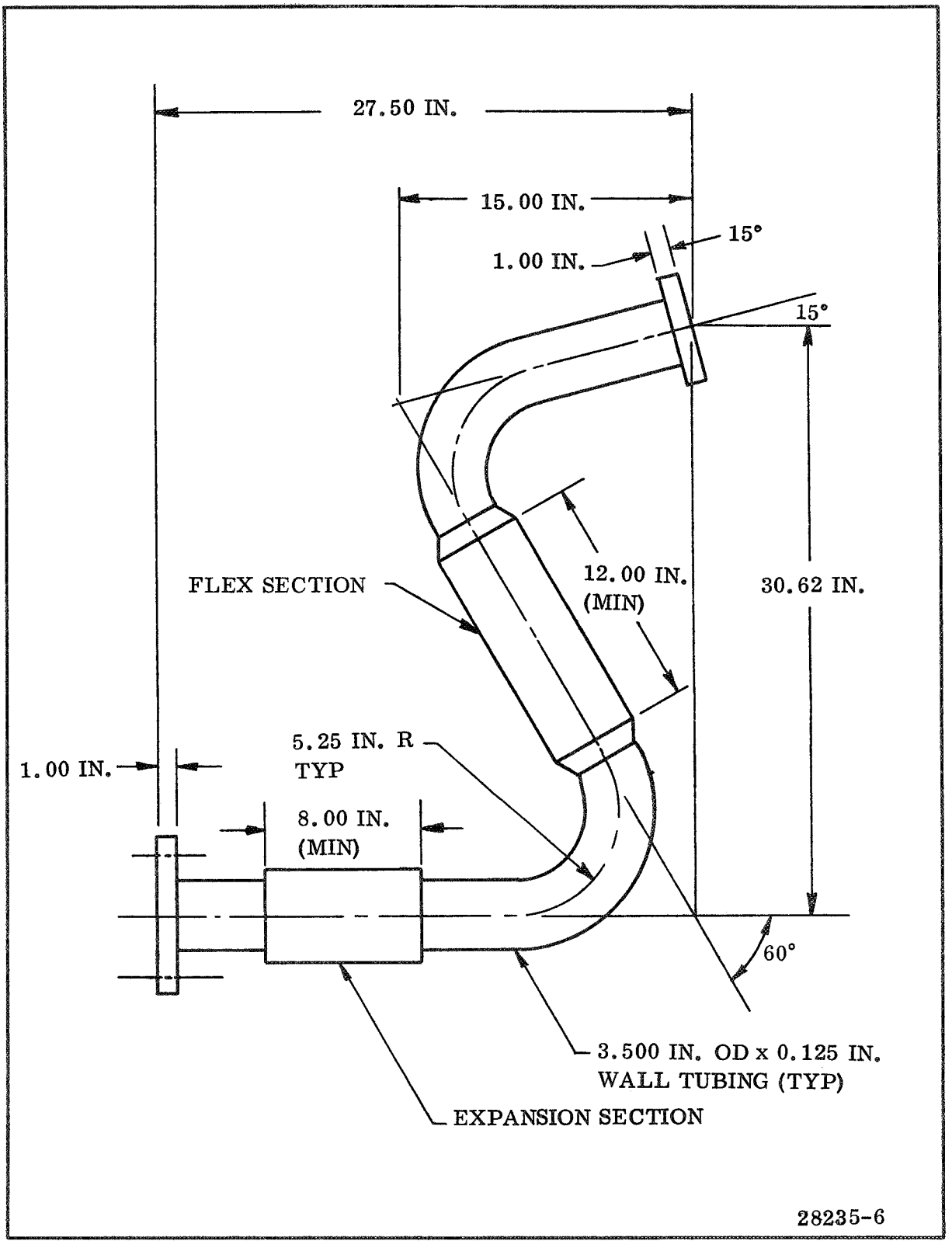

Figure 4-23. N_2O_4 Transfer Duct Design

4.6 Final LITVC System Studies

4.6.4 Electromechanical Injector Valve

ELECTROMECHANICALLY ACTUATED PINTLE VALVE DESCRIBED

The electromechanically actuated pintle-type valves achieve the required slew rates by modulating N_2O_4 flow rates from 0 to 169 lbm/sec (76.7 kg/sec) at 800 psi (5.516×10^6 N/m^2) and 0 to 120 lbm/sec (54.4 kg/sec) at 400 psi (2.758×10^6 N/m^2).

Injection valve housings attached to the nozzle provide support for each of the injector valve assemblies. A full scale cross sectional view of the LTV electromechanical (EM) injector valve and valve housing configuration used for the final LITVC system design is presented in Thiokol Drawing TUL-13085. A side view of the EM valve (housing excluded), that was designed, built, and tested to Titan III C specifications by LTV, is shown in Figure 4-24.

The major components of the EM injector valve are displayed in Figure 4-25. The LTV valve employs a dc "pancake" motor directly driving a ball screw which converts rotary motion into linear motion to actuate the injector pintle. The pancake torque motor and ball screw have the following advantages over other injector systems.

1. Rugged components.
2. Fully reversible for fail-safe closure.
3. Motor specially adapted for quasi-static positioning.
4. Ball screw 90 percent efficient in converting rotary to linear motion.
5. High coupling stiffness and torque-to-inertia ratio.
6. Compact, frameless design.

This electromechanically actuated pintle type valve varies the flow rate by changing the effective flow area. The servocontrolled assemblies are capable of modulating N_2O_4 flow from 0 to 169 lbm/sec (76.7 kg/sec) at 800 psi (5.516×10^6 N/m^2 and from 0 to 120 lbm/sec (54.4 kg/sec) at 400 psi (2.758×10^6 N/m^2). The injector valves use developed servocomponents to provide valve opening and closing time capabilities for achieving the required slew rates.

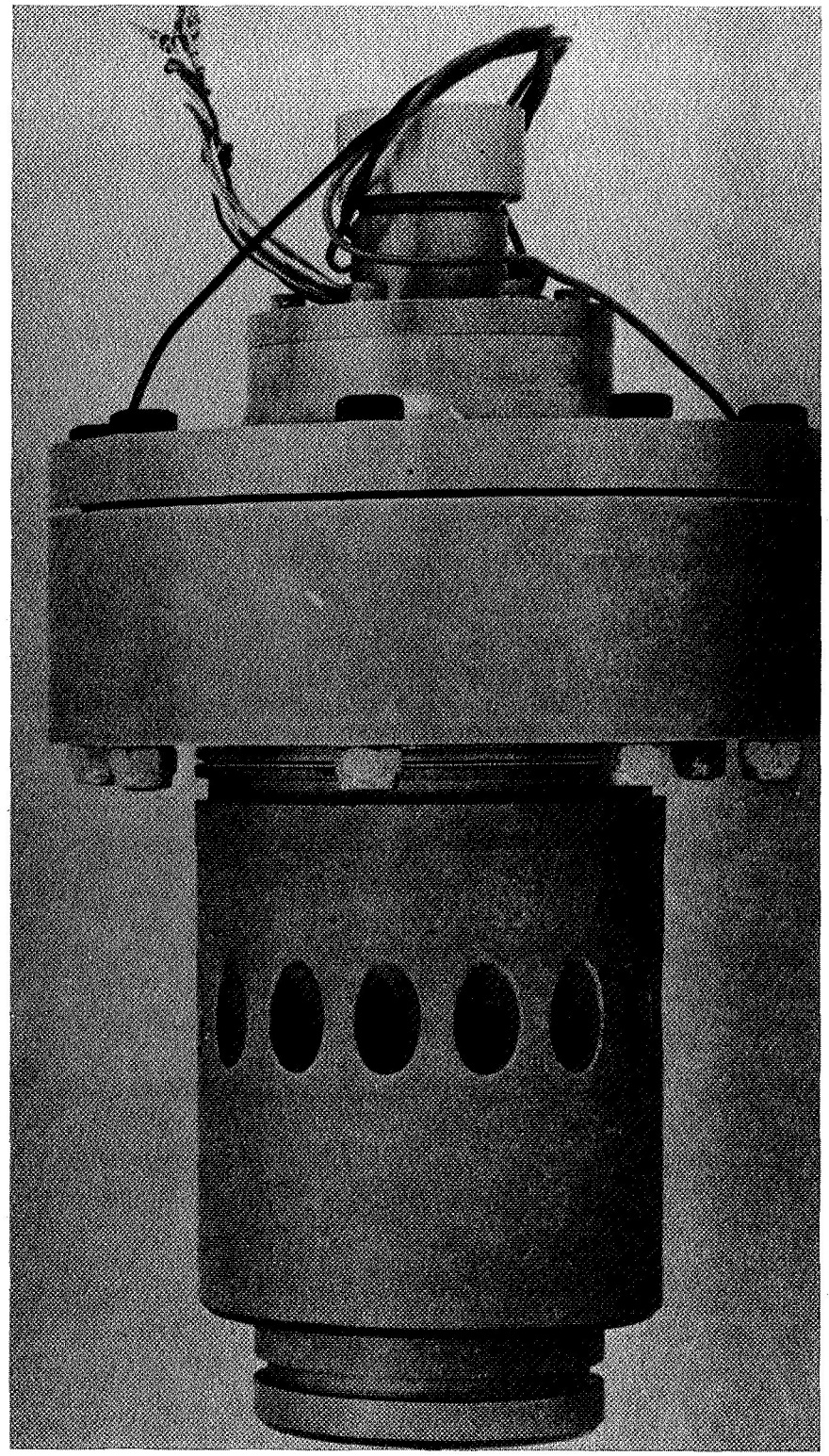

Figure 4-24. Side View of LTV Electromechanical Injector Valve

(Scale Approx 2/3)

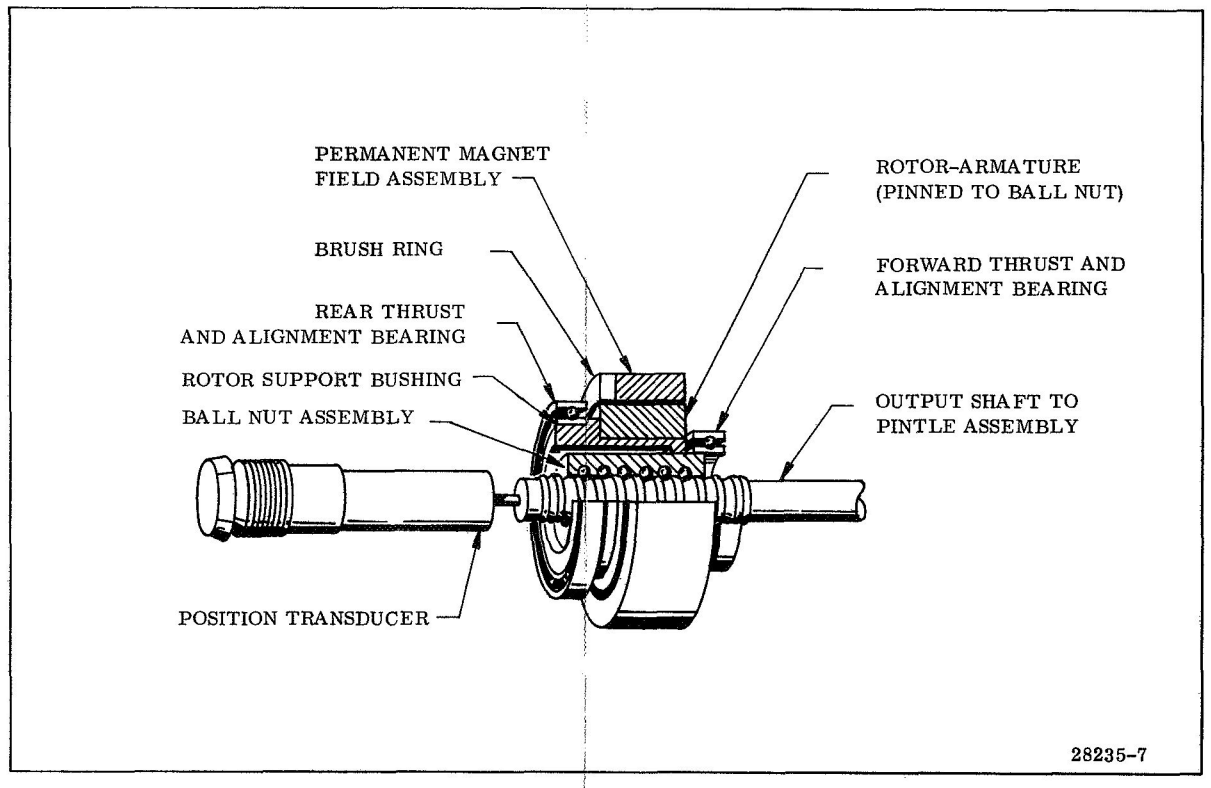

Figure 4-25. Major Component Parts of LTV Electromechanical Injector Valve

4.6 Final LITVC System Design

4.6.5 LITVC Control System

LITVC CONTROL SYSTEM DESCRIBED

The basic LITVC control system has the capability of providing correction for all transient and steady-state perturbations in the pitch and yaw axes. The pitch and yaw controller subsystem provides (1) servodrive amplifiers and coupling between the autopilot command signals and the injection valves, (2) a linearization of the side force voltage relation, (3) compensation for quadrant interaction, and (4) controller integration of the liquid dump commands with the TVC requirements.

Most flights will not require the use of all the N_2O_4 injectant. Therefore, after evaluating several alternate dump schemes, a continuous injectant dump system incorporating a liquid level transducer (Kavlico Electronics, Inc.) was selected to minimize the performance penalty of carrying all N_2O_4 injectant to first stage burnout. The system (Figure 4-26) continuously compares the residual injectant quantity (sensed by the liquid level transducer in the injectant storage tank) with a preprogramed residual quantity which varies as a function of flight time. An error signal, proportional to the excess of injectant over the preprogramed quantity, is added with the guidance commands to each control servo, resulting in superposition of control and symmetrical dump commands. Optimum TVC depletion profile and residual limits should be established in the design phase of the program to take full advantage of actual injectant utilization system accuracy and LITVC performance information.

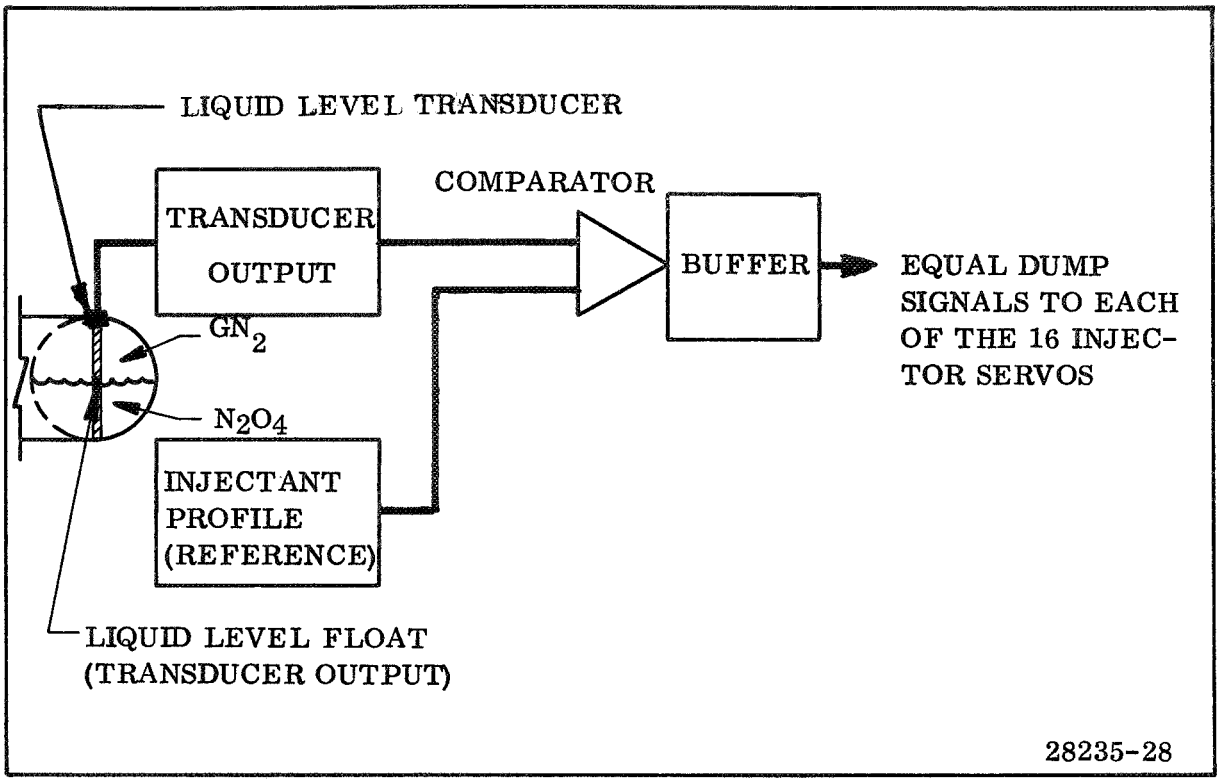

Figure 4-26. LITVC Dump System, Schematic

4.6 Final LITVC System Design

4.6.6 LITVC System Weights

FINAL LITVC SYSTEM WEIGHTS DEFINED

The LITVC system components and fixed nozzle initially weighed 92,748 lbm (42,070 kg); the total burnout weight was calculated at 63,553 lbm (28,828 kg). However, thrust augmentation from the N_2O_4 injection duty cycle will reduce the motor propellant requirements by 7,940 lbm (3,602 kg).

A component weight breakdown (nozzle excluded) of the 260 in. LITVC system is presented in Table 4-16. The initial weight is 38,801 lbm (17,600 kg); the burnout weight is 14,804 lbm (6,715 kg). The total initial, expended, and burnout weights of the nozzle and LITVC system are shown in Table 4-17. The total initial nozzle and LITVC system weight is 92,748 lbm (42,070 kg); the total burnout weight is 63,553 lbm (28,828 kg).

Thrust augmentation during the 260 in. SRM liquid injection duty cycle was investigated. A correlation of Titan III N_2O_4 injection data of axial thrust augmentation as a function of side force generated is shown in Figure 4-27. Using the correlation of Figure 4-27 and the 260 in. SRM side force duty cycle, a thrust augmentation impulse of 2,018,600 lbf-sec (8.98×10^6 N-sec) was calculated (an increase in axial impulse of 0.233%). This reduces motor propellant requirements by 7,940 lbm (3,602 kg) (2,018,600 ÷ 254.34).

TABLE 4-16

LITVC SYSTEM COMPONENT WEIGHTS
(Nozzle Excluded)

Component	Weight (lbm)	Weight (kg)
Injectant-pressurant tank assembly	10,470	4,749
Injectant: nitrogen tetroxide (N_2O_4)	24,634*	11,174
Pressurant: nitrogen gas (GN_2)	1,690	766
Burst disc assembly	3	1.36
Operational pressure transducer	1	0.45
Liquid level indicator	8	3.63
Relief valve	3	1.36
Solenoid vent valve	5	2.27
GN_2 pressure charge valve	2	0.91
Solenoid fill and drain valve	5	2.27
Quick disconnect and dust cap	2	0.91
Injector valves (16 at 20 lbm) (with electronics)	320	145.2
Injector housings (16 at 12 lbm)	192	87.1
Tank to injector N_2O_4 transfer lines (16)	240	108.9
Axial supports (16)	392	177.8
Radial supports (2)	103	46.7
Aft skirt support mounting brackets (18)	455	206.4
Pitch and yaw controller	30	13.6
Control system battery	40	18.1
Power transfer switch	8	3.63
Electrical harness assembly	160	72.6
Injector valve drain manifold assembly	18	8.16
Relief and solenoid vent valve tubing assembly	16	7.26
Burst disc assembly tubing assembly	4	1.81
Total initial weight (lbm)	38,801	17,600
Total burnout weight (lbm)	14,804**	6,920

*Initial N_2O_4 = 24,634 lbm (11,174 kg)
**Expended N_2O_4 = 23,997 lbm (10,885 kg)

TABLE 4-17

NOZZLE AND LITVC SYSTEM WEIGHTS

Total Initial Nozzle and LITVC System Weight
Nozzle = 53,947 lbm (24,470 kg)
LITVC system = 38,801 lbm (17,600 kg)
Total = 92,748 lbm (42,070 kg)

Total Expended Nozzle and LITVC System Weight
Nozzle = 5,198 lbm (2,358 kg)
LITVC system = 23,997 lbm (10,885 kg)
Total = 29,195 lbm (13,243 kg)

Total Burnout Nozzle and LITVC System Weight*
Nozzle = 48,749 lbm (22,113 kg)
LITVC system = 14,804 lbm (6,715 kg)
Total = 63,553*lbm (28,828 kg)

*Thrust augmentation excluded.

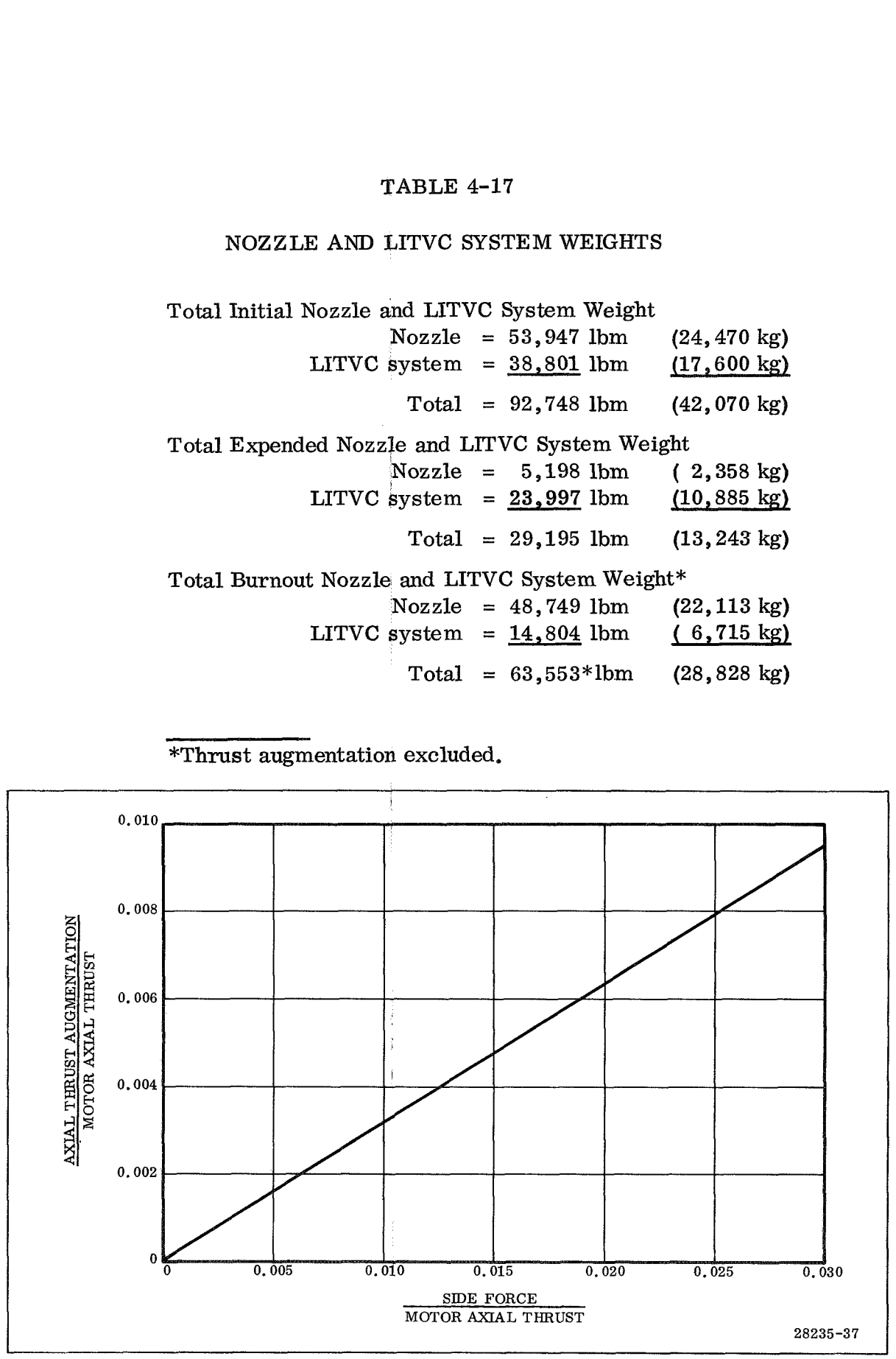

Figure 4-27. Axial Thrust Augmentation Correlation

4.6 FINAL LITVC SYSTEM DESIGN

4.6.7 Major LITVC System Characteristics

MAJOR LITVC SYSTEM CHARACTERISTICS SUMMARIZED

A summary of the NASA 260 in. SRM final LITVC system design characteristics follow.

The major final LITVC system design characteristics (general, N_2O_4-GN_2 reservoir, fixed nozzle, and injection subsystem) are shown in Table 4-18.

TABLE 4-18

MAJOR LITVC SYSTEM CHARACTERISTICS

1. GENERAL	
Injectant fluid	N_2O_4
Pressurant gas	Nitrogen (GN_2)
Nozzle-LITVC system reliability prediction	0.9886
Initial CG to aft equator, Y_{Go} (in.)	661
Aft equator to nozzle throat station (in.)	121
Nozzle throat station to nozzle injection station, x (in.)	98
Equivalent point of side force insertion (in.)	880
L* = 661 + 121 in. (in.)	782
Vacuum specific impulse (lbf-sec/lbm)	254.35
Total vacuum axial impulse (lbf-sec)	864,776,960
Control impulse capabilities (lbf-sec)	6,289,000
Control impulse capabilities (°-sec)	60
Control impulse-to-total vacuum axial impulse (%)	0.727
Axial impulse gained by thrust augmentation (lbf-sec)	2,018,600
Thrust augmentation-to-total vacuum axial impulse (%)	0.233
2. N_2O_4 AND GN_2 RESERVOIR	
Shape	Toroid
Number required	1
Total tank assembly weight (dry) (lbm)	10,470
Total storage volume (cu ft)	702
Initial N_2O_4 volume (cu ft)	274
Initial N_2O_4 weight (lbm)	24,634
Initial GN_2 volume (cu ft)	428
Initial GN_2 weight (lbm)	1,690
Operating pressure of GN_2 blowdown system	
Initial (psi)	800
Burnout (psi)	400
Proof pressure (psi)	1,200
Burst pressure (psi)	2,000
Material	17-4 PH CRES (175,000 psi min yield)
Major diameter of torus (nominal) (in.)	236
Minor ID of torus (nominal) (in.)	45.3
Wall thickness (in.)	0.300
Envelope diameter of toroidal tank assembly (in.)	281.8 ± 0.5
3. LITVC FIXED NOZZLE	
Insulation (initial) (lbm)	38,562
Silica and asbestos filled Buna rubber	
Carbon cloth phenolic	
Silica cloth phenolic	
Canvas	
Structure (initial) (lbm)	15,385
Alloy steel (4130)	
Fiberglass	
Total initial nozzle weight (lbm)	53,947
Total expended nozzle weight (lbm)	5,198
Total burnout nozzle weight (lbm)	48,759
Nozzle axial length from throat to exit, L (in.)	277.86
Nozzle axial length from throat to injection station, x (in.)	98
Injection station, x/L	0.353
Initial nozzle expansion ratio at injection station	2.69:1
4. INJECTION SUBSYSTEM	
Type of injector valve	Single pintle-type injectors (LTV design)
Type of injector actuation system	Electromechanical actuators; battery power source
Number of valves per nozzle quadrant	4
Angle between adjacent injector port centerlines (°)	22.5
Injector location	
x/L	0.353
Area ratio	2.69:1
Injection angle	+15° upstream of a perpendicular to the nozzle centerline
Injection system slew rate capabilities (°/sec)	3
LITVC control system scheme	Pitch-yaw + dump controller
Maximum required equivalent thrust vector angle (each-pitch and yaw) (°)	1.2
Maximum required equivalent side force (lbf)	114,000
Maximum required N_2O_4 flow rate per quadrant (NPV = 4) (lbm/sec)	440
Maximum required N_2O_4 flow rate per injector port for NPV = 4 (lbm/sec)	110
Maximum N_2O_4 flow rate capabilities per injector port	
P_i = 800 psi (lbm/sec)	169
P_i = 400 psi (lbm/sec)	120
Maximum N_2O_4 flow rate capabilities per quadrant (NPV = 4)	
P_i = 800 psi (lbm/sec)	676
P_i = 400 psi (lbm/sec)	480

NPV = No. of Single Pintle Injectors per Quadrant.

4.0 LITVC System Studies

4.7 Detailed Cost Analysis of LITVC System

DETAILED COST ANALYSIS PRESENTED

This subsection presents a detailed cost breakdown of the LITVC system. Tabular matter itemizes costs as follows.

1. Overall cost summary.
2. Unit cost of components.
3. Bench test hardware costs.
4. Fixed nozzle costs.
5. Material costs.
6. Labor costs.
7. Freight, travel, and computer costs.

Prior to developing the detailed cost estimates for the LITVC system, a system development and qualification program plan, which described the recommended individual system and component testing for developing the TVC system was prepared. This development plan is included in this report as Appendix E.

Table 4-19 is an overall summary for the expected costs to be incurred in developing and producing the LITVC system chosen for the detailed design.

A tabulation of the individual TVC system components on a unit cost basis is indicated in Table 4-20.

The bench test hardware costs to support the system and component testing described in Appendix E is shown in Table 4-21.

The basic fixed nozzle, after allowing for structural modifications, was priced as indicated in Table 4-22. It can be seen here as well as in movable nozzle pricing that the importance of low cost ablative materials cannot be overemphasized.

All material costs for the development and production phases are shown in Table 4-23.

Labor in terms of hours and dollars are spread in Tables 4-24 and 4-25.

Table 4-26 shows the other direct costs, which could be expected during the actual program.

TABLE 4-19

LITVC SYSTEM DEVELOPMENT AND PRODUCTION SUMMARY

	1971		1972		1973		1974		1975		1976		1977		
	First	Second	First	Second	First	Second	First	Second	First	Second	First	Second	First	Second	Total
1. Design															
Labor	140,800	146,960	27,120	14,140	--	--	--	--	--	--	--	--	--	--	329,020
2. Component development and system testing															
Labor	12,219	69,312	--	--	--	--	--	--	--	--	--	--	--	--	81,531
Material	340,667	583,859	--	--	--	--	--	--	--	--	--	--	--	--	924,526
3. Qualification (3 R & D systems)															
Labor	--	2,542	925,146	--	--	--	--	--	--	--	--	--	--	--	927,688
Material	--	265,000	2,583,861	--	--	--	--	--	--	--	--	--	--	--	2,848,861
4. PFRT (7 PFRT systems)															
Labor	--	--	301,516	1,833,888	--	--	--	--	--	--	--	--	--	--	2,135,404
Material	--	--	1,622,574	4,056,435	--	--	--	--	--	--	--	--	--	--	5,679,009
5. Production (20 systems)															
Labor	--	--	--	--	538,737	561,304	569,607	593,003	601,306	626,421	635,552	662,235	671,473	699,688	6,159,326
Material	--	--	--	--	1,622,574	1,622,574	1,622,574	1,622,574	1,622,574	1,622,574	1,622,574	1,622,574	1,622,574	1,622,574	16,225,740
6. Administration and support															
Labor	84,261	87,823	89,110	92,927	94,266	98,327	99,777	104,018	105,525	110,038	111,633	116,409	118,078	123,149	1,435,341
Other direct	12,969	15,860	58,082	81,970	26,373	27,438	27,828	28,933	29,326	30,511	30,940	32,198	32,635	33,966	469,029
Total direct cost	590,916	1,171,356	5,607,409	6,079,360	2,281,950	2,309,643	2,319,786	2,348,528	2,358,731	2,389,544	2,400,699	2,433,416	2,444,760	2,479,377	37,215,475
Estimated overhead	421,530	648,052	2,974,601	3,848,479	2,281,950	1,355,878	1,370,522	1,411,973	1,426,682	1,471,135	1,487,222	1,534,360	1,550,739	1,600,594	22,417,689
Total cost	1,012,446	1,819,408	8,582,010	9,927,839	3,597,872	3,665,521	3,690,308	3,760,501	3,785,413	3,860,679	3,887,921	3,967,776	3,995,499	4,079,971	59,633,164

TABLE 4-20

260 IN. LITVC SYSTEM COMPONENTS
(ROM Cost Summary)

Item No.	Component	Vendor Tooling and Devel Costs	Per Unit Costs
1	Injectant - pressurant tank assembly	$150,000	$ 75,000
2	Injectant - nitrogen tetroxide (N_2O_4)	--	1,600
3	Pressurant - nitrogen gas (GN_2)	--	280
4	Burst disc assembly	--	20
5	Operational pressure transducer	--	1,250
6	Liquid level sensor	--	1,800
7	Relief valve	--	350
8	Solenoid vent valve	--	385
9	GN_2 pressure charge valve	--	75
10	Solenoid fill and drain valve	--	385
11	Quick disconnect and dust cap	--	80
12	Injector valves (with electronics) - (16 at $3,800 each)	--	60,800
13	Injector housings - (16 at $200 each)	--	3,200
14	N_2O_4 - transfer lines (16 at $755 each)	2,600	12,080
15	Supports and brackets		
	Axial supports (16)	--	--
	Radial supports (2)	--	--
	Aft skirt support mounting brackets - (18)	--	--
	36 units = 950 lb at $.47/lb	--	447
16	Pitch and yaw controller	--	16,000
17	Control system battery	--	4,200
18	Power transfer switch	--	1,700
19	Electrical harness assembly	--	8,000
20	Injector valve drain manifold assembly	--	270
21	Relief and solenoid vent valve tubing assembly	--	100
22	Burst disc assembly, tubing assembly	--	45
		$152,600	$188,067

NOTES:

Unit cost based on 30 system buy.

All prices are based on inhouse engineering estimates or catalog prices, except: items (1) injectant - pressurant tank assembly, (6) liquid level sensor, (8) solenoid vent valve, (10) solenoid fill and drain valve, and (14) tank to injector transfer line, which are vendor quotes.

TABLE 4-21

260 IN. LITVC BENCH TEST HARDWARE
(ROM Cost Summary)

Description	Total Cost
LITVC flow stand (fixture)	$ 35,000
Dummy nozzle	15,000
Receiver tank (stainless)	5,000
Injectant - freon II (25,000 lb at $.10/lb)	2,500
Gaseous nitrogen (4 fills) - (200,000 SCF at $.01)	2,000
S/steel tubing - 1-1/2 x 0.058 in. (500 ft at $2.00/ft)	1,000
S/steel tubing - 1/4 x 0.028 in. (500 ft at $1.25/ft)	625
Connector - fittings (200 each at $5.00 each)	1,000
Harness (2 sets at $2,000 each)	4,000
Bread board controller	15,000
Instrumentation (lab test)	5,000
Vibration fixture	100,000
Hydroburst fixture	20,000
Injectant nitrogen tetrox (25,000 lb at $.065/lb)	1,600
Total	$207,725

All estimates are Thiokol Chemical Corporation engineering estimates based on historical data or catalog prices.

TABLE 4-22

260 IN. FIXED EXTERNAL NOZZLE (LITVC SYSTEM)
(ROM Cost Summary)

A preliminary survey revealed that all facilities required, such as autoclave, hydroclave and presses, are available in the industry on a rental basis. With the exception of an exit cone mandrel, all tooling also appears to be available. Slight modifications will be required.

				Per Unit Cost
Tooling: Exit Cone Mandrel				$180,000
Facilities: Rental				85,000
Materials:				
897.5 lb V-44	at	$ 4.30	$ 3,859	
11,156.1 lb carbon wrap tape	at	$18.50	206,388	
3,977.2 lb carbon bias tape	at	$19.50	77,555	
5,764.1 lb silica wrap tape	at	$ 5.10	29,397	
2,453.8 lb glass wrap tape	at	$ 2.80	6,871	
13,201.6 lb canvas wrap tape	at	$ 1.50	19,802	
13,967.4 lb machined steel	at	$20.00	279,348	623,220
Total materials and tooling				$888,220
Total labor hours				35,200

All estimates are Thiokol Chemical Corporation engineering estimates based on historical data gained through various other nozzle programs.

TABLE 4-23

LITVC SYSTEM DEVELOPMENT MATERIAL

	1971		1972		1973		1974		1975		1976		1977		Total	Remarks
	First	Second	First	Second	First	Second	First	Second	First	Second	First	Second	First	Second		
1. Design	--	--	--	--	--	--	--	--	--	--	--	--	--	--	--	
2. Component development and system testing (3 systems)																
System components	188,067	376,134	--	--	--	--	--	--	--	--	--	--	--	--	564,201	3 system components at $188,067 each
Bench test hardware	--	207,725	--	--	--	--	--	--	--	--	--	--	--	--	207,725	Engineering pricing sheet
Vendor tooling	152,600	--	--	--	--	--	--	--	--	--	--	--	--	--	152,600	
3. Qualification (3 R & D units)																
System components	--	--	564,201	--	--	--	--	--	--	--	--	--	--	--	564,201	3 system components at $188,067 each
Nozzles	--	--	1,869,660	--	--	--	--	--	--	--	--	--	--	--	1,869,660	3 nozzles at $623,220 each
Operations assembly tooling	--	--	150,000	--	--	--	--	--	--	--	--	--	--	--	150,000	Engineering estimate
Nozzle fabrication tooling	--	180,000	--	--	--	--	--	--	--	--	--	--	--	--	180,000	Engineering estimate
Nozzle fabrication facilities	--	85,000	--	--	--	--	--	--	--	--	--	--	--	--	85,000	Engineering estimate
4. PFRT (7 PFRT units)																
System components	--	--	376,134	940,335	--	--	--	--	--	--	--	--	--	--	1,316,469	7 system components at $188,067 each
Nozzles	--	--	1,246,440	3,116,100	--	--	--	--	--	--	--	--	--	--	4,362,540	7 nozzles at $623,220 each
5. Production (20 units)																
System components	--	--	--	--	376,134	376,134	376,134	376,134	376,134	376,134	376,134	376,134	376,134	376,134	3,761,340	20 system components at $188,067 each
Nozzles	--	--	--	--	1,246,440	1,246,440	1,246,440	1,246,440	1,246,440	1,246,440	1,246,440	1,246,440	1,246,440	1,246,440	12,464,400	20 nozzles at $623,220 each
Total	340,667	848,859	4,206,435	4,056,435	1,622,574	1,622,574	1,622,574	1,622,574	1,622,574	1,622,574	1,622,574	1,622,574	1,622,574	1,622,574	25,678,136	

TABLE 4-24

LITVC SYSTEM DEVELOPMENT AND PRODUCTION
(Labor Hours)

	1971		1972		1973		1974		1975		1976		1977		Total	Remarks
	First	Second	First	Second	First	Second	First	Second	First	Second	First	Second	First	Second		
1. Design																
Engineering	22,000	22,000	4,000	2,000	--	--	--	--	--	--	--	--	--	--	50,000	Engineering estimate
2. Component development and system testing																
Engineering component development	1,020	--	--	--	--	--	--	--	--	--	--	--	--	--	1,020	Engineering estimate
System testing	--	7,650	--	--	--	--	--	--	--	--	--	--	--	--	7,650	Engineering estimate
Quality control	233	816	--	--	--	--	--	--	--	--	--	--	--	--	1,049	Statistical hours to matl cost (rec insp)
Manufacturing	1,000	3,000	--	--	--	--	--	--	--	--	--	--	--	--	4,000	Independent engineering estimate bracket fabrication
3. Qualification (3 R & D systems)																
Engineering	--	--	36,000	--	--	--	--	--	--	--	--	--	--	--	36,000	Engineering estimate
Manufacturing - brackets	--	--	3,000	--	--	--	--	--	--	--	--	--	--	--	3,000	Independent engineering estimate
Assembly	--	--	2,880	--	--	--	--	--	--	--	--	--	--	--	2,880	Independent engineering estimate
Technician	--	--	105,600	--	--	--	--	--	--	--	--	--	--	--	105,600	Engineering estimate - nozzle fabrication
Quality control	--	487	4,364	--	--	--	--	--	--	--	--	--	--	--	4,851	Statistical hours to matl cost (rec insp)
4. PFRT (7 PFRT systems)																
Engineering	--	--	10,000	60,000	--	--	--	--	--	--	--	--	--	--	70,000	Engineering estimate
Manufacturing - brackets	--	--	1,000	6,000	--	--	--	--	--	--	--	--	--	--	7,000	Independent engineering estimate
Assembly	--	--	960	5,760	--	--	--	--	--	--	--	--	--	--	6,720	Independent engineering estimate
Technician	--	--	35,200	211,200	--	--	--	--	--	--	--	--	--	--	246,400	Engineering estimate
Quality control	--	--	2,725	6,813	--	--	--	--	--	--	--	--	--	--	9,538	Statistical estimate hours to matl cost (rec insp)
5. Production (20 systems)																
Engineering	--	--	--	--	8,000	8,000	8,000	8,000	8,000	8,000	8,000	8,000	8,000	8,000	80,000	Engineering estimate
Manufacturing - brackets	--	--	--	--	2,000	2,000	2,000	2,000	2,000	2,000	2,000	2,000	2,000	2,000	20,000	Independent engineering estimate
Assembly	--	--	--	--	2,400	2,400	2,400	2,400	2,400	2,400	2,400	2,400	2,400	2,400	24,000	Independent engineering estimate
Technician	--	--	--	--	70,400	70,400	70,400	70,400	70,400	70,400	70,400	70,400	70,400	70,400	704,000	Engineering estimate
Quality control	--	--	--	--	2,725	2,725	2,725	2,725	2,725	2,725	2,725	2,725	2,725	2,725	27,250	Statistical hours to matl cost (rec insp)
6. Administration and support																
Prog Mgmt	3,510	3,510	3,510	3,510	3,510	3,510	3,510	3,510	3,510	3,510	3,510	3,510	3,510	3,510	49,140	
Fin & Admin	1,776	1,776	1,776	1,776	1,776	1,776	1,776	1,776	1,776	1,776	1,776	1,776	1,776	1,776	24,864	
Requirements	3,432	3,432	3,432	3,432	3,432	3,432	3,432	3,432	3,432	3,432	3,432	3,432	3,432	3,432	48,048	
Project Engrg	4,038	4,038	4,038	4,038	4,038	4,038	4,038	4,038	4,038	4,038	4,038	4,038	4,038	4,038	56,532	

TABLE 4-25

LITVC SYSTEM DEVELOPMENT
(Labor Dollars)

	1971		1972		1973		1974		1975		1976		1977		
	First	Second	First	Second	First	Second	First	Second	First	Second	First	Second	First	Second	Total
1. Design															
Engineering	140,800	146,960	27,120	14,140	--	--	--	--	--	--	--	--	--	--	329,020
2. Component development and system testings															
Engineering	6,528	51,102	--	--	--	--	--	--	--	--	--	--	--	--	57,630
Quality control	1,181	4,260	--	--	--	--	--	--	--	--	--	--	--	--	5,441
Manufacturing	4,510	13,950	--	--	--	--	--	--	--	--	--	--	--	--	18,460
3. Qualification (3 R & D systems)															
Engineering	--	--	244,080	--	--	--	--	--	--	--	--	--	--	--	244,080
Technician	--	--	630,432	--	--	--	--	--	--	--	--	--	--	--	630,432
Quality control	--	2,542	22,998	--	--	--	--	--	--	--	--	--	--	--	25,540
Manufacturing	--	--	27,636	--	--	--	--	--	--	--	--	--	--	--	27,636
4. PFRT (7 PFRT units)															
Engineering	--	--	67,800	424,200	--	--	--	--	--	--	--	--	--	--	492,000
Technician	--	--	210,144	1,315,776	--	--	--	--	--	--	--	--	--	--	1,525,920
Quality control	--	--	14,360	36,994	--	--	--	--	--	--	--	--	--	--	51,354
Manufacturing	--	--	9,212	56,918	--	--	--	--	--	--	--	--	--	--	66,130
5. Production (20 systems)															
Engineering	--	--	--	--	57,360	59,840	60,720	63,280	64,160	66,960	67,920	70,880	71,920	74,960	658,000
Technician	--	--	--	--	444,928	463,936	470,976	390,688	497,728	518,848	526,592	549,120	556,864	580,800	5,100,480
Quality control	--	--	--	--	14,933	15,396	15,559	16,023	16,186	16,677	16,840	17,331	17,521	18,012	164,478
Manufacturing	--	--	--	--	21,516	22,132	22,352	23,012	23,232	23,936	24,200	24,904	25,168	25,916	236,368
6. Administration and support															
Program management	26,009	27,097	27,483	28,676	29,097	30,326	30,782	32,081	32,537	33,941	34,433	35,907	36,433	37,978	442,780
Finance and admin	9,998	10,425	10,567	11,028	11,188	11,668	11,828	12,343	12,520	13,053	13,248	13,817	14,012	14,616	170,311
Requirements	17,606	18,361	18,635	19,425	19,699	20,557	20,866	21,758	22,067	23,028	23,371	24,367	24,710	25,774	300,224
Project engineering	30,648	31,940	32,425	33,798	34,282	35,776	36,301	37,836	38,401	40,016	40,581	42,318	42,923	44,781	522,026
Total	237,280	306,637	1,342,892	1,940,955	633,003	659,631	669,384	697,021	706,831	736,459	747,185	778,644	789,551	822,837	11,068,310

TABLE 4-26

LITVC SYSTEM DEVELOPMENT
(Other Direct)

	1971		1972		1973		1974		1975		1976		1977			
	First	Second	First	Second	First	Second	First	Second	First	Second	First	Second	First	Second	Total	Remarks
1. Freight	78	195	967	932	373	373	373	373	373	373	373	373	373	373	5,902	0.023% of material costs
2. Travel	9,491	12,265	53,715	77,638	25,320	26,385	26,775	27,880	28,273	29,458	29,887	31,145	31,582	32,913	442,727	4% of direct labor dollars
3. Computer	3,400	3,400	3,400	3,400	680	680	680	680	680	680	680	680	680	680	20,400	50 hr per year thru PFRT - 10 hr per year production
Total	12,969	15,860	58,082	81,970	26,373	27,438	27,828	28,933	29,326	30,511	30,940	32,198	32,635	33,966	469,029	

CONTENTS
SECTION 5.0

5.0 Movable Nozzle - Flexible Seal

5.1 Literature Search

LITERATURE SEARCH REVEALS COMMON DESIGN FEATURES; THIOKOL'S TVC APPROACH UNIQUE FOR LARGE SOLID ROCKET MOTORS

The literature search was conducted by making a survey of TVC systems designed for large 156 (3.96m) to 260 in. (6.6m) solid propellant missile systems that used movable nozzles. It was concluded that hydraulic power with linear servoactuators will be required for the 260 in. (6.6m) solid rocket motor.

The systems studied all had one common design feature; they all used hydraulics as the means of transmitting power to the load and used linear servo-actuators. A solid propellant gas generator was consistently used as the primary power source except for the Sundstrand design and Stage II design of the Douglas study. Sundstrand proposed a hydrazine gas generator to drive a turbine-pump system while the Stage II 260 in. vehicle used by Douglas in the comparative study of TVC systems used two electric motors to drive the hydraulic pumps. In the latter case, a large accumulator was used to supplement pump flow during peak periods.

BIBLIOGRAPHY

Final Report for the 260-Inch Diameter Solid Rocket Motor Gimbal Nozzle Thrust Vector Control Study (U), TWR-1447. Contract NAS7-542. Thiokol Chemical Corporation, Brigham City, Utah, August 1967.

Auxiliary Power Unit for Movable Nozzle TVC Systems to Aerojet - General Corporation. Sundstrand Engineering Proposal No. 2304A-P1. Sundstrand Aviation, Rockford, Illinois, February 1967.

Comparative Study of Thrust Vector Control Systems for Large, Solid Fueled Launch Vehicles. Volumes I & II. Contract NAS1-7109. Douglas Aircraft Co., Huntington Beach, California, November 1967.

Design Study and Cost Estimate for Application of Lockseal to 260-Inch Solid Motor. Contract NAS7-477. LPC Report No. 759-F. Lockheed Propulsion Company, Redlands, California, December 1966.

Hydraulic Power Unit for Thiokol Chemical Corporation Rocket Motor Nozzle Actuation. Technical Proposal by AiResearch Manufacturing Division, Los Angeles, California, May 1964.

5.0 Movable Nozzle - Flexible Seal

5.2 Design Requirements

TVC DESIGN REQUIREMENTS ESTABLISHED

The design requirements for the movable nozzle TVC system was originally defined as 1.5° (0.026 RAD) maximum vector angle, 3°/sec (0.052 RAD/sec) maximum slew rate and 8°/sec^2 (0.139 RAD/sec^2) maximum slew acceleration. These requirements were later modified during the preliminary design phase.

The vector angle of $\pm$1.5° (0.026 RAD) in any plane was changed to $\pm$1.61° (0.028 RAD) due to the change in pivot point location in the Aerojet bearing design. The design slew rate was 3.0°/sec (0.052 RAD/sec) and 8°/sec^2 (0.139 RAD/sec^2) maximum slew acceleration. The duty cycle in the RFP was modified by NASA and is shown in Figure 5-1. The duty cycle is identical for both planes except for the pitchover event at 10 sec. At this point the yaw actuator maintains its steady state position. All components used in the actuation system were to be flight-type and flightweight. Development of components was to be kept to a minimum and use of existing items and techniques were to be employed wherever possible to minimize cost and increase reliability.

5.3 Nozzle Torque

5.3.1 Seal Spring Torque

SEAL SPRING TORQUE CALCULATED

Seal spring torque results from the shear stress produced by the seal's elastomer layers upon nozzle vectoring.

An actuation system for a movable nozzle assembly cannot be designed efficiently or effectively unless the total forces on the nozzle's movable section are defined accurately. This total is made up of components such as friction, inertial, dynamic spring, offset and aerodynamic. Maximum torque for the nozzle and seal system was computed to be 8.60 million in.-lb (0.972×10^6 N-m) and occurred at ignition. The following data applies only to the AGC design as it was decided to eliminate the Thiokol concept in favor of the AGC nozzle.

The seal spring torque component was calculated by Thiokol's Advanced TVC Computer Program for the Thiokol movable nozzle; this component was supplied by NASA for the AGC design. The equation used by the Advanced TVC Computer Program is:

$$T_{seal} = \delta\,(9.57 \times 10^{-4})\,(G)\,(ASEAL)^4\,(\sin\beta m)\,(1 + \cos^2\beta m)\,(\beta 2 - \beta 1)/(TR)\,(TRNO) \quad (1)$$

where:

δ = vector angle
G = elastomer's shear modulus
ASEAL = spherical radius of the mean shim
βm = angle between nozzle centerline and line joining pivot point to the center of the mean shim
$\beta 2$ and $\beta 1$ = angles between nozzle centerline and line from pivot point to outer and inner edge, respectively, of the mean shim
TR = elastomer thickness
TRNO = number of elastomer layers

For $0 < t \leq 60$ sec, the torque component was 4.063 million in.-lb (0.46×10^6 N-m) for the Thiokol nozzle, and 4.05 million in.-lb (0.457×10^6 N-m) for the AGC nozzle. After 60 sec into the firing, the vector angle requirement drops from 1.61° (0.028 RAD) to 1.18° (0.0206 RAD) and the seal torque drops to 2.97 million in.-lb (0.336×10^6 N-m) for the AGC nozzle, as illustrated in Figure 5-2.

No attempt was made to calculate any torque component as a function of time for the Thiokol design due to the decision to eliminate it from further consideration. The torque vs time curves appearing in this subsection, as well as the following subsections, apply to the AGC nozzle only.

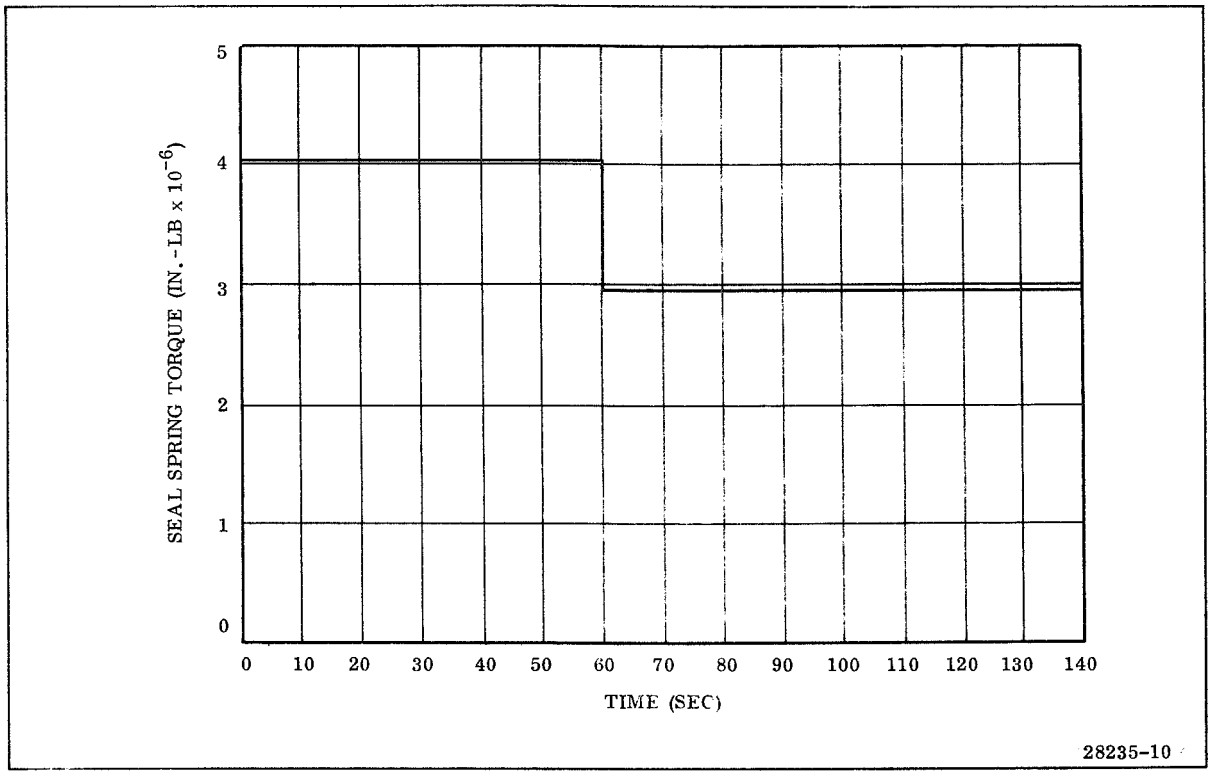

Figure 5-2. Aerojet Seal Spring Torque as a Function of Time

5.3 Nozzle Torque

5.3.2 Internal Aerodynamic Torque

INTERNAL AERODYNAMIC TORQUE CALCULATED

Internal aerodynamic torque is the result of flow asymmetry in the deflected nozzle, producing a pressure differential in the plane of actuation. This torque has been observed to vary linearly with deflection angle and, for this reason, is a spring torque (force proportional to angular displacement).

The internal aerodynamic torque can be calculated by summing the force components produced by pressure differential acting on the nozzle wall multiplied by the perpendicular distance from each force vector to the nozzle pivot. The general equation describing the internal aerodynamic torque may be written:

$$T_{\text{int. aero}} = \int_{X_1}^{X_2} \int_{o}^{2} P \sin \Theta \, (R\,X + R^2 \tan\alpha) \, d\Theta \, dX \qquad (2)$$

where:

Θ = nozzle vector angle (radians)
R = nozzle radius at point of force application
X = axial distance from pivot to point of calculation in the nozzle
P = static pressure
α = nozzle wall slope

This equation requires knowledge of the wall static pressure and pressure differentials which exist in the nozzle. Two procedures are available for calculating the internal wall pressure distribution in the vectored nozzle. They are air flow simulation tests (cold flow) and a two dimensional method of characteristics solution.

The axial location (x) may be expressed as a function of the throat diameter and the internal aerodynamic torque may then be expressed as a function of chamber pressure and the cube of the throat diameter for geometrically similar designs.

The effect of varying the axial location of the pivot point has been considered analytically, by assuming that the pressure distribution is not affected by the pivot point location. Error in this assumption is magnified as the distance from the pivot point to the nozzle throat is increased. However, hot firing data have verified the validity of this technique for pivot points located within one throat diameter of the nozzle throat. For the 260 in. movable nozzle, the pivot point location is 0.68 throat diameters.

By expressing the axial location to the pivot point as a function of throat diameter, aerodynamic torque, as a function of chamber pressure and throat diameter, is as follows:

$$T_{int.\ aero} = \Theta \left[-0.0007 - 0.00555 \left(\frac{XPIV}{DTINT} \right) \right] \left[(PMAX)\ (DTINT)^3 \right] \qquad (3)$$

where:

Θ = vector angle
XPIV = distance from nozzle throat to pivot point
DTINT = initial throat diameter
PMAX = instantaneous upper 3 sigma value of pressure

Propellant grain configuration has a major influence on internal aerodynamic torque. In the 0 sec web time configuration, the gas has a relatively high velocity at the aft end of the grain and the turning of the gas within the nozzle during vector results in a nozzle wall pressure differential in the plane of actuation. However, as the propellant burns out, a plenum of low velocity gas is created in the aft end near the nozzle and subsequent nozzle vectoring has a rapidly decreasing influence on the nozzle pressure distribution. For this reason, internal aerodynamic torque for submerged movable nozzles decreases greatly with burning time.

Equation (3) does not take the above grain burnout into consideration. Instead, it is used to calculate maximum aerodynamic torque. It was therefore necessary to apply a propellant burn factor to Equation (3) when establishing the aerodynamic torque vs time trace in Figure 5-3 . Cold flow testing and hot firing data have yielded burn factors at two points: 0 sec web time; and motor burnout. The intermediate points establishing propellant burn factor vs time trace were estimated. The curve chosen showed the burn factor decreased exponentially with time. This selection was based on the assumption of linear increase in plenum radius with time which, in turn, increases plenum area and reduces flow velocity exponentially.

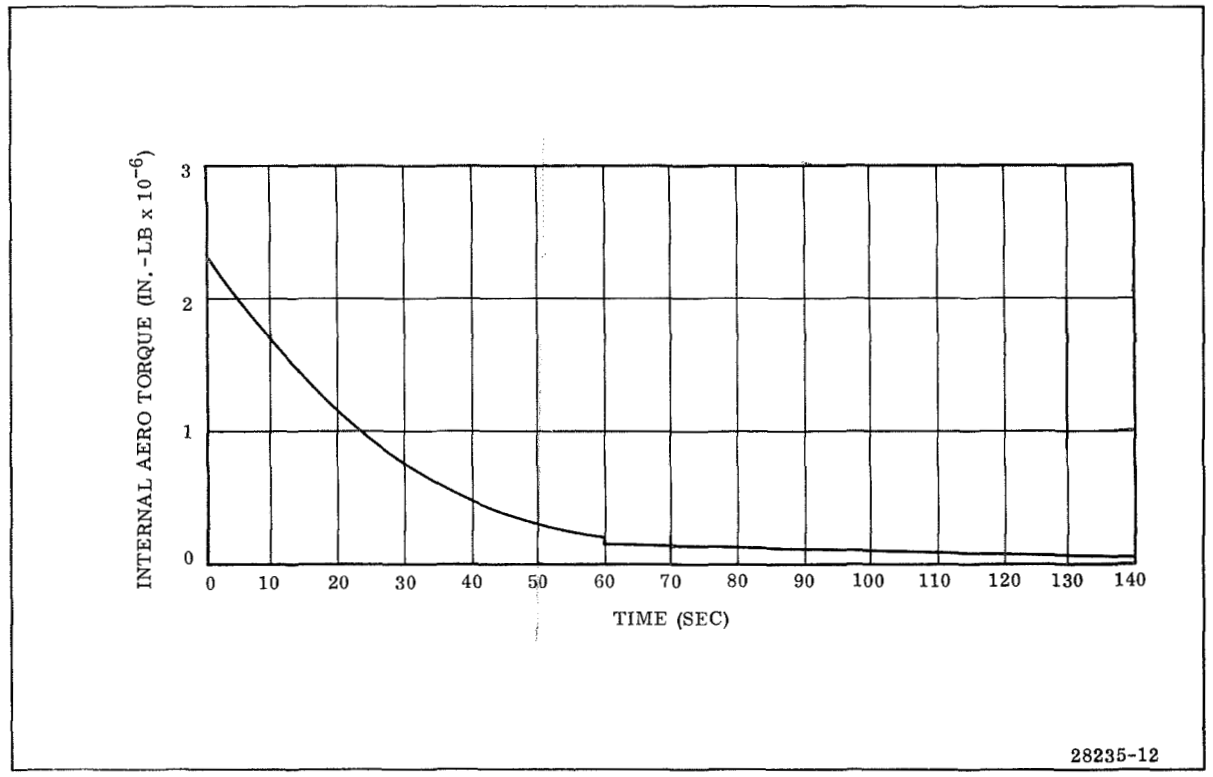

Figure 5-3. Aerojet Internal Aerodynamic Torque as a Function of Time

5.3 Nozzle Torque

5.3.3 Offset Torque

NOZZLE OFFSET TORQUE CALCULATED

This torque component is defined as the null position internal aerodynamic torque resulting from asymmetrical gas flow in the unvectored nozzle. Factors contributing to asymmetrical flow are the fabrication tolerance buildup, uneven ablative erosion, and uneven propellant burn.

Empirical cold flow and hot firing data from past programs have been used to estimate the effect of offset torque as a function of pivot point distance from the throat (XPIV), chamber pressure (Pc), and throat diameter (DTINT). The equation used is:

$$T_{offset} = (0.0067)\ (XPIV)\ (Pc)\ (DTINT^3) \qquad (4)$$

Figure 5-4 shows offset torque vs time for the AGC nozzle. The maximum value for this component was 2.523 million in.-lb (0.286×10^6 N-m) and it occurred at 108 sec into the motor firing.

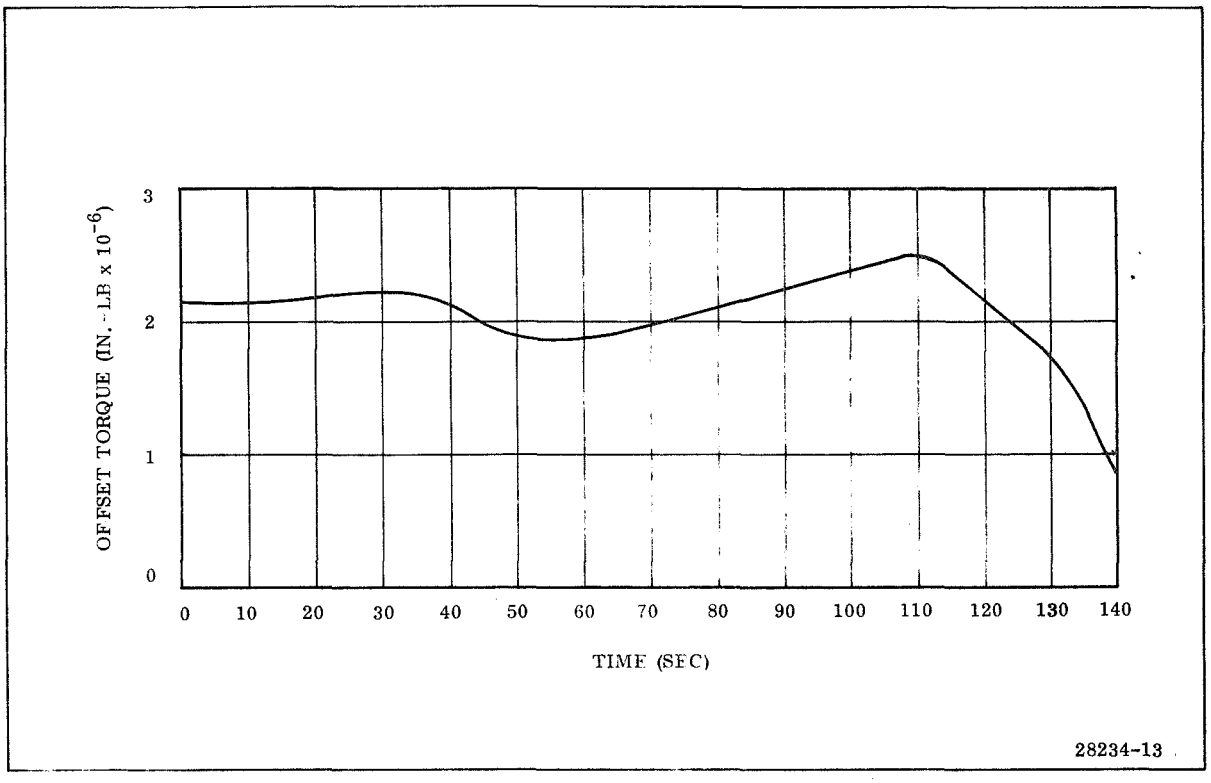

Figure 5-4. Aerojet Offset Torque as a Function of Time

5.3 Nozzle Torque

5.3.4 Boot Spring Torque

NOZZLE BOOT TORQUE CALCULATED

Boot spring torque is the result of stress in the boot when the nozzle is vectored.

Boot spring torque was calculated from a previous bench test on a similar boot. The decrease in elastomer thickness of the AGC was compensated for in the calculation. The AGC 260 in. boot is approximately the same thickness and same cross sectional area as was the 156 in. (3.96 m) motor boot. In the 156-9 flexible seal bench test, boot torque was 4 percent of the seal torque. However, the total elastomer height in the 156-9 seal was 2.075 in. (5.27 cm); whereas, the elastomer height in the AGC 260 flexible seal is only 1.50 in. (3.81 cm). This decrease in elastomer thickness (height) results in a stiffer seal and changes the ratio of boot torque to flexible seal torque in inverse proportion.

Therefore, maximum AGC boot torque (Figure 5-5) was calculated as:

at $0 \leq t \leq 60$: $T_{boot} = (T_{seal})\ (0.04)\ \left(\frac{2.075}{1.500}\right) =$ 0.224 million in.-lb (2.53×10^4 N-m)

at $t > 60$: $T_{boot} = (T_{seal})\ (0.04)\ \left(\frac{2.075}{1.500}\right) =$ 0.164 million in.-lb (1.85×10^4 N-m)

Maximum boot torque for the Thiokol nozzle was 0.160 million in.-lb (1.809×10^4 N-m) (4 percent of Thiokol seal torque).

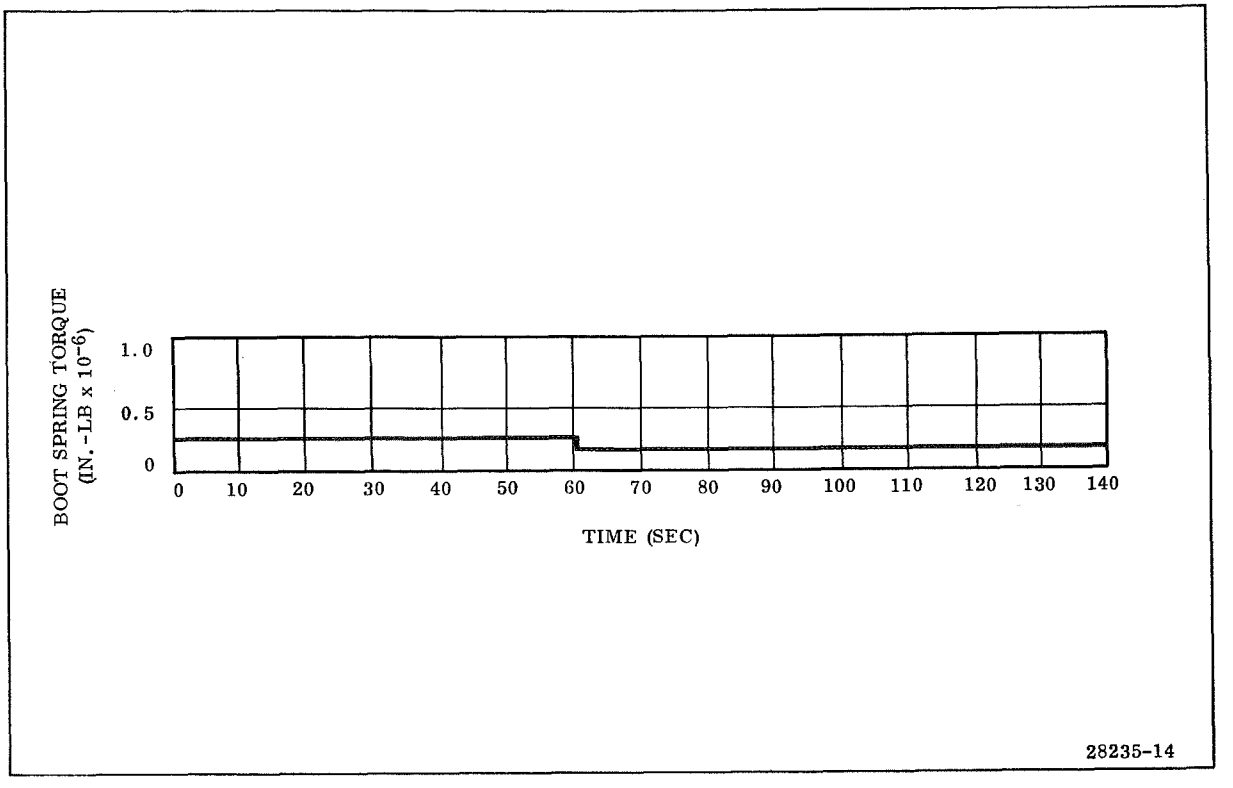

Figure 5-5. Aerojet Boot Spring Torque as a Function of Time

5.0 Movable Nozzle - Flexible Seal

5.4 Preliminary Screening

DESIGN APPROACHES RECEIVED PRELIMINARY SCREENING

The ground rules applied to the program required that state-of-the-art components be selected. Low cost, low development risk, and simplicity of operation were stressed in the design.

At the beginning of the preliminary screening process, it was determined by past experience and by the literature survey that hydraulic power would be required in order to stay within the basic ground rules. Linear electrohydraulic servoactuators were selected to drive the nozzle. The primary task in the preliminary screening was to select a power source to drive the actuators. Staying within the guidelines established, the power sources listed on the opposite page were investigated in some detail. Under each category listed, several different configurations were studied. The torque values used were obtained from computer runs made at Thiokol using the AGC bearing design. During the screening process, the same torque values were used for all configurations studied. The servoactuators were sized at the beginning of the study and used for all power sources. The torque was later reduced at the preliminary design review; however, the auxiliary power supply studied during the preliminary design used the initial torque values.

POWER SOURCES STUDIED FOR TVC SYSTEM

1. Warm gas solid propellant generator
    a. Blowdown
    b. Turbine pump
2. Warm gas liquid propellant generator
3. Cold gas blowdown

5.4 Preliminary Screening

5.4.1 Warm Gas Solid Propellant Gas Generator Turbine Pump Systems With Accumulator

PRELIMINARY SCREENING GIVEN TO WARM GAS SOLID PROPELLANT GAS GENERATOR TURBINE PUMP SYSTEM WITH ACCUMULATOR

The most conventional system investigated was a warm gas solid propellant warm gas generator driving a turbine-gearbox-hydraulic pump combination.

The propellant considered for the preliminary design had a density of 0.053 lb/cu in. (1.468×10^{-3} kg/cm^3) and a burning rate of 0.086 ips (0.218 cm/sec). Chamber pressure was assumed to be 1,000 psi (70.3 kg/cm^2) and the adiabatic head was 556,000 ft (169,700 m). A relief valve is used on all systems to prevent over-pressurization of the gas generator. The warm gas drives a partial admission axial flow turbine which is coupled directly through a gear box to a variable displacement hydraulic pump. The gear box reduces the speed by a factor of 10 or 15 to 1 and is provided with a self contained lubrication system. Various size hydraulic pumps were used in the following designs but all are of the positive-displacement, axial piston type which have found application throughout the aerospace industry. The flow of the pumps is controlled by the speed of rotation of the pump and the piston displacement. Pump rotational speed can be set by the turbine-gearbox arrangement; however, piston stroke is regulated by the pump itself. During periods of low flow demand, the yoke angle is reduced to shorten piston stroke. System pressure is maintained; however, the flow is reduced to that sufficient to supply internal leakage.

A bootstrap reservoir is used on all systems requiring a hydraulic pump. The reservoir is sized to contain sufficient hydraulic fluid to allow for thermal expansion, leakage, and the filling of the blowdown accumulator when used. In addition, the reservoir supplies inlet pressurization to the pump in the range of 50 to 100 psi (344×10^3 to 689×10^3 N/m^2).

A nitrogen precharged accumulator is used in many applications to supplement hydraulic flow during peak demand periods. For systems studied in this program which required accumulators, a piston type accumulator precharged to 2,200 psi ($15,105 \times 10^3$ N/m^2) was used. During startup time, the pumping unit pumped fluid from the reservoir into the accumulator compressing the nitrogen to system pressure. System pressure for all designs was 4,000 psi ($27,600 \times 10^3$ N/m^2).

Miscellaneous items such as filters, disconnects, checkvalves, etc, are included in the complete preliminary design but were not included in the initial

screening process since they are present in all systems and represent a small part of the total system. Hydraulic tubing also was not considered since the length and size will be approximately the same for all systems.

Equations used in preliminary design of major components are given below:

Equations Used for Preliminary Design of Major Components

$$\text{Pump Input Horsepower} = \frac{\text{hp}}{\text{Pump Eff}} = \text{hpp} \tag{5}$$

$$\text{Required Gas HP} = \frac{\text{hpp}}{\text{Turbine Eff}} = \text{GHP} \tag{6}$$

$$\text{Gas Generator Flow} = \dot{W} = \frac{(\text{GHP})\ (550)}{(\text{Adiabatic Head})} \tag{7}$$

$$\text{Accumulator Volume} = V_{33} = \frac{V_o \left(\frac{P_{20}}{P_{33}}\right)^{\frac{1}{\gamma}}}{1 - \left(\frac{P_{20}}{P_s}\right)^{\frac{1}{\gamma}}} \tag{8}$$

$$\text{Propellant Weight} = \dot{W}\ (t_b + 27) = \text{WGGP} \tag{9}$$

$$\text{Gas Generator Weight} = \frac{\text{WGGP}}{\sigma} \tag{10}$$

5.4 Preliminary Screening

5.4.2 Servoactuator Sizing

EFFECTIVE AREA OF SERVOACTUATOR COMPUTED AS 47.2 SQ IN. (304 CM^2).

The servoactuator effective area was sized during preliminary screening assuming a stall torque of 17.726 x 10^6 in.-lb (1.95 x 10^6 N-m) a lever arm of 96.5 in. (245 cm) and a hydraulic system pressure of 4,000 psi (27,600 x 10^3 N/m^2). The area was computed from equation 11.

The torque figure used was obtained at the 1.61° (0.028 RAD) vector angle. A slew rate of 3.0°/sec (0.0524 RAD/sec) in an oblique plane requires a rate of 2.12° /sec (0.037 RAD/sec) in both the yaw and pitch planes. The flow necessary to meet this rate is 87 gpm (equation 12) or 43.5 gpm (2.74 l/sec) per actuator. For preliminary design it was decided to use a 50 gpm (3.15 l/sec) servovalve (standard production model) to meet this requirement. The servovalve is a two stage, four-way electrohydraulic unit. The actuator stroke required to give a vector angle of 1.61° (0.028 RAD) is 2.71 in. (6.88 cm) (equation 13). The maximum vector angle on the duty cycle presented by NASA was 0.948° (0.0165 RAD) at approximately 20 sec. The slew rate at that time was 1.84° /sec (0.032 RAD/sec) and the torque is 14.8 x 10^6 in.-lb (1.67 x 10^6 N-m). The flow rate required to meet this slew rate is 38 gpm (2.39 l/sec) (equation 14). At 20 sec, the pressure drop across the actuator is 3,250 psi (22,400 x 10^3 N/m^2) (equation 15) and the resulting valve flow is 40.3 gpm (2.54 l/sec) (equation 16) which is adequate to meet the 1.84° /sec (0.032 RAD/sec) slew rate. These values were used for the first phase of the preliminary design.

$$A_p = \frac{T}{l P_s} = \frac{17.726 \times 10^6}{96.5 \times 3,900} = 47.2 \text{ sq in. } (304 \text{ cm}^2) \quad (11)$$

$$Q_m = \frac{2 A_p \dot{x}}{3.85} = \frac{2 A_p l \dot{\delta}}{3.85 (57.3)} = \frac{2 (47.2) (96.5) (2.12)}{3.85 (57.3)} = 87 \text{ gpm } (5.48 \text{ l/sec}) \quad (12)$$

$$x = \frac{l \delta}{57.3} = \frac{96.5 (1.61)}{57.3} = 2.71 \text{ in. } (6.88 \text{ cm}) \quad (13)$$

$$Q_c = \frac{A_p l \dot{\delta}}{3.85 (57.3)} = \frac{47.2 (96.5) (1.84)}{3.85 (57.3)} = 38 \text{ gpm } (2.39 \text{ l/sec}) \quad (14)$$

$$\Delta P = \frac{T}{A_p l} = \frac{14.8 \times 10^6}{47.2 (96.5)} = 3,250 \text{ psi } (22.4 \times 10^6 \text{ N/m}^2) \quad (15)$$

$$Q = 50 \sqrt{\frac{P_v}{1,000}} = 50 \sqrt{\frac{4,000 - 3,250 - 100}{1,000}} = 40.3 \text{ gpm } (2.54 \text{ l/sec}) \quad (16)$$

5.4 PRELIMINARY SCREENING

5.4.3 Accumulator Sizing

ACCUMULATOR SIZED DURING PRELIMINARY SCREENING

The accumulator was sized using the hydraulic flow response obtained from an analog computer study.

The precharged accumulator is used to supplement hydraulic flow during peak demand periods where the demand exceeds the output capability of the pump. In the top sketch on the opposite page, $\dot{\delta}$ (nozzle vector rate) is depicted as a triangular wave and the resulting flow is shown directly below. Pump capacity, Q_p, is indicated by the horizontal line. The flow required from the accumulator flow is shown by the shaded area. During the time between accumulator flow demands, the pump recharges the accumulator. It is obvious that the accumulator cannot supply more than half the flow if recharging between demands is required. The lower sketch shows a typical flow curve obtained from the computer. For preliminary design it was assumed that the response would be independent of power supply design. By varying Q_p and integrating the area above the line, the flow from the accumulator could be determined. This method was used to size all accumulators for the preliminary design.

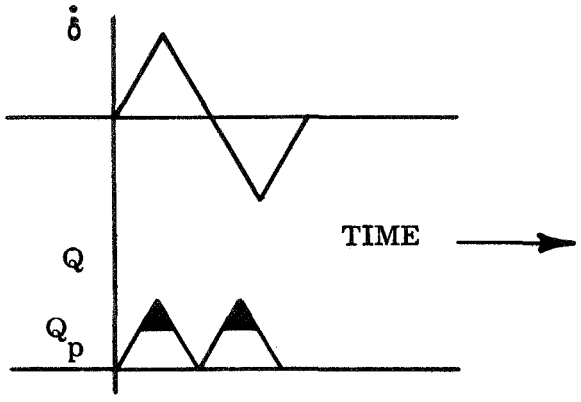

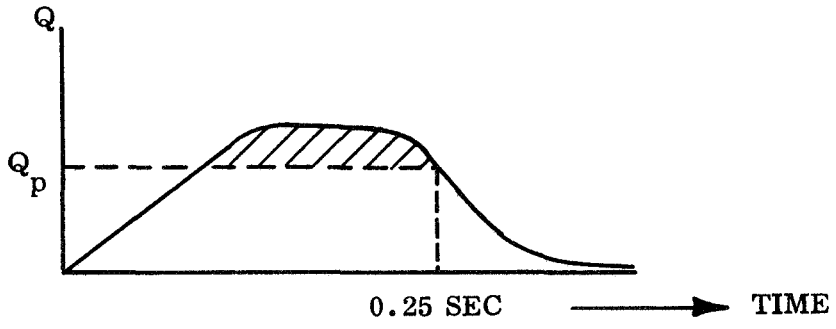

28235-36

5.5 Preliminary Designs

5.5.1 Warm Gas Solid Propellant Gas Generator Turbine Pump System With and Without Accumulator

PRELIMINARY TRADE STUDY SHOWS ACCUMULATOR BETTER

The most conventional system is a warm gas solid propellant generator driving a turbine-gearbox-hydraulic pump combination. Hydraulic flow is supplemented by a nitrogen precharged accumulat

Accumulators are usually included in the design of hydraulic power packages to reduce the size of the pumping unit; however, they have a serious limitation in that if unanticipated rapid demands are made, the system pressure may drop to a level which will prevent attaining maximum vector angle or slew rate.

The pump selected for this design is a variable displacement type capable of flowing 60 gpm (3.78 l/sec) at 7,100 rpm. Turning at a higher rpm requires a larger gas generator but a smaller accumulator. The efficiency used for the pump was 0.8 and an efficiency of 0.5 was assumed for the turbine-gearbox which is higher than normally used; however, in recent contracts with a turbine manufacturer, they have stated that this value is within state-of-the-art. A schematic of the system is shown in Figure 5-6. The pressure control valve and sonic orifice act as a regulator and relief valve for the gas generator. Use of a variable displacement pump requires a turbine speed control to prevent excess turbine speed during time of no flow requirement. The accumulators were sized as described in subsection 5.4.3. The pressure was allowed to decay from 4,000 (27.6×10^6 N/m^2) to 3,800 psi (26.2×10^6 N/m^2) during the blowdown cycle. This allowed sufficient supply pressure to meet duty cycle requirements. Design parameters and major component weight are shown in Table 5-1.

Without Accumulator

The maximum flow as determined by equation 12 in subsection 5.4.2 is 87 gpm (5.48 l/sec). The pump selected for this design was the B70 pump developed by Vickers. The pump will flow 100 gpm (6.3 l/sec) at 4,000 psi (27.6×10^6 N/m^2). This is more than sufficient to meet the requirements for this particular program. The weight of the pump 98 lb (44.4 kg) offsets any possible weight advantage of dropping the accumulator. The weight of the major components exceeds those given in Table 5-1 by approximately 100 lb (45.3 kg). This weight penalty plus the additional cost for the pump and turbine-gearbox eliminated this design from further consideration.

TABLE 5-1

WARM GAS SOLID PROPELLANT GAS GENERATOR - TURBINE PUMP SYSTEM
(SINGLE PUMP WITH ACCUMULATOR)

	Value	
	English Units	SI Units
Design Parameters		
Pump flow	60 gpm	3.78 l/sec
Horsepower	140 hp	104.5×10^3 watts
Pump input	175 hp	130.5×10^3 watts
Gas horsepower	350 hp	261×10^3 watts
Gas generator flow rate	0.35 lb/sec	0.157 kg/sec
Propellant weight	59.5 lb	27 kg
Accumulator volume	600 cu in.	9.85 l
Weights		
Gas generator	82.5 lb	37.4 kg
Accumulator	37	16.75
Reservoir	15.5	7.02
Turbine gear box	42.5	19.25
Hydraulic fluid	13.2	5.98
Pump	19.8	8.96
Total Weight	210.5 lb	95.5 kg

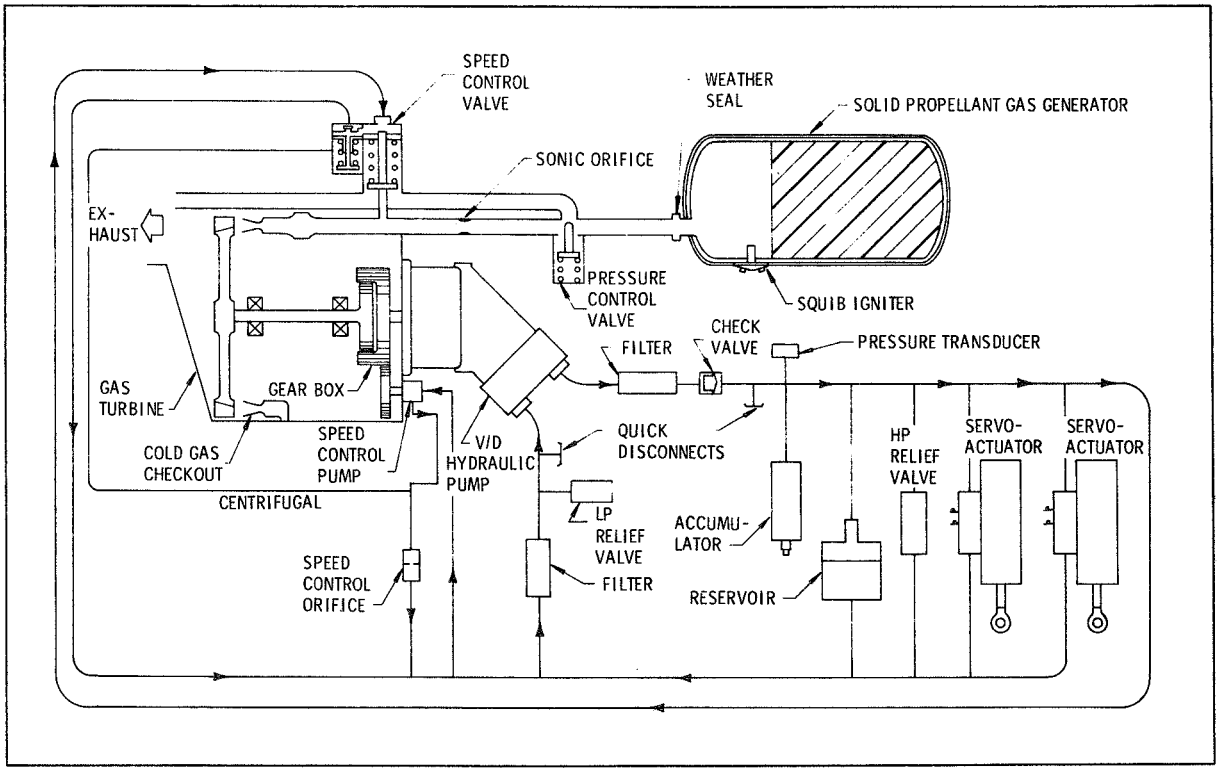

Figure 5-6. Variable Displacement Pump Approach, Schematic

5.5 PRELIMINARY DESIGNS

5.5.2 Warm Gas Solid Propellant Gas Generator Turbine Pump System with Dual Pump - No Accumulator

DUAL PUMP DESIGN WITHOUT ACCUMULATOR CONSIDERED

To overcome the difficulties encountered by a single large pump, consideration was given to dual pumps driven by a common turbine-gearbox arrangement. Weight difference is insignificant but the additional pump adds complexity which may decrease reliability.

The variable displacement pumps, each capable of delivering 48 gpm (3.02 l/sec) at 4,000 psi (27.6 x 10^6 N/m^2) were selected for this design. The combined flow of 96 gpm (6.05 l/sec) was more than sufficient to meet the slew rate requirement. Pump speed for this flow rate is 5,650 rpm and is identical with the pump used in Subsection 5.5.1. This design is similar to the previous with the exception of the dual pumps and the elimination of the accumulator. Using dual pumps allows for a more severe duty cycle which would impose serious limitations on a system which depended on an accumulator. The weight difference is insignificant for a preliminary design tradeoff. The addition of a second pump adds complexity to the system and as such may decrease reliability. The cost of the dual pump will be partially offset by the addition of the large accumulator in the single pump system. Design parameters and preliminary component weights are given in Table 5-2.

TABLE 5-2

DUAL PUMP SYSTEM - NO ACCUMULATOR

	Value	
	English Units	SI Units
Design parameters		
Pump flow (2) (gpm)	96	6.05 l/sec
Power		
Pump output (hp)	224	167×10^3 watts
Pump input (hp)	264	197×10^3 watts
Gas (hp)	528	394×10^3 watts
Gas generator flow rate (lbm/sec)	0.528	0.239 kg/sec
Grain weight (lb)	89.6	40.6 kg
Component weight (lb)		
Gas generator	123	55.8 kg
Reservoir	11	4.98
Turbine-gearbox	47	21.3
Hydraulic fluid	7	3.17
Pump (2)	39.6	17.92
Total	227.6	103 kg

5.5 Preliminary Designs

5.5.3 Warm Gas Solid Propellant Gas Generator Turbine Pump System with Small Dual Pumps - Precharged Accumulator

SMALL DUAL PUMPS WITH PRECHARGED ACCUMULATOR CONSIDERED

The same two pumps used in the design described in subsection 5.5.2 were used in conjunction with a small accumulator to reduce horsepower requirements. Although some advantages are realized (eg, lower output horsepower required; better pump efficiency), system is more complex.

The two pumps were run at a reduced speed of 3,750 rpm at which the total hydraulic flow is 64 gpm (4.03 l/sec). Using the value of 87 gpm (5.48 l/sec) as the required flow to meet the design slew rate, the accumulator will be required to flow 23 gpm (1.45 l/sec) which is approximately one-fourth of the total flow. The lower flow results in a proportionally lower output horsepower and, in addition, running the pumps at lower speed increases the pump efficiency thereby reducing the input power requirement even more. The design parameters and major component weight are listed in Table 5-3. As may be noted, the weight difference is again insignificant especially when the overall motor and movable nozzle TVC system is considered. Again, an additional component is added to the system and, although it is a simple, highly reliable component it does add complexity to the system.

TABLE 5-3

DUAL PUMP SYSTEM PRECHARGED ACCUMULATOR
(2,200 psi GN_2) (15.105 x 10^6 N/m^2)

	Value	
	English Units	SI Units
Design parameters		
Pump flow (2)	64 gpm	4.03 l/sec
Power		
Pump output	149 hp	111 x 10^3 watts
Pump input	166 hp	124 x 10^3 watts
Gas	332 hp	248 x 10^3 watts
Gas generator flow rate	0.33 lb/sec	0.1495 kg/sec
Grain weight	56.4 lb	25.5 kg
Accumulator volume	440 cu in.	7.22 l
Component weights		
Gas generator	77 lb	34.8 kg
Accumulator	37	16.75
Reservoir	13.6	6.16
Turbine-gearbox	43	19.5
Hydraulic fluid	10.4	4.71
Pump (2)	39.6	17.92
Total	220.6 lb	100 kg

5.5 Preliminary Designs

5.5.4 Warm Gas Solid Propellant Gas Generator with Small Pump and Large Accumulator

SMALL TURBINE PUMP WITH LARGE ACCUMULATOR CONSIDERED

Thiokol decided to compare system specified in subsection 5.5.3 with a design which would use the smallest pump size capable of meeting the duty cycle requirements with the aid of a large precharged accumulator. This design is similar to that described in subsection 5.5.1.

Use of a smaller hydraulic pump flow reduces the size of the solid propellant gas generator required. However, the accumulator and reservoir increase in size so that the net weight difference is slightly in favor of the larger pumping unit. The pump used was the same size but was turned at 5,650 rpm instead of 7,100 rpm. Design parameters and component weights are given in Table 5-4. The weight difference again is negligible, the main difference being in the accumulator. The pressure was allowed to decay to only 3,800 psi (26.2×10^6 N/m^2) which resulted in the large volume. This value of pressure was used in all designs in order to compare systems on the same basis.

TABLE 5-4

SMALL PUMP SYSTEM WITH LARGE ACCUMULATOR

	Values	
	English Units	SI Units
Design parameter		
Pump flow	48 gpm	3.02 l/sec
Power		
Pump output	112 hp	83.5×10^3 watts
Pump input	132 hp	98.5×10^3 watts
Gas	264 hp	197×10^3 watts
Gas generator flow rate	0.264 lb/sec	0.1195 kg/sec
Grain weight	44.8 lb	20.3 kg
Accumulator volume	1,050 cu in.	17.2 l
Component weight		
Gas generator	63.2 lb	28.6 kg
Accumulator	65	29.4
Reservoir	18	8.15
Turbine gearbox	40	18.1
Hydraulic fluid	18	8.15
Pump	19.8	8.98
Total	224 lb	101.5 kg

5.5 Preliminary Designs

5.5.5 Warm Gas Solid Propellant Gas Generator with Precharged Accumulator

PRECHARGING ACCUMULATOR FROM WARM GAS GENERATOR CONSIDERED

One of the primary disadvantages of a precharged accumulator is that during peak flow demands, system pressure decays as the accumulator discharges fluid. To overcome this difficulty a design was considered which charged the accumulator from the warm gas generator instead of using nitrogen.

The added complexity of the valving plus the heavier gas generator and accumulator eliminated this concept.

By using a warm gas generator, the system pressure can be maintained at essentially 4,000 psi (2.758×10^7 N/m^2) during the time the accumulator is discharging fluid. A switching arrangement can be provided so that between cycles, the pump will fill the accumulator with hydraulic fluid making it ready for the next demand. There are several disadvantages with this type of system. In order to use a 4,000 psi (2.758×10^7 N/m^2) supply pressure it would require either a gas generator operating at this pressure or a differential area type accumulator. A high pressure gas generator would have a lower mass fraction, resulting in a heavier generator. A differential area type accumulator would also be much heavier than its equal area counterpart. Since the generator would have to drive not only the turbine but also supply sufficient gas to the accumulator to provide the necessary hydraulic flow, the total gas flow rate would be high, thus increasing the size of the generator even more. The higher gas flow would also require a larger warm gas relief valve on the gas generator. A priority valve arrangement would be required to allow refilling of the accumulator between demands. The added complexity of the valving plus the heavier gas generator and accumulator would not offset the advantage of maintaining system pressure for this application. For this reason this system was not given further consideration in the preliminary design.

5.5 Preliminary Designs

5.5.6 Warm Gas Liquid Propellant - Turbine Pump

LIQUID FUELED TURBINE PUMP SYSTEM CONSIDERED

This system uses the same components as previous designs except for the gas generator and accessories necessary for the liquid propellant gas generator. Lack of experience and heavy development effort eliminated this design.

For the warm gas liquid fueled generator scheme, hydrazine was used as a fuel and pumped to a catalyst bed by a centrifugal fuel pump. A schematic of the liquid fueled system is shown in Figure 5-7 . The fuel pump can be mounted on a common shaft with the turbine so that it will always turn at turbine speed. Fluid is pumped through a fuel valve which controls flow to the catalyst bed and hence to the turbine. The output pressure of the fuel pump is essentially independent of flow but a direct function of pump speed and consequently turbine speed. The fuel valve senses pump output pressure and varies flow to the turbine as a function of this pressure. Thus turbine speed is controlled and can be maintained at almost constant speed over the entire hydraulic flow range. Low pressure warm gas is bled off at the turbine and fed back to the fuel tank to create a slight back pressure on the fluid. The system is started by firing a cartridge propellant which drives the turbine to its operating speed. This cartridge also raises the temperature of the catalyst bed to assist decomposition of the fuel during startup.

The system was sized using two different hydraulic pump speeds with a precharged accumulator to supply additional flow for peak demands. Design parameters and major component weights are listed in Table 5-5 . As may be noted, these weights are slightly less than those for a solid propellant gas generator system; however, this weight difference is not significant when compared to the overall system weight. In reviewing the current usage and development status of the hydrazine system it was decided that the weight difference would not overcome the lack of experience and development required for the use of liquid system of this size.

TABLE 5-5

LIQUID FUELED GAS GENERATOR SYSTEM

	Pump Speed			
	7,100 RPM		5,650 RPM	
	English Units	SI Units	English Units	SI Units
Design parameters				
Pump flow	60 gpm	3.02 l/sec	48 gpm	3.78 l/sec
Power				
Pump output	140 hp	83.5 x 10^3 watts	112 hp	104.5 x 10^3 watts
Pump input	175 hp	98.5 x 10^3 watts	132 hp	130.5 x 10^3 watts
Gas	350 hp	197 x 10^3 watts	264 hp	261 x 10^3 watts
Gas Generator flow rate	0.283 lb/sec	0.097 kg/sec	0.214 lb/sec	0.128 kg/sec
Fuel weight	48 lb	16.5 g	36.4 lb	21.7 kg
Accumulator volume	600 cu in.	17.2 l	1,050 cu in.	9.85 l
Component weight				
Gas generator	60 lb	22.6 kg	50 lb	27.2 kg
Accumulator	37	29.4	65	16.75
Reservoir	15.5	8.15	18	7.02
Turbine-gear box	42.5	18.1	40	19.25
Hydraulic fluid	13.2	8.15	18	5.98
Pump	19.8	8.98	19.8	8.98
Accessories	10	3.62	8	4.53
Total	198 lb	99.2 kg	218.8 lb	89.8 kg

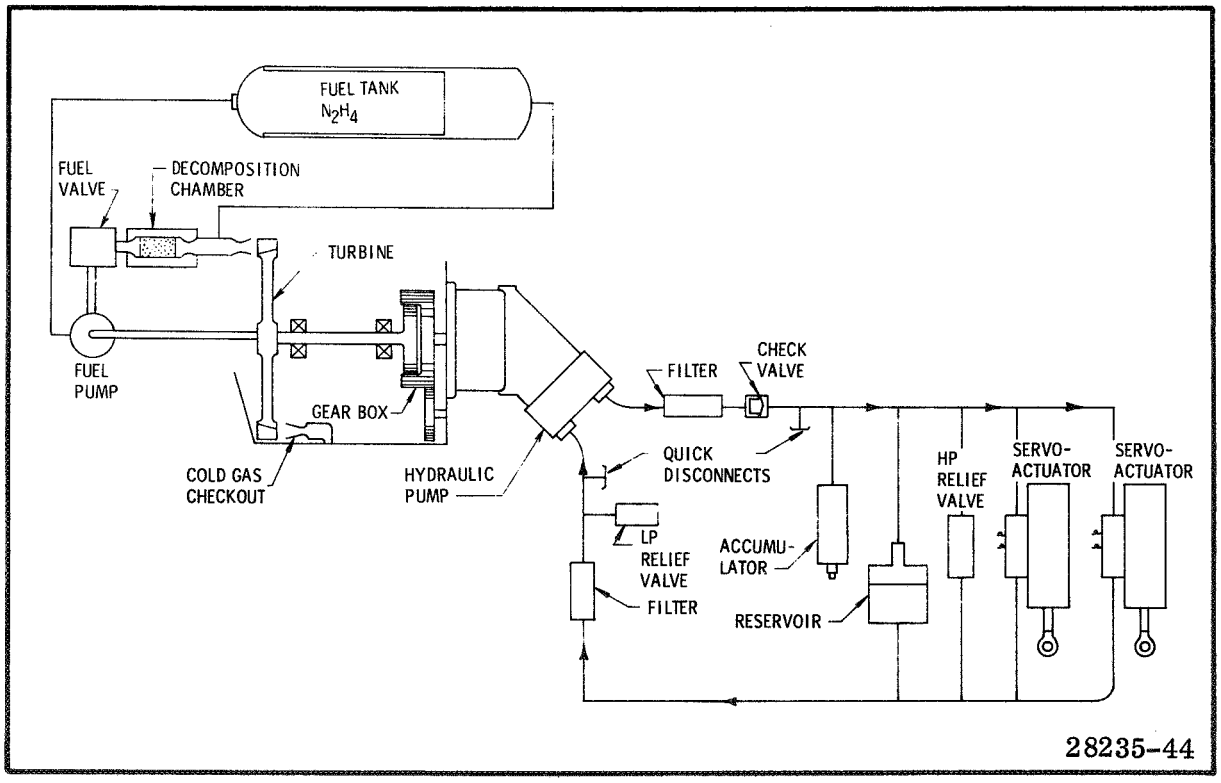

Figure 5-7. Liquid Fuel System (Hydrazine)

5.5 Preliminary Designs

5.5.7 Warm Gas Blowdown

WARM GAS BLOWDOWN SYSTEM CONSIDERED

A warm gas blowdown system is one of the least complex of the systems studied. It utilizes a solid propellant warm gas generator to pressurize an accumulator which contains sufficient hydraulic fluid to meet duty cycle requirements. Because this system requires additional weight and is duty cycle limited, it was considered inferior to the more conventional turbine pump system.

The most critical item in the design of a blowdown system is the sizing of the blowdown accumulator. The duty cycle obtained from NASA presented $\dot{\delta}$ vs time. The integral of the absolute value of $\dot{\delta}$ gave 18.92° (0.314 RAD) for the pitch and yaw signals. Using a safety factor of 1.2 resulted in 1,800 cu in. (29.5 l) of fluid to be used for the duty cycle. Servovalve leakage flow was assumed to be 0.5 gpm (0.0315 l/sec) per servovalve. Over the entire action time, this amounts to 655 cu in. (10.75 l) of fluid used due to leakage. The total quantity of hydraulic oil is then 2,455 cu in. (40.2 l). The equations 17 thru 21 were used in sizing the system. Component weights are 234 lb (106 kg) for gas generator, 73.5 lb (33.3 kg) for hydraulic oil, 150 lb (67.9 kg) for accumulator, and 6.0 lb (2.72 kg) for relief valve making a total weight of 463.5 lb (210 kg). As may be noted, the weight is considerably more than the turbine pump systems. In order to use the same size actuators, a 4,000 psi (27.6×10^6 N/m^2) gas generator was used. This requires a heavier case and the mass fraction goes down to 0.45. The other alternative is to use a 2,000 psi (13.8×10^6 N/m^2) gas generator with an unbalanced area accumulator. This would also increase the weight considerably. Prelaunch checkout is accomplished by attaching ground hydraulic power to the two quick disconnects shown in the schematic (Figure 5-8).

The blowdown system has the advantage of simplicity but has the distinct disadvantage of being duty cycle limited. A very good knowledge of the expected duty cycle is required for any blowdown system. As may be noted from the schematic, once the hydraulic fluid passes through the servovalve, it is dumped and not available for reuse. Because of this, it is necessary that the duty cycle be well defined in order to predict the amount of fluid necessary to meet thrust vector requirements. Although this system is considerably simpler, and only slightly heavier considering the weight of the booster inerts, Thiokol decided that a turbine pump system would be preferable.

A closed cycle blowdown system in which the hydraulic fluid is recycled instead of being dumped as in the open cycle was also investigated. The blowdown accumulator and the amount of hydraulic oil in storage would be reduced; however, the complexity of the system would be increased considerably. Thiokol concluded that the added complexity and consequent reduction in reliability and increase in cost would not justify the use of the closed cycle system.

Equations Used in Sizing Warm Gas Blowdown System

$$V_x = \frac{A_p l}{57.3} \int_{t=-30}^{t=140} \left(\left|\dot{\delta}_y\right| + \left|\dot{\delta}_p\right| \right) dt = 1,500 \text{ cu in. } (24.6 \text{ l}) = \text{volume of oil expelled} \quad (17)$$

$$V_{TB} = 1,800 + Q_L (t_b + 27) = 1,800 + (3.85)(170) = 2,455 \text{ cu in. } (40.2 \text{ l}) = \text{total volume} \quad (18)$$

$$\dot{W} = 3.85 \rho Q_M = 3.85 (1.84 \times 10^{-3}) (87) = 0.62 \text{ lb/sec } (0.281 \text{ kg/sec}) \quad (19)$$

$$WGGP = \dot{W} (t_b + 27) = 0.62 (170) = 105 \text{ lb } (47.5 \text{ kg}) \quad (20)$$

$$G.G.W. = \frac{WGGP}{\sigma} = \frac{105}{0.45} = 234 \text{ lb } (106 \text{ kg}) \quad (21)$$

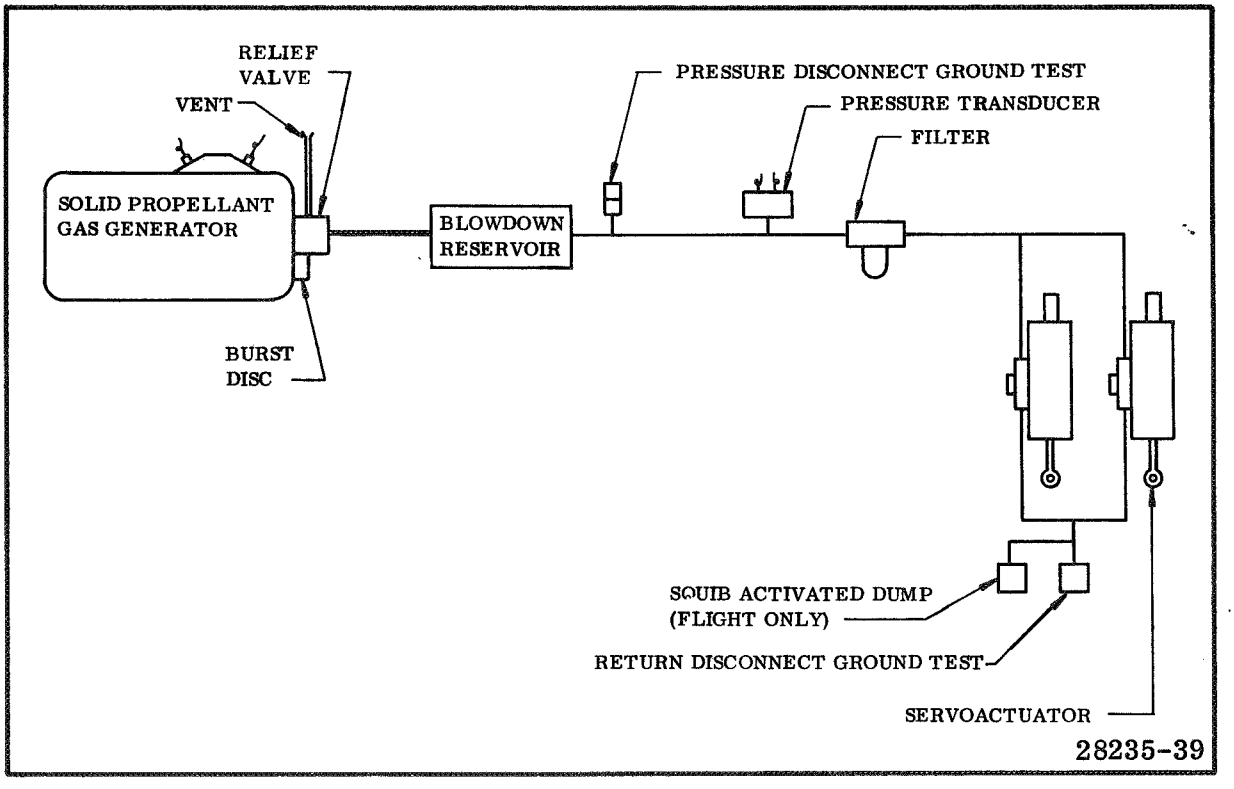

Figure 5-8. Warm Gas Blowdown System, Schematic

MOVABLE NOZZLE - FLEXIBLE SEAL TVC SYSTEM PRESENTED TO NASA AS CANDIDATE FOR DETAIL DESIGN STUDIES

The design presented to NASA as the candidate for detail design was the one described in subsection 5.5.1 (with accumulator). This actuation system was used on both the Thiokol and AGC nozzles. Since the torques for the two seal designs were within 10 percent of each other, the same actuation system was used with each.

This system uses solid propellant gas generator driving a turbine-gearbox, a single hydraulic pump turning at 7,100 rpm and the Thiokol flex bearing. A weight breakdown of the individual actuation system components is shown in Table 5-6 . Actual weight of components supplied by vendors were used wherever possible. If such data were not available, the Thiokol-TVC Preliminary Design Computer Program was used to estimate weight. This system was selected because it is the most conventional system involving the least development risk. There would be little component development; although the system as a whole will require extensive checkout and bench test to insure adequate performance and response characteristics. A layout of the system is shown in Figure 5-9 .

The turbine-gearbox, gas generator, pump, and reservoir are grouped together and are located midway between the pitch and yaw servoactuators. Stainless steel tubing is run to the plane of actuation where flexible hose connects the solid tubing to the actuators. Tubing for the preliminary design was 1.25 (3.18 cm) by 0.095 in. (2.41 cm) wall thickness for both pressure and return lines. The accumulator volume was 600 cu in. (9.85 l) which allowed supply pressure to decay to 3,800 psi (26.2×10^6 N/m^2). Crosstalk for a 1.61° (0.028 RAD) vector angle pitch or yaw command is approximately 0.036° (6.28×10^{-4} RAD). This implies that if a 1.61° (0.028 RAD) pitch or yaw command is made the actuator in the other quadrant must extend an equivalent of 0.036° (6.28×10^{-4} RAD) in order to obtain 1.61° (0.028 RAD) in a pure pitch or yaw plane. The equation for computing this error is listed on the opposite page as equation 22. Crosstalk is an inherent feature of all flexible bearings and is a function of pivot point location and geometry of actuator mounting. Crosstalk can be eliminated by positioning the actuator fixed pivot point in the same plane as the nozzle pivot point. For this condition $b = a \sin \alpha$ and as can

be seen from equation 22, ϵ goes to zero. For the preliminary design:

$b = 75.6$ in. (192 cm)

$a = 28.3$ in. (72 cm)

$\alpha = 38.197°$ (0.666 RAD)

$\epsilon = 0.06121$ in. (0.155 cm)

$$\epsilon = \left[4b\,(b - a \sin\alpha)\,\sin^2 \delta/2 + a^2\right]^{1/2} - a \qquad (22)$$

where:

ϵ = Change in actuator length to give pure pitch or yaw vector angle

a = Length of actuator at null

b = Distance along centerline of nozzle from the pivot point to the plane that intersects the nozzle clevis

δ = Vector angle

α = Angle between the actuator centerline and a line from the actuator fixed pivot point perpendicular to the centerline of the nozzle

TABLE 5-6

WEIGHT BREAKDOWN OF SELECTED SYSTEM

Component	Weight English Units (lb)	SI Units (kg)
Gas generator	82.5	37.4
Pump	19.8	8.98
Accumulator	37.0	16.75
Hydraulic fluid	40.0	18.1
Reservoir	15.5	7.02
Turbine-gearbox	42.5	19.25
Tubing and fittings	50.0	22.6
Filter and disconnect	14.0	6.35
Actuator (2)	480.0	217
Servovalves (2)	40.0	18.1
	821.3	372
+10% for brackets and contingencies	82.0	37.1
Total	902.3	408

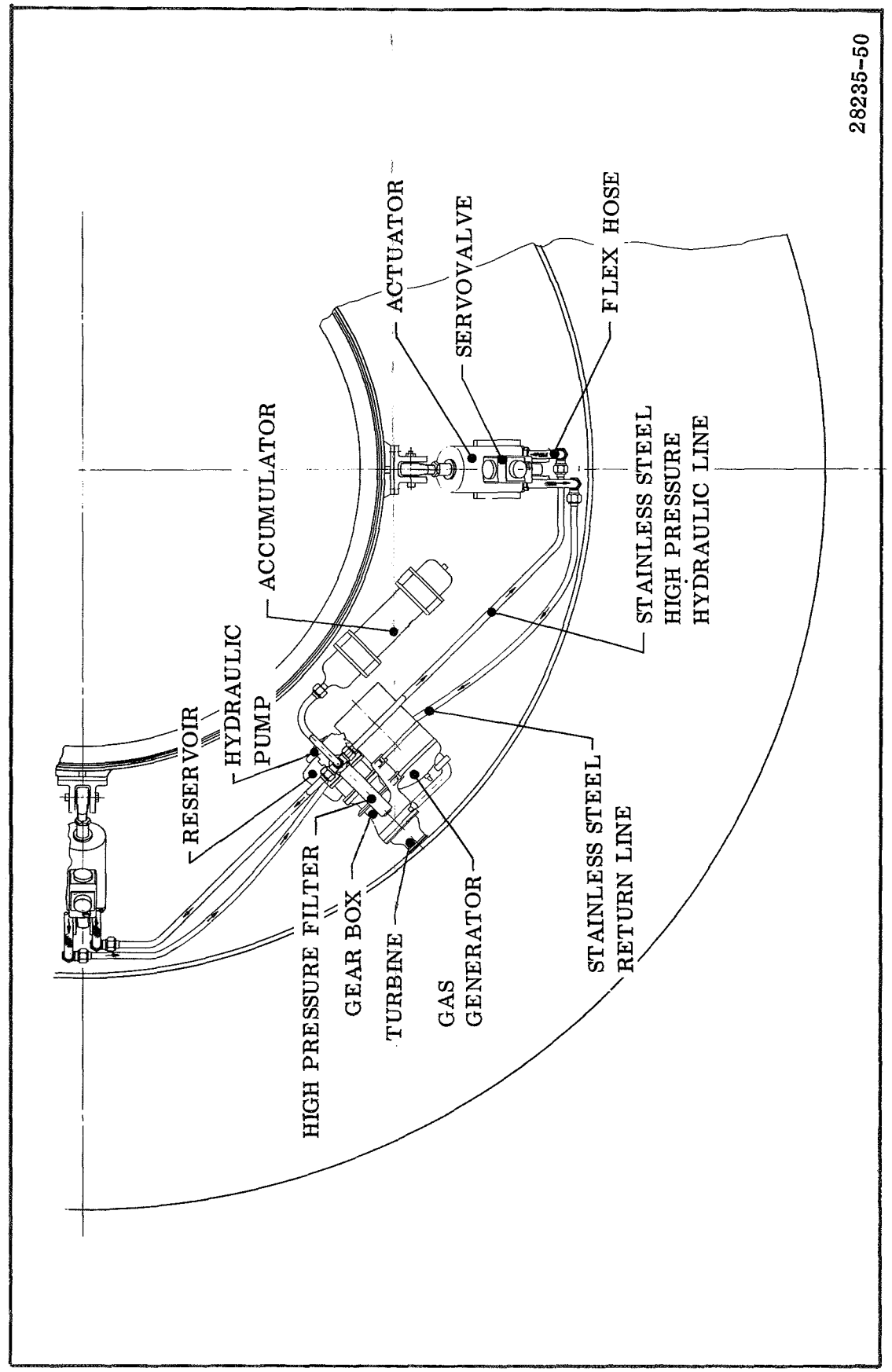

Figure 5-9. Layout of Candidate System, Movable Nozzle - Flexible Seal

5.6 Preliminary Design Review

5.6.1 Major Component Cost

MAJOR COMPONENT COST BREAKDOWN GIVEN FOR CANDIDATE SYSTEM

The preliminary cost figures for all the major components were obtained from vendors. The quotes were based on quantities required for a total of 30 complete motors using a new complete actuation system on each motor.

The major components priced for the preliminary design were: solid propellant warm gas generator, turbine-gearbox, hydraulic pump, accumulator, actuators and servovalves. A tabulation of the cost per item with nonrecurring cost where applicable is presented in Table 5-7. Two additional systems were added for bench testing to determine response and performance characteristics.

TABLE 5-7

MAJOR COMPONENT COST BREAKDOWN OF CANDIDATE SYSTEM
(TURBINE PUMP)

Item	Recurring Cost/Unit ($)	No. of Units	Cost ($)	Nonrecurring ($)	Total ($)
Gas generator	500	32	16,000	--	16,000
Actuator*	20,000	64	1,280,000	150,000	1,430,000
Turbine gearbox	20,000	32	640,000	200,000	840,000
Hydraulic pump	1,450	32	46,400	--	46,400
Accumulator	950	32	30,400	--	30,400
Servovalve*	1,472	64	94,208	--	94,208
Total	65,844			350,000	2,457,008

*Two required per system.

5.6 Preliminary Design Review

5.6.2 Preliminary Design Review Meeting for Candidate TVC System Selection - Movable Nozzles

IMPORTANT CHANGES MADE IN DESIGN PHILOSOPHY AND REQUIREMENTS

During the preliminary design review meeting the following important changes were made.

1. Torque requirements were reduced.
2. Duty cycle multiplied by $\sqrt{2}$.
3. Slew rate redefined to 3°/sec (0.0524 RAD/sec) average velocity.
4. AGC bearing selected.
5. Preliminary design phase extended to investigate passive cold gas blowdown system.

Because of the orientation of the motor during static test and because of the zero gravity conditions during flight, gravity torque would not be a component of the total required torque. The maximum torque value used for the design was 8.86×10^6 in.-lb (0.1×10^6 N-m). Total torque and torque component vs time are shown in Figure 5-10. The duty cycle was multiplied by $\sqrt{2}$ and a 1.61° (0.028 RAD) event was added at 60 sec. This occurred on both the pitch and yaw axis. The new duty cycle is shown in Figure 5-11. The slew rate was defined as 3° /sec (0.0524 RAD/sec) average velocities when taken from hardover in one direction to 90 percent of full travel. The Aerojet bearing was selected by NASA LeRC to be used for the detail design phase of the program. NASA stressed that simplicity was the most important parameter and, consequently, extended the preliminary design phase to investigate a cold gas blowdown system. A turbine-pump system was redesigned using the new torque and slew rate values.

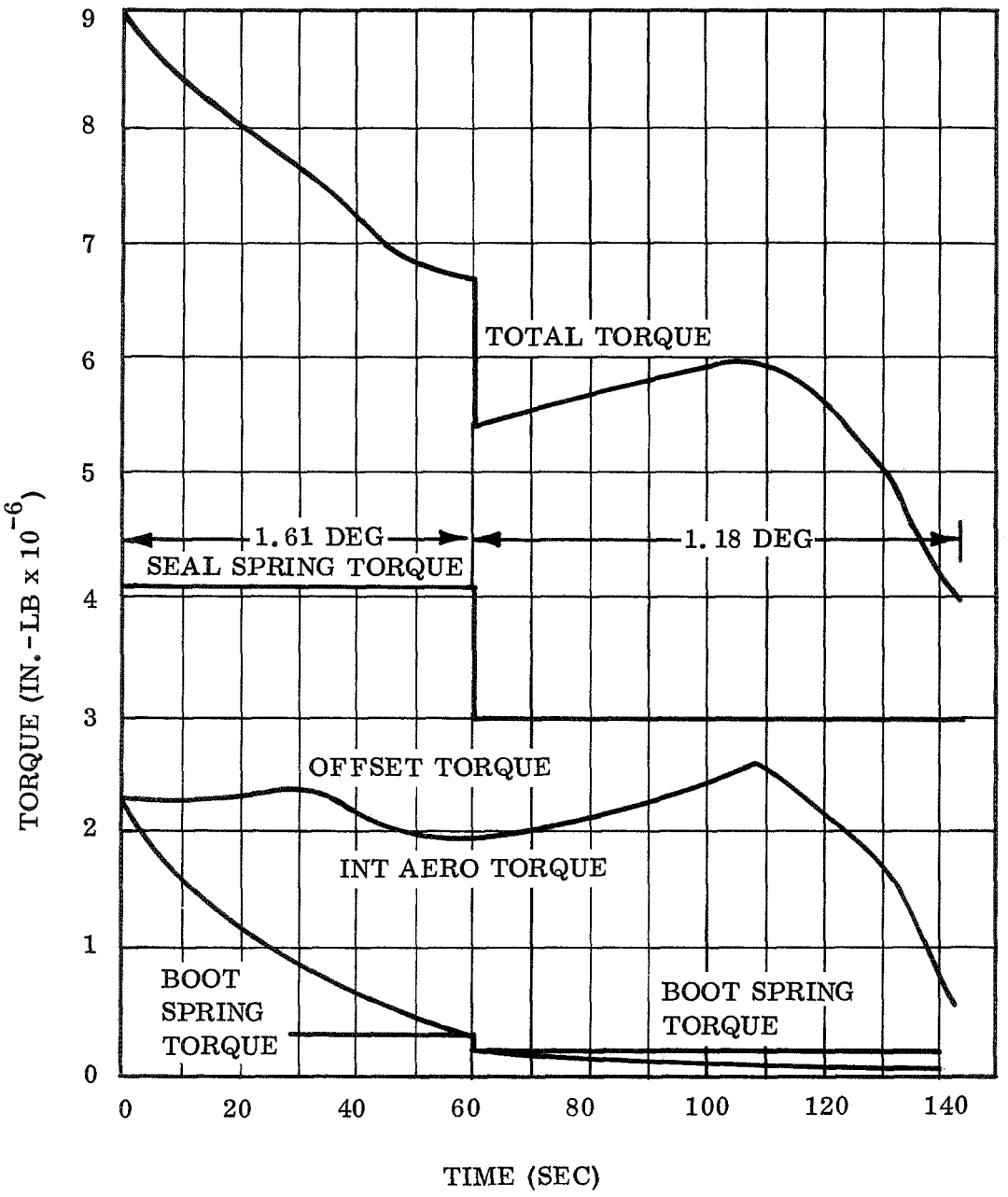

Figure 5-10. Nozzle Torque vs Time

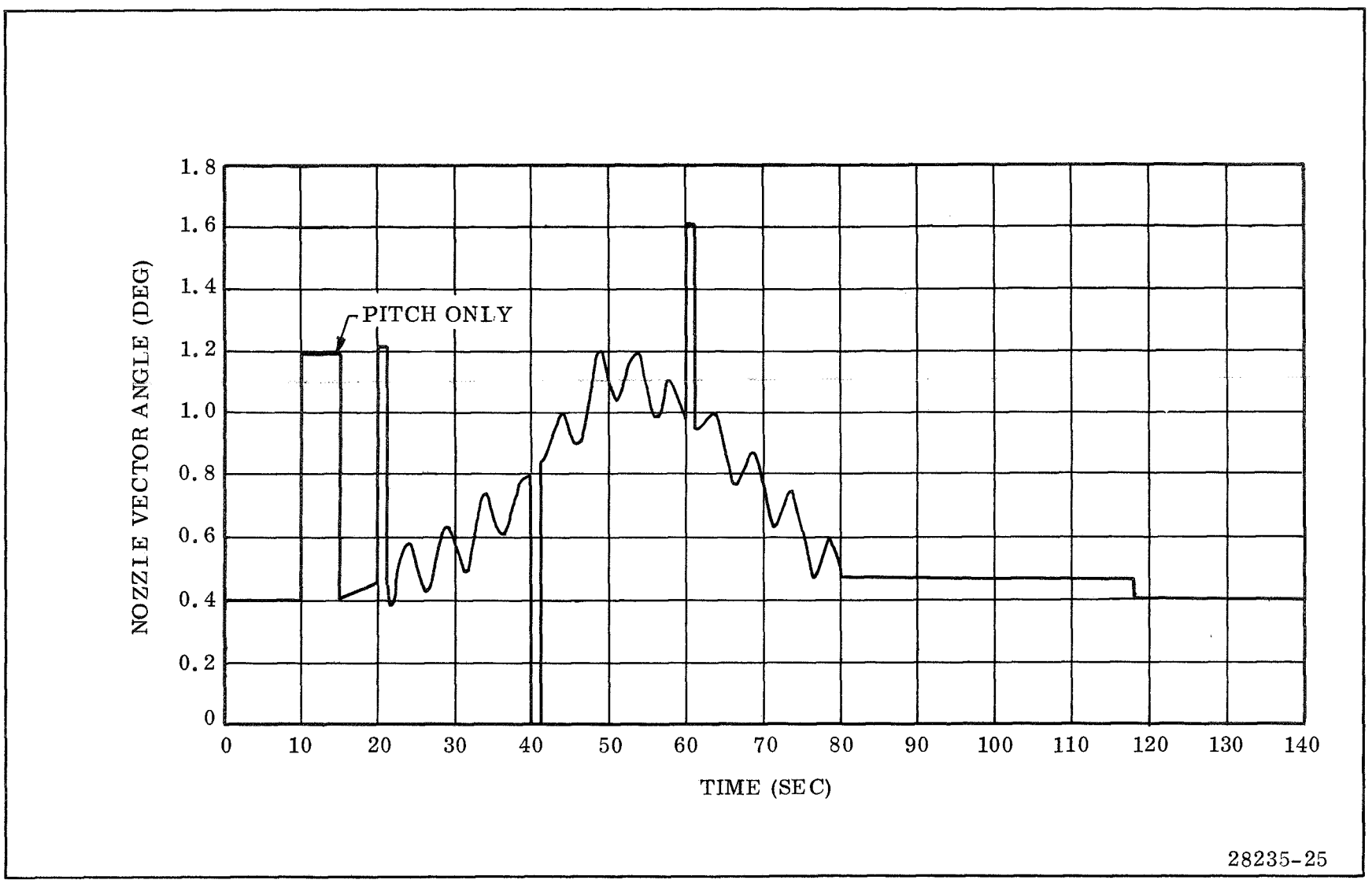

Figure 5-11. Movable Nozzle Duty Cycle

5.6 Preliminary Design Review

5.6.3 Cold Gas - Passive Blowdown

PASSIVE COLD GAS BLOWDOWN SYSTEM INVESTIGATED

The passive blowdown system consists primarily of a single tank in which both the pressurant and hydraulic fluid is contained. The system considered did not use either a piston or bladder to separate the pressurant from the fluid.

The two most critical items in the design of a passive blowdown system are to insure adequate fluid and pressure to meet the design duty cycle. Initial pressure of time equal zero was set at 4,000 psi (27.6×10^6 N/m^2). As pressure decays there will be less vector angle capability.

For the passive blowdown system (Figure 5-12), the initial pressure was set at 4,000 psi (27.6×10^6 N/m^2). The actuator area was sized by assuming a supply pressure of 3,000 psi (20.7×10^6 N/m^2) at 110 sec and a torque of 8.8×10^6 in.-lb (0.995×10^6 N-m). This resulted in an area of 30.4 sq in. (196 cm^2). The torque figure was later found to be in error and was actually 7.65×10^6 in.-lb (0.865×10^6 N-m); however, the analysis had proceeded to the point where it was decided to continue with the previously calculated area.

The response rate used was an average of 3.0°/sec (0.0524 RAD/sec) where the system was stepped from +1.61° (0.028 RAD) to 90 percent of full travel. It was assumed that this time was approximately 1 sec. To determine the maximum rate during that interval a second order system with a damping ratio of 0.8 was used to simulate the actuation system. Using nondimensional charts of second order systems, the time (nondimensional) to reach 90 percent of the final output is 2.95.

From equations 28 and 29 the natural frequency of the system is 2.95 RAD/sec.

This second order system then would reach a maximum velocity of 4.02°/sec (0.0702 RAD/sec) at 0.364 sec. The vector angle at that time would be 0.74° (0.0129 RAD). The slew rate in a single plane would be $4.02/\sqrt{2^\circ}$/sec or 2.84°/sec (0.0495 RAD/sec). Hydraulic flow for a single actuator would be 37.8 gpm (2.38 l/sec) as found from equation 30. For two actuators, the flow would be 75.6 gpm (4.76 l/sec). For a single actuator moving the nozzle at 4.02°/sec (0.0702 RAD/sec) the flow is 53.5 gpm (3.37 l/sec). These values of area and flow were used in both the blowdown and pumping system Phase I studies.

The duty cycle in Figure 5-11 was integrated using the new area to obtain the quantity of fluid required. The total amount of fluid expelled was 1,820 cu in. (29.8 l). This included both pitch and yaw events and was calculated using an actuator area of 30.4 sq in. (196 cm^2) and 1 gpm (0.063 l/sec) leakage. A 25 percent pad was added along with an expulsion efficiency of 90 percent. The total fluid on board is given by equation 24.

With the introduction of the 1.61° (0.028 RAD) event at 60 sec and the reduced torque, it was decided to size the system so that the pressure would decay to 3,000 psi (20.7×10^6 N/m^2) at that time.

The amount of fluid expelled at 60 + sec (after +1.61° (0.028 RAD) vector angle has been attained) is 1,156 cu in. (18.95 l). Equations 25 and 26 were used to determine the initial gas volume required to result in a pressure of 3,000 psi (20.7×10^6 N/m^2) at this time. This volume is 5,060 cu in. (83 l) (equation 27). The tank volume is then 7,590 cu in. (124.5 l). Again using equation 25 but solving for P20 when the V20 = 6,880 cu in. (113 l) (gas volume when 1,820 cu in. (29.8 l) of fluid displaced) yields a final pressure of 2,600 psi (17.9×10^6 N/m^2). Figure 5-13 shows the volume of fluid expelled, the resulting supply pressure and the pressure required to give 1.61° (0.028 RAD) of vector angle for the first 60 sec and 1.18° (0.023 RAD) for the remainder of the flight.

Figure 5-14 depicts the passive blowdown system in the preliminary design phase. A solenoid valve which will be closed until just prior to launch is mounted on the outlet of the pressure vessel. The purpose of the valve is to prevent hydraulic fluid leakage through the servovalves during the hold period on the launch pad. This valve could be replaced by a squib valve. Quick disconnects are located on the pressure and return lines for ground checkout after assembly.

The blowdown accumulator, designed with a safety factor of 1.5, is of steel construction with walls 0.25 in. (0.635 cm) thick. There is no bladder or piston between the cold gas and hydraulic fluid. No mounting brackets are shown on the accumulator as it is shown in this position for clarity only. Table 5-8 lists the components and preliminary system weight.

$$A_p = \frac{T}{l\Delta P} = \frac{8.8 \times 10^6}{96.5\ (3,000)} = (196\ \text{cm}^2) \tag{23}$$

$$V_{TH} = \frac{1,820\ (1.25)}{0.9} = (41.5\ \text{l}) \tag{24}$$

$$P_s V_i^{\gamma} = P_3 V_3^{\gamma} \tag{25}$$

$$V_3 = V_i + 1,156 \tag{26}$$

$$V_i = \frac{1,156}{\left(\frac{4,000}{3,000}\right)^{\frac{1}{\gamma}} - 1} = (83\ \text{l}) \tag{27}$$

$$w_o t = 2.95 \tag{28}$$

$$w_o = \frac{2.95}{t} = \frac{2.95}{1.0} = (169°/\text{sec}) \tag{29}$$

$$Q = A_p \dot{X} = \frac{A_p l \dot{\delta}}{(57.3)} = \frac{30.4\ (96.5)\ (2.84)}{(57.3)} = (2.42\ \text{l/sec}) \tag{30}$$

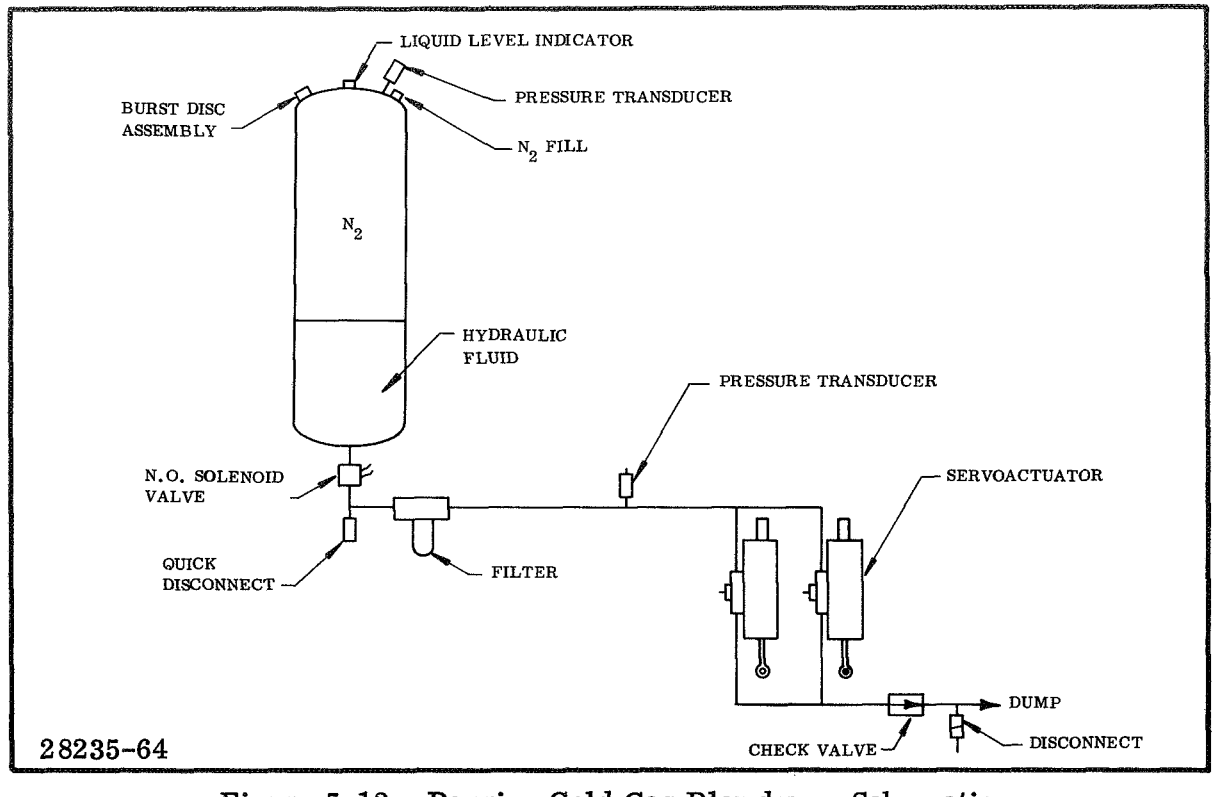

Figure 5-12. Passive Cold Gas Blowdown, Schematic

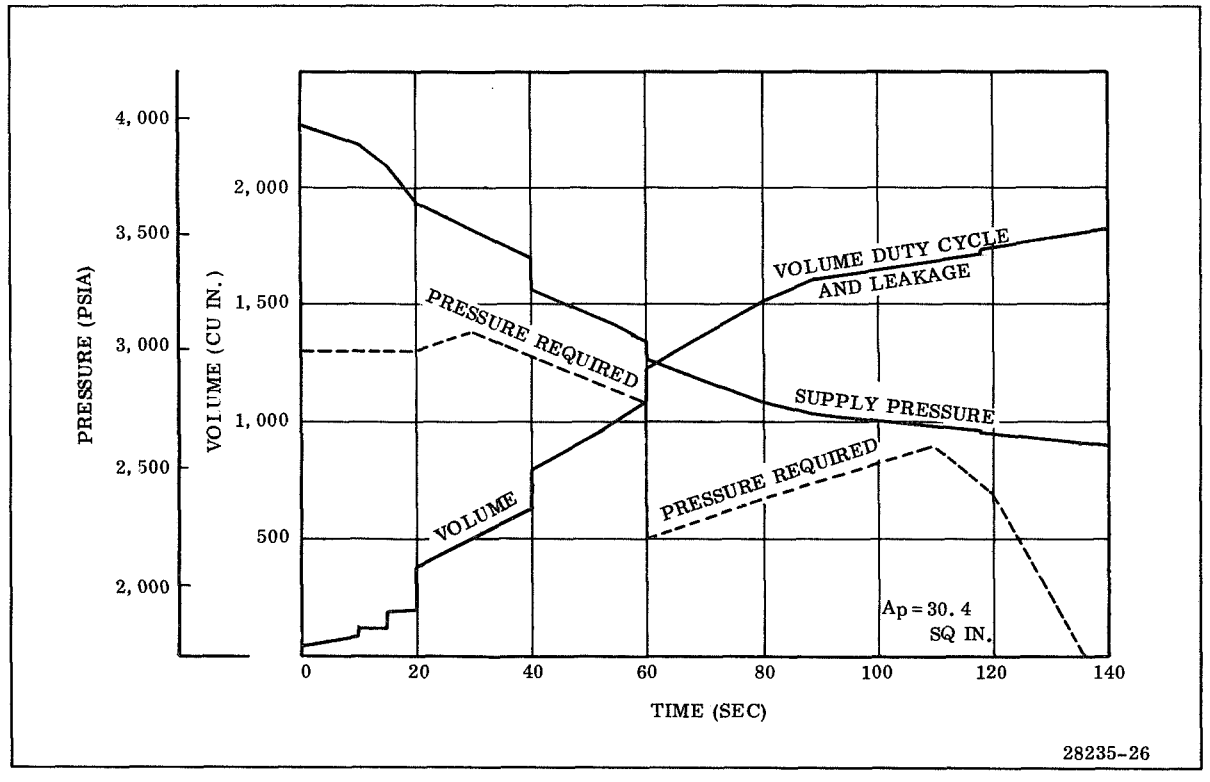

Figure 5-13. Passive Cold Gas Blowdown System Duty Cycle

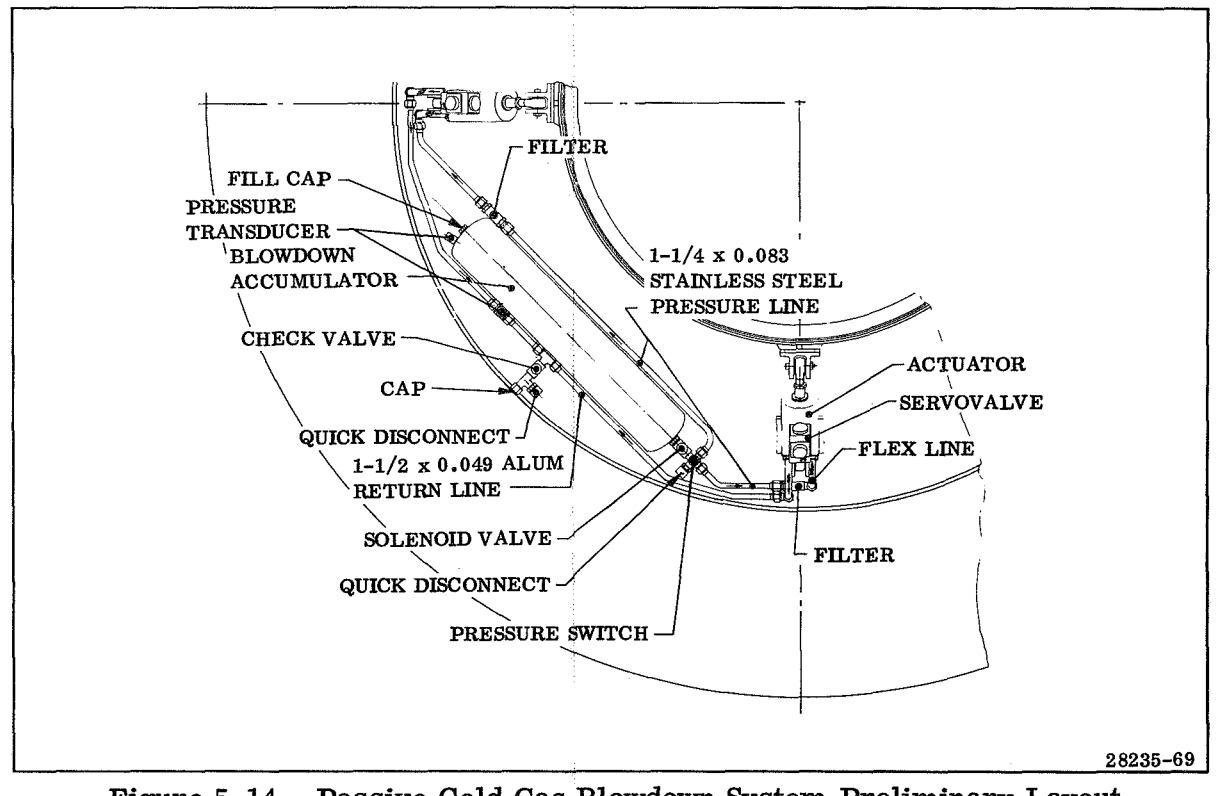

Figure 5-14. Passive Cold Gas Blowdown System Preliminary Layout

TABLE 5-8

COMPONENT WEIGHT PASSIVE BLOWDOWN SYSTEM
(Preliminary Design)

Item	Weight (lb)	SI Units (kg)
Accumulator	250	113.5
Actuator (2)	370	168.0
Servovalve (2)	38	17.2
Tubing, hose, and fitting	48	21.8
Hydraulic fluid	97	44.0
Filter (2)	14	6.35
Pressure transducer and switch	3	1.36
Quick disconnect	4	1.815
Solenoid valve	10	4.53
Nitrogen	29	13.15
Total weight	863	391.5
+10%	86	39.0
	949	430.0

5.6 Preliminary Design Review

5.6.4 Redesigned Warm Gas Solid Propellant Gas Generator Turbine Pump Systems

REDESIGNED GAS GENERATOR TURBINE PUMP SYSTEM EVALUATED TO ASSESS IMPACT OF CHANGED DESIGN REQUIREMENTS

This system is similar to the one shown by Figure 5-9 . Three different systems were redesigned differing only in the hydraulic pump output capability in order to assess the impact of the revised design requirements.

System I used a large pump without an accumulator. The required flow (using the 30.4 sq in. (196 cm^2) actuator area) is 68 gpm (4.28 l/sec) at 4,000 psi (27.6 x 10^6 N/m^2) outlet pressure.

The pump selected for System I is capable of 70 gpm (4.41 l/sec) at a speed of 5,400 rpm.

Systems II and III used a pump turning at 5,650 and 4,500 rpm, respectively. The output flow is 48 gpm (3.02 l/sec) for the former and 40 gpm (3.52 l/sec) for the latter. Accumulators were included with these systems to make up for the additional flow requirement.

Component weights for these three systems are shown in Table 5-9. The weight differences between these systems appear insignificant.

TABLE 5-9

WEIGHT BREAKDOWN OF TURBINE PUMP SYSTEM
USING REDUCED TORQUE VALUES

Item	System and Weight (lb) I	kg	II	kg	III	kg
Gas generator	115	52.2	78	35.4	67	30.4
Pump	28	12.7	19.8	8.98	19.8	8.98
Hydraulic fluid	27.7	12.55	30	13.6	31	14.05
Reservoir	11	4.99	15	6.8	17	7.7
Accumulator	--	--	20	9.07	24	10.9
Turbine gearbox	44	19.95	40	18.15	38	17.25
Tubing and fitting	50	22.7	50	22.7	50	22.7
Filter, disconnects and pressure transducer	20	9.07	20	9.07	20	9.07
Actuator (2)	370	168	370	168	370	168
Servovalve (2)	38	17.25	38	17.25	38	17.25
N_2	--	--	1.7	0.77	2.4	1.09
	703.7	319	682.5	309	677.2	307
+10% contingencies	70.3	31.9	68	30.8	68	30.8
	774	352	750.5	340	745	338

5.0 Movable Nozzle - Flexible Seal

5.7 Selection for Detail Design

PASSIVE BLOWDOWN SYSTEM SELECTED FOR DETAIL DESIGN

The passive blowdown system was chosen for further consideration in the detailed design task.

From a weight standpoint, the turbine pump system offers considerable advantage. It is also more flexible from a growth or demand viewpoint. The blowdown system is much more simple with less components and moving parts. The development risk with such a system is almost nonexistent.

The primary disadvantage with any blowdown system is the duty cycle limitation. The system presented here has a 25 percent pad which could be increased by increasing the size of the accumulator.

The blowdown system seems to have the advantage over the turbine system in every category except weight, where the advantage is slight, and the above mentioned limitation.

A cost comparison of major components is shown in Table 5-10. The cost figures are for each motor based on a total of 30 motors.

NASA LeRC selected the passive blowdown system for detail design. The major factor to be stressed is simplicity of design using the least number of components.

TABLE 5-10

PRELIMINARY COST COMPARISON OF
BLOWDOWN AND TURBINE SYSTEM

Item	System		Nonrecurring
	Blowdown	Turbine	
Gas generator	--	700	--
Actuators	40,000	40,000	150,000
Servovalves	2,944	2,944	--
Turbine gearbox	--	20,000	200,000
Pump	--	2,000	--
Accumulator	700	400	--
Total	43,644	66,044	350,000

DETAILED COLD GAS PASSIVE BLOWDOWN SYSTEM DESIGN PRESENTED

The system closely follows that presented in subsection 5.6.3 and schematic (Figure 5-12). The major components consist of two servoactuators located 90° (1.57 RAD) apart and a high pressure reservoir used as the expulsion device to provide hydraulic power to the system.

A layout of the actuation system is shown in Figures 5-15 and 5-16. The fixed end of the actuators are mounted to brackets which are bolted to the nozzle aft mounting flange. The reservoir, made of 4340 steel, is mounted on the aft skirt with the reservoir centerline parallel to the longitudinal axis of the motor. The tank contains no barrier between the pressurant and hydraulic fluid. For static test, the tank is reversed and the plumbing to the filter bracket rerouted.

Hydraulic power is supplied to the two servoactuators through flexible hose attached to hard tubing at the actuator mounting bracket. The tubing follows the nozzle aft mounting flange to the filter bracket.

Stainless steel tubing is used for all high pressure lines except for flexible hose which connect both pressure and return tubing to the actuators. Aluminum return lines, which are designed for low operating pressure, reduce system weight. The high pressure supply line has an outside diameter of 1-1/4 in. (3.18 cm) and a wall thickness of 0.089 in. (0.226 cm). This gives a safety factor of 3.8 or a burst pressure of 15,200 psi (0.105×10^9 N/m^2). One inch lines branch off the main supply line at the 180 in. (456 cm) bolt circle and follow the bolt circle to the actuator bracket where they are connected to flexible hose with swivel connectors. The 1 in. (2.54 cm) line has a wall thickness of 0.065 in. (0.165 cm) yielding a safety factor of 3.5. Burst pressure for the 1-1/4 (3.18 cm) and 1.0 in. (2.54 cm) aluminum return lines are 1,440 (9.92×10^6 N/m^2) and 1,800 psi (12.4×10^6 N/m^2) respectively. The high pressure flex hose has a burst pressure of 12,000 psi (82.7×10^6 N/m^2) while the low pressure hose has a burst pressure of 4,200 psi (29×10^6 N/m^2).

A normally open solenoid valve located at the pressurization tank outlet is closed after filling the tank to the required level with hydraulic fluid. This valve remains closed during the prefiring checkout to prevent loss of fluid and pressure through servovalve leakage. This leakage is estimated at 1.0 gpm (0.063 l/sec) for both valves. At a predetermined time before firing, the valve is opened to pressurize the system. A solenoid valve was used rather than an explosive operated valve so that it could be reclosed if a hold occurred during the final stages of the countdown.

A filter located in the hydraulic supply line has a rating of 10 micron (10×10^{-6} m) nominal/25 micron (25×10^{-6}m) absolute. The filter is secured to a bracket which mounts to the 180 in. (456 cm) bolt circle. Two quick disconnects also are mounted on the filter bracket and used to supply ground hydraulic power for prelaunch checkout of the actuation system. The high pressure quick disconnect is also used to fill the system with hydraulic fluid. A check valve designed to open at 50 psi (0.344×10^6 N/m^2) differential pressure is the return line near the filter bracket.

Four brackets mounted on the 180 in. (456 cm) bolt circle secure the pressure and return tubing in a fixed position. Details of the brackets as well as the actuator mounting brackets, flexible boss brackets, and the filter bracket are shown in Thiokol Drawing TUL 13113.

In order to fill and check out the system, the solenoid valve is de-energized. Ground hydraulic power and return lines are connected to the two quick disconnects mounted on the filter bracket. The input flow must be well filtered. A hose attached to the quick disconnect on the forward end of the tank is left open to the atmosphere to allow venting of air during filling with hydraulic fluid.

Hydraulic power is applied and the tank is allowed to fill slowly. When the liquid level transducer indicates that the tank contains the required amount of fluid, the solenoid valve is energized. With the hydraulic power still applied at low pressure, the flexible hose is bled and attached to the actuators.

The actuators are removed from the nozzle clevis and operating pressure applied to the system to check for leakage. Following this check, the actuator should be actuated from hardover to hardover for several times to rid the system of any remaining entrapped air. The actuators are then mounted to the nozzle clevis and the nozzle may be vectored if desired. Ground hydraulic power may be detached at any time prior to launch.

The pressurization tank is pressurized with GN_2 through the hose connector to the forward quick disconnects. Pressurization must be done slowly to prevent entrapment of N_2 in the hydraulic fluid and to allow time for temperature stabilization. Disconnecting the hose from the tank completes the procedure and the system is ready for operation.

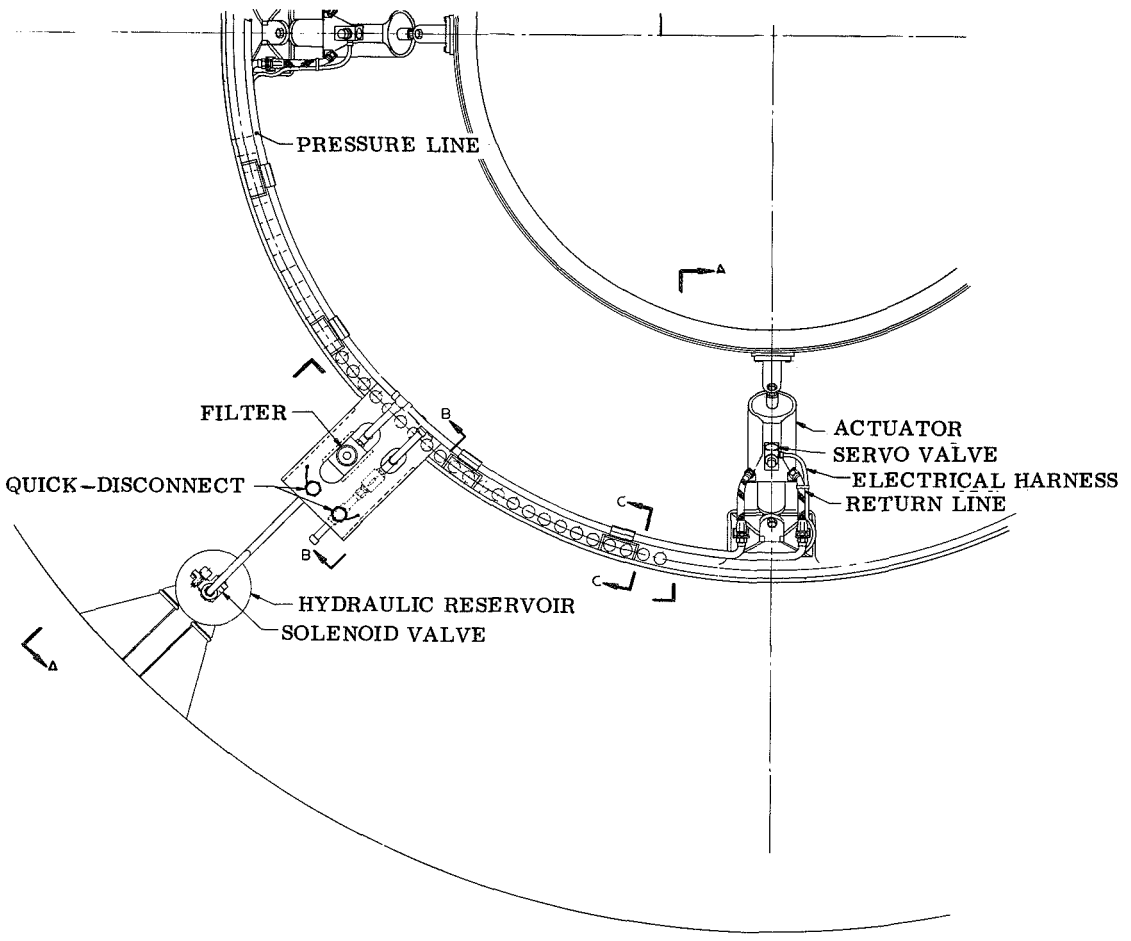

Figure 5-15. Actuation System for Movable Nozzle

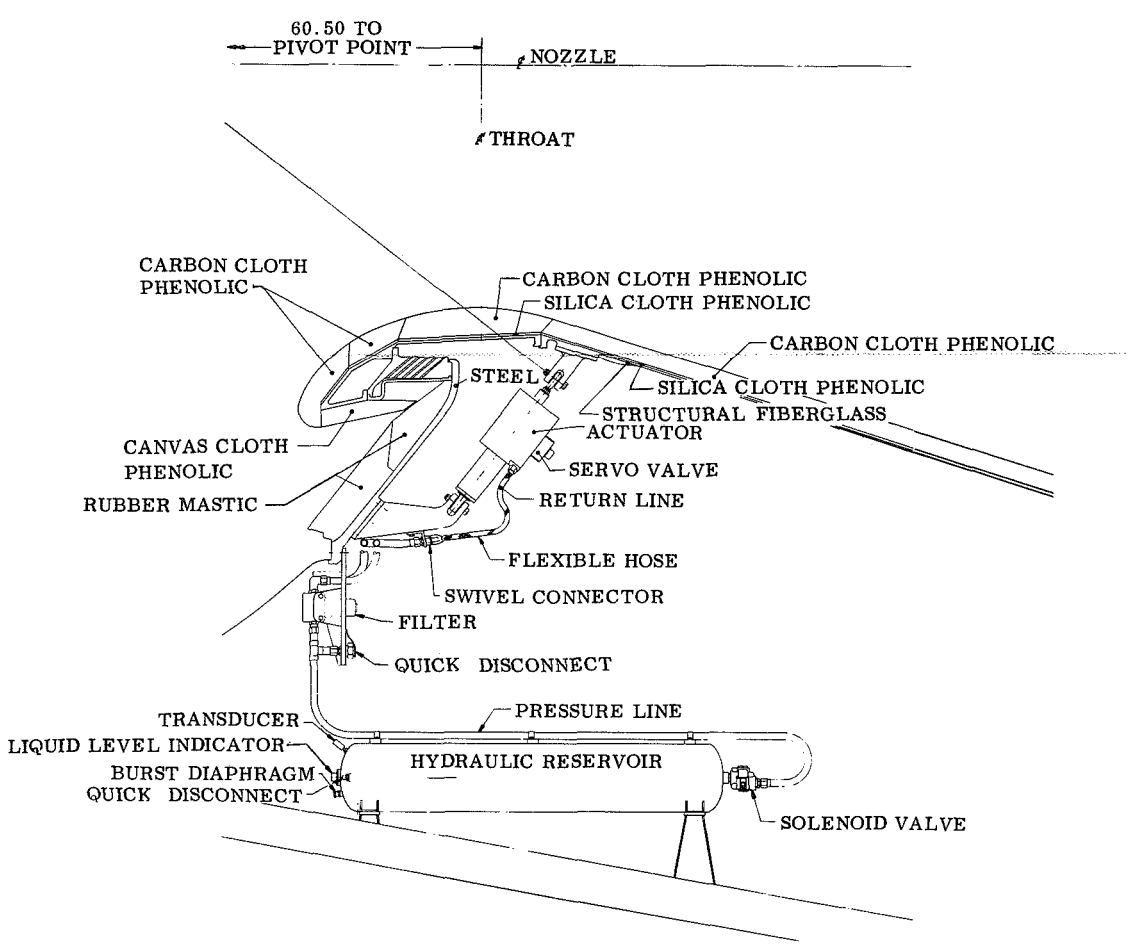

Figure 5-16. Actuation System for Movable Nozzle

5.8 Detailed Cold Gas Passive Blowdown Design

5.8.1 Analog Computer Simulation

ANALOG COMPUTER PROGRAM USED TO STUDY STABILITY AND RESPONSE CHARACTERISTIC OF TVC SYSTEM SELECTED FOR DETAIL DESIGN

The analog computer program used in this study has been in use at Thiokol for several years. The primary purpose of the program is to study the stability and response characteristics of TVC system. The results obtained with this program have agreed well with test data from static tests. A high degree of confidence has been attained in the ability of the program to predict performance of TVC actuation systems.

A block diagram of the computer setup is shown in Figure 5-17. Equations 31 thru 47 are used to generate this block diagram. The servoamplifier which sums the input and feedback signals is represented by equations 31 and 32. Since the response of the servoamplifier is much greater than the rest of the system, the dynamics are neglected and the amplifier is represented by a pure gain K_I. The servovalve dynamics are assumed to be second order as shown by equation 33. The damping ratio and natural frequency were obtained from vendor's literature. The control flow through one part of the servovalve is expressed by equations 34 and 35 where A_s is proportional to the valve flow areas. The volume of the cylinder on the high pressure side is given by equation 36 where V_0 is the volume with the piston at midstroke. Equation 37 is a flow continuity equation where the left hand term is the flow due to the compressibility of the fluid in the volume V_1. Equations 38 thru 41 are similar to the above flow equations but are for the other side of the servovalve.

The force balance on the actuator is given by equation 42 in terms of torque. The term on the left side of the equation represents the pressure force exerted by the differential pressure on the effective area (A_p) of the actuator multiplied by the lever arm to give the resulting torque available. The terms on the right side are in order: inertial torque, viscous torque, coulomb torque, seal spring and boot torque, offset torque, and internal aerodynamic torque. Some of these terms (viscous and coulomb) are difficult to define analytically; however, past experience indicates they are present to a certain degree. Although coulomb or viscous torque are not presented in the torque tabulations, they were included in the analog computer studies.

Experience with flexible bearing nozzle actuation systems indicates that the coulomb torque is approximately 5 to 10 percent of the maximum total torque. Torque is maximum at the initiation of the duty cycle and is approximately 8.8×10^6 in.-lb (0.995×10^6 N-m). This implies that coulomb torque would be between 440,000 and 880,000 in.-lb (49,700 and 99,500 N-m). For the computer study, it was decided to use as low a value as possible while still maintaining a stable system. The value used was 75,000 in.-lb (8,460 N-m).

"Twang" tests conducted on the 156 in. (396 cm) flexible bearing, fabricated and tested by Thiokol, demonstrated a damping ratio of approximately 0.2. This value of damping ratio was used initially on the analog computer and then reduced along with the coulomb friction until the minimum values were reached at which stability could still be assured. The final value of the damping ratio was 0.062.

The internal aerodynamic torque was made a function of time to account for the change in chamber pressure and grain configuration throughout the motor burning time. The function $f_3(t)$ is presented in Figure 5-18.

Equation 43 relates the actuator position to the nozzle position. The nozzle and bracket compliance is considered as a spring located between the actuator and nozzle having a rate of K_a. It may be noted that if the compliance is infinite, the actuator position is directly proportional to the nozzle position.

Equations 46 and 47 are used to generate the hydraulic supply pressure as the gas pressure decays. It was assumed that the hydraulic pressure was equal to the gas pressure in the tank at all times. The total gas volume at any time is equal to the initial volume (V_i) plus the amount of hydraulic fluid used to move the actuators plus a term for leakage.

Nomenclature for the above equations is given in Appendix H and the constants used in the final runs of the computer study are listed in Table 5-11. These constants were varied during the study to insure stability at all vector angle positions as well as to determine the capability of the system to meet the maximum vector angle and angular rate requirements.

Step inputs were applied to the program and the gains were varied in order to insure stability and the required response. System pressure was held constant for these steps since they were of short duration. Response and stability characteristics were studied at a pressure of 4,000 psi (27.6×10^6 N/m^2) and 3,000 psi (20.7×10^6 N/m^2). When system pressure was 4,000 psi (27.6×10^6 N/m^2) the torque shown in Figure 5-19 at a time of zero seconds was used. For the 3,000 psi (20.7×10^6 N/m^2) case, the torque at a time of 60 sec was used. Figures 5-20 and 5-21 show the response to a step input of hardover to hardover for the 4,000 psi (27.6×10^6 N/m^2) and 3,000 psi (20.7×10^6 N/m^2) cases, respectively. For the step from -1.61° to +1.61° (-0.028 to +0.028 RAD) note that the angular velocity peaks at approximately 4.5°/sec (0.0785 RAD/sec) at 3,000 psi (20.7×10^6 N/m^2) system supply pressure. The velocity is lower in this direction due to the manner in which offset torque is input.

A step of hardover to hardover implies a step of 3.22° (0.0562 RAD). Ninety percent of this value is 2.898° (0.0505 RAD) or approximately 1.3° (0.0227 RAD) in the positive direction. To average 3°/sec (0.0524 RAD/sec) over 2.898° (0.0505 RAD) requires a time of 2,898/3 which is 0.966 sec. From the trace in Figure 5-21 it may be seen that it takes approximately 0.9 sec to reach +1.3° (0.0227 RAD). This gives an average of 3.22°/sec (0.0562 RAD/sec).

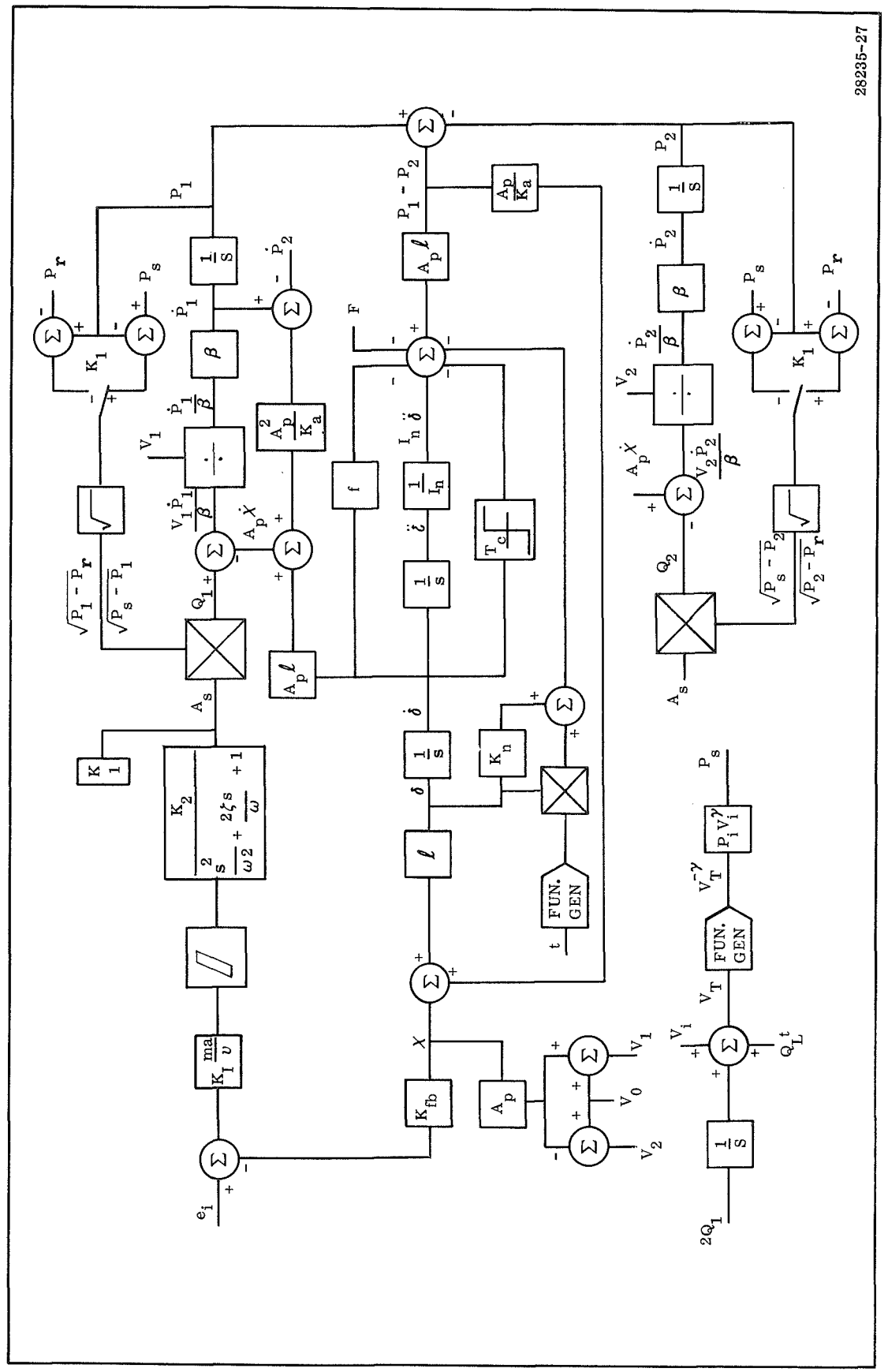

Figure 5-17. Computer Block Diagram

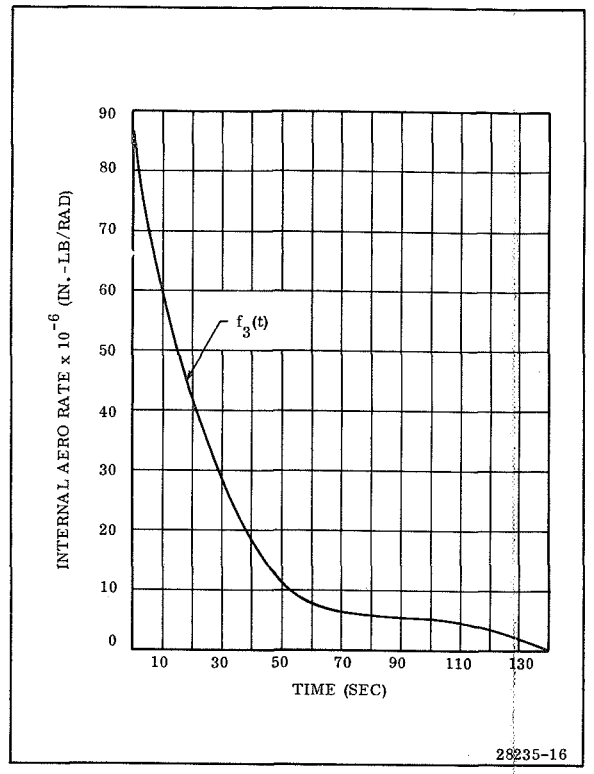

Figure 5-18. Internal Aerodynamic Spring Rate vs Time

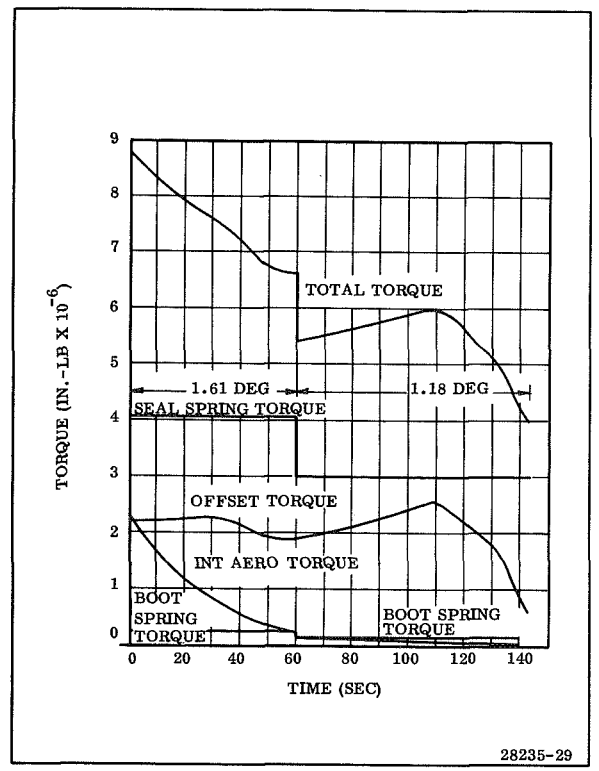

Figure 5-19. Nozzle Torque vs Time

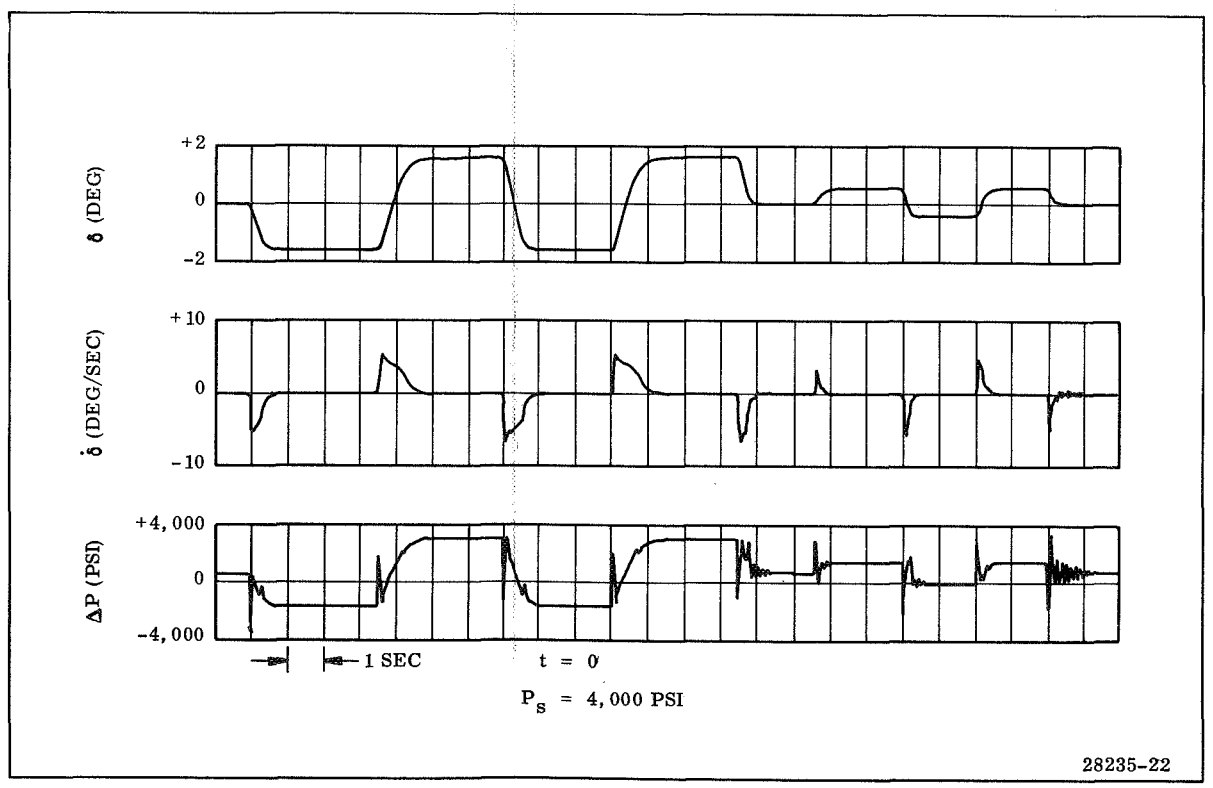

Figure 5-20. Analog Analysis

5.8 Detailed Cold Gas Passive Blowdown Design (Cont)

5.8.1 Analog Computer Simulation (Cont)

Figures 5-20 and 5-21 also show the response of the system to small step changes. This was done to insure stability for small disturbance about the null position.

The duty cycle shown in Figure 5-11 was put on magnetic tape and used as an input to the analog computer. The results are shown in Figures 5-22 and 5-23. The results of the step inputs described above prove the stability and response of the system; hence, the purpose of the duty cycle input is primarily to demonstrate the ability of the blowdown reservoir to supply sufficient pressure to allow compliance with the duty cycle over the total motor burning time. Note that at the initiation of the 1.61° (0.028 RAD) event, supply pressure had decayed to approximately 3,100 psi (21.4×10^6 N/m^2) and dropped to 3,000 psi (20.7×10^6 N/m^2) at the conclusion of the event (Figure 5-23). System pressure at the end of firing was 2,680 psi (18.5×10^6 N/m^2). The volume of oil expended over the duration of motor firing was 1,660 cu in. (27.2 l) as shown in trace 6 of Figure 5-23 and the resultant gas volume at this time is 6,720 cu in. (110 l).

Trace 3 of Figure 5-23 is essentially the pressure margin which exists at anytime. The pressure P_r is that which is required to meet the vector angle at that particular time.

The difference between supply and required pressure ($P_s - P_r$) is essentially the pressure drop across the servovalve and is a measure of the flow to the actuator. Note that the smallest pressure margin occurs at the +1.61° (0.028 RAD) event when the pressure drop is approximately 1,450 psi (10×10^6 N/m^2) at the initiation of the event and 800 psi (5.51×10^6 N/m^2) during steady state. The pressure margin increases near the end of motor burning time due to the decrease in torque and the low vector angle requirement.

As with the step inputs, flows and velocities are higher in the negative direction. This results from the fact that both the offset torque and the spring torque assist in returning the nozzle to the null position. The differential pressure across the actuator becomes very small (in fact it becomes negative for a very short period of time), allowing a large flow through the servovalve.

In general, the nozzle position follows the command very well except that a slight rounding occurs where step inputs are applied. Note that the nozzle position for the 1.61° (0.028 RAD) event (Trace 2, Figure 5-22) is slightly less than 1.60° (0.028 RAD). This is due to the structural compliance which was assumed to be 2×10^6 lb/in. (3.53×10^6 N/m).

Nozzle angular velocity reaches 3.6° /sec (0.0628 RAD/sec) in the positive direction and approximately 6.0° /sec (0.105 RAD/sec) in the negative direction. Again the high velocity occurs because the spring torque assists return of the nozzle.

The nozzle acceleration peaks at 70° /sec^2 (1.22 RAD/sec^2) in positive direction and 110° /sec^2 (1.92 RAD/sec^2) in the negative direction. These high values of acceleration result from the fact that step inputs are used to excite the system.

Using the duty cycle tape as the input, the constants listed in Table 5-11 were varied in order to determine an optimum system. Final values are those listed in the table.

TABLE 5-11

CONSTANTS USED IN COMPUTER STUDY

A_p	30 sq in. (193.5 cm^2)	V_o	90 cu in. (1.47 l)
I_n	5.296×10^6 in.-lb-sec^2 (0.597×10^6 m-N-sec^2)	β	250,000 psi (1.725×10^9 N/m^2)
K_a	2×10^6 lb/in.	ζ	1.0
K_{fb}	5.0 ν/in. (1.97 v/cm)	ω	75.39 RAD/sec
K_I	2.1 ma/ν	f_v	3.5×10^6 in.-lb sec/RAD (0.396×10^6 m-N sec/RAD)
K_n	1.52×10^8 in.-lb/RAD (0.172×10^8 m-N/RAD)	P_i	4,000 psi (27.6×10^6 N/m^2)
K_2	0.518 in.^{4}/sec lb$^{1/2}$ ma (32.0 cm^4/sec kg$^{1/2}$ ma)	V_i	5,060 cu in. (82.6 l)
l	94.5 in. (240 cm)	γ	1.4
P_o	50 psi (0.345×10^3 N/m^2)	I_{max}	10 ma
T_c	7.5×10^4 in.-lb (0.847×10^4 m-N)		

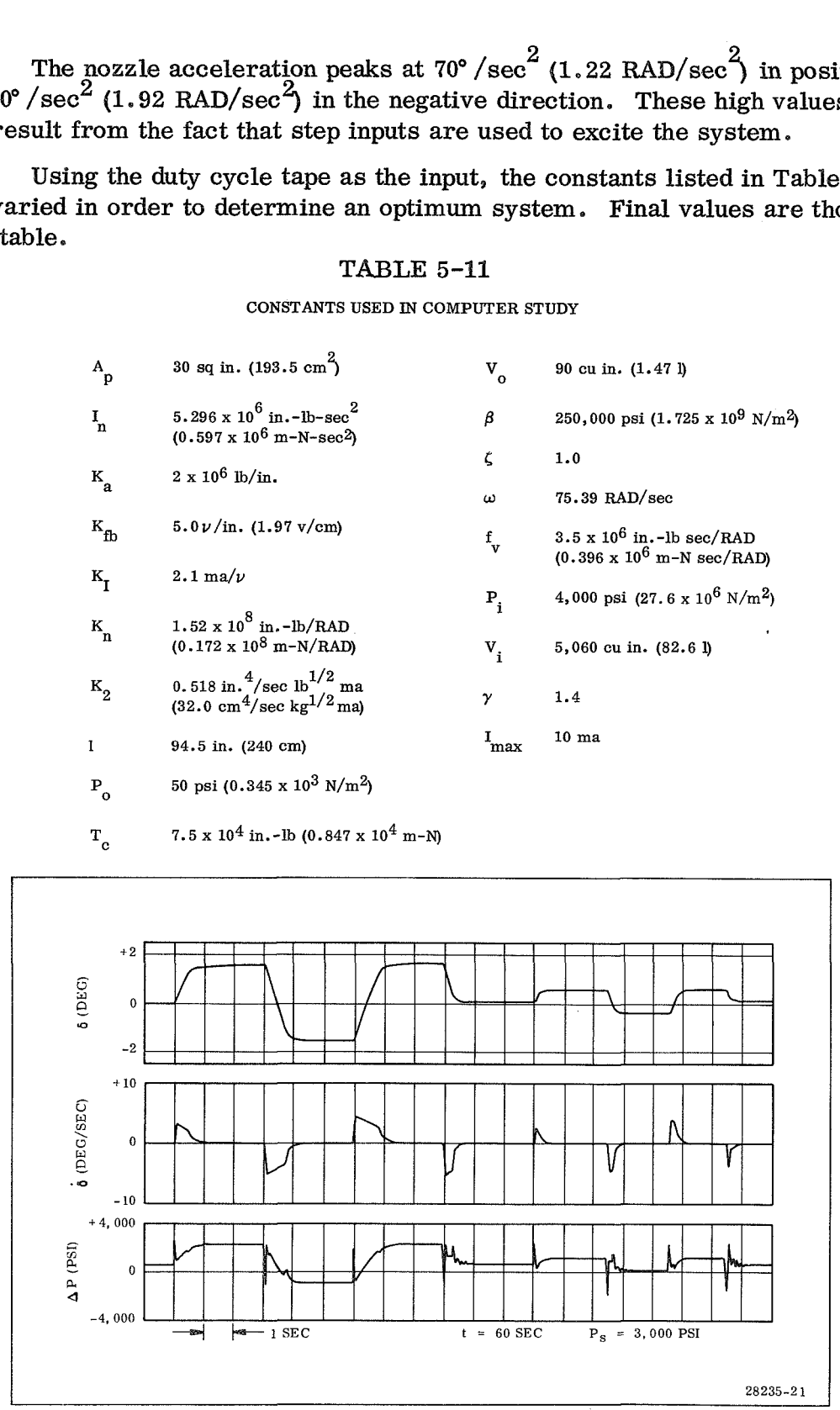

Figure 5-21. Response to Step Inputs

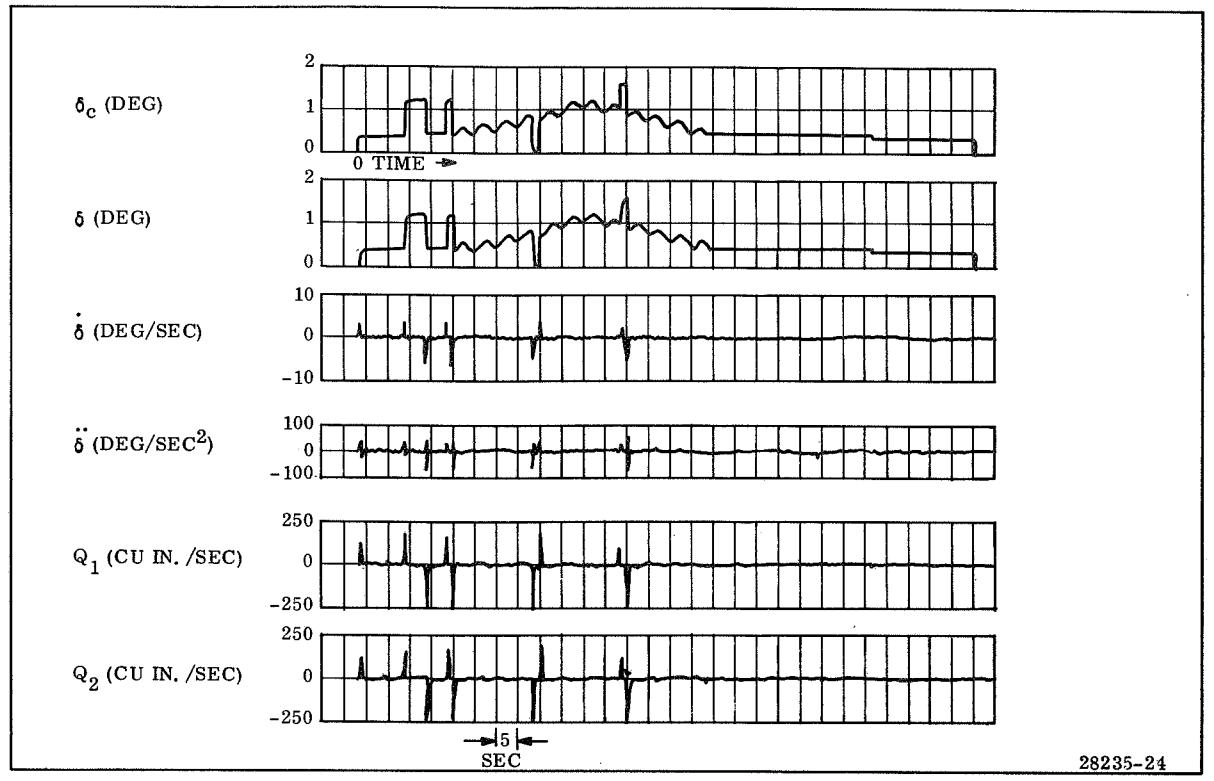

Figure 5-22. Analog Analysis

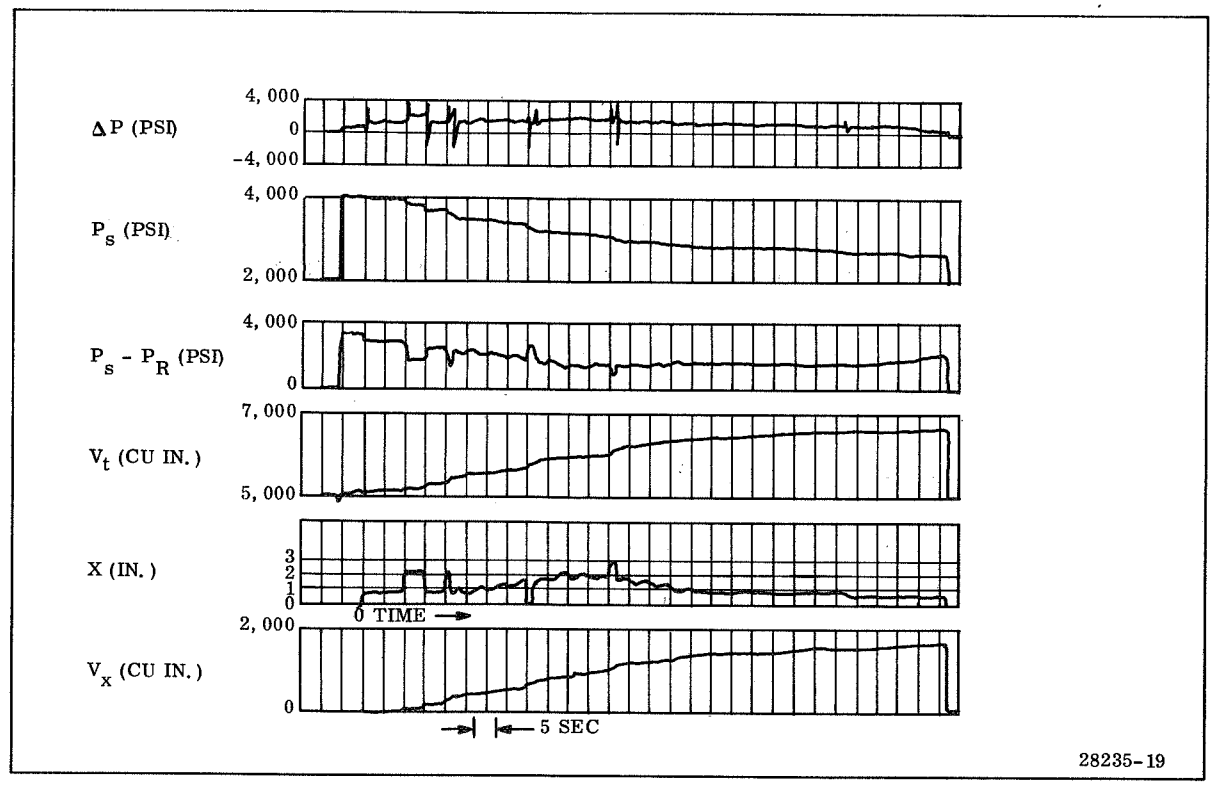

Figure 5-23. Analog Analysis

$$\epsilon = (e_i - K_{fb} x) \quad (31)$$

$$I = K_I \epsilon \quad (32)$$

$$K_2 I = \frac{\ddot{A}_s}{\omega^2} + \frac{2\zeta \dot{A}_s}{\omega} + A_s \quad (33)$$

$$Q_1 = A_s \sqrt{P_s - P_1} \qquad A \geq 0 \quad (34)$$

$$Q_1 = A_s \sqrt{P_1 - P_o} \qquad A < 0 \quad (35)$$

$$V_1 = V_o + A_p x \quad (36)$$

$$\frac{V_1 \dot{P}_1}{\beta} = Q_1 - A_p \dot{x} \quad (37)$$

$$Q_2 = A_s \sqrt{P_2 - P_o} \qquad A \geq 0 \quad (38)$$

$$Q_2 = A_s \sqrt{P_s - P_2} \qquad A < 0 \quad (39)$$

$$V_2 = V_o - A_p x \quad (40)$$

$$\frac{-V_2 \dot{P}_2}{\beta} = Q_2 - A_p \dot{x} \quad (41)$$

$$A_p (P_1 - P_2) = I_n \ddot{\delta} + f_v \dot{\delta} + T_c \frac{\dot{\delta}}{|\dot{\delta}|} + K_n \delta + F + \delta f_3(t) \quad (42)$$

$$x = A_p \frac{(P_1 - P_2)}{K_a} + \delta \quad (43)$$

$$\dot{x} = \frac{A_p (\dot{P}_1 \dot{P}_2)}{K_a} + \dot{\delta} \quad (44)$$

$$F = f_2(t) \quad (45)$$

$$P_s = P_i V_i^{\gamma} V_T^{-\gamma} \quad (46)$$

$$V_T = V_i + 2 \int_0^{143} \left(A \sqrt{P_1 - P_o} \right| dt) + 3.85\, t \quad (47)$$

5.8 Detailed Cold Gas Passive Blowdown Design

5.8.2 Servoactuator Design

SERVOACTUATOR DESIGN FOR COLD GAS PASSIVE BLOWDOWN SYSTEM DESCRIBED

The design of the servoactuator is primarily dependent upon three parameters: force, stroke, and linear rate. The force is derived from nozzle torque and actuator geometry. The stroke can be readily determined from the required nozzle vector angle and the lever arm. The linear rate can be obtained from the nozzle slew rate and lever arm.

The lever arm is defined as the perpendicular distance from the flexible bearing pivot point to the line of action of the actuator. The actuator was positioned so that the lever arm passed through the center of the rod end bearing attaching the actuator to the nozzle clevis. This distance was 94.5 in. (240 cm) and was used in all calculations in the detail design. The stroke determined from equation 13 was $\pm$2.66 in. ($\pm$6.75 cm). The actuator was designed to have a stroke of $\pm$ 2.90 in. ($\pm$7.36 cm) allowing an overtravel of 0.14 in. (0.355 cm) in either direction. A drawing of the actuator is shown in Figure 5-24.

The cylinder, constructed of 4340 steel, has an inside bore diameter of 6.474 in. (16.43 cm). Drilled passages 1/2 in. (1.27 cm) in diameter supply hydraulic fluid to both sides of the piston. The actuator rod is 2 in. (5.08 cm) in diameter and machined from 4340 steel. The piston is an integral part of the rod. Both piston and rod are chrome plated to reduce friction and increase the life of the actuator.

A linear variable differential transformer (LVDT) inserted inside the actuator rod measures actuator position for feedback to the servoamplifier. The base of the LVDT is rigidly mounted to the fixed housing, while the core is attached to the piston. The electrical leads from the LVDT are routed to a NAS type connector mounted on the fixed housing of the actuator.

Spherical self-aligning bearings are used at either end of the actuator. The bearing located in the fixed housing end of the actuator attaches to a bracket which is bolted to the aft closure near the 180 in. (456 cm) bolt circle. The rod end bearing is mounted to the nozzle clevis.

The 30 gpm (1.89 l/sec) servovalve mounts directly on the actuator as shown in Figure 5-24. The servovalve used in this application is a standard ABEX Model 425 which normally flows 25 gpm (1.575 l/sec) but with slight modification can be upgraded to obtain 30 gpm (1.89 l/sec) required to meet the design slew rate.

Servoamplified Design

Two servoamplifiers provide signals to the servovalves. The amplifiers are independent in operation but are located in the same chassis and have a common power supply.

Complete solid state circuitry consistent with current state-of-the-art technology assures high reliability with little development required. A detail design of the servoamplifier was not made because there are many current designs and operational systems similar to the one required.

A modulator-demodulator incorporated in the design will supply the necessary signals to the LVDT in the actuator and provide feedback signals through appropriate electrical network.

The nominal gain of 2.1 ma/v can be adjusted during bench tests to arrive at an optimum setting. A null bias adjust will also be incorporated. The unit requires an input power of 28 vdc at 1.0 amp.

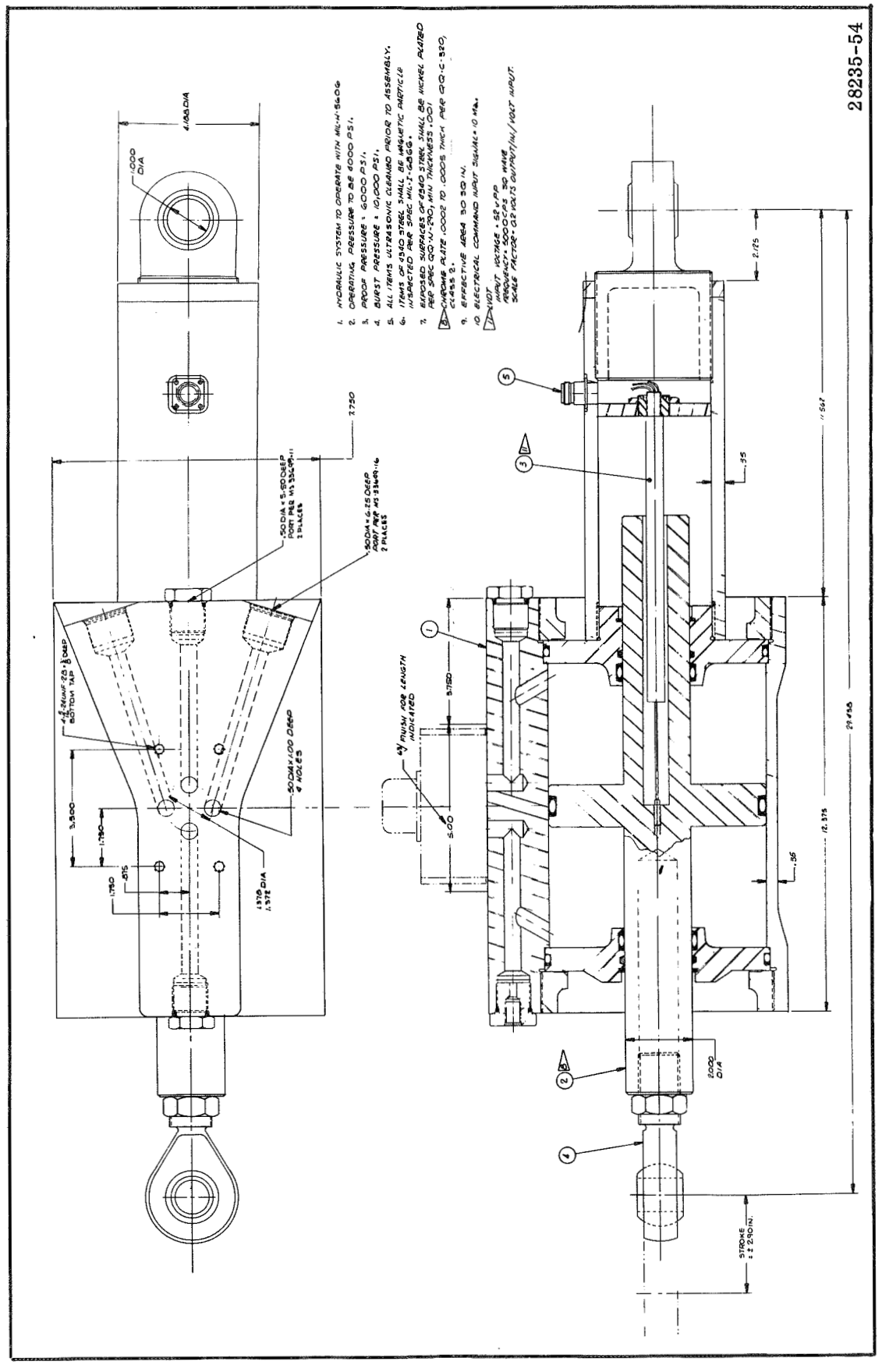

Figure 5-24. Movable Nozzle Actuator

5.8 Detailed Cold Gas Passive Blowdown Design

5.8.3 Pressurization Tank

PRESSURIZATION TANK OF COLD GAS PASSIVE BLOWDOWN SYSTEM DESCRIBED

The pressurization was sized to have a total volume of 7,590 cu in. (124.5 l). The tank was constructed of 4340 steel and heat treated to 200,000 psi (1.38×10^9 N/m^2). The tank operates at 4,000 psi (27.6×10^6 N/m^2) and is designed for a proof pressure of 6,000 psi (41.4×10^6 N/m^2) and burst pressure of 10,000 psi (68.9×10^6 N/m^2).

The pressurization tank shown in Figure 5-25 is cylindrical with elliptical end domes. The inside diameter is 12 in. (30.5 cm) and the wall thickness is 0.3 in. (0.761 cm). The length of the cylindrical section is 64.1 in. (163 cm) and the overall is 72.8 in. (185 cm). The main body of the tank is fabricated by welding the two end domes to the cylindrical center section. A vortex breaker mounted in the aft end dome is welded in place prior to the tank assembly.

The forward dome has four ports which are used for: (1) pressure transducer, (2) liquid level transducer, (3) burst disc assembly, and (4) quick disconnect for GN_2 filling. Since the drawing does not show welds around the ports, the vendor suggested a spin forming technique to fabricate the end domes. The cost of the tank reflects this technique.

Four pads welded on the cylindrical section are used to attach the tank supporting brackets which are mounted to the aft skirt. Three brackets are welded on the opposite side of the tank to support the hydraulic supply line. All brackets are symmetrically placed on the tank so that when the tank is reversed for static test, no modifications to the tank are required.

Structural analysis of the tank is given in a separate section. Longitudinal growth due to pressurization is obtained from equation 48 and amounts to 0.0328 in. (0.0834 cm). Assuming that the growth is symmetrical, this will result in an expansion of 0.0164 in. (0.0416 cm) at each set of mounting brackets. A final detailed bracket design would allow for this.

Since the tank is mounted parallel to the centerline of the motor, it is assumed that the vehicle acceleration forces will result in the hydraulic fluid being contained in the aft end of the tank with the liquid surface perpendicular to the centerline of the tank. Consequently, no barrier was placed between the pressurant and the hydraulic fluid.

$$\Delta L_p = \frac{(1 - 2\nu)\, L P_s R}{2 t_w E} \tag{48}$$

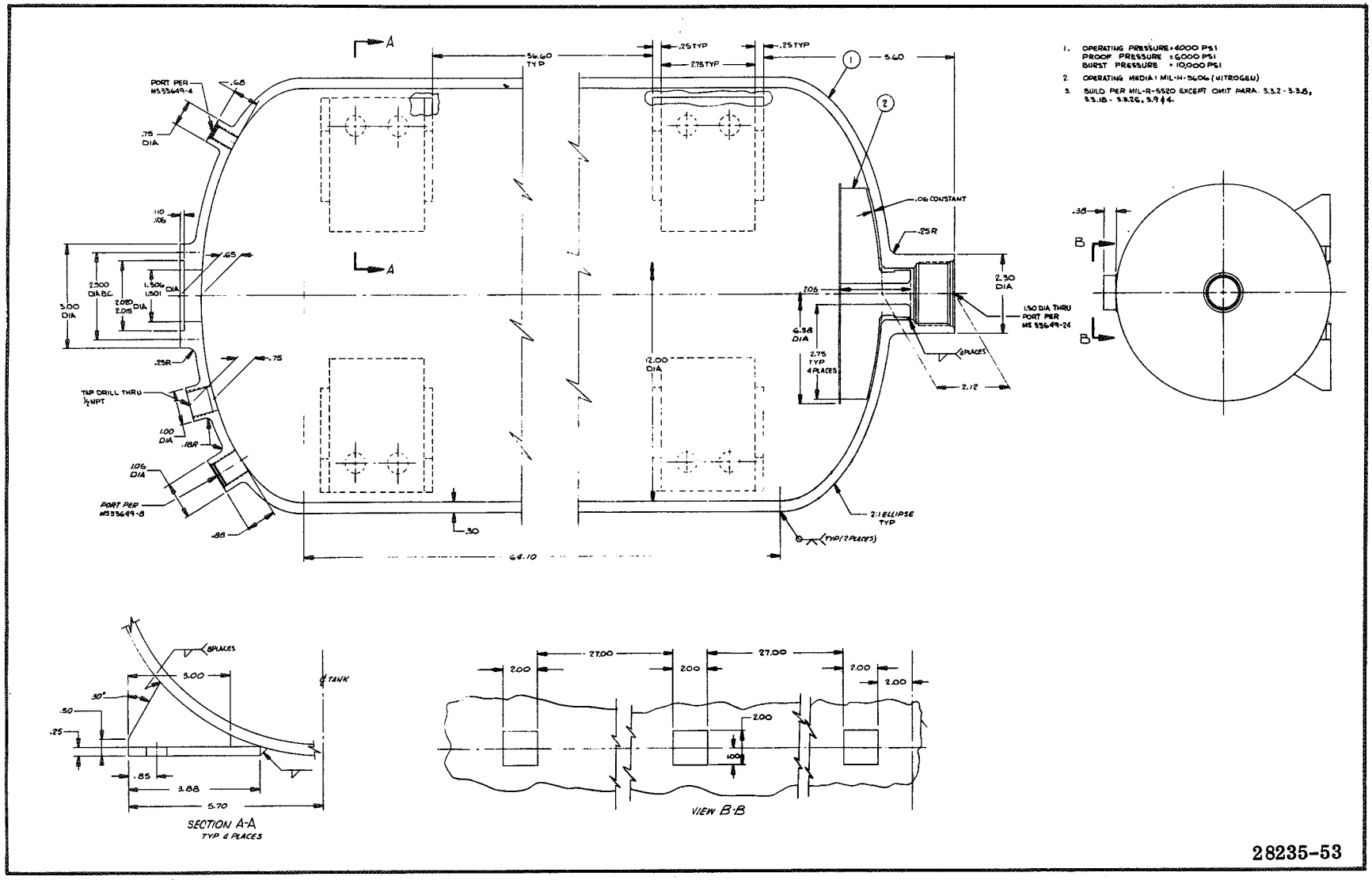

Figure 5-25. Pressurization Tank for Movable Nozzle

5.8 Detailed Cold Gas Passive Blowdown System

5.8.4 Component Weight Analysis

COMPONENT WEIGHTS OF COLD GAS PASSIVE BLOWDOWN SYSTEM PRESENTED

Actuation system total weight is 881.4 lb (400 kg). Including nozzle, the launch weight is 55,775 lb (25,300 kg). Burnout weight is 50,725 lb (23,000 kg).

Weights of the actuator, pressurization tank, and brackets were computed from drawings. Other component weights were obtained from vendors or standard tables. The total weight of the actuation system is 881.4 lb (400 kg) which includes the hydraulic fluid and the pressurant. Including the nozzle weight of 54,893.7 lb (24,900 kg) the total launch weight is 55,775.1 lb (25,300 kg). During the motor firing, hydraulic fluid will be expelled and some nozzle material will be eroded away. The weight expended amounts to 5,000 lb (2,270 kg) for the nozzle and 50 lb (22.7 kg) of hydraulic fluid. The burnout weight is 50,725 lb (23,000 kg). Component weights are shown in Table 5-12.

TABLE 5-12

ACTUAL AND COMPUTED COMPONENT WEIGHT
FOR MOVABLE NOZZLE - FLEXIBLE SEAL

Item		Weight (lb)	kg
Actuator (2)		257.0	116.5
Servovalve (2)		5.5	2.49
Actuator bracket (2)		66.1	30.0
Tank		244.5	111.0
Solenoid valve		5.2	2.36
Tank mounting brackets		14.5	6.57
GN_2		58.0	26.3
Filter bracket		30.1	13.65
Filter		4.5	2.04
Tubing and fittings		38.7	17.55
Hydraulic fluid		106.1	48.2
Miscellaneous brackets and hardware		36.3	16.45
Accessory equipment		14.9	6.75
	Subtotal	881.4	400
Nozzle weight		54,893.7	24,900
	Total	55,775.1	25,300
Burnout weight (lb)	50,725	23,000	

5.8 Detailed Cold Gas Passive Blowdown System Design

5.8.5 Critical Area Stress Analysis

CRITICAL AREA STRESS ANALYSIS PERFORMED TO SIZE CRITICAL ACTUATION SYSTEM COMPONENTS

To properly size the major actuation system components for the movable nozzle-flexible seal, a critical area stress analysis was performed. The detailed analysis is included as Appendix G.

The primary approach employed in the analysis of the actuator cylinder was a strain compatibility solution for determining stress in a thin-walled pressure vessel. This discontinuity analysis was performed using a computer program. The pressure vessel is divided into various geometrical shapes, and expressions found for their deflection and rotation in terms of pressure, moment, and shear. The equations are solved and stresses determined at the free body junctures. The actuator is designed for an operating pressure of 4,000 psig (27.6×10^6 N/m^2), a proof pressure of 6,000 psig (41.4 N/m^2) and an ultimate pressure of 10,000 psig (68.9×10^6 N/m^2).

After this general analysis procedure is applied, there are areas which require specialized analysis. The actuator rod is in both tension and compression depending on direction of movement; therefore, it is sized to withstand both tensile stress and compressive column buckling. The end plates on the actuator must withstand the same pressures as the cylinder itself and so it was assumed they were circular plates with a uniform pressure and simply supported. The equations for circular plates were taken from "Formulas for Stress and Strain," by Raymond J. Roark.

The connecting linkage such as pins, clevises, actuator brackets, and threads was analyzed for stresses and deflections caused by the actuator loads. The pins were assumed to be a uniformly loaded pin ended beam. Shearout and bearing stresses were calculated on the connecting clevises and threads. The actuator bracket was designed for the bending moment caused by the lever arm between the case and the actuator. The bolts and welds that attach the bracket to the case were designed to withstand this same moment. The deflections of these parts were caused by the same loads and were calculated for nozzle compliance.

The pressurization tank was designed with a 12 in. (30.5 cm) cylinder ID and 2:1 elliptical domes. An ultimate pressure of 10,000 psig (68.9×10^6 N/m^2) was used to calculate the basic wall thickness. To assure compatibility between the domes and cylinder, a discontinuity analysis was made on the computer. The pressure vessel was divided into various geometrical shapes and expressions found for their

deflection and rotation in terms of pressure, moment, and shear. The equations are solved and stresses determined at the free body junctures. The cylinder and 2:1 elliptical domes proved compatible.

5.0 Movable Nozzle - Flexible Seal

5.9 Cost Analysis for Detail Design

COST BREAKDOWN PROVIDED FOR MOVABLE NOZZLE - FLEXIBLE SEAL

The cost breakdown for the movable nozzle flexible seal includes the following.

1. Overall cost summary.
2. Unit cost of components.
3. Test hardware costs.
4. Materials, tooling, and facility costs.
5. Labor costs.
6. Freight, travel, and computer rental.

In order to prepare cost estimates for the development and production of the movable nozzle flexible seal TVC system, extensive planning was done. This planning included preparation of manufacturing plans which detailed the various assembly and inspection operations, and development program plans, which describe what is considered to be a reasonable development and qualification effort for the TVC system. The development program plan is included in this report as Appendix F.

The overall cost summary for the movable nozzle-flexible seal program is spread in Table 5-13.

Table 5-14 provides a breakdown of the system components on a unit cost basis.

Table 5-15 describes the estimated cost of the test hardware required for system development testing. This testing is described in Appendix F.

As can be seen in Tables 5-16 and 5-17, the costs for the submerged movable nozzle are significantly higher than the other system components. The importance of having low cost ablative materials is emphasized when working with nozzles of such large proportions.

Table 5-18 is shown to describe the material costs breakdown for the estimated period of performance.

Labor costs in terms of hours and dollars are spread in Tables 5-19 and 5-20.

Miscellaneous costs which could be expected during the forecasted development and production program are shown in Table 5-21.

TABLE 5-13

FLEX BEARING TVC SYSTEM SUMMARY

	1971		1972		1973		1974		1975		1976		1977		
	First	Second	First	Second	First	Second	First	Second	First	Second	First	Second	First	Second	Total
1. Design															
Labor	96,000	100,200	20,340	14,140	--	--	--	--	--	--	--	--	--	--	230,680
2. Component development and system testing															
Labor	3,143	70,631	--	--	--	--	--	--	--	--	--	--	--	--	73,774
Material	377,814	201,075	--	--	--	--	--	--	--	--	--	--	--	--	578,889
3. Qualification (3 R & D systems)															
Labor	--	2,531	848,886	--	--	--	--	--	--	--	--	--	--	--	851,417
Material	--	265,000	2,153,716	--	--	--	--	--	--	--	--	--	--	--	2,418,716
4. PFRT (7 PFRT systems)															
Labor	--	--	219,512	1,801,093	--	--	--	--	--	--	--	--	--	--	2,020,605
Material	--	--	684,572	4,107,432	--	--	--	--	--	--	--	--	--	--	4,792,004
5. Production (20 systems)															
Labor	--	--	--	--	522,386	544,343	552,427	575,187	583,271	607,697	616,585	642,551	651,534	679,003	5,974,984
Material	--	--	--	--	1,369,144	1,369,144	1,369,144	1,369,144	1,369,144	1,369,144	1,369,144	1,369,144	1,369,144	1,369,144	13,691,440
6. Administration and support															
Labor	84,261	87,823	89,110	92,927	94,266	98,327	99,777	104,018	105,525	110,038	111,633	116,409	118,078	123,149	1,435,341
Other direct	8,782	11,914	49,125	78,630	25,320	26,360	26,742	27,822	28,205	29,362	29,782	31,012	31,438	32,740	437,234
Total direct cost	570,000	739,174	4,065,261	6,094,222	2,011,116	2,038,174	2,048,090	2,076,171	2,086,145	2,116,241	2,127,144	2,159,116	2,170,194	2,204,036	32,505,084
Estimated overhead	346,910	488,903	2,409,629	3,804,976	1,230,487	1,269,383	1,283,647	1,323,993	1,338,320	1,381,575	1,397,238	1,443,138	1,459,072	1,507,636	20,684,904
Total cost	916,910	1,228,077	6,474,890	9,899,196	3,241,603	3,307,557	3,331,737	3,400,164	3,424,465	3,497,816	3,524,382	3,602,254	3,629,266	3,711,672	53,189,989

TABLE 5-14

MOVABLE NOZZLE SYSTEM COMPONENTS
(ROM Cost Summary)

Item No.	Component	Vendor Tooling and Devel Costs	Per Unit Costs
1	Pressurization tank No. TUL 13098	$112,191	$ 7,057
2	Solenoid valve	--	385
3	Quick disconnect	--	40
4	Burst disc assembly	--	20
5	Pressure transducer - (2 each at $1,200 each)	--	2,400
6	Liquid level sensor	--	1,800
7	Hydraulic fluid (15.3 gal at $2.25/gal)	--	34
8	GN_2 - (800 cu ft at $0.01 SCF)	--	8
9	Brackets and clamps		
	Nozzle clevis (2)	--	--
	Actuator mount (2)	--	--
	Filter (1)	--	--
	Flex hose mounting (4)	--	--
	Tank mounting (4)	--	--
	Main hydraulic supply line (3)	--	--
	Pressure and return clamp (4)	--	--
	Total 20 units = 141.5 lb - No. 4130 steel at $0.47 lb	--	67
10	Actuators (No. TUL 13093) - (2 each at $4,620 each)	44,745	9,240
11	Servovalve - (2 each at $1,000 each)	--	2,000
12	Filter	--	165
13	Check valve	--	103
14	Quick disconnects - (2 each at $50 each)	--	100
15	Servoamplifiers/elec harness	--	9,000
16	ΔP transducers - (2 each at $500 each)	--	1,000
17	Tubing		
	1-1/4 in. x 0.089 S/Steel (136 in. at $3.50/ft)	--	40
	1-1/4 in. x 0.035 aluminum (16 in. at $3.50/ft)	--	5
	1 in. x 0.065 S/Steel (142 in. at $3.50/ft)	--	41
	1 in. x 0.035 aluminum (142 in. at $3.50/ft)	--	41
18	Flex hose (high pressure) - (2 each at $85)	--	170
19	Flex hose (low pressure) - (2 each at $85)	--	170
20	Swivel connectors 1 in. (4 each at $15)	--	60
21	Unions 1 in. (8 each at $5)	--	40
22	Tee 1 in. (2 each at $5)	--	10
23	90° elbow - 1-1/4 in. (2 each at $5)	--	10
24	Tee - 1-1/4 in. (2 each at $7)	--	14
		$156,936	$34,020

NOTE:
All estimates are Thiokol Engineering estimates or catalog prices, except items numbered: (1) pressurization tank, (2) solenoid valve, (4) burst disc assembly, (6) liquid level sensor, (10) actuators, (11) servovalve, (12) filter, and (13) check valve, which were obtained from a vendor quote.

TABLE 5-15

260 IN. FLEXIBLE BEARING NOZZLE BENCH TEST HARDWARE
(ROM Cost Summary)

Description	Total Cost
Flex bearing test fixture	$62,451
Environmental test fixture	15,000
Burst test fixture	2,000
Laboratory test materials	2,000
Hydraulic oil - (144 gal at $2.25/gal)	325
Gaseous nitrogen (5 cu ft) - (10,000 SCF at $0.01/SCF)	100
S/steel tubing, 1-1/4 in. x 0.065 - (500 ft at $2.00/ft)	1,000
S/steel tubing, 1 in. x 0.065 - (500 ft at $2.00/ft)	1,000
S/steel tubing, 3/4 in. x 0.049 - (500 ft at $1.50/ft)	750
S/steel tubing, 1/4 in. x 0.028 - (500 ft at $1.25/ft)	620
Fittings (misc size) - (200 each at $5.00)	1,000
Harness - (2 sets at $1,000/set)	2,000
Instrumentation (lab test)	3,000
Total	$91,246

All estimates are Thiokol Engineering estimates based on historical data or catalog prices, except for the flexible bearing test fixture which is an AGC figure provided by Mr. J. Pelouch, NASA Program Manager.

TABLE 5-16

260 IN. SUBMERGED FLEX SEAL NOZZLE
(ROM Cost Summary)

A preliminary survey revealed that all facilities required, such as autoclave, hydroclave and presses, are available in the industry on a rental basis. With the exception of an exit cone mandrel, all tooling also appears to be available. Slight modifications will be required.

kg			Per Unit Costs
	Tooling: exit cone mandrel		$180,000
	Facilities: rental		85,000
	Materials:		
12,180	26,808 lb canvas wrap tape at $ 1.50	$ 40,212	
3,460	7,636 lb carbon wrap tape at $18.50	141,266	
1,660	3,658 lb carbon bias tape at $19.50	71,331	
2,780	6,127 lb silica wrap tape at $ 5.10	31,248	
1,960	4,251 lb mastic NBR at $ 4.50	19,130	
2,078	4,570 lb glass wrap tape at $ 2.80	12,796	
5,870	12,938 lb machined steel at $20.00	258,760	574,743
	Total materials and tooling		$839,743
	Total labor hours		35,000

All estimates are Thiokol Engineering estimates based on historical data gained through various other nozzle programs.

TABLE 5-17

260 INCH FLEXIBLE SEAL, NOZZLE
(ROM Cost Summary)

Non-Recurring Costs	
Design	$ 59,992
Rubber tubing tooling	14,751
Special tooling	36,306
	$111,049
Flex Seal Fabrication (Unit Cost)	
Materials and laboratory	$ 52,042
Labor	23,767
	$ 75,809

NOTE:
Costs are Aerojet costs for a two seal program, provided by Mr. J. Pelouch of NASA. The cost for the test fixture, the two flex-seals and associated testing, have been incurred by NASA; consequently, these costs could be subtracted from the program summary to determine the net expenditure.

TABLE 5-18

FLEX BEARING TVC SYSTEM MATERIAL

	1971		1972		1973		1974		1975		1976		1977		Total	Remarks
	First	Second	First	Second	First	Second	First	Second	First	Second	First	Second	First	Second		
1. Design	--	--	--	--	--	--	--	--	--	--	--	--	--	--	--	
2. Components development and system testing																
Flex seal - Components	75,809	75,809	--	--	--	--	--	--	--	--	--	--	--	--	151,618	2 flexible seals at 75,809 each
Tooling	111,049	--	--	--	--	--	--	--	--	--	--	--	--	--	111,049	Aerojet supplied cost
System - Components	34,020	34,020	--	--	--	--	--	--	--	--	--	--	--	--	68,040	2 component systems at 34,020 each
Tooling	156,936	--	--	--	--	--	--	--	--	--	--	--	--	--	156,936	Engineering estimate
Bench test hardware	--	91,246	--	--	--	--	--	--	--	--	--	--	--	--	91,246	Engineering estimate
3. Qualification (3 R & D systems)																
Flex seals	--	--	227,427	--	--	--	--	--	--	--	--	--	--	--	227,427	3 flexible seals at 75,809 each
System components	--	--	102,060	--	--	--	--	--	--	--	--	--	--	--	102,060	3 component system components at 34,020 each
Nozzles	--	--	1,724,229	--	--	--	--	--	--	--	--	--	--	--	1,724,229	3 nozzles at 574,734 each
Operational assembly tooling	--	--	100,000	--	--	--	--	--	--	--	--	--	--	--	100,000	Independent Engineering estimate
Nozzle fabrication tooling	--	180,000	--	--	--	--	--	--	--	--	--	--	--	--	180,000	
Nozzle fabrication facilities	--	85,000	--	--	--	--	--	--	--	--	--	--	--	--	85,000	
4. PFRT (7 PFRT units)																
Flex seals	--	--	75,809	454,854	--	--	--	--	--	--	--	--	--	--	530,663	7 flexible seals at 75,809 each
Nozzles	--	--	574,743	3,448,458	--	--	--	--	--	--	--	--	--	--	4,023,201	7 nozzles at 574,743 each
System components	--	--	34,020	204,120	--	--	--	--	--	--	--	--	--	--	238,140	7 systems at 34,020 each
5. Production																
Flex seals	--	--	--	--	151,618	151,618	151,618	151,618	151,618	151,618	151,618	151,618	151,618	151,618	1,516,180	20 flexible seals at 75,809 each
Nozzles	--	--	--	--	1,149,486	1,149,486	1,149,486	1,149,486	1,149,486	1,149,486	1,149,486	1,149,486	1,149,486	1,149,486	11,494,860	20 nozzles at 574,743 each
System components	--	--	--	--	68,040	68,040	68,040	68,040	68,040	68,040	68,040	68,040	68,040	68,040	680,400	20 systems at 34,020 each
Total	377,814	466,075	2,838,288	4,107,432	1,369,144	1,369,144	1,369,144	1,369,144	1,369,144	1,369,144	1,369,144	1,369,144	1,369,144	1,369,144	21,481,049	

TABLE 5-19

FLEX BEARING TVC SYSTEM
(Labor Hours)

	1971		1972		1973		1974		1975		1976		1977		Total	Remarks
	First	Second	First	Second	First	Second	First	Second	First	Second	First	Second	First	Second		
1. Design																
Engineering	15,000	15,000	3,000	2,000	--	--	--	--	--	--	--	--	--	--	35,000	Engineering estimate
2. Component development and system testing																
Engineering - flexible bearing test	--	4,200	--	--	--	--	--	--	--	--	--	--	--	--	4,200	Engineering estimate
System testing	--	4,920	--	--	--	--	--	--	--	--	--	--	--	--	4,920	Engineering estimate
Manufacturing - brackets	--	1,674	--	--	--	--	--	--	--	--	--	--	--	--	1,674	Independent engineering estimate
Quality control - receiving inspection	620	369	--	--	--	--	--	--	--	--	--	--	--	--	989	Statistically estimated - hours to material cost
3. Qualification (3 R & D systems)																
Engineering - flexible bearing acceptance	--	--	600	--	--	--	--	--	--	--	--	--	--	--	600	Engineering estimate
Support static test	--	--	26,000	--	--	--	--	--	--	--	--	--	--	--	26,000	Engineering estimate
Manufacturing - brackets	--	--	2,511	--	--	--	--	--	--	--	--	--	--	--	2,511	Independent engineering estimate
Assembly	--	--	1,920	--	--	--	--	--	--	--	--	--	--	--	1,920	Independent engineering estimate
Technician - nozzle fabrication	--	--	105,000	--	--	--	--	--	--	--	--	--	--	--	105,000	Engineering estimate
Quality control - receiving inspection	--	485	3,959	--	--	--	--	--	--	--	--	--	--	--	4,444	Statistically estimated - hours to material cost
4. PFRT (7 PFRT systems)																
Engineering - flexible bearing acceptance	--	--	--	1,400	--	--	--	--	--	--	--	--	--	--	1,400	Engineering estimate
Support test	--	--	--	56,000	--	--	--	--	--	--	--	--	--	--	56,000	Engineering estimate
Manufacturing - brackets	--	--	837	5,022	--	--	--	--	--	--	--	--	--	--	5,859	Independent engineering estimate
Assembly	--	--	--	4,480	--	--	--	--	--	--	--	--	--	--	4,480	Independent engineering estimate
Technician - nozzle fabrication	--	--	35,000	210,000	--	--	--	--	--	--	--	--	--	--	245,000	Engineering estimate
Quality control - receiving inspection	--	--	1,258	7,550	--	--	--	--	--	--	--	--	--	--	8,808	Statistically estimated - hours to material cost
5. Production (20 systems)																
Engineering - test support	--	--	--	--	7,000	7,000	7,000	7,000	7,000	7,000	7,000	7,000	7,000	7,000	70,000	Engineering estimate
Flexible bearing test	--	--	--	--	400	400	400	400	400	400	400	400	400	400	4,000	Engineering estimate
Manufacturing - brackets	--	--	--	--	1,674	1,674	1,674	1,674	1,674	1,674	1,674	1,674	1,674	1,674	16,740	Independent engineering estimate
Assembly	--	--	--	--	1,600	1,600	1,600	1,600	1,600	1,600	1,600	1,600	1,600	1,600	16,000	Independent engineering estimate
Technician - nozzle fabrication	--	--	--	--	70,000	70,000	70,000	70,000	70,000	70,000	70,000	70,000	70,000	70,000	700,000	Engineering estimate
Quality control - receiving inspection	--	--	--	--	2,516	2,516	2,516	2,516	2,516	2,516	2,516	2,516	2,516	2,516	25,160	Statistically estimated - hours to material cost
6. Support																
Program Management	3,510	3,510	3,510	3,510	3,510	3,510	3,510	3,510	3,510	3,510	3,510	3,510	3,510	3,510	49,140	
Finance and Administration	1,776	1,776	1,776	1,776	1,776	1,776	1,776	1,776	1,776	1,776	1,776	1,776	1,776	1,776	24,864	
Requirements	3,432	3,432	3,432	3,432	3,432	3,432	3,432	3,432	3,432	3,432	3,432	3,432	3,432	3,432	48,048	
Project Engineering	4,038	4,038	4,038	4,038	4,038	4,038	4,038	4,038	4,038	4,038	4,038	4,038	4,038	4,038	56,532	

TABLE 5-20

FLEX BEARING TVC SYSTEM
(Labor Dollars)

	1971		1972		1973		1974		1975		1976		1977		
	First	Second	First	Second	First	Second	First	Second	First	Second	First	Second	First	Second	Total
1. Design															
Engineering	96,000	100,200	20,340	14,140	--	--	--	--	--	--	--	--	--	--	230,680
2. Components development and system testing															
Engineering	--	60,921	--	--	--	--	--	--	--	--	--	--	--	--	60,921
Quality control	3,143	1,926	--	--	--	--	--	--	--	--	--	--	--	--	5,069
Manufacturing	--	7,784	--	--	--	--	--	--	--	--	--	--	--	--	7,784
3. Qualification (3 R & D systems)															
Engineering	--	--	180,348	--	--	--	--	--	--	--	--	--	--	--	180,348
Technician	--	--	626,850	--	--	--	--	--	--	--	--	--	--	--	626,850
Quality control	--	2,531	20,863	--	--	--	--	--	--	--	--	--	--	--	23,394
Manufacturing	--	--	20,825	--	--	--	--	--	--	--	--	--	--	--	20,825
4. PFRT (7 PFRT systems)															
Engineering	--	--	--	405,818	--	--	--	--	--	--	--	--	--	--	405,818
Technician	--	--	208,950	1,308,300	--	--	--	--	--	--	--	--	--	--	1,517,250
Quality control	--	--	6,629	40,996	--	--	--	--	--	--	--	--	--	--	47,625
Manufacturing	--	--	3,933	45,989	--	--	--	--	--	--	--	--	--	--	49,922
5. Production (20 systems)															
Engineering	--	--	--	--	50,190	52,360	53,130	55,370	56,140	58,590	59,430	62,020	62,930	65,590	575,750
Technician	--	--	--	--	442,400	461,300	468,300	487,900	494,900	515,900	523,600	546,000	553,700	577,500	5,071,500
Quality control	--	--	--	--	13,787	14,215	14,366	14,794	14,945	15,397	15,548	16,001	16,177	16,630	151,860
Manufacturing	--	--	--	--	16,009	16,468	16,631	17,123	17,286	17,810	18,007	18,530	18,727	19,283	175,874
6. Administration and support															
Program management	26,009	27,097	27,483	28,676	29,097	30,326	30,782	32,081	32,537	33,941	34,433	35,097	36,433	37,978	442,780
Finance and administration	9,998	10,425	10,567	11,028	11,188	11,668	11,828	12,343	12,520	13,053	13,248	13,817	14,012	14,616	170,311
Requirements	17,606	18,361	18,635	19,425	19,699	20,557	20,866	21,758	22,067	23,028	23,371	24,367	24,710	25,774	300,224
Project engineering	30,648	31,940	32,425	33,798	34,282	35,776	36,201	37,836	38,401	40,016	40,581	42,318	42,923	44,781	522,026
Total	183,404	261,185	1,177,848	1,908,170	616,652	642,670	652,204	679,205	688,796	717,735	728,218	758,960	769,612	802,152	10,586,811

TABLE 5-21

FLEX BEARING TVC SYSTEM
(Other Direct)

	1971		1972		1973		1974		1975		1976		1977			
	First	Second	First	Second	First	Second	First	Second	First	Second	First	Second	First	Second	Total	Remarks
1. Freight	86	107	652	944	314	314	314	314	314	314	314	314	314	314	4,929	0.023% of material cost
2. Travel	7,336	10,447	45,113	76,326	24,666	25,706	26,088	27,168	27,551	28,208	29,128	30,358	30,784	32,086	423,465	4% of labor
3. Computer rental	1,360	1,360	1,360	1,360	340	340	340	340	340	340	340	340	340	340	8,840	20 hr per year thru PFRT - 5 hr per year production
Total	8,782	11,914	49,125	78,630	25,320	26,360	26,742	27,822	28,205	29,362	29,782	31,012	31,438	32,740	437,234	

CONTENTS
SECTION 6.0

6.0 Mechanical Interference TVC Systems

6.1 Literature Search

MECHANICAL INTERFERENCE TVC SYSTEM LITERATURE SEARCH CONDUCTED.

Using reliability as the main criterion, a literature search was conducted for mechanical interference TVC systems. The six systems studied were mechanical probes jetavators, jet tabs, supersonic splitline, flexible exit cone, and jet vanes. Data was scarce and generally not applicable to large motors with small vector angles.

A major criterion of this study was reliability; accordingly, only those systems which had either been demonstrated or which were potentially attractive in the light of current technology were considered and reviewed. The six mechanical interference TVC systems studied were; mechanical probes, jetavators, jet tabs, supersonic splitline, flexible exit cone, and jet vanes.

In all cases choice of materials proved to be a considerable problem but in varying degrees of severity; the worst case being jet vanes because of their continuous exposure to the exhaust environment. Design data on jet vanes was particularly scarce; generally a vane configuration evolved from testing many empirical designs.

It became apparent during the search that development of mechanical interference TVC systems had concentrated on obtaining the maximum TVC angle out of each system for its particular application. Little data were available on small vector angles (1° to 2°) (0.01745 to 0.0349 RAD) such as the thrust vector requirement for the 260 in. diameter launch vehicle.

Because of the variety of systems considered in this category, the following sections describe the results of the literature search by system.

6.1 Literature Search

6.1.1 Mechanical Probes

MECHANICAL PROBE LITERATURE SEARCH REVEALS NEED FOR CONSIDERABLE DEVELOPMENT WORK

The data available on mechanical probes was related to high vector angles on small motors. These data indicated that a great deal of development effort is required before considering probes as a high reliability method of TVC. A bibliography is shown on the facing page.

The initial investigation into this concept was undertaken in two firings at the Allegany Ballistics Laboratory (ABL) in 1958[1]. Probes of molybdenum and steel survived 4 sec exposures to nonaluminized rocket exhaust gas.

Lockheed Missiles and Space Company (LMSC) conducted a cold flow test program in 1959[2] using nitrogen gas. Solid probes, with and without accompanying gas injection, were tested in a conical nozzle having a 17.5° (0.304 RAD) half angle 1.128 in. (2.86 cm) throat diameter and 6.25:1 expansion ratio. Thrust vector deflection and approximate axial thrust change were related to probe size and location. A maximum TVC angle of 8.5° (0.148 RAD) was achieved at an axial location x/L = 0.78. The depth of insertion was 0.75 in. (1.9 cm) and an axial thrust loss of approximately 4.6 percent of the total axial thrust was recorded.

The Bendix Corporation began investigation into the cooled probe TVC concept in 1960. A proposal by Bendix to ABL in 1962[3] resulted in an experimental probe effort[4,5,6] in which water-cooled probes were subjected to a program of static firings, subscale thermal exposure tests, and subscale cold flow tests.

Thrust vector deflections up to 5° (0.0872 RAD) were obtained in the solid propellant firing and 14° (0.244 RAD) in cold gas tests. Axial thrust decrement was approximately 40 percent of the measured side force. Severe erosion of the graphite nozzle liner occurred in the case of a solid flat tab and a closely spaced array of prongs.

Cylindrical probes of Inconel and stainless steel survived when cooled at a rate of 0.2 lb/sec per sq in. (0.014 kg/sec cm^2) of probe projected area. Each of the hot firings lasted 78 sec but the total insertion time (at full insertion) for any one probe never exceeded 37.5 sec. The 29 in. (73.6 cm) diameter end burning motor used DDP-75 aluminized propellant.

An attempt was made to reduce cooling requirements. Cooled cylindrical refractory probes in the form of porous sinters were exposed in subscale torch tests.

Problems were experienced with cracking of specimens and leakage at the seals.

All but one of the probes tested were less than 1 in. in diameter (0.7 to 0.8 in.) (1.78 to 2.03 cm). A test of a single 1.33 in. (3.38 cm) diameter probe, which became stuck after one insertion and retraction, proved inconclusive.

A probe TVC program was initiated between Bendix and LMSC in April 1962, in which full scale firings were to be conducted at Aerojet-General Corporation (AGC) facilities. Of the two tests which took place, the first resulted in the destruction of the cooled probes while the second was almost completely successful. Subscale tests at LMSC Santa Cruz facility were completed in March 1963. Eight JATO motors (7 sec burning time) were used to test various probe designs.

In 1963 Thiokol Chemical Corporation, Wasatch Division, conducted a mechanical probe TVC program[7] under Air Force Contract AF 33(600)-36514, to provide analytical and empirical design criteria for advanced TVC systems for possible application to the Wing II thru IV Minuteman motors. Lack of funds necessitated early termination of the program. Although not all of the objectives were met, a sufficient number of parametric tests were conducted to provide a preliminary design procedure. Optimum probe location appeared to lie between $x/L = 0.5$ and $x/L = 0.7$. Since the tests were of short duration (3.15 sec), fixed noneroding probes were installed in the expansion core. The probes were made of tungsten, or 98 percent tungsten 2 percent thoria. Probe diameters tested were 0.25, 0.375, and 0.50 in. (0.635 cm, 0.952 cm, and 1.27 cm). Throat diameter was 0.815 in. (2.07 cm), nozzle half angle was 15° (0.262 RAD), and expansion ratio 10:1.

During this program, a correlation of test data from LMSC, Bendix, ABL, and Thiokol was made. The proportionality of side force to probe area blockage ratio was clearly established during this correlation.

Early in 1963, a subscale Stage I Flightweight Minuteman Development Motor was static fired[8]. Each nozzle incorporated one uncooled tungsten probe. The probes were designed to penetrate the exhaust stream to various depths (up to 1 in.) (2.54 cm) to induce TVC. The probes failed to extend when actuated 42 sec into the firing. Tungsten carbide formations and aluminum oxide deposits friction-bound the probes in the carbide sleeves.

Recently, in June 1969, a probe actuated flexible seal nozzle designed and fabricated by United Technology Center (UTC) was static test fired on an AFRPL 36 in. (91.4 cm) diameter char motor[9]. The wire wound tungsten probe, fabricated from a plasma spray bonding process, was ejected from the nozzle approximately 2 sec after motor injection. The probe was located at an area ratio of 2.5. Nozzle throat diameter was 2.75 in. (6.98 cm) and the motor operated at a chamber pressure of 685 psia (4.72×10^6 N/m^2), and gas temperatures were of the order of 5,700°F (3,150°C).

MECHANICAL PROBE BIBLIOGRAPHY

1. Mann, J. K., et al.: "Oblique Shock Thrust Vector Control Firings," IRBM Inert Components Study - 1501 Progress Reports ABL, March and April 1958 (Confidential).

2. Tryk, D. B. and Engler, J. F.: "Report of Experimental Results of the Nozzle TAB Control Program, Phase I," LMSC, July 1959.

3. "Proposal for Thrust Vector Control of a Rocket Engine by Injection of a Cooled Probe into the Exhaust Nozzle," Bendix Products Aerospace Division. Proposal No. 863-328, January 1962 and 863-338, March 1962.

4. Leining, R. B.: "The Use of Probes for Rocket Thrust Vector Control," ABL P. Dev. No. 4045, 1963 (Confidential).

5. Eastman, J. M. and Leining, R. B.: "Cooled Probe Thrust Vector Control," January 1963 (Confidential).

6. Firing Reports, 29D-260C-MT-36, 37, 39, 42, 43, ABL, 1963 (Confidential).

7. Final Report "Mechanical Probe Thrust Vector Control Development Engineering Program - Wing II thru IV, Stage I Minuteman Motor," TWR-577, Thiokol Chemical Corporation, Wasatch Division, July 1964 (Confidential).

8. "Individual Motor Report for the TU-222-301.11 Subscale, Stage I Flight Weight Minuteman Development Motor," Thiokol Chemical Corporation, Wasatch Division, TWR-417, August 1963 (Confidential).

9. Ellison, J. R., Lt. USAF: "Test Firing of a Spike Actuated Flexible Seal Nozzle," AFRPL-TR-69-191, August 1969.

6.1 Literature Search

6.1.2 Jetavators

JETAVATOR LITERATURE SEARCH REVEALS NO EXPERIENCE WITH LARGE MOTORS, SMALL VECTORING ANGLES, OR EXTENDED BURN TIMES

A jetavator is an aerodynamically contoured ring or ring segment that fits around the nozzle circumference at the exit plane. It is mounted on bearings on opposite sides of the nozzle so that it can be rotated past the rim of the nozzle and down into the exhaust stream. A shock wave is formed in the nozzle. Downstream of this shock there is a high pressure region in the gas flow, which acts on the jetavator ring providing the necessary side force. Here again the literature revealed no experience with either large motors or small vectoring angles.

The concept of the jetavator as a TVC device was originally proposed by Dr. W. Fiedler, then of U.S. Naval Air Missile Test Center, Pt. Mugu, California. The feasibility of this concept was established[10] between 1951 and 1954 in subsequent development tests at Pt. Mugu.

Jetavators have been used on Polaris, Subroc, and Bomarc Missiles. Initial development of Polaris Jetavators is given in ref 11 and a more detailed description of the development and perfection of the jetavator for first stage Polaris Model A1 can be found in ref 12. Brief descriptions of the principles of jetavator operation may be found in ref 13, 14, 15 and 16.

The Subroc jetavators are briefly described in ref 17 which describes the whole Subroc propulsion system. Maximum jetavator deflection was 25° (0.436 RAD) producing about 14° (0.244 RAD) of jet deflection. Maximum dwell time in the fully deflected position was 1 sec during the first part of the firing with a sinusoidal variation thereafter. Total burning time for the Subroc missile is 26 sec.

The design and development of the Bomarc TVC system is reported in ref 18 and details of the qualifications program in ref 19 and 20.

Although the Bomarc missile used aerodynamic control surfaces to control its attitude and direction, these are ineffective at the relatively low missile speeds encountered during the first few seconds of flight. The XM51 Rocket Motor which is used to launch the Bomarc was equipped with a jetavator TVC system to control the missile during this critical launch period.

Bomarc was the first operational missile to incorporate pitch and yaw jetavators on a single nozzle. Both Polaris and Subroc have a four-nozzle configuration using separate jetavators for pitch and yaw.

A major problem in both the Polaris and Subroc programs was the development of an adequate seal to prevent blowback of the exhaust gases through the annular gap between the jetavator rings and the nozzle. The solution employed in both programs was to eliminate the seal. On the Subroc a flashback shield deflects the gases to the rear again and on Polaris protection is provided by heat shields and insulation. A flashback shield also was used on Bomarc.

On all programs a severe materials problem existed. Polaris used molybdenum inserts for the facing material and either titanium or stainless steel for the support structure. The steel was insulated from the molybdenum in order to maintain the steel at a more uniform temperature to take the loads.

JETAVATOR BIBLIOGRAPHY

10. Fiedler, W.: "Thrust Direction Control by Jetavator," U.S. Naval Air Missile Test Center, Pt. Mugu, California, May 1955. Summary Report No. 15 (Confidential).

11. Cottrell, R. F. and Archer, H. J.: "Thrust Vector and Thrust Termination Systems for Control of Solid Propellant Rockets," Bulletin of 14th Meeting JANAF Propellant Group, Volume I, pp. 151-191, May 1958 (Confidential).

12. Davis, R. E., et al.: "The Jetavator as a Vector Control Device Development of the Polaris Jetavator," Bulletin of Interagency Solid Propulsion Meeting, Vol. IV, pp. 391-401, July 1963 (Confidential).

13. Bankston, L. T.: "Thrust Vectoring Methods," Nots TP 2123, NAVORD Report 6423, China Lake, California, December 1958 (Confidential).

14. Ritchey, H. W.: "Thrust Control of Solid Propellant Rockets," Institute of Aeronautical Sciences, IAS Report No. 59-55.

15. Babazadeh, H.: "Thrust Vector Control for Solid Propellant Rocket Motors," CPIA 1963, Interagency Solid Propulsion Meeting, July 1963 (Confidential).

16. McCullough Jr. F.: "Critical Analysis of Existing Techniques and Future Potentialities for Thrust Vector Control," U.S. Naval Ordnance Test Station, NAVWEPS Report 7754, NOTS TP 2722, September 1961 (Confidential).

17. Growen, L. F.: "Subroc Propulsion System," Bulletin 16th Meeting JANAF Solid Propellant Group Volume I, June 1960 (Confidential).

18. "Special Report on Design and Development of a Thrust Axis Control Unit for XM51 Rocket Motor," Thiokol Chemical Corporation, Redstone Division, Report No. C-A-62-127A, March 1962 (Confidential).

19. "Final Report on Design and Development and Qualification of the XM51 Bomarc Booster Rocket Motor, Thiokol Chemical Corporation, Alpha Division, Report No. C-A-24A, September 1962.

20. Summary Report of "XM51 Qualification Program," Thiokol Chemical Corporation, Redstone Division, Report No. C-A-61-30A, June 1961.

6.1 Literature Search

6.1.3 Jet Tabs

JET TAB LITERATURE SEARCH REVEALED APPLICABLE EXPERIENCE

The jet tab concept is based, as in the case of a mechanical probe, on the generation of a shock wave around the leading edge of a blunt object inserted in the exhaust stream. Higher pressures are generated behind the shock than on the opposing wall of the nozzle, thereby providing the control force. Unlike the probe, however, the jet tab is located at the exit plane of the nozzle.

The literature revealed experience with large motors using jet tab TVC. Lockheed Propulsion Company's 156 in. (396 cm) motor provided an important source of information for 260 in. application.

In 1961, Aerojet was awarded a study under Contract AF 04(611)-6094[22] to determine the TVC methods best suited for large solid-rocket boosters with motors 100 in. (254 cm) and larger in diameter. Results of the study indicated that the jet tab system is the most advantageous for use on large solid rocket motors. Criteria for the study were reliability, availability, adaptability, economy, logistics, and performance.

Subsequently Aerojet was awarded a contract (AF 04(611)-8012) to demonstrate a tab facing material capable of withstanding the exhaust blast[23]. Three firings were conducted, each 120 sec in duration comprising two subscale motors (7 in. (17.8 cm) diameter throat) and one large scale motor (100 in. (254 cm) diameter with a 25.3 in. (64.2 cm) diameter throat). Test results indicated that tungsten was the most suitable facing material. The feasibility of the jet tab TVC system for large solid motors was proven. Problem areas were identified which indicated that no extension of 1963 technology was necessary for their solution. Also, side force, drag, torque, and performance characteristics were established.

In 1963, Lockheed Propulsion Company began an advanced state-of-the-art large solid rocket motor program initiated by the Air Force (Contract AF 04(695)-364). The objectives were to test a large ablative throat nozzle and to demonstrate a jet tab TVC system by static firing two 156 in. (396 cm), 1 million lb thrust (4.448×10^6 N), segmented, solid propellant motor. A brief account of this program up to the first large scale test can be found in ref 24. Full details may be found in LPC's final report[25].

Results indicated a jet tab side force deflection capability up to 7° (0.122 RAD). Axial thrust degradation was approximately 50 percent of the side force. The necessary jet tab construction to withstand the severe exhaust environment was further defined and the structural integrity of this size tab established. Minimum maintainable tab-nozzle gas was essential to side force effectiveness. This was achieved using a molybdenum erosion ring at the exit cone extension, thus minimizing nozzle erosion at this location.

Jet tabs were considered in a TVC study[26] performed by Hercules Inc. (ABL) in 1967 for an Advanced Surface-to-Air Missile System (ASMS). Selection criteria for this study were performance, envelope, feasibility and development cost. Jet tabs were rejected because of envelope violations and possible high development costs because of the severe conditions imposed by ASMS (6,500°F (3,600°F) - 2,000 psia (13.78×10^6 N/m^2)).

JET TAB BIBLIOGRAPHY

21. LMSC-800917, Jet Tab Thrust Vector Control, Lockheed Aircraft Corporation, December 1961.

22. Final Report for Phase I of the Large Solid Rocket Program (U), Report No. 0436-FR-July 1962, Aerojet-General Corporation (Confidential).

23. Auble, C. M. and Spielberger, L. J.: Jet Tab Thrust Vector Control for Large Solid Rockets (U), p 241, Volume III, Bulletin of the Interagency Solid Propulsion Meeting, July 1963 (Confidential).

24. Coverdale, J. S. and Opplinger G. T.: 156-Inch Diameter Motor and Jet Tab TVC Program (U), p 9, Volume III, Bulletin of 20th Interagency Solid Propulsion Meeting, July 1964 (Confidential).

25. 156-Inch Diameter Motor Jet Tab TVC Program (U), Final Report AFRPL-TR-64-167, January 1965 (Confidential).

26. Final Report, Thrust Vector Control System for the Advanced Surface to Air Missile System (U), Hercules Inc. (ABL), ABL-TR-67-19, June 1967 (Confidential).

26a. Final Report, Advanced TVC Preliminary Design Computer Program, (U) AFRPL-TR-67-318, January 1968 (Confidential).

6.1 Literature Search

6.1.4 Supersonic Splitline

LITERATURE SEARCH REVEALED BOTH PROBLEMS AND SUCCESSES

Because of the many advantages of movable nozzles for TVC, an extensive effort has been conducted during the last decade on the development of movable nozzle concepts[27]. Two TVC systems which have evolved from movable nozzle technology are the supersonic splitline and the flexible exit cone (Flex-X). In both concepts, the joint between the movable and fixed portions of the nozzle is located downstream of the throat in the supersonic flow section. Optimum splitline location appears to lie between expansion ratio of 1.5 and 2.5.

Development of the supersonic splitline has been delayed by material design problems, particularly at the point of gas reattachment on the downstream edge of the splitline, and also because of high aerodynamic torques. However, several supersonic splitline nozzles have been successfully tested. During Stage I Wing II Minuteman development, Marquardt Corporation fabricated a nozzle for a Stage I Minuteman Motor, which was successfully tested by Thiokol[28]. The nozzle used an O-ring for the splitline seal, which was located at an area ratio of 1.6. Throat diameter was 7.5 in. (19 cm) and burning time was 47 sec at an average chamber pressure of 747 psia (5.15 x 10^6 N/m^2). A vector angle of 6-1/2° (0.113 RAD) was achieved in this test which produced maximum torques of 61,400 in.-lb (6,940 N-m).

During the development of 1st Stage Polaris, Model A-3, Aerojet successfully tested several Pneumo-Dynamics designed nozzles using a bellows seal at the splitline[29]. Throat diameter of these nozzles was 4.9 in. (XX cm), burning time was 65 sec, and average chamber pressure 668 psia (4.6 x 10^6 N/m^2). Force amplification, factors of 1.2 were achieved.

Recently a successful test was conducted at AFRPL[30] on a nozzle designed by ARDE Portland Inc. under subcontract to Rocketdyne. Measured torque to actuate the nozzle was about 670 in.-lb/° (4,450 N-m/RAD) and a maximum vector angle of 5.2° (0.091 RAD) was achieved. The motor used for this test was the AFRPL 84 in. (213 cm) Char Motor. Burning time was 36 sec at an average chamber pressure of 640 psia (4.41 x 10^6 N/m^2). Nozzle throat diameter was 5.3 in. (13.45 cm), expansion ratio was about 10:1. Splitline location was at an expansion ratio of approximately 2.3:1.

All tests to date have incorporated a gimbal ring as the means for nozzle rotation.

Use of a flexible bearing in the splitline location has not yet been demonstrated but this would offer considerable weight savings with the elimination of the gimbal ring. Sealing problems at the splitline would also be eliminated. Flexible bearing technology has reached the point where a minimum amount of development effort would be required for this.

In 1967, Thiokol successfully static test fired an omniaxial flexible bearing nozzle on a 1 million lb (4.448×10^6 N) thrust class, 156 in. (396 cm) diameter motor[31]. Maximum actuation torques of 1.6 million in.-lb (0.18×10^6 N-m) were measured. [Much of the data obtained in the Flex-X (see 6.1.5) program can be directly applied to the supersonic splitline, since both concepts involve deflection of part of the supersonic section of the nozzle. Joint location, pivot point location, vector angle and force amplification are among the design variables common to both systems.]

Optimum splitline location appears to lie between expansion ratios of 1.5 and 2.5 with the pivot point located as near to the splitline as possible consistent with good joint design.

SUPERSONIC SPLITLINE BIBLIOGRAPHY

27. Desjardins, S. P. and Wilson, J.: "Evolution of Omniaxial Movable Nozzle Thrust Vector Control Systems," AIAA/ICRPG, 3rd Solid Propulsion Conference, 4-6 June 1968 (Confidential).

28. Final Test Results First Stage Minuteman Marquardt Corporation TVC Nozzle MA-103-XBA Using the TU-137-120 Rocket Motor (U), TW-217-3-62, Thiokol Chemical Corporation, Wasatch Division, March 1962 (Confidential).

29. Hoover, G. H.: An Omnivector Nozzle for Thrust Vector Control, Aerojet-General Corporation, Sacramento, California.

30. Strome, R. K.: Test Firing of a Supersonic Splitline Nozzle, AFRPL Report 1969.

31. Development and Demonstration of an Omniaxial Flexible Seal Movable Nozzle for Thrust Vector Control (U), Final Report AFRPL-TR-67-196, October 1967 (Confidential).

6.1 Literature Search

6.1.5 Flexible Exit Cone

LITERATURE SEARCH REVEALS NO DEVELOPMENT EXPERIENCE FOR LARGE MOTOR FLEXIBLE EXIT CONES

The flexible exit cone (Flex-X) consists of a standard nozzle - submerged or external in which a section of the exit cone is replaced by a flexible joint composed of layers of elastomer and plastic reinforcements. There is no development experience for large motor Flex-X TVC systems.

Thiokol is currently conducting a program, funded by AFRPL, to demonstrate this concept[32, 33] which combines the advantages of the supersonic splitline (lower nozzle ejection loads and side force amplification) with those of a flexible bearing (no gimbal ring or splitline seal).

A comprehensive cold flow program has been conducted to determine the effect of design variables such as location of the joint, pivot point location, exit cone half-angle expansion ratio, and the effect of vector angle on force amplification factor and internal aerodynamic torque. Results of this program indicated force amplification factors as high as 1.8 can be achieved through proper joint location. Torque requirements are likely to be high.

The demonstration phase has not yet been completely successful. Problems appear to lie in the area of joint processing and fabrication.

FLEXIBLE EXIT CONE BIBLIOGRAPHY

32. Wilson, J. W. "Development of a Flexible Exit Cone Omniaxial Movable Nozzle TVC System." AIAA 5th Propulsion Joint Specialist Conference, 9-13 June 1969.

33. Flexible Exit Cone Nozzle Development Program, Phase II Report. AFRPL-TR-68-124, Volumes I and II.

6.1 Literature Search

6.1.6 Jet Vanes

LITERATURE SEARCH REVEALED MAJOR MATERIAL DEVELOPMENT PROBLEMS WITH EXTENDED BURNING TIMES

Jet vanes are aerofoils located in the exhaust stream of a nozzle, usually just aft of the exit plane. Deflection of the vane produces a lift force, which is a lateral force relative to the direction of axial thrust, resulting in a turning moment about the vehicle cg. A drag force on the vane always exists during firing resulting in a continuous loss in axial thrust. The literature revealed that major material development problems would occur with the extended burning time of the 260 in. motor.

Jet vanes have been used on several operational guided missiles, viz: V-2 (Redstone), NASA Scout, Corporal, Sergeant, and Pershing. In all cases firing times have been relatively short or the vanes have been designed for only the first few seconds of firing, after which aerodynamic fins took over.

The Corporal achieved satisfactory performance using graphite vanes, with a molybdenum leading edge. However, the graphite was brittle and difficult to handle.

A 5 yr development program[34, 35] was conducted to develop a vane configuration suitable for use with the Sergeant guided missile system. During the course of this program, 14 vane configurations using 13 different body materials (including 11 types of fiberglass) and 10 types of leading edge were tested. The result was a moldable vane using chopped glass fiber and phenolic resin. No improvement was found for the molybdenum leading edge. Molding the vane resulted in a 90 percent cost reduction over machining the vane.

The vanes were designed to operate for a full duration of 26 sec and were capable of correcting 1/2° (0.0085 RAD) of thrust misalignment in the 45,000 lb (2.02×10^6 N) thrust motor, a requirement of 14 lb (62.8 N) lift force per degree vane deflection. Total vane deflection was 14° (0.244 RAD) and submerged planform area was 12 sq in. (77.5 cm^2). Nozzle throat diameter was 8.55 in. (21.7 cm) and exit diameter approximately 20 in. (50.8 cm).

Control of the Pershing missile[36, 37, 38] is provided by three jet vanes in the motor exhaust and three air vanes, on both stages. Jet and air vanes are interconnected and are capable of $\pm 26°$ (± 0.454 RAD) maximum deflection during flight. First stage vanes are required only during the first 15 sec of flight, after which the air vanes become effective. Conversely, second stage air vanes become virtually ineffective at high altitude during the latter part of the second stage burning and jet vanes are required for the full 40 sec duration.

An extensive materials evaluation program was required[39] to discover a material that would withstand the 5,500°F (3,040°C) gas temperature and solidified particles of Al_2O_3 to which the vanes are subjected in the PBAA propellant exhaust.

Numerous materials and alloys were investigated including graphite, molybdenum, tantalum, tungsten, ceramics and plastics. Many fabrication processes were utilized including sintering, forging, pressing, rolling, and casting. A transpiration cooled vane was investigated, but an unsuccessful test of this concept terminated any further development.

The vane selected for first and second stages was an arc-cast alloy of 15 percent molybdenum/85 percent tungsten, and exhibited a 10 percent planform area loss during full duration testing. This was deemed acceptable. First Stage vanes had a planform area of 25 sq in. (161 cm^2). The nozzle had a 6.2 in. (15.7 cm) diameter throat and 7.32 expansion ratio.

Design of jet vanes has generally been based on the results of testing experimental configurations. P. N. Rowe[40] attempted to gather information which would enable a designer to choose a vane configuration which would meet the requirements of a particular application. Unfortunately practical considerations limited his investigation to experiments with small nozzles discharging air. Some of the results of this investigation are of interest. Side thrust was found to vary linearly with vane deflection except at very small angles (<3°) (<0.0524 RAD). Up to this point the increase in side force amounted to 0.75 percent of axial thrust per degree of vane deflection. This was for a center vane only and may not apply to vanes located on the periphery of the exit diameter. Thrust loss increases approximately as the square of the thickness ratio of the vane.

Torque requirements can be reduced to a minimum by locating the hinge axis near to the center of pressure of the vane. This center generally lies about 25 percent aft of the leading edge but varies with vane angle.

JET VANES BIBLIOGRAPHY

34. Robinson, D. J., and Montgomery, L. C.: "Sergeant Motor Jet Vanes." JPL Report No. 20-136, June 1960.

35. "Reports on Sergeant Motor Static Firing Tests," 1 thru 46, various JPL Reports from Dec 1954 to June 1960.

36. Jones, A. T.: "Large Motor Program for Pershing Missile." Bulletin 15th Meeting JANAF Solid Propellant Group Vol I, 1959.

37. Mitchell, C. M., and Jones, A. T.: "Pershing Propulsion Program," Bulletin 16th Meeting JANAF Solid Propellant Group Vol I, 1960.

38. Dale, W. I., and Wise, D. E.: "New Developments in the Pershing Propulsion System." Bulletin 18th Meeting JANAF Solid Propellant Group Vol I, 1962.

39. "Results of Pershing Jet Vanes Aerodynamic Tests." Numerous ABMA Reports published in 1960.

40. Rowe, P. N.: "Supersonic Jet Deflection." Part IV Deflection by Vane. Imperial College of Science and Technology Report No. JRL-27.

6.0 Mechanical Interference TVC Systems

6.2 Design Requirements and Selection Criteria

CANDIDATE MECHANICAL INTERFERENCE TVC SYSTEMS EVALUATED

Each mechanical interference TVC system was evaluated with respect to specified design requirements. Selection of the most promising system was based primarily on its reliability with respect to current technology and its potential cost. Secondary factors such as weight, development history, etc, were considered when necessary.

The duty cycle was as shown in Figure 4-1 multiplied by 1.16. Total injection impulse was 69.6°-sec (1.215 RAD-sec). Maximum equivalent TVC angle was 1.4° (0.0244 RAD). This applied for an equivalent point of side force insertion located 772 in. (19.6 m) aft of the initial vehicle center of gravity. The magnitude of the side force requirement varied depending upon its point of application in the nozzle. Adjustments were made accordingly, and the turning moment acting on the vehicle was maintained constant at 109.6×10^6 in.-lb (12.4×10^6 N-m). Maximum slew rate was 3°/sec (0.0524 RAD/sec) and motor burning time was 143 sec. Combustion gas temperature was assumed to be about 5,800°F. These requirements are tabulated in Table 6-1.

The vehicle for which each TVC system was sized is a 260 in. diameter solid propellant booster (a modified S-IV-B second stage with a payload).

Selection of the most promising TVC system was based primarily upon its reliability with respect to current technology and upon its potential cost. Wherever two or more TVC systems compared closely, weight, performance loss, development history, and current development status were determined to provide secondary evaluation criteria.

TABLE 6-1

MITVC DESIGN REQUIREMENTS

Parameter	English Unit Value	SI Unit Value
Total injection impulse	69.6°-sec	1.215 RAD-sec
Maximum equivalent TVC angle	1.4°	0.0244 RAD
Equivalent point of side force insertion - distance aft of cg	772 in.	19.6 m
Maximum required equivalent slew rate	3°/sec	0.0524 RAD-sec
Motor burning time	143 sec	
Combustion gas temperature	5,800° F	3,478°K

6.0 Mechanical Interference TVC Systems

6.3 Preliminary Design and Screening

PRELIMINARY SCREENING NARROWED TO SIX CONCEPTS

Only those systems which are (or have been) operational, or are under development were investigated. This restriction was imposed primarily by considerations of reliability and cost, the two most important criteria of this study.

The six candidates design concepts considered and the selection criteria imposed are listed on the facing page.

Mechanical probes could be either cooled or uncooled. Supersonic splitline could employ either a gimbal ring or flexible bearing to provide thrust vectoring capability. Each of these, in turn, was investigated.

To insure inherent reliability of each system a conservative approach was taken. Existing materials, material configurations, and fabrication techniques previously demonstrated were employed wherever possible. However, in the case of jet vanes, it appears that a breakthrough in current materials technology is necessary before a vane can be built which will reliably withstand the relatively long burning time of the 260 in. motor.

Experimental and theoretical data were used to size specific control elements; tabs, probes, etc. It should be realized, however, that a general lack of scale-up data and in some cases (probes) lack of data at small TVC angles, resulted in many approximations. Wherever possible, system parameters were optimized (probe location, pivot point, splitline location, etc) but often parametric data of this kind were severely lacking.

Although sizes, weights, and performance penalties are preliminary, all reflect the same state-of-the-art and completeness in design and are considered valid for comparative purposes.

Preliminary Design Concepts Considered

- Mechanical probes
- Jetavators
- Jet tabs
- Supersonic splitline
- Flexible exit cone (flex-X)
- Jet vanes

Selection Criteria

- Reliability
- Cost
- Development risk
- Flexibility
- Weight and performance

6.3 Preliminary Design and Screening

6.3.1 Mechanical Probes

6.3.1.1 Probe Sizing and Location

BLOCKAGE RATIO SEEN AS MOST IMPORTANT FACTOR IN DETERMINING PROBE SIZE AND LOCATION

The most significant parameter in determining available side force and probe size from mechanical probe systems is blockage ratio.

Analysis of available probe data indicates that the side force ratio F_s/F_a of an optimum probe system is directly proportional to the blockage area ratio at the probe insertion point, ie,

$$F_s/F_a = K \frac{A_p}{A_i} \quad \text{where } K = 1$$

F_s = side force ~ (lb)

F_a = nominal axial thrust ~ (lb)

A_p = probe projected area ~ (sq in.)

A_i = nozzle cross sectional area at probe insertion point (sq in.)

The constant of proportionality, K, or linearity factor, may be likened to the amplification factor associated with hot gas or LITVC. Studies in ref 7 indicate that K varies with probe location, and at x/L ratios less than 0.5, K may be less than 1.0. For preliminary sizing purposes, K was taken to be 1.0.

In order to maintain a constant turning moment about the vehicle cg, side force ratio requirements necessarily vary with probe location. Figure 6-1 shows the side force and probe projected area requirements at various locations within the nozzle of the 260 in. vehicle. The pressure immediately behind the bow shock wave acting on the front face of the probe is also shown.

It can be seen that as probe location moves closer to the throat the required projected area of the probe becomes less, resulting in a smaller probe. However, at low x/L ratios, there is the possibility that the shock produced by the probe may interact with the opposite wall of the nozzle causing a reduction in the side force produced.

Ref 7 indicates probe optimum location to be between x/L = 0.5 and 0.7 inserted perpendicular to the nozzle wall. Table 6-2 shows the variation of probe size for x/L ratios of 0.4, 0.5, and 0.6; and for one, two, and three probes per quadrant. Probe sizes indicated, are extremely large, relative to those previously tested, most of which have been less than 1 in. (2.54 cm) in diameter. A single cooled probe 1.33 in. (3.38 cm) in diameter was tested by Bendix, but this only made one insertion and retraction before it became stuck. The test proved inconclusive.

Probe location was selected at x/L = 0.5, for the 260 in. motor application. The projected area required for each probe in a single probe/quadrant system is 490 sq in. (3,160 cm^2) or a square whose sides are 22.1 in. (56.1 cm) long. A probe with these dimensions at x/L = 0.5 would cover an arc of 14.5° (0.253 RAD). Actual insertion depth would be slightly greater than 22.1 in. (56.1 cm) to account for loss of area due to this curvature.

With probe dimensions of this magnitude, it becomes desirable to use a flat plate type of probe rather than the cylindrical probe. This reduces nozzle cutout area and actuation loads. The only probe of this type to be tested was water cooled and failed because of poor coolant distribution. Severe erosion of the nozzle liner also was experienced.

TABLE 6-2

APPROXIMATE PROBE DIMENSIONS

x/L = 0.4 A_p = 405 sq in.			x/L = 0.5 A_p = 490 sq in.			x/L = 0.6 A_p = 580 sq in.		
No. Probes	D_p	H	No. Probes	D_p	H	No. Probes	D_p	H
1	17.8	22.7	1	5	98.0	1	5	116.0
1	22.3	18.2	1	10	49.0	1	10	58.0
1	26.7	15.2	1	20	24.5	1	20	29.0
1	31.2	13.0	1	30	16.3	1	30	19.3
1	35.6	11.4	1	40	12.3	1	40	14.5
2	5	40.5	2	5	49.0	2	5	58.0
2	10	20.3	2	10	24.5	2	10	29.0
2	15	13.5	2	15	16.4	2	15	19.3
2	20	10.2	2	20	12.3	2	20	14.5
2	30	6.8	2	30	8.2	2	30	9.7
3	5	27.0	3	5	32.6	3	5	38.6
3	10	13.5	3	10	16.3	3	10	19.3
3	15	9.0	3	15	10.9	3	15	12.9
3	20	6.8	3	20	8.2	3	20	9.7
3	30	4.5	3	30	5.5	3	30	6.45

A_p = Approximate probe projected area (sq in.)

D_p = Approximate probe diameter (or width) (in.)

H = Approximate probe inserted height (in.)

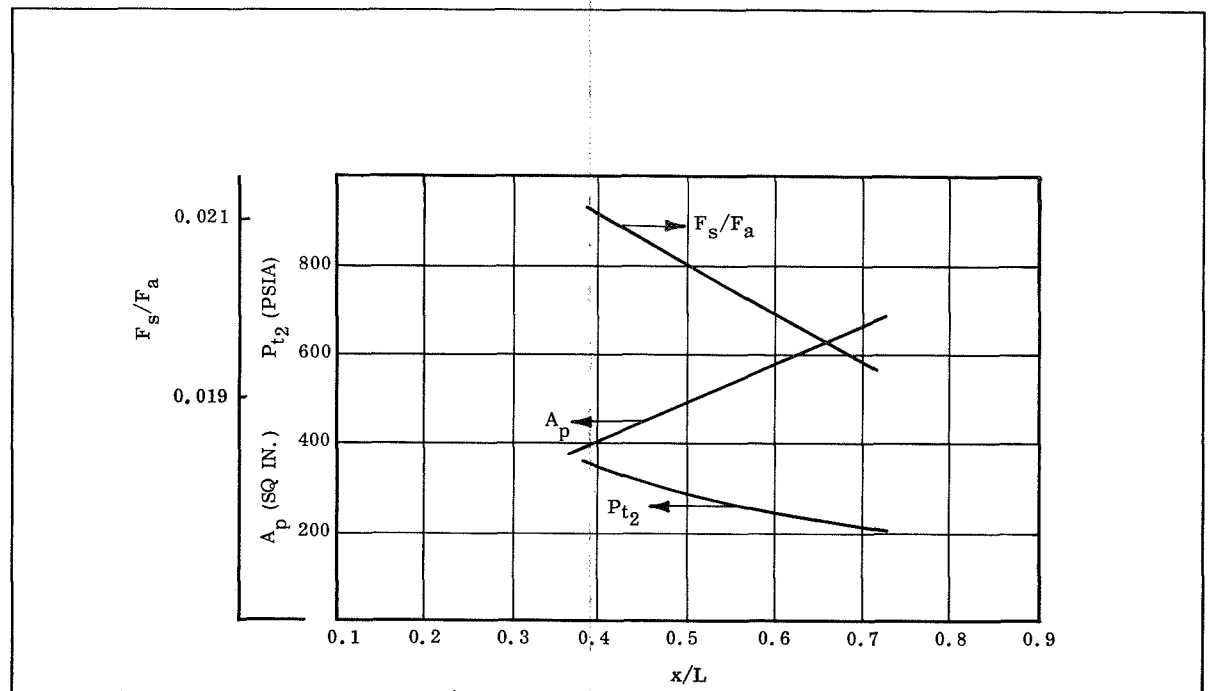

NOTES: 1. ALL POINTS ALONG F_s/F_a CURVE GIVE CONSTANT TURNING MOMENT FOR VEHICLE.
2. $F_s/F_a = A_p/A_i$

28235-17

Figure 6-1. Probe Projected Area Requirements

6.3 Preliminary Design and Screening

6.3.1 Mechanical Probes

6.3.1.2 Design Considerations

PROBES APPEAR UNATTRACTIVE FOR LARGE MOTORS WITH LONG BURNING TIMES BECAUSE OF CURRENT DESIGN FACTORS

Many factors influence the overall probe design, bending moment, probe grouping and materials, and nozzle orifice size. The combined impact of these factors make probes unattractive for large motors with extended burning times.

A major problem area is the seal between the nozzle cutout and the actuation system. A minimum gap must be left between the probe periphery and the nozzle cutout to absorb any unequal thermal expansions in the nozzle wall and probe. Many probes have become stuck, simply because this gap was too small.

In a practical single probe design, the length of the probe external envelope will be between 2 and 4 times the maximum probe insertion depth. With probes of this size the actuation mechanism could be located within the probe itself. As there is approximately 90 in. (228 cm) between the 260 in. nozzle outer wall and the skirt at an $x/L = 0.5$, a mechanical probe system is not expected to violate the envelope.

Use of multiple probes would reduce individual probe dimensions as reflected in Table 6-2. However, little work has been done on what an optimum grouping of the probes should be. Bendix tested a four pronged array and found that distance between probes was critical if severe nozzle erosion was to be minimized.

In addition to probe profile and probe grouping, other areas in which development is required is that of materials for uncooled probe design. Unlike jet tabs, probes are completely immersed within the exhaust flow and a configuration is required which will withstand this environment. Uncooled probes tested so far have been small enough so that solid tungsten could be used. For the 260 in. booster application some form of outer refractory shell with an inner graphite-type heat sink would be required. This form of construction appears to be the only one to have reliably demonstrated survival in the severe exhaust environment expected from the 260 in. motor.

Wire-wound tungsten probes appear attractive from many aspects, but the recent failure at UTC of this type of probe indicates that development problems in the fabrication process still await solution.

Ablative probes can only be considered for short duration burning times. They are inefficient in that they must be overdesigned for the initial part of any duty cycle. The larger probe size results in larger bending moments and heavier, higher-load-carrying bearings. A sharp relief angle at the probe tip could not be maintained in an ablative design. Eventually as the probe tip became rounded, a component of the front face pressure force would act on the probe tip in the retract direction greatly increasing actuation requirements over those of a noneroding design. It is conceivable that an ablative probe design could be heavier than a noneroding design as a result of heavier actuators, heavier bearings, and resultant heavier nozzle structure.

Bending moments acting on the probe are very high. The minimum distance from the center of pressure of the probe (at full insertion) to any kind of bearing surface is 1.5 times the full insertion depth, or 33.2 in. (84.2 cm). Since the bearing must be thermally protected from hot exhaust gases passing through the nozzle cutout/probe gap, actual distance to the bearing surface will probably be greater than this. Figure 6-1 shows that the pressure acting on the front face of the probe decreases as probe location moves nearer the exit plane. It decreases at approximately the same rate as the probe area requirement increases, resulting in an approximately constant probe loading of 141,000 lb (632,000 N).

The resulting bending moment on a 22.1 in. (56.1 cm) square probe is 4.68×10^6 in.-lb (0.528×10^6 N-m), or 38 percent greater than the bending moment on the jet tab of an equivalent dual jet tab system. A reduction in bending moment can be achieved in two ways: (1) reduce the insertion depth by increasing probe width, and (2) adopt a multiple probe system. The former merely lowers probe aspect ratio. Cold flow tests performed by Lockheed show that probe efficiency $\frac{F_s/F_a}{A_p/A_i}$ is actually increased at low insertion depth/width ratios. Typical dimensions from Table 6-2 would be a probe 30 in. (76.1 cm) wide and inserted to a maximum depth of 16.3 in. (41.4 cm), an aspect ratio of 0.544. Total probe loading is still the same but the bending moment is reduced to (1.5) (16.3) (141,000) = 3.44×10^6 in.-lb (0.389×10^6 N-m). However, the arc covered by a 30 in. (76.1 cm) wide probe at an $x/L = 0.5$ has risen to 19.7° (0.344 RAD) and insertion depth would be slightly greater than 16.3 in. (41.4 cm).

An estimate of probe performance loss can be obtained from Figure 6-2. This is a mean curve drawn through cold flow test data from Bendix and LMSC, in which excellent correlation was noted. The curve is taken from ref 7 and shows a thrust loss of approximately 0.5 percent at a TVC angle of 1.175° (0.0205 RAD). This is the thrust vector requirement at a probe location of $x/L = 0.5$ to maintain the turning moment on the vehicle specified in the design requirements of this report.

$F_a = 6.047 \times 10^6$ lb $\Delta F_a = (0.005)\ (6.047 \times 10^6) = 30{,}200$ lb (135,200 N)

Total injection impulse = $60 \times 1.16 = 69.6°$-sec (1.215 RAD-sec).

Impulse loss = 30,200/1.175 (69.6) = 1.789×10^6 lb-sec (8.01×10^6 N-sec) = 0.21%. Additional propellant necessary to achieve total impulse

= $1.789 \times 10^6/254 = 7{,}040$ lb (31,500 N)

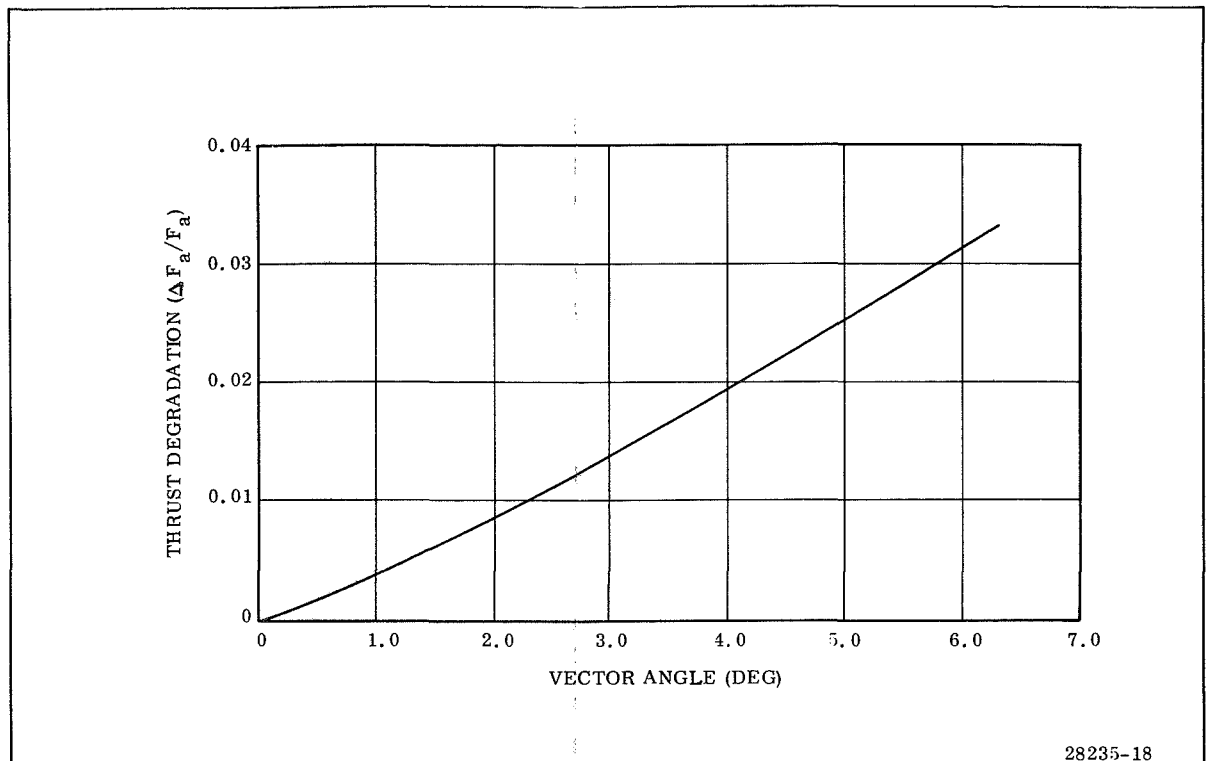

Figure 6-2. Thrust Degradation vs Thrust Vector Angle for Mechanical Probes Cold Flow Test Data

6.3 Preliminary Design and Screening

6.3.1 Mechanical Probes

6.3.1.3 Cooled Probes

COOLED PROBES HAVE DEVELOPMENT PROBLEMS AND INCREASE SYSTEM WEIGHT

Cooled probes have the potential for reducing probe size, but have the disadvantage of increasing the overall system weight by the amount of coolant required.

Considerable development work is required in many areas of cooled probe design before it can be considered a reliable means of TVC. Three major areas still to be investigated further are the side force contribution of the coolant, an optimum coolant distribution for different probe configurations and whether the best coolant should be inert or chemically reactive with the exhaust gases. Bendix used only water in their cooled probe program. The effects of any selected coolant on probe materials would also have to be fully investigated.

The lowest flow rate at which probes survived was 0.2 lb/sec per sq in. (0.014 kg/sec cm^2) of probe projected area. Using this as a minimum, a mechanical probe TVC system for the 260 in. booster would require more than 8,000 lb (3,620 kg) of water as coolant in order to meet the duty cycle requirements of this study.

It has been suggested (Ref 5) that use of a chemically reactive coolant would lower this weight penalty. Gross calculations performed on injectants usually associated with LITVC suggest that this may not be true and water may, in fact, be the best available probe coolant, from a coolant weight standpoint. Assume:

$$\frac{F_{s_p}}{F_a} = K_1 \frac{A_p}{A_i} \qquad \text{where } K_1 = 1$$

and

$$\frac{F_{s_i}}{F_a} = K_2 \frac{\dot{\omega}_c}{\dot{\omega}_a} \qquad \text{where } K_2 \text{ varies with injectant}$$

F_{s_p} = probe contribution to side force, lb

F_{s_i} = injectant contribution to side force, lb

$\dot{\omega}_c$ = coolant flow rate, lb/sec

$\dot{\omega}_a$ = motor flow rate, lb/sec

Total side force ratio is thus given by

$$\frac{F_s}{F_a} = \frac{F_{s_p}}{F_a} + \frac{F_{s_i}}{F_a} = K_2 \frac{\dot{\omega}_c}{\dot{\omega}_a} + \frac{A_p}{A_i}$$

using 0.2 lb/sec per sq in. projected area as a minimum flow rate for water and adjusting this according to the heat capacity of the injectant, i.e.,

$$\dot{\omega}_c = 0.2 A_p \frac{C_{p_{water}}}{C_{p_{injectant}}}$$

$$\frac{F_s}{F_a} = K_2 \frac{0.2 A_p}{\dot{\omega}_a} \frac{C_{p_{water}}}{C_{p_{injectant}}} + \frac{A_p}{A_i}$$

From this equation, a useful comparison may be made of probe projected area requirements and total coolant weights for various injectants. Table 6-3 shows the results of this comparison.

The following assumptions were made in generating this comparison:

1. Probe location at $x/L = 0.5$
2. For probe, linearity factor $K_1 = 1$, ie, $F_s/F_a = A_p/A_i$
3. For injectant; amplification factors, K_2, taken from LITVC data. These values are optimistic since injection efficiency is probably reduced when injecting through or in front of a probe.

The coolant requirement was based on test data obtained with water and was adjusted only for the heat capacity of each injectant. The heat of vaporization was not included. The relative merits of injectants would change if the coolant was allowed to vaporize before leaving the probe. However, it should be pointed out that the transition from nucleate boiling to film boiling which would occur in such a system, is accompanied by a drastic reduction in coolant heat transfer coefficient, seriously increasing the possibility of probe burnout. Additionally, the tests from which the coolant requirement was taken, employed Inconel and stainless steel probes. Increasing probe operating temperature by the use of refractory materials would no doubt reduce overall cooling requirements. However, the relative standing of each injectant would be the same from a coolant-weight standpoint. Total coolant weight was based upon satisfying the TVC requirements of the design duty cycle.

Water, hydrazine, and aqueous strontium perchlorate solution appear the better injectants with water offering the lowest coolant weight and the strontium the smaller probe size. It is interesting to note that the Freons are such poor coolants that a very high flow rate is required to sufficiently cool the probes. This high flow rate significantly contributes to side force reducing probe projected area requirements considerably.

Although mechanical probes have been shown to be feasible, and may be attractive from a weight standpoint, extensive development is still required in many areas to show that they are a reliable method for TVC. In view of their rather poor development history mechanical probes were eliminated from further consideration.

TABLE 6-3

MECHANICAL PROBE POTENTIAL COOLANT COMPARISON

	Uncooled	Water	N_2O_4	N_2H_4	Freon 114-B2	Freon 113	Aqueous Strontium Perchlorate
A_p (sq in.)	490	477	352	441	330	359	423
Weight coolant (lb)	--	8,000	16,000	10,000	29,300	27,600	10,100
K_2	--	0.2	0.9	0.5	0.5	0.5	0.7
C_p (Btu/lb°F)	--	1.0	0.368	0.736	0.166	0.218	0.700

Notes:

1. Weight of coolant calculated to meet NASA duty cycle
2. A_p = probe projected area (sq in.)

Assumptions:

1. Probe location at $x/L = 0.5$
2. For probe, linearity factor $K_1 = 1$ $F_s/F_a = K_1 (A_p/A_i)$
   F_s = side force from probe A_p = probe projected area
   F_a = nominal axial thrust A_i = nozzle cross sectional area at probe location
3. K_2 = measure of injectant efficiency obtained from LITVC data.
4. Weight of coolant adjusted only for heat capacity of injectant. Heat of vaporization neglected.
5. Weight of coolant based upon satisfying total side impulse requirements of 260 in. diameter launch vehicle.

6.3 Preliminary Design and Screening

6.3.2 Jetavators

6.3.2.1 Design Considerations

JETAVATOR SYSTEM DESIGN REQUIRES ACCEPTANCE OF WEIGHT PENALTY AND EXTENSIVE MATERIAL DEVELOPMENT

Jetavators applicable to 260 in. solid rocket motors would be extremely heavy and would require extensive material development. The spherical jetavator was selected as the best tradeoff profile.

It became apparent from the literature search that application of the jetavator concept to a 260 in. nozzle would result in an extremely large and very heavy control element. Jetavator deflection requirements directly affect the width of the jetavator ring which in turn affects the weight of the ring. Since the mean diameter of the jetavator ring will be somewhat greater than 260 in. only a small increase in width is necessary to produce a significant increase in weight. It was thus desirable to keep deflection requirements to a minimum.

Of the various shapes that the inner ring surface may take, a spherical profile offers the minimum jetavator deflection for small TVC angles (Figure 6-3b). In addition, it can be seen that the side force produced by a spherical jetavator is a linear function of angular position. Figure 6-3a shows the relative actuation torque requirements and Figure 6-3c shows the relative thrust loss for the same inner ring surface profiles. Actuation torque requirements are dependent upon the location of the jetavator pivot axis; however, in the case of the spherical jetavator, the force vector passes through (or very close to) the pivot axis reducing the actuation torque almost to zero.

In terms of thrust loss, the spherical jetavator was inferior to the cylindrical and conical profiles. The cylindrical ring is also easier to manufacture. However, the advantages of the spherical jetavator are considered to outweigh these latter two considerations, and this shape was selected.

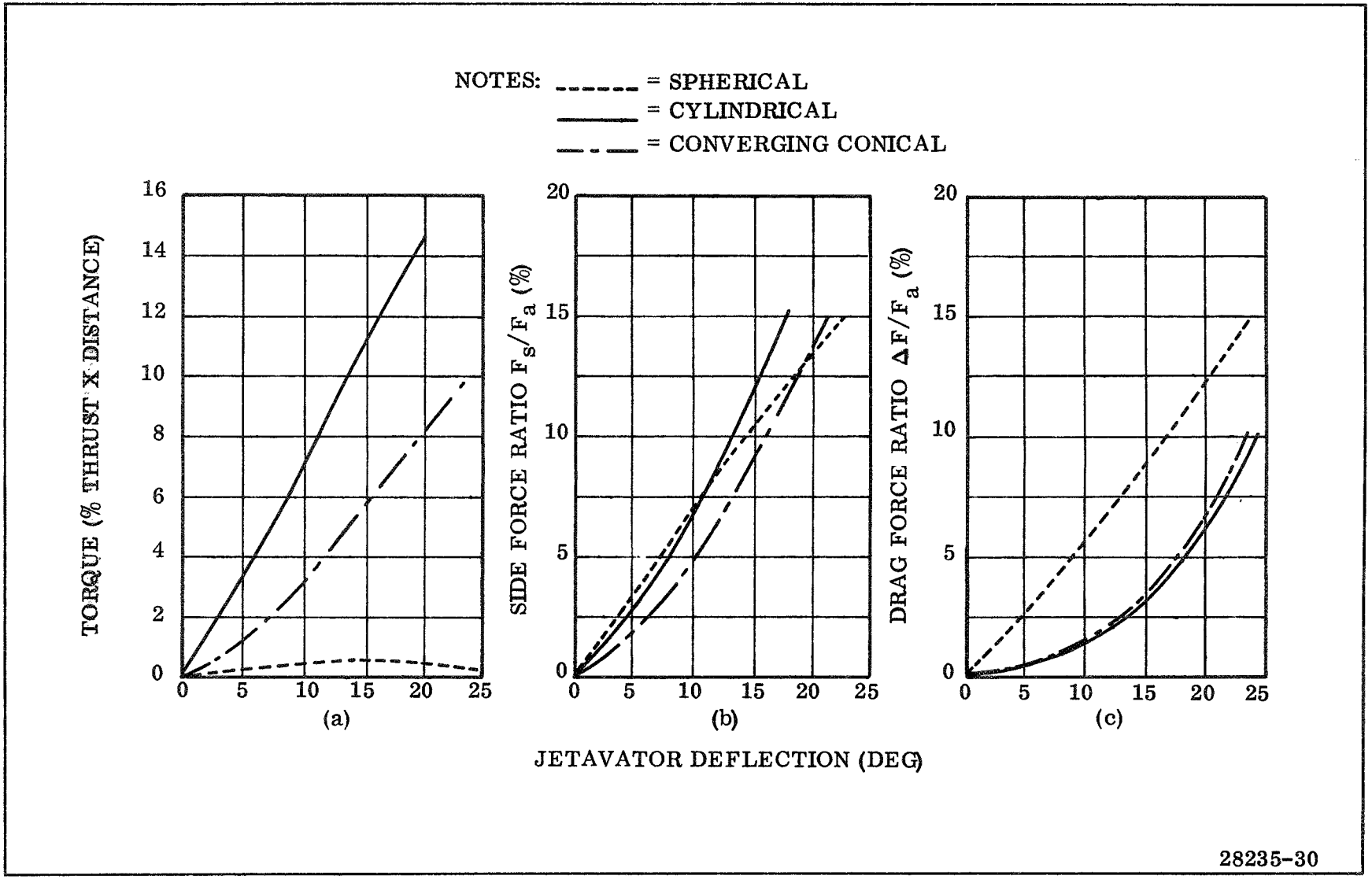

Figure 6-3. Relative Effect of Jetavator Inner Surface Profile on Torque, Side Force, and Drag

6.3 Preliminary Design and Screening

6.3.2 Jetavators

6.3.2.2 Performance Loss

JETAVATOR SYSTEM DESIGN REQUIRES CONSIDERABLE PERFORMANCE LOSS

One of the major disadvantages of jetavators is the inherent performance loss associated with the insertion of the rings into the exhaust stream.

Side force requirements at the exit plane are 104,000 lb (467,000 N) or F_s/F_a = 0.0179 (a TVC angle of 1.03° (0.018 RAD) at the exit plane). Data from Polaris and Bomarc (Figure 6-4), which both used spherical jetavators, suggest a deflection angle of about 5° (0.0872 RAD) is necessary. Figure 6-5, which presents thrust loss data from the Bomarc and Polaris program as a function of jetavator deflection angle, indicates a thrust loss between 0.5 and 0.6 percent is likely at the full deflection angle of 5° (0.0872 RAD).

$\frac{0.55}{100}$ (5.824×10^6) = 32,000 lb (144,000 N) loss of thrust for 1.03° (0.018 RAD) TVC. Total impulse loss for NASA duty cycle = $\frac{32,000}{1.03}$ (69.6) = 2.16×10^6 lb-sec (9.7×10^6 N-sec) = 0.25%. Additional propellant required to compensate for impulse loss = $\frac{2.16 \times 10^6}{254}$ = 8,500 lb (3,850 kg).

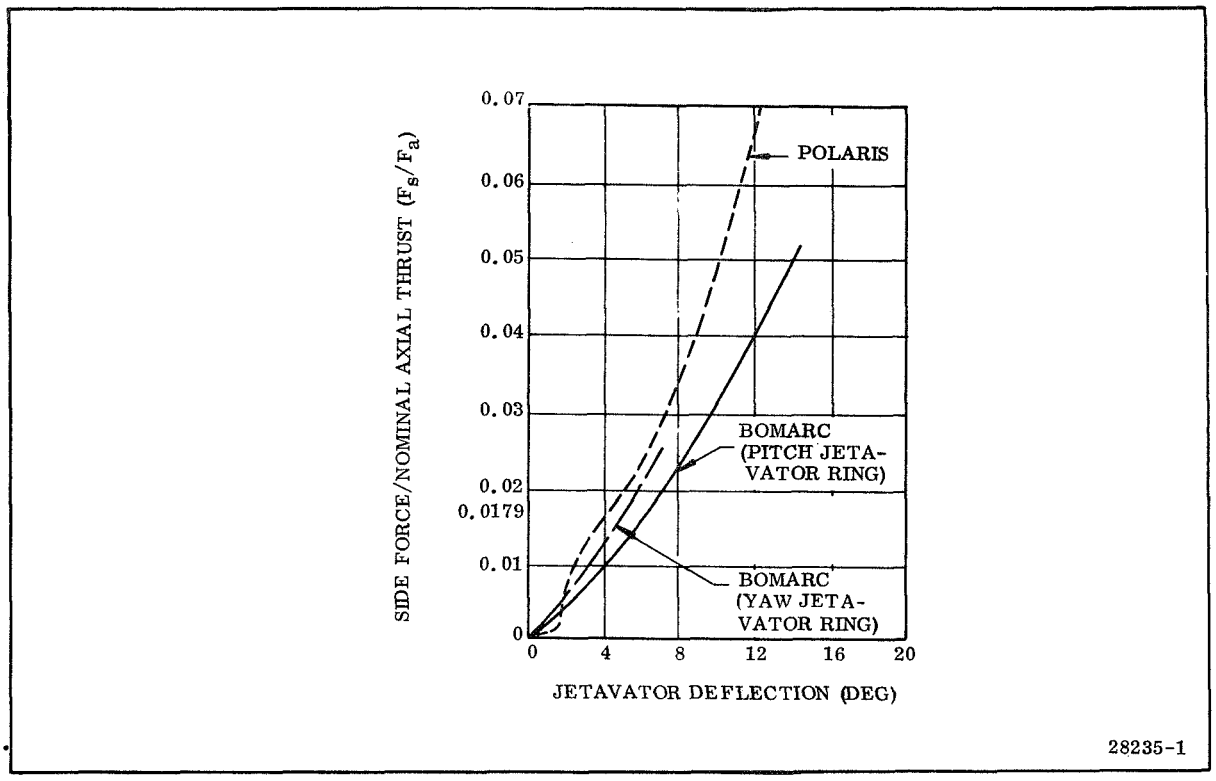

Figure 6-4. Side Force Ratio vs Jetavator Deflection Angle, Polaris and Bomarc Test Data (Spherical)

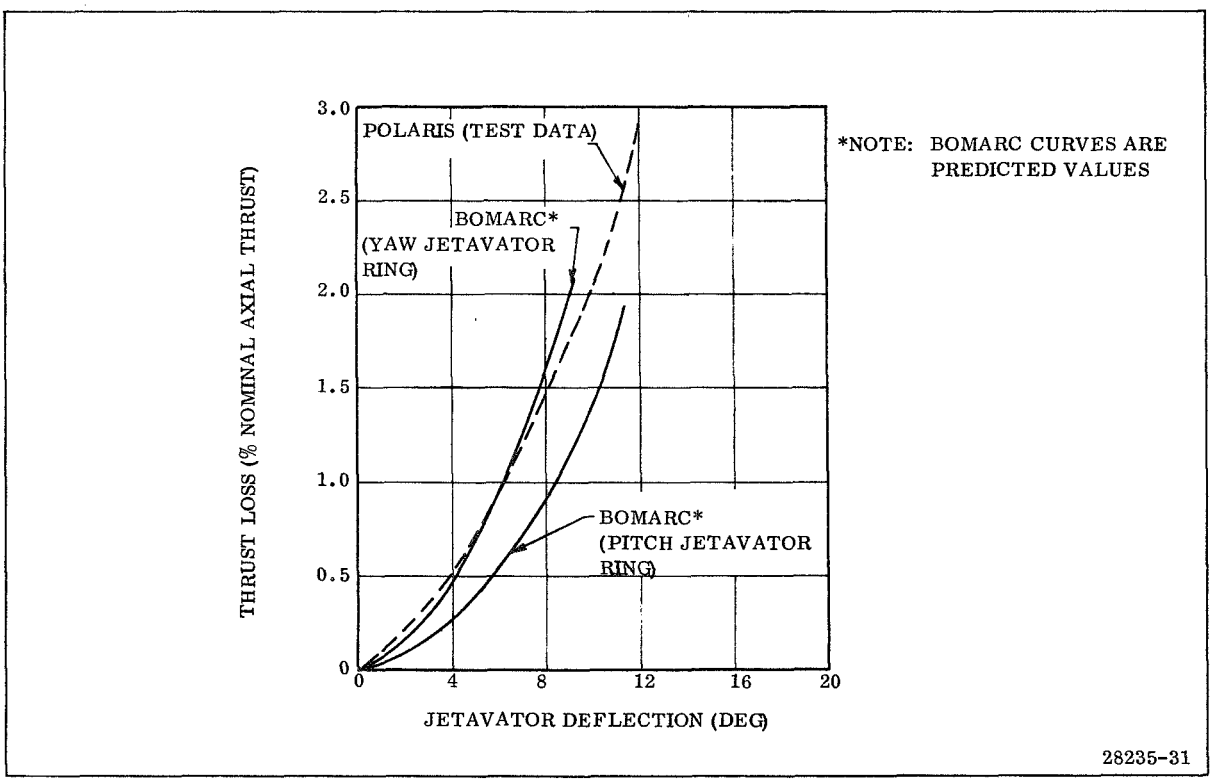

Figure 6-5. Thrust Degradation vs Jetavator Deflection Angle

6.3 Preliminary Design and Screening

6.3.2 Jetavators

6.3.2.3 Jetavator Weight Estimate, Configuration, and Torque Requirements

JETAVATOR SYSTEM ELIMINATED DUE TO WEIGHT AND COMPLEXITY

The concentric ring approach was selected for preliminary sizing purposes. These rings would weigh approximately 11,040 lb (5,010 kg). Actuation torque requirements would be 290,000 in.-lb (32,800 N-m)/jetavator. The jetavator was eliminated from further consideration during the screening phase due to its weight and overall complexity.

To effect both pitch and yaw control, the jetavator can be used with its pivot axis located on a gimbal ring or two concentric rings may be used. A third approach, suggested by Fiedler[10] employed a spherical jetavator in a spherical seat (Figure 6-6) and actuated by two push-pull rods located 90° (1.57 RAD) apart. This latter approach was not considered because problem areas are undefined as it has never been tested. It was considered less reliable than the other two since unequal thermal expansion could cause the ring to bind in its seat resulting in possible failure of the whole mission.

Of the remaining two systems, there appears little difference from a weight standpoint and since experience had been gained with the concentric ring approach on the Bomarc missile system this was selected for preliminary sizing.

The two jetavator rings were assumed to be mounted concentrically about the same center but rotating about axes at right angles to each other.

As in Bomarc there is a region of each ring stretching approximately 50° on each side of the support bearings, which does not contribute to side force and which can be reduced in width. The final width and thickness of this section depends only upon the supporting loads required. A lightweight ablative type material can be used for thermal protection.

That part of the ring which does contribute to side force must be reliable and noneroding. The only configurations which have a demonstrated capability to successfully withstand the anticipated environment of the 260 in. motor are sandwich type structures. These comprise a high temperature-resistant face plate (usually refractory), a heat sink core, and a load-bearing backup structure protected from downstream recirculation of exhaust gases by a layer of insulation (Figure 6-7).

Considerable weight reduction could be achieved by replacing the refractory facing of the jetavator ring and the heat sink core by an ablative material. However, the savings in weight would be partially offset by the larger size of jetavator ring required and larger structural bending loads.

There is no guarantee that each control element would erode in a uniform manner, and the eroding surface would change the side force/jetavator deflection characteristics, thus introducing unpredictable control requirements. Deflection requirements are increased, by an amount which is determined by the erosion rate of the ablative material used.

One requirement for the 260 in. motor is the capability to correct up to 1/4° (0.00436 RAD) of thrust misalignment. The jetavator ring could therefore be inserted a small distance into the exhaust stream for the complete duration of the firing, 143 sec.

The only application of an ablative jetavator system appears to be on vehicles with relatively short duration burning times. They are considered less reliable than noneroding jetavators and for these reasons were not investigated further.

Torque requirements were scaled from Polaris data which showed a maximum of 2,000 in.-lb (226 N-m). A more correct average value would appear to be 1,500 in.-lb (169.5 N-m). Torque is a function of the pressure acting on the inserted inner surface of the jetavator blade. It is also a function of the distance of the resultant force vector from the pivot axis. Since the force vector is supposed to pass through the pivot axis in a spherical jetavator system, this distance is ideally zero. However, misalignment during jetavator assembly to the nozzle and erosion during operation are two possible causes of deviation from the ideal. Making two gross assumptions that similar pressure forces act on the jetavator blade and similar deviations of the force vector from the pivot axis exist in both systems, an order of magnitude number can be calculated for the actuation torque.

The increase in exposed jetavator surface area increases as the square of the diameter.

$$\text{Thus } \left(\frac{278}{20}\right)^2 \times 1{,}5000 = 290{,}000 \text{ in.-lb } (32.8 \times 10^3 \text{ N-m})/\text{jetavator}$$

Stroke requirements are very large. Arc = R θ = 139 (5) /180

$$= \pm 12.1 \text{ in. } (\pm 30.7 \text{ cm})$$

Clearly some stroke reduction is necessary.

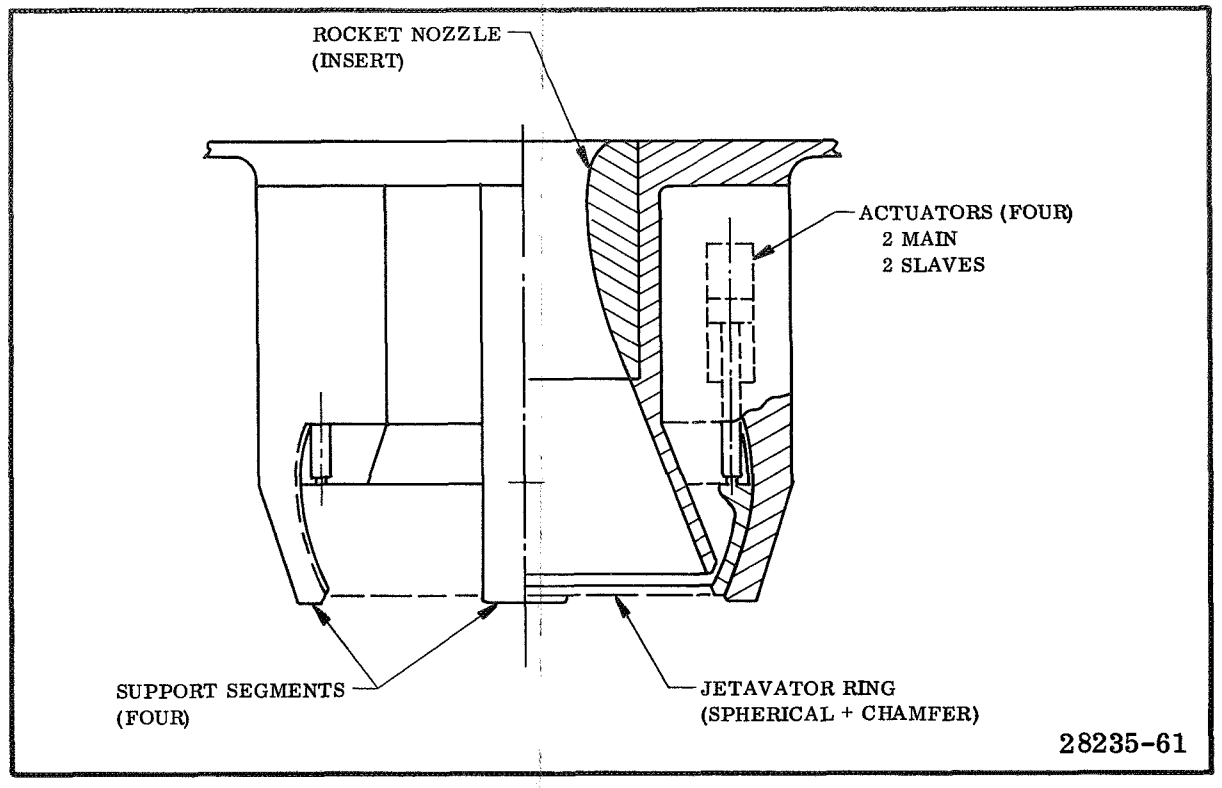

Figure 6-6. Jetavator for Omnidirectional Thrust Deflection

In calculating the approximate weight of each ring it was assumed that the width was 20 percent greater than the arc swept by the ring during maximum deflection. A total of 160° of each ring was assumed to have the sandwich type construction shown in this figure. Average diameter was taken to be 278 in.

Arc = $R\theta$ = (136) (5) π /180 = 11.9 in. Width = 11.9 + 20% = 14.3 in.

Total weight of sandwich construction = $(278)\pi \frac{320}{360}$ (14.3) $\left[(0.75)(0.56) + (2.5)(0.0686) + (0.5)(0.283) + (0.063)\right]$ = 8,900 lb

Total weight of support structure = $(278)\pi \frac{400}{360}$ $\left[(0.75)(14.3)(0.5)(0.283) + (0.063)\right.$ = 2,140 lb$\left.\right]$

Total weight of both rings excluding bearings = 11,040 lb

To eliminate sealing problems between the nozzle and jetavator rings but protect the actuation system and nozzle structure from exhaust gas blowback, a flash back shield was located just forward of the jetavators. Assuming 1/4 in. thick steel plate insulated each side to a thickness of about 1/2 in., the weight of this shield is approximately

260π (12) $\left[(0.25)(0.283)(0.75) + 0.063\right]$ = 1,130 lb

This assumes 25 percent of steel shield is scalloped out to reduce weight.

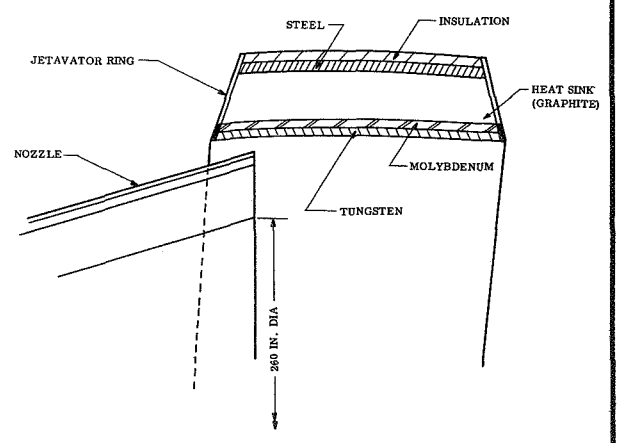

Figure 6-7. Typical Jetavator Configuration with Calculations

6.3 Preliminary Design and Screening

6.3.3 Flexible Exit Cone

FLEXIBLE EXIT CONE CONCEPT ELIMINATED BECAUSE OF LIMITED DEVELOPMENT HISTORY

A flexible exit concept was eliminated from further design consideration in view of its limited development history.

The flexible exit cone (Flex-X) concept, in which a section of the exit cone is replaced by a flexible joint to permit vectoring, offers considerable potential over other methods of TVC. It combines the advantages of a supersonic splitline nozzle (lower nozzle ejection loads and force amplification) with the advantages of a flexible bearing (elimination of the gimbal ring and O-ring seal). The result is a lightweight nozzle, which, because of the smaller, simpler flexible seal, offers a high reliability potential. The major drawback appears to be large actuation requirements as a result of the high internal aerodynamic torque.

Development of this concept is still in its early stages. Subscale materials tests have shown that the flexible exit cone nozzle joint can survive exposure to the rocket exhaust gas environment.

Design of a flexible exit cone may be broken down into three primary areas: (1) selection of pivot point and joint location, (2) selection of joint design, and (3) actuation requirements.

Figure 6-8 shows the major geometric variables of a flexible exit cone joint. Selection of the pivot point involves consideration of the following parameters: joint torque, (T_J); joint length, (L_{JT}); elastomer strain, (σ); ramp angle, (α_V); aerodynamic torque, (T_A); and side force amplification, (F_A).

Cold flow test data suggests the pivot point should be located as near to the joint as possible consistent with good joint design. An aft pivot, ie, one that is downstream of the joint, indicated force degradation rather than force amplification.

Side force amplification is generally reduced as joint location is moved downstream. This is primarily due to the reduced surface area downstream of the joint. There is, however, an upstream limit on location of the joint. This occurs when the shock produced by the joint during vectoring interacts with the opposite wall of the nozzle causing a reduction ir side force. Optimum location appears to lie between expansion ratios 1.5 and 2.5

Figure 6-9 shows three possible approaches to joint design. The first is a laminated flexible joint section exposed directly to the exhaust environment. The second is a recessed design, relying upon a narrow gap between shims to protect the

elastomer from the exhaust gas. The third is a protected joint, separated from the exhaust gases by a thermal barrier. The latter design is more complex than either of the other two designs, and requires more development. However, there is a higher confidence in the design and fabrication of the protected joint, since conventional flexible bearing materials (polyisoprene and stainless steel) can be employed.

Preliminary design of the flexible exit cone TVC system for the 260 in. motor based upon test data and analytical studies, would employ a flexible joint located at an expansion ratio of 2.0:1.

The angle, β_i, was made as large as possible consistent with a conservative joint design. This turned out to be approximately 55° (0.96 RAD) resulting in a pivot point location of 22.5 in. (57.2 cm) downstream of the throat.

Overall weight of the Flex-X nozzle is approximately 3,500 lb less than that of the supersonic splitline. The major portion of this difference resulting from smaller, lighter, end rings, either side of the bearing. Performance loss is negligible.

Torque requirements are virtually the same for the Flex-X as for the supersonic splitline and for the purpose of comparison with other TVC systems may be considered the same. For the 260 in. motor TVC requirements, a torque of about 27×10^6 in.-lb (3.05×10^6 N-m) will be required. The actuation system required to meet such large torques is more fully discussed in subsection 6.1.4, Supersonic Splitline.

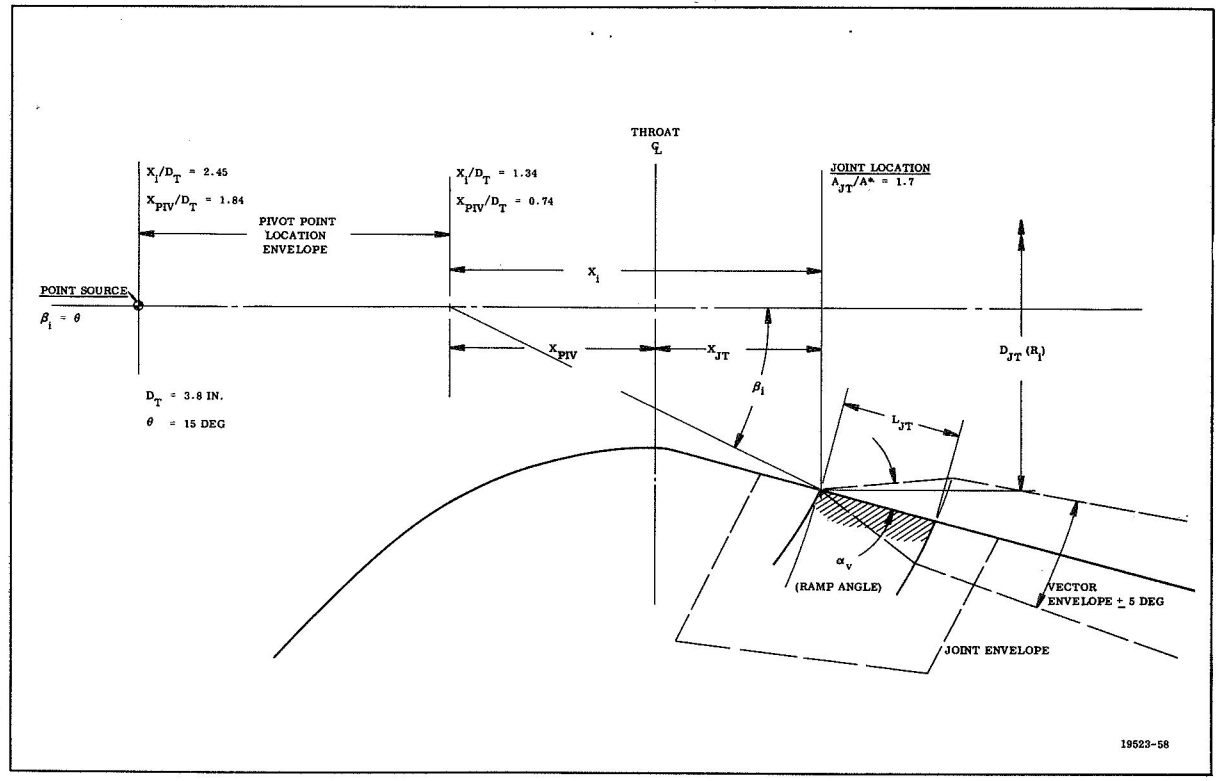

Figure 6-8. Pivot Point Location and Joint Nomenclature

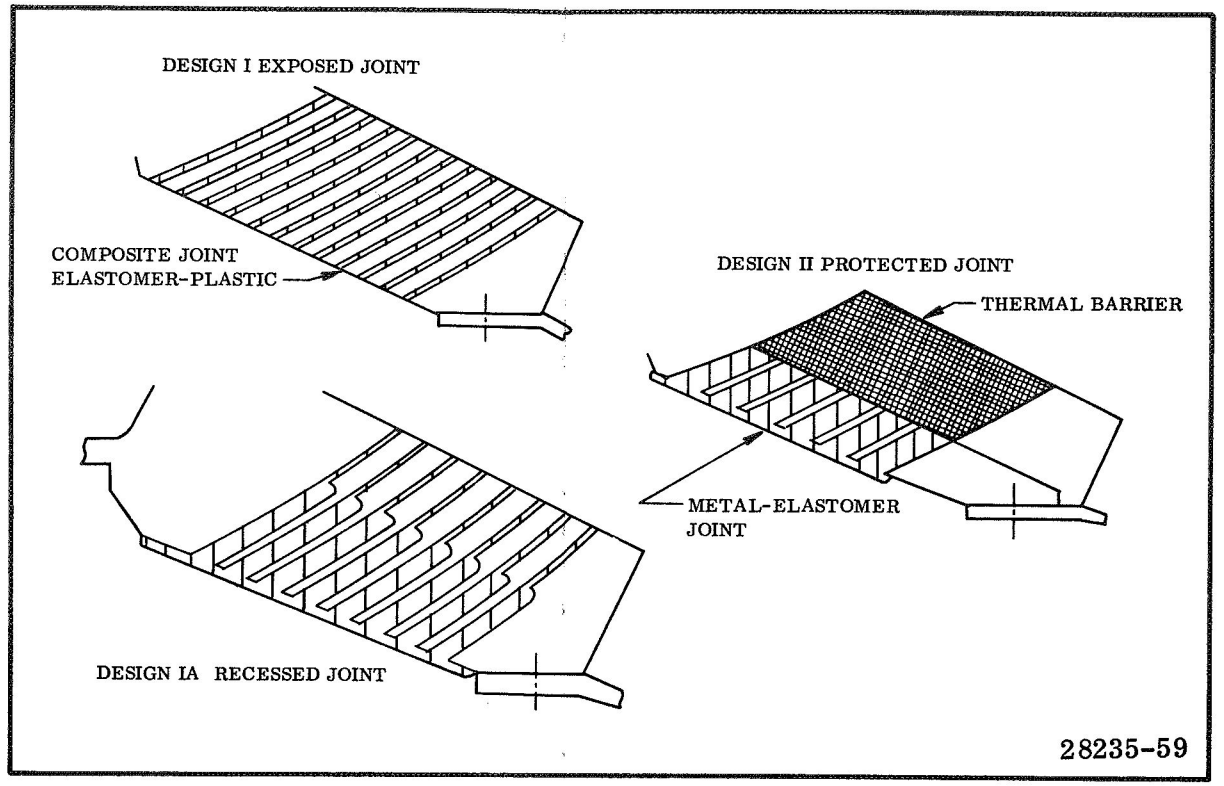

Figure 6-9. Flexible Exit Joint Design

6.3 Preliminary Design and Screening

6.3.4 Jet Vanes

JET VANES ELIMINATED BECAUSE OF MATERIAL DEVELOPMENT PROBLEMS

Jet vanes were eliminated from further consideration because of the material development problems that could be expected in view of the constant exposure to the motor exhaust.

Design data on jet vanes proved scarce. Theoretical predictions of the flow around a vane deflection system have been of little use to the designer, primarily because of the nonuniform type of flow in a rocket exhaust and because of the significant modification to the flow caused by the deflecting vane. Consequently, vane design, particularly vane profile, has proceeded largely on an experimental basis, usually for a specific application, as in the Sergeant and Pershing missile programs.

Jet vanes are necessarily subjected to continuous exposure of the exhaust environment. The resulting materials problem has never been fully solved, despite two extensive materials testing programs conducted during the development of the above two missiles. Severe erosion occurred in both cases although total burning time was relatively short compared to those currently in existence. The Sergeant motor burned for about 26 sec and the Pershing for approximately 39 sec. In the latter case, the final acceptable vane configuration sustained a 10 percent loss in planform area. The vane was constructed of 85 percent tungsten and 15 percent molybdenum.

Operating time for the 260 in. booster is 143 sec. Again, an extensive materials program would be necessary to determine a vane configuration which would withstand this duration. Such a program would carry a high development risk since a significant step forward in current materials technology would be required. Success of this type of program is highly questionable.

To reduce erosion, materials possessing a higher tungsten content would have to be investigated. A program of this nature would prove extremely costly as also would the final vane configuration.

Ablative jet vanes would be lighter and very much cheaper. However, because of the continuously eroding surface, the vane would possess continuously changing deflection angle/side force (lift) characteristics thus affecting response of the system in an unpredictable way. There is no guarantee that the vane would erode uniformly, possibly introducing a different side force in pitch-up than in pitch-down for the same vane deflection angle.

Jet vanes carry the highest performance penalty of all mechanical interference systems studied. Unlike other systems, thrust degradation occurs throughout the firing even when the vanes are not providing TVC. The Sergeant vane deflection system was designed to correct for 1/2° (0.0087 RAD) of thrust misalignment and drag losses varied between 0.45 and 0.7 percent during the test program. The Pershing missile sustained 0.6 percent thrust loss when providing zero vane deflection and this rose to 1.2 percent when providing the same TVC requirements as this study.

No scale-up data was available, but assuming a thrust loss of between 0.5 and 1.0 percent as typical for the 260 in. booster, an additional 17,000 to 34,000 lb (7,700 to 15,400 kg) of propellant would be required to achieve the total impulse requirements of this vehicle.

In any case, jet tabs, jetavators, and mechanical probes can provide the same degree of TVC without such a large performance penalty and with a considerably less severe materials problem.

One advantage of vanes is that it offers roll control in addition to TVC.

6.3 Preliminary Design and Screening

6.3.5 Supersonic Splitline

6.3.5.1 Design Concepts

SUPERSONIC SPLITLINE CONCEPT A CANDIDATE FOR FURTHER DESIGN EFFORT

The lightweight and development history of the supersonic splitline concept made it a candidate for further design effort.

The supersonic splitline approach to TVC has evolved from movable nozzle technology. The splitline between the fixed and movable sections of the nozzle is located in the supersonic section of the nozzle. The main advantages being lower nozzle ejection loads and force amplification. Considerations in selection of pivot point location and joint location are the same for all supersonic splitline concepts including that of the flexible exit cone discussed in a previous subsection. Cold flow test data suggest a joint location at an expansion ratio of 2.0:1 is near optimum. Pivot point location, depends partly on joint design, but ideally should be located as near to the splitline as possible.

Following selection of the pivot point and joint locations, the supersonic splitline may take one of two configurations: (1) the aft, movable portion of the exit cone may be vectored by means of a gimbal ring situated around the exit cone at the splitline or (2) the movable portion of the exit cone may be connected to the fixed section by a flexible bearing comprised of alternate layers of elastomer and steel shims.

In the case of the gimbal ring, the seal between the fixed and movable portions is usually in the form of an O-ring. This O-ring has been the source of continual problems with the gimbal ring approach. The flexible bearing becomes highly attractive at very large diameters when the gimbal ring becomes excessively heavy. The O-ring seal is also eliminated.

A TVC computer program is available at Thiokol for comparison of these two concepts. In addition to selecting pivot point and joint location; the design vector angle, required as input to the program, was based on a point of side force insertion halfway between the splitline and the exit plane. The resultant vector angle satisfying design requirements for the 260 in. motor was 1.15° (0.02 RAD).

HIGH TORQUE REQUIREMENT SEEN AS DISADVANTAGE OF SUPERSONIC SPLITLINE CONCEPT

One of the disadvantages of the supersonic splitline concept is the high torque requirement. For the two systems considered, the gimbal ring maximum torque was 24 x 10^6 in.-lb (2.71 x 10^6 N-m) and the flexible bearing 27 x 10^6 in.-lb (3.05 x 10^6 N-m).

A force amplification factor of 1.4 and torque amplification factor of 1.8 were considered reasonable assumptions for the comparison based upon cold flow test data obtained at Thiokol.

Results of this comparison showed that the torque requirements were extremely high, 24 x 10^6 in.-lb (2.71 x 10^6 N-m) for the gimbal ring and 27 x 10^6 in.-lb (3.05 x 10^6 N-m) for the flexible bearing. Total nozzle weights were 82,600 lb (37,500 kg) for the gimbal ring, of which the ring itself weighed 17,600 lb (7,980 kg), and 58,900 lb (36,700 kg) for the flexible bearing. Performance loss in each case is negligible.

Assuming a lever arm of 100 in. (254 cm) (ie, the distance from the pivot point to the line of action of the actuator) and a 4,000 psi hydraulic supply pressure, the cross sectional area of the actuator piston is

$$A_P = \frac{27 \times 10^6}{3,900 \times 100} = 70 \text{ sq in. } (452 \text{ cm}^2),\ D_P = 9.55 \text{ in. } (24.2 \text{ cm}).$$

Where D_P is the piston diameter.

The stroke requirement is:

$$\frac{(100)(0.82)}{57.3} = 1.43 \text{ in. } (3.63 \text{ cm})$$

Although the design vector angle is 1.15° (0.02 RAD), because of force amplification, the angle actually turned through by the nozzle is only 0.82° (0.0143 RAD).

For a slew rate of 3°/sec (0.0524 RAD/sec) in the oblique plane, a slew rate of 2.12°/sec (0.037 RAD/sec) is required in the pitch and yaw planes.

Pump flow requirements are then,

$$Q = A_X = (70)\ \frac{(1.43)\ (2.12)}{(0.82)} = 259 \text{ cu in./sec } (4.25 \text{ l/sec/actuator})/\text{actuator}.$$

$$= \frac{2 \times 259}{3.85} = 135 \text{ gpm } (8.5 \text{ l/sec}).$$

A tradeoff of various actuation systems has been conducted in the Movable Nozzle section (Section 5.0) of this study, where power requirements were also very large, approximately 17 x 10^6 in.-lb (1.92 x 10^6 N-m).

The most promising means of supplying this requirement appears to be a warm gas turbine system driving a variable displacement pump. To satisfy peak power demands an accumulator is incorporated on the delivery side of the pump. A typical combination would be a Vickers PV3-300 pump incorporating a 500 cu in. accumulator.

6.3 Preliminary Design and Screening

6.3.5 Supersonic Splitline

6.3.5.3 Description of Candidate Design

HIGH TORQUE REQUIREMENTS AND SEVERE THERMAL ENVIRONMENT SEEN AS MAIN AREAS OF DEVELOPMENT EFFORT

A preliminary layout of the supersonic splitline was accomplished in order to reasonably size the system.

High aerodynamic torque is inherent in this design as well as a severe thermal environment. Minimizing these two factors was seen as the main development effort.

Figure 6-10 shows the preliminary layout of the supersonic splitline system selected for the tradeoff study. The supersonic splitline TVC system for the 260 in. motor may be divided into three basic sections: (1) flexible bearing, (2) nozzle support structure, and (3) actuation system.

Location of the splitline was at an expansion ratio of 2.0:1 and the pivot point was located approximately 11.6 in. (29.4 cm) downstream of the throat.

Of the mechanical interference TVC nozzle designs studied, this concept required the greatest amount of modification to the basic convergent-divergent nozzle. The exit cone was "split" into two separate sections with the section forward of the splitline fixed, and the section aft of the splitline movable. The interface between the forward and aft sections of the exit cone was spherical in contour and the two sections were joined by a flexible seal consisting of 20 spherical, metal (304 CRES) shims and 21 layers of elastomer. The metal shims were each 0.050 in. (0.127 cm) thick, while the elastomer layers were each 0.025 in. (0.0635 cm) thick.

The flexible seal was supported by two load carrying steel rings; the forward end ring was located forward of the bearing and the aft end ring located aft of the seal. An I-beam shaped exit ring was added to the movable section of the exit cone structure to distribute the load applied by the hydraulic actuators. The exit ring and aft end ring were designed as integral parts of the movable section's support structure; the forward end ring was designed as a separate piece bolted to the fixed section's support structure.

A rubber boot was incorporated into the design in order to protect the flexible seal from the radiant heat associated with the hot gas.

The steel support structure was terminated aft of the exit ring, and structural fiberglass was employed as the support material for the remaining length of the exit cone, as with the basic fixed nozzle. The interface between the steel and fiberglass support structures was joined by an overwrap of structural fiberglass.

The nozzle assembly weight was calculated to be 58,890 lb (26,700 kg), an increase of 10,990 lb (4,980 kg) over the basic fixed nozzle. Of this increase, 220 lb (99.8 kg) was attributable to the flexible seal; 4,693 lb (2,125 kg) resulted from the fixed section structure (including forward end ring) buildup; and the remaining 6,077 lb (2,760 kg) was in the support structure of the movable section.

The total torque required to vector the nozzle was 27.18 million in.-lb (3.06 x 10^6 N-m), broken down as follows:

Internal aerodynamic torque	15,486,575 in.-lb	1.748 x 10^6 N-m
Offset torque	3,871,643 in.-lb	0.437 x 10^6 N-m
Gravity torque	5,113,798 in.-lb	0.579 x 10^6 N-m
Seal torque	2,343,989 in.-lb	0.265 x 10^6 N-m
Boot torque	366,662 in.-lb	41,400 N-m

The major contributing factor to the total torque was the internal aerodynamic component. This is inherent in the design and is the main disadvantage with supersonic splitline nozzles, regardless as to whether movement is provided by a flexible seal, gimbal ring, or ball and socket. Also inherent with this nozzle concept is the severe thermal environment at the point of gas reattachment on the downstream edge of the splitline, which causes a high rate of erosion.

The attempt to minimize these two factors would constitute the main development effort. Establishing the splitline location at the point of maximum amplification factor will reduce the physical vector angle required to obtain the desired vehicle steering and thus reduce aerodynamic torque. Determining the precise thermal environment at the splitline is a prerequisite to designing for that environment.

Vectoring of the movable portion of the exit cone is achieved by hydraulic linear servoactuators driven by a variable displacement pump. Warm gas turbine system supplies the power for the pump. This type of actuation system was the most attractive from a weight and reliability standpoint. A servopump system was also considered but as servopumps are not generally off the shelf items they were rejected for reasons of cost.

The weight breakdown of the supersonic splitline is as follows:

Nozzle assembly	58,890	26,700 kg
Servoactuators (2)	400	181.5 kg
Gas generator	280	127 kg
Pump	28	12.7 kg
Turbine gearbox	42	19.05 kg
Hydraulic fluid	76	34.5 kg
Accumulator	33	14.98 kg
Miscellaneous (lines, filters, reservoir, etc)	226	102.5 kg
Total weight	59,975	27,200 kg

The flexible bearing weighed 220 lb (99.8 kg) and is included in the nozzle assembly. The support structure necessary to contain the bearing added a total of 10,990 lb (4,980 kg) to the baseline nozzle design.

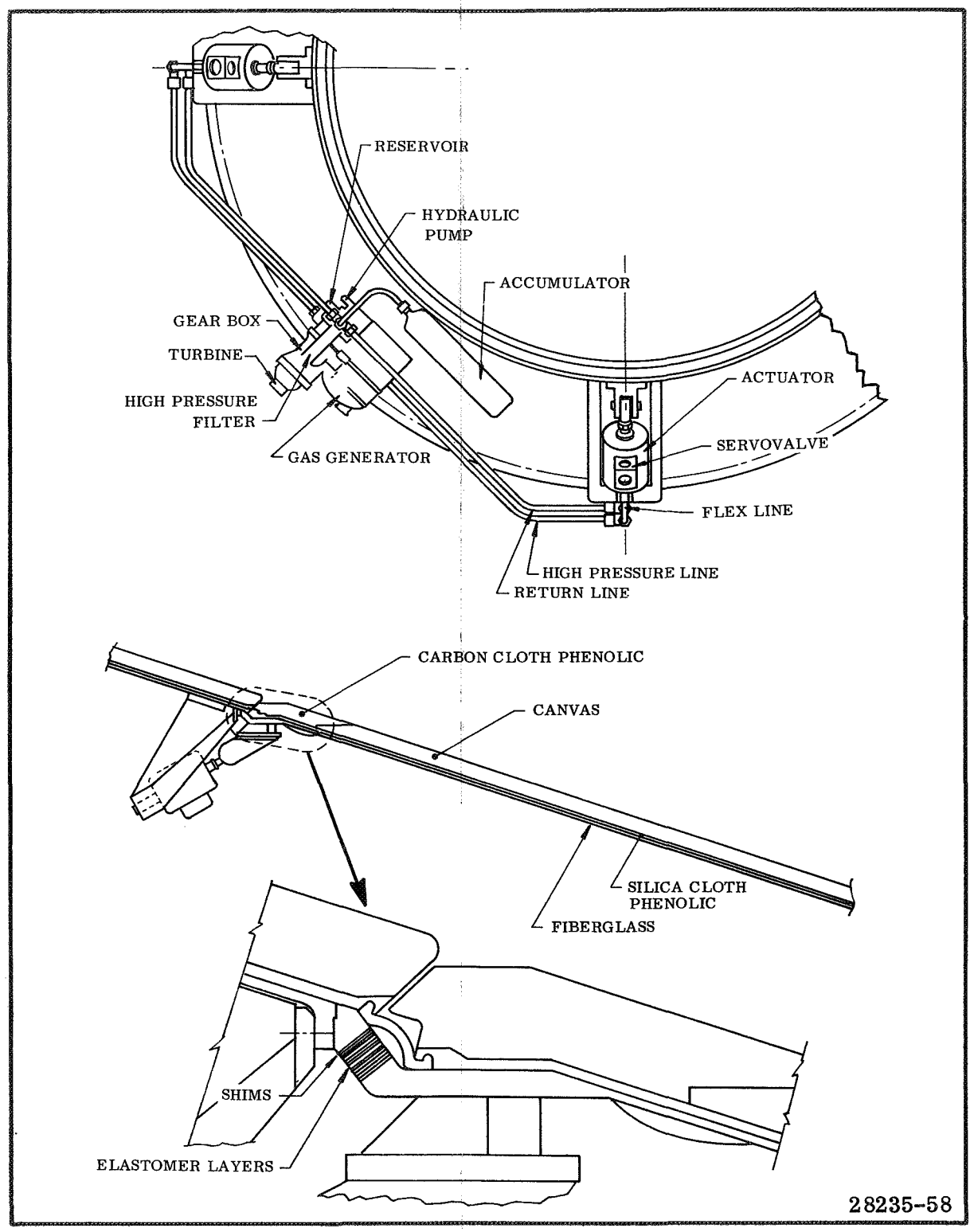

Figure 6-10. Supersonic Splitline

6.3 Preliminary Design and Screening

6.3.6 Jet Tabs

JET TABS CONCEPT SELECTED FOR FURTHER DESIGN EFFORT - LOCKHEED TECHNOLOGY USED

Jet tab design was largely based on data from Lockheed's 156 in. (396 cm) diameter motor program. Two main reasons for this were (1) Lockheed's tabs alone would produce almost 60 percent of the side force requirement of the 260 in. diameter launch vehicle and (2) a tab configuration had evolved from materials evaluation testing, conducted during the 156 in. (396 cm) program, that successfully demonstrated the capability for survival in the extreme conditions of the exhaust environment. Much of Lockheed's technology thus could be applied directly to the 260 in. diameter motor jet tab design.

Because of the extensive design history, the jet tabs concept was chosen for further design effort.

Figure 6-11 shows the relationship between exhaust jet deflection and exit area blockage ratio. At the exit plane, a TVC angle of 1.03° (0.018 RAD) or side force ratio (F_s/F_a) of 0.017 is required. This results in a blockage ratio of 0.03 or a tab projected area of 1,592 sq in. (10,280 cm^2). Construction and handling of tabs with these dimensions would be exceedingly difficult. Adopting two tabs per quadrant results in a tab area of 850 sq in. (5,480 cm^2), or slightly more than half that of a single tab. In any case, the single tab violates the aft skirt envelope of the 260 in. launch vehicle.

In addition to minimizing tab size, there are certain other advantages in selecting a dual tab system. A smaller tab better fits the envelope. Power requirements per tab are reduced. Tab geometry is not restricted to a profile which must maintain the side force vector directly in the pitch or yaw plane, ie, equal areas of each tab remaining on either side of the pitch or yaw plane which results in an undesirable nonlinear area/tab rotation angle relationship. Reliability of the launch vehicle is increased by using the redundancy inherent in a multiple tab system, despite the increased complexity of additional components. Should the failure of a complete tab occur, adjacent tabs can contribute as much as 70 to 80 percent of the required control force.

A dual tab system may also be adapted to provide roll control by tilting the tab surface 1° to 2° (0.01745 to 0.0349 RAD).

As a first approximation, assume the side force per tab acts in a direction 22-1/2° (0.393 RAD) from either the pitch or yaw plane.

Then $F_s = 2\ F_t \cos 22\text{-}1/2°$

where: F_s = resultant side force in pitch/yaw plane (lb)

F_t = side force per tab (lb)

Now: $$\frac{F_s}{F_a} = 0.0179\ \frac{F_t}{F_a} = \frac{0.0179}{2 \cos 22\text{-}1/2°} = 0.00968$$

From Figure 6-11 $$\frac{A_{TAB}}{A_{EXIT}} = 0.016$$

$$A_{TAB} = 850 \text{ sq in. } (5{,}480 \text{ cm}^2).$$

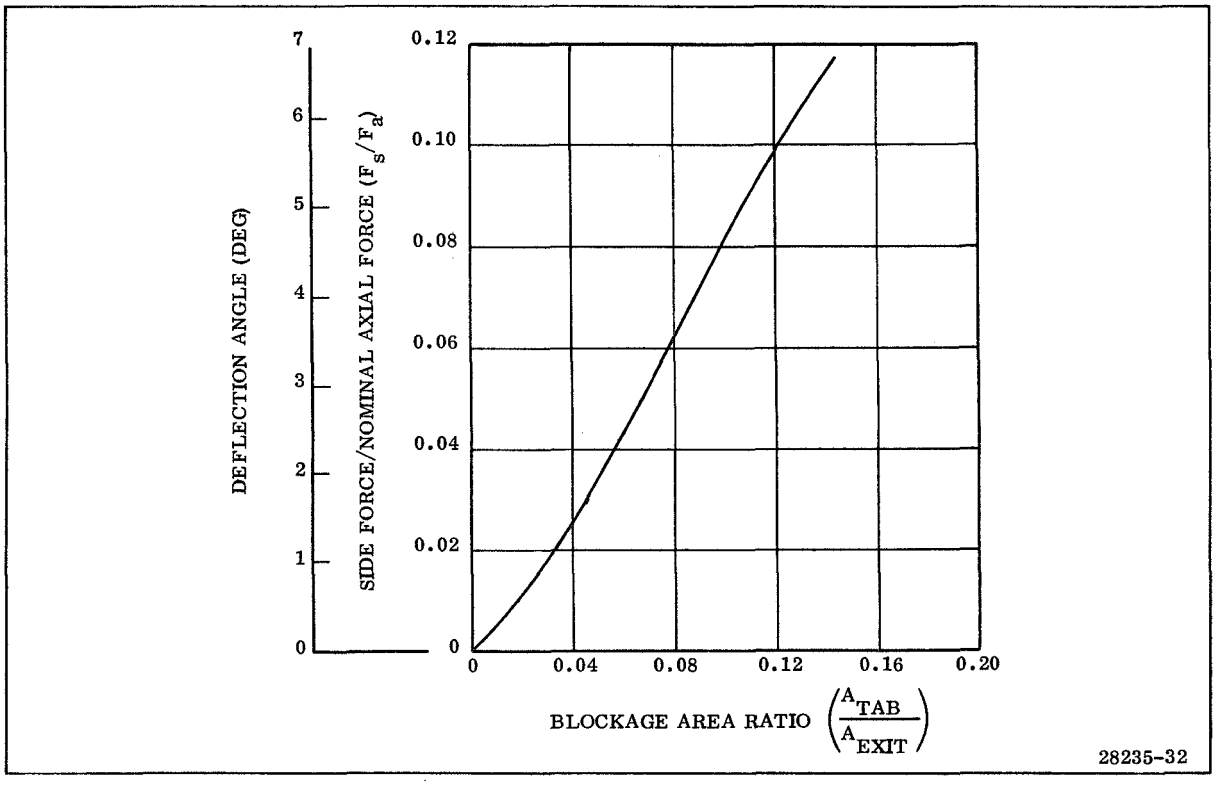

Figure 6-11. Typical TVC Angle and Side Force Ratio vs Jet Tab Blockage Area Ratio

6.3 Preliminary Design and Screening

6.3.6 Jet Tabs

6.3.6.1 Design Considerations

JET TAB DESIGN DESCRIBED

Lockheed's 156 in. (396 cm) SRM tab design information was used as the basis for the 260 in. SRM jet tabs.

Jet tab construction is a composite structure comprising a refractory face plate, a backup plate also refractory, heat sink, insulation, steel support structure and outer insulation.

Preliminary data were used to arrive at a typical jet tab configuration for the 260 in. motor application from which an estimated weight could be obtained. The face plate of each tab is composed of 3/8 in. (0.952 cm) thick segmented unalloyed tungsten. This facing is backed by 3/8 in. (0.952 cm) thick sections of 70 percent molybdenum, 30 percent tungsten plate. The heat sink is ATJ graphite, approximately 2.5 in. (6.35 cm thick, backed by an insulator of silica cloth phenolic. Each tab assembly is held together with refractory bolts. Two typical face retention configurations are shown in the prelimin layout drawing (Figure 6-12). The first (detail-a) shows short tungsten bolts threaded into a block of 70 percent molybdenum, 30 percent tungsten, which extends into the graphite heat sink. This, in turn, is bolted to the steel structure by means of molybdenum bolts. This type of construction allows for thermal expansion of the face plates and minimizes the loads taken by the tungsten bolts. The second (detail-b) simply shows tungsten bolts passing through the complete tab section to the steel support structure. In both cases, Belleville washers maintain constant tension in the bolts as the tab structure expands.

An important factor to be considered is jet tab relief angle. This affects side force on the tab and hence affects the aerodynamic torque. For the design selected the relief angle is 20° (0.349 RAD), however this angle is representative and not necessar the final design angle.

The jet tabs are supported by a large steel structure, the torque box, which houses the tab shafts and bearing cages. A total of three bearings is necessary, two to take the radial load and one the thrust load. The tabs are mounted to the shaft on keyways to insure positive rotary location. The forward end of each shaft is provided with a clevis for attachment of the linear hydraulic servoactuators.

The torque box is by far the heaviest component of the jet tab TVC system. Because the diameter of the torque box is so large, approximately 280 in. (7.1 m) diameter, the overall weight is significantly affected by very small changes in torque box dimensions. During design of the torque box emphasis must be placed on reducing these dimensions to a minimum consistent with good design practice and accepted margins of safety.

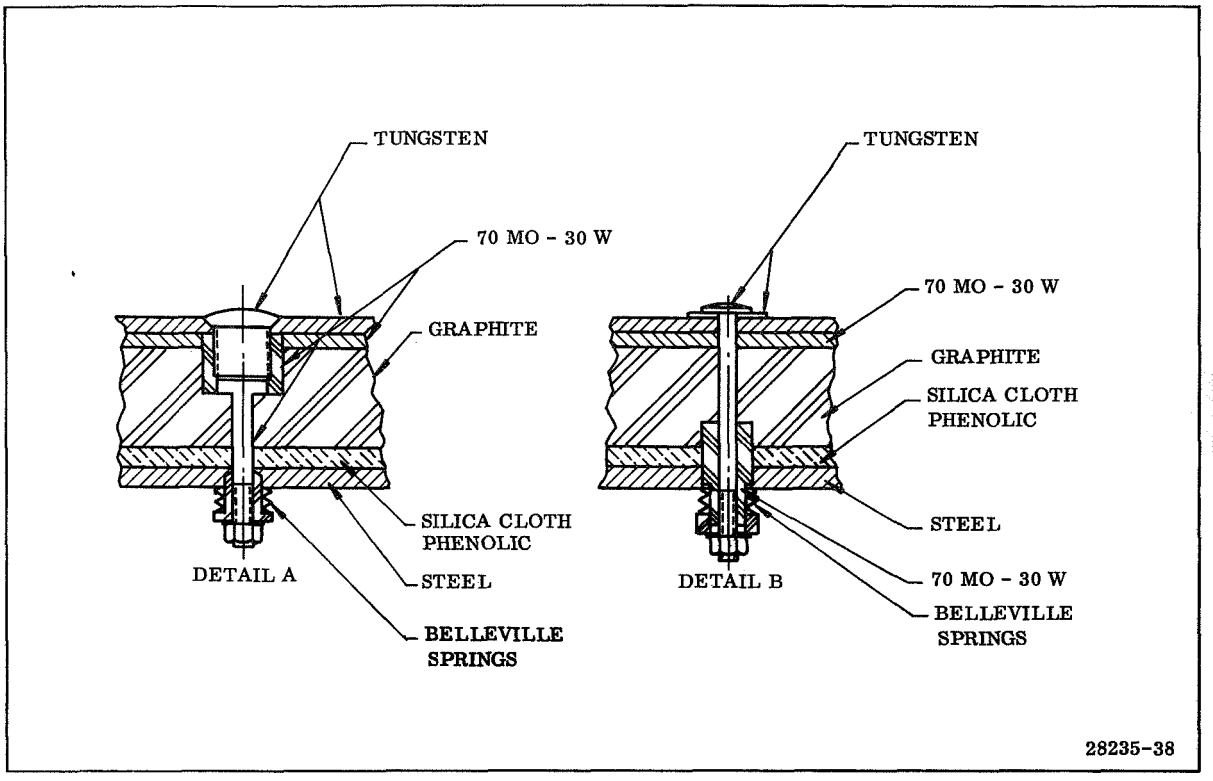

Figure 6-12. Typical Jet Tab Face Plate Retention Configuration

6.3 Preliminary Design and Screening

6.3.6 Jet Tabs

6.3.6.2 Actuation System and Power Requirements

WARM GAS TURBINE SYSTEM WITH LINEAR SERVOACTUATORS SELECTED

The maximum torque requirement for a 260 in. SRM jet tab system is approximately 107,800 in.-lb (12,200 N-m). Because of weight advantage, a warm gas turbine system using linear hydraulic servoactuators was selected for the jet tabs actuation system.

The forces acting on the jet tabs are comprised of aerodynamic, inertia, and friction forces. The sum of these components determines the required actuation torque. Aerodynamic torque is a function of the tab side pressure distribution which in turn is a function of tab relief angle. Maintaining the sharpness of the tab leading edge is a mandatory design requirement if low aerodynamic torques are to be achieved. If the tab edge erodes and becomes rounded the aerodynamic torque rises because a component of the tab front face pressure acts in a direction of the torque load. Face pressures are considerably higher than tab side pressures. Figure 6-13 shows tab side pressures as a function of blockage area computed from AGC hot firing test data. The figure shows that tungsten tabs generally have the lowest side pressures and when an eroding material such as graphite was used pressure levels and hence torque values rose by factors of 3 to 5.

Estimated aerodynamic torque was calculated as follows.

$$T_a = A_{ts} \cdot x_{scp} \cdot \frac{\left(P_{ts}\right)}{P_c} P_{max} = (370)\ (24)\ (0.007)\ (764) = 47,500 \text{ in.-lb } (5,360 \text{ N-m})$$

where:

A_{ts} = tab side surface area (sq in.)

x_{scp} = distance of tab side center pressure from axis of jet tab shaft (in.)

$\frac{\left(P_{ts}\right)}{P_c}$ = tab side pressure ratio

P_{max} = maximum expected operating pressure (psi)

The friction torque is a result of bearing loads applied during cycling of the tabs. Bearing friction was calculated from the equation:

$$T_{fr} = \frac{M_B \mu_{fr} r_s}{l_B} = \frac{(3.4 \times 10^6)\ (0.03)\ (3.75)}{25} = 15,300 \text{ in.-lb } (1,730 \text{ N-m})$$

where:

$M_B = F_T x_{acp} = (107,000)\ (31.8) = 3.4 \times 10^6$ in.-lb $(0.384 \times 10^6$ N-m)

M_B = axial tab bending moment (in.-lb)

F_T = maximum axial force on tab face (lb)

x_{acp} = distance of jet tab axial center of pressure from tab shaft centerline (in.)

μ_{fr} = coefficient of friction

r_s = radius of tab shaft (in.)

l_B = distance between bearing centers (in.)

Friction torque is significantly affected by the distance between bearing centers. In order to reduce torque box size (and hence weight) to a minimum consistent with good design practice, friction torque necessarily increases. The location of the torque box is at such a large diameter, that the savings in weight achieved by even a small reduction in torque box length, is far more significant than the small increase in actuation system weight as a result of increased torque requirements.

Inertia torque is a function of jet tab weight and acceleration of the system. The weight of each tab, including the tab shaft, was estimated at approximately 1,050 lb (1.77 kg). As no system response was given in the design requirements, and acceleration was determined by assuming the tabs rotated in a sinusoidal manner according to the function, then

$$\theta = A \text{ Sin } (2\pi f \cdot t)$$

where:

θ = tab rotation angle (deg)

A = amplitude (deg)

f = frequency (cps)

t = time (sec)

Maximum slew rate then becomes

$$\dot{\theta} = A\,(2\,\pi\,f)$$

and maximum acceleration is,

$$\ddot{\theta} = A\,(2\,\pi\,f)^2$$

A design requirement is a maximum slew rate of 3°/sec (0.0524 RAD/sec). Since a 60° (1.048 RAD) tab rotation produces 1° (0.01745 RAD) of TVC, the maximum slew rate of the tab is 180°/sec (3.142 RAD/sec). This is equivalent to a frequency of 1 cps. The maximum acceleration is then,

$$\ddot{\theta} = \frac{30.(2\,\pi)^2}{57.3} = 20 \text{ rad/sec}^2 \ (1{,}145°/\text{sec}^2)$$

Maximum inertia force is then $\frac{(1,100)}{32.2} \cdot (20) \cdot \frac{(28)}{12} = 1{,}600$ lb (7,170 N)

Maximum inertia torque becomes $T_{in} = (1{,}600)\ (28) = 45{,}000$ in.-lb (5,090 N-m)

Total torque requirements per tab are,

$$T_a + T_{fr} + T_{in} = 47{,}500 + 15{,}300 + 45{,}000 = 107{,}800 \text{ in.-lb } (12{,}200 \text{ N-m})$$

A comparison was made between linear and rotary actuators and between a warm gas turbine and warm gas blow system to meet the power requirements of the jet tab system. The results are summarized below.

	Torque			System Weight			Torque		Weight	
	(in.-lb)	(N-m)	Actuator	(lb)	(kg)	Actuator	(in.-lb)	(N-m)	(lb)	(kg)
Blowdown:	120,000	13,560	Linear	2,988	1,355	Linear	100,000	11,300	29.8	13.5
	120,000	13,560	Rotary	4,217	1,910	Linear	120,000	13,560	33.5	15.2
						Linear	140,000	15,810	37.2	16.85
Turbine:	120,000	13,560	Linear	1,138	516	Rotary	100,000	11,300	87.0	39.4
	120,000	13,560	Rotary	1,931	875	Rotary	120,000	13,560	95.5	43.3
						Rotary	140,000	15,810	102.5	46.5

The warm gas blowdown system is considerably heavier than the warm gas turbine system. Most of the difference between the two systems can be accounted for in the weight of the accumulator and the weight of oil expended, which together take up about 50 percent of the total weight of the blowdown system.

Linear actuators appear to weigh about one-third that of rotary actuators and also offer a lower weight penalty to increased torque requirements.

Consequently, a warm gas turbine system using linear hydraulic servo-actuators was selected for the actuation system.

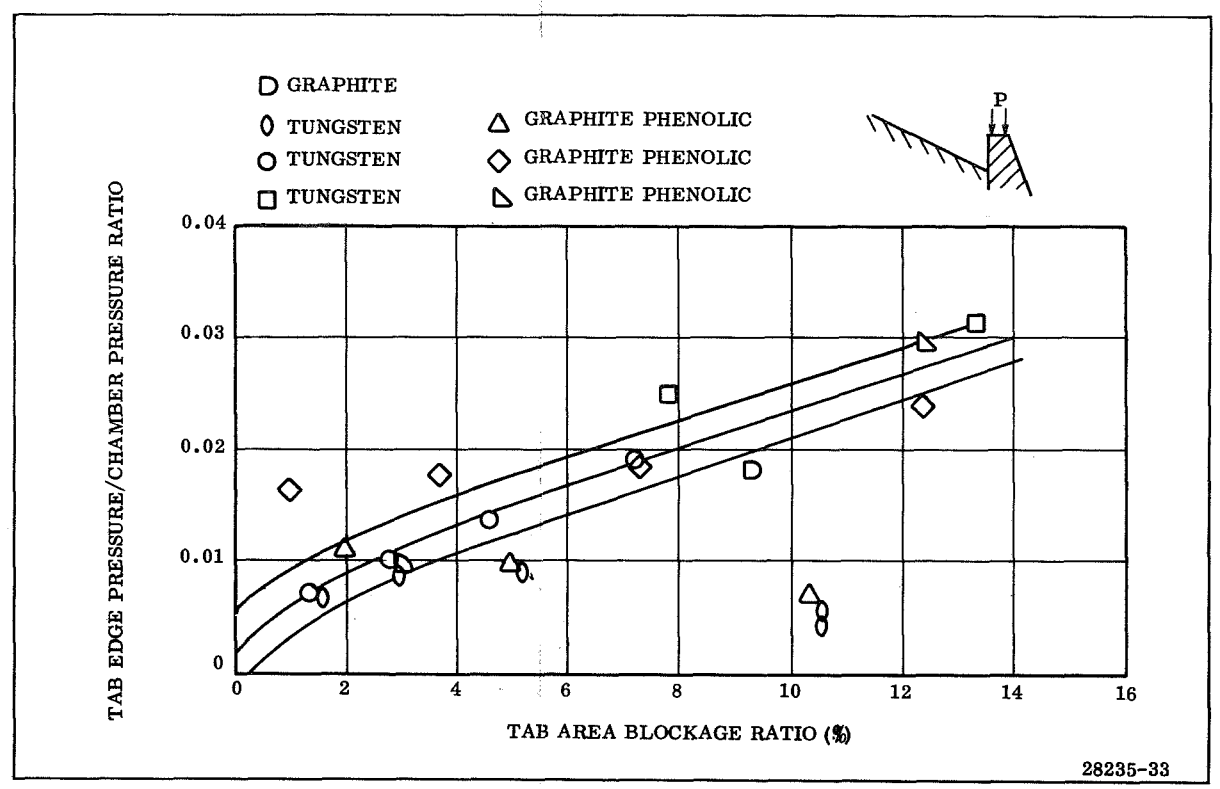

Figure 6-13. Jet Tab Side Force Pressure vs Blockage Area Ratio

CANDIDATE SYSTEM DESCRIBED

Design of the candidate jet tab system included an efficient multiple tab system. Redesign of the last 45 in. (114.1 cm) of the exit cone to accommodate the jet tabs raised the nozzle weight by 17,593 lb (7,960 kg). The actuation system consisting of a warm gas, high speed turbine driving a fixed displacement hydraulic pump (with accumulator) was designed to produce a torque of 140,000 in.-lb (15,810 N-m).

Figures 6-14 and 6-15 show the preliminary layout of the jet tab TVC system selected for the tradeoff study. The design is based largely on the results of Lockheed's 156 in. diameter motor test program which successfully demonstrated jet tabs to be an effective and reliable means of TVC on large motors. In fact, Lockheed's tabs, per se, would provide over 60 percent of the side force requirements of the 260 in. launch vehicle under consideration.

A multiple tab system, two tabs per quadrant, was selected over a single tab system. This has the advantage of reducing tab dimensions to manageable proportions. Other advantages of a dual tab system are increased tab efficiency, increased vehicle reliability, and the potential of roll control.

The jet tab TVC system consists of three basic sections: (1) the jet tabs, (2) the jet tab support structure, and (3) the actuation system.

Each of these, in turn, is described below together with the power requirements and modifications to the baseline nozzle.

A composite structure was assumed for the tab configuration A refractory faceplate, graphite heat sink, and insulated support structure. Tab weight was estimated as follows:

$$W_{TAB} = A_{TAB}\left[\rho_1 T_1 + \rho_2 T_2\right] + \text{-----} \rho_n T_n$$

where:

A_{TAB} = area tab face = 850 sq in. (5,480 cm^2)

ρ_1 = density of first material, etc (lb/cu in.)

T_1 = thickness of first material, etc (in.)

Total tab weight was 1,050 lb (476 kg), comprising 783 lb (355 kg) for the tab and 267 lb (121 kg) for the shaft.

The shaft and bearings must be designed to withstand the axial load acting on the face of the tab (F_{TAB}) and the resultant bending moment about the shaft. The axial load was estimated to be:

$$F_{TAB} = k\, P_{max}\, A_{TAB} = (0.165)(764)(850)$$
$$= 107,000 \text{ lb } (480,000 \text{ N})$$

where k was taken from ref 26a and P_{max} is MEOP. The resultant bending moment is thus,

$$(107,000)(318) = 3.4 \times 10^6 \text{ in.-lb } (0.384 \times 10^6 \text{ N-m})$$

Modification to the basic convergent-divergent nozzle required for the needs of the jet tab method of TVC consisted of replacing the canvas liner with carbon cloth phenolic at the aft end of the exit cone and substituting steel in place of fiberglass as the exit cone structure material.

Carbon cloth phenolic was substituted for canvas as the liner material for the last 45 in. (1.141 cm) of the exit cone. This was necessary because of the excessive erosion in this area due to the oblique shock wave created by the insertion of the jet tabs into the exhaust stream during vectoring.

The structure consisted of two steel cones bolted together. The first, 0.3 in. (0.761 cm) thick, extended from the nozzle exit cone interface to a point 233 in. (5.92 m) aft of the nozzle throat. The second, 0.75 in. (1.9 cm) thick, extended the remaining length (45 in.) (114.1 cm) of the exit cone. The buildup in structure thickness was necessitated by the aerodynamic forces exerted upon the tab by the nozzle exhaust. The interface between the two sections was designed to coincide with the initiation of the carbon cloth liner in the aft section of the exit cone to facilitate fabrication.

It was decided to design the exit cone structure in two separate sections, as opposed to a single piece with a gradual thickness increase along the length, for reasons of fabrication and assembly ease. The aft structural cone carries the entire vectoring system. This includes tabs, shafts, bearings, torque box, and actuators. The ability to assemble these components to a separate, bolt-on steel cone allows jet tab checkout tests and any necessary rework to be performed prior to final nozzle assembly.

The nozzle assembly weight, excluding jet tabs, shafts, bearings, torque box, or actuators was 65,494 lb (29,620 kg) (38,251 lb (17,350 kg) insulation and 26,123 lb (11,840 kg) structure . This was an increase of 17,593 lb (7,960 kg) over the unmodified fixed nozzle weight. The 134 lb (60.8 kg) insulation weight increase was due to the substitution of carbon cloth for canvas in the aft end of the exit cone. The remaining 17,454 lb (7,910 kg) increase was due to the structural buildup in the exit cone.

A conservative approach was adopted for the actuation system which was designed to produce a torque of 140,000 in.-lb (15,800 N-m) in the stall condition. A warm gas, high speed turbine driving a fixed displacement hydraulic pump was selected for the jet tab power supply. An accumulator is incorporated in the delivery side of the pump to supply sufficient fluid to meet peak power demands. Linear servoactuators provide

the force necessary for tab rotation. Rotary actuators proved to be almost three times as heavy as linear actuators for the same torque requirements. Consideration was given to a blowdown system as a power source; however, the weight penalty incurred by the expended fluid and the blowdown accumulator was considered too high (1,800 lb) (816 kg).

The selected actuation system weight is approximately 835 lb (378 kg), assuming one actuator per tab. Should torque requirements be increased, the pump selected is capable of a 25 percent increase in power output simply by increasing its speed. The only weight penalty incurred is that of additional propellant in the warm gas generator. For the full 25 percent increase in pump horsepower, the additional propellant would weigh about 31 lb (14.05 kg).

The following is a weight breakdown, by component, of the selected jet tab TVC system.

	Pounds	kg
Modified nozzle (excluding torque box)	65,360	29,600
Torque box	12,000	5,440
Shafts (8)	2,128	965
Tabs (8)	6,264	2,840
Servoactuators (8)	280	127
Pump	20	9.06
Turbine gearbox	40	18.12
Hydraulic fluid	35	15.88
Accumulator	25	10.32
Miscellaneous (lines, filter, disconnect, and etc)	200	90.6
Total	86,475	39,200

The torque box weight estimate is the most approximate of those listed. Because of the complex nature of the torque box loading, a detailed structural analysis is required to accurately estimate an adequate torque box geometry (thicknesses, etc).

It is assumed that the total allowable deflection of the jet tab when fully inserted is to be selected by the designer. The smaller the total deflection allowed, the heavier the torque box.

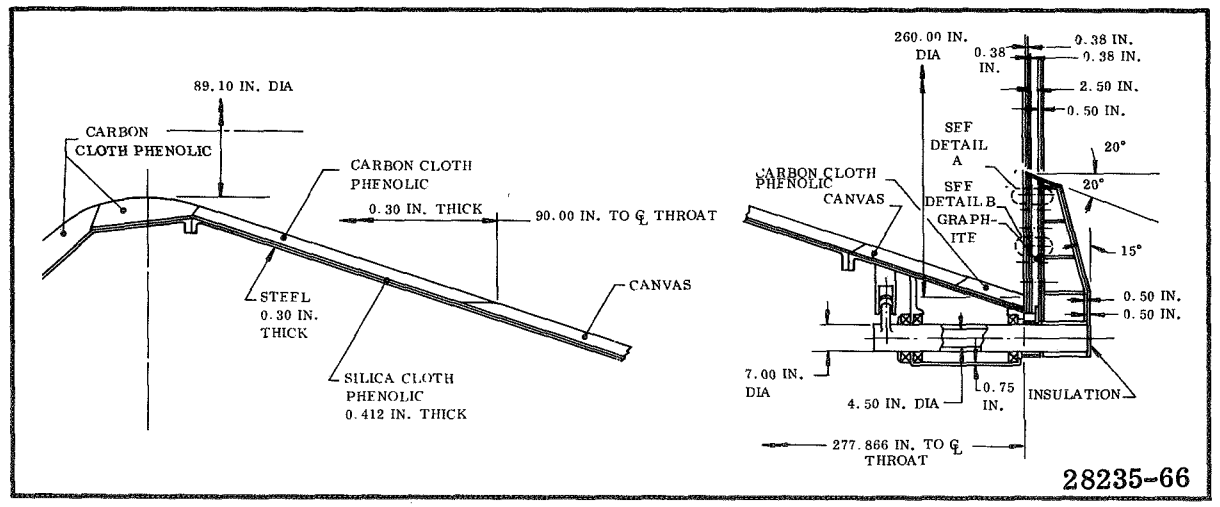

Figure 6-14. Jet Tabs

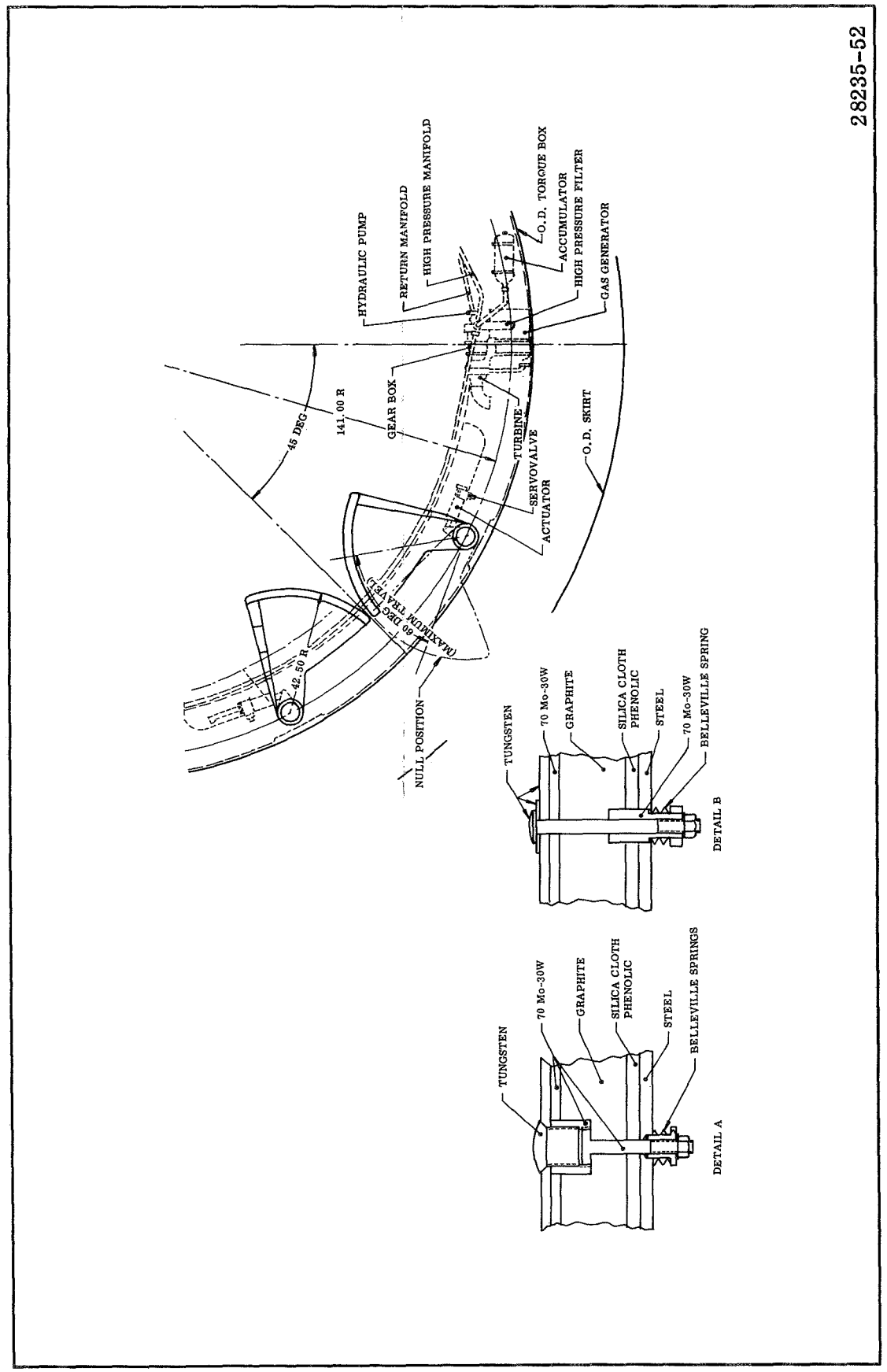

Figure 6-15. Jet Tabs

6.3 Preliminary Design and Screening

6.3.6 Jet Tabs

6.3.6.4 Performance Loss

PERFORMANCE LOSS PREDICTED WITH JET TABS

One of the disadvantages of the jet tab concept is the performance loss incurred as the result of inserting the tab into the motor exhaust.

Figure 6-16 shows the thrust loss as a function of side force ratio.

For: $\frac{F_t}{F_a} = 0.00968$ $\frac{\Delta F_a}{F_a} = 0.003$ $F_a = 17{,}500$ lb/tab (78,500 N-m)

Total injection impulse = 60 x 1.16 = 69.6°-sec (1.215 RAD-sec)

Total impulse loss = $\frac{2(1.75 \times 10^4)}{1.03} \cdot (69.6) = 2.365 \times 10^6$ lb-sec

(4.121×10^4 RAD-sec)

$$= \frac{2.365 \times 10^6}{8.647 \times 10^8} = 0.27\%$$

Additional propellant required to achieve total impulse requirement is

$$\frac{2.365 \times 10^6}{254} = 9{,}330 \text{ lb } (4{,}230 \text{ kg})$$

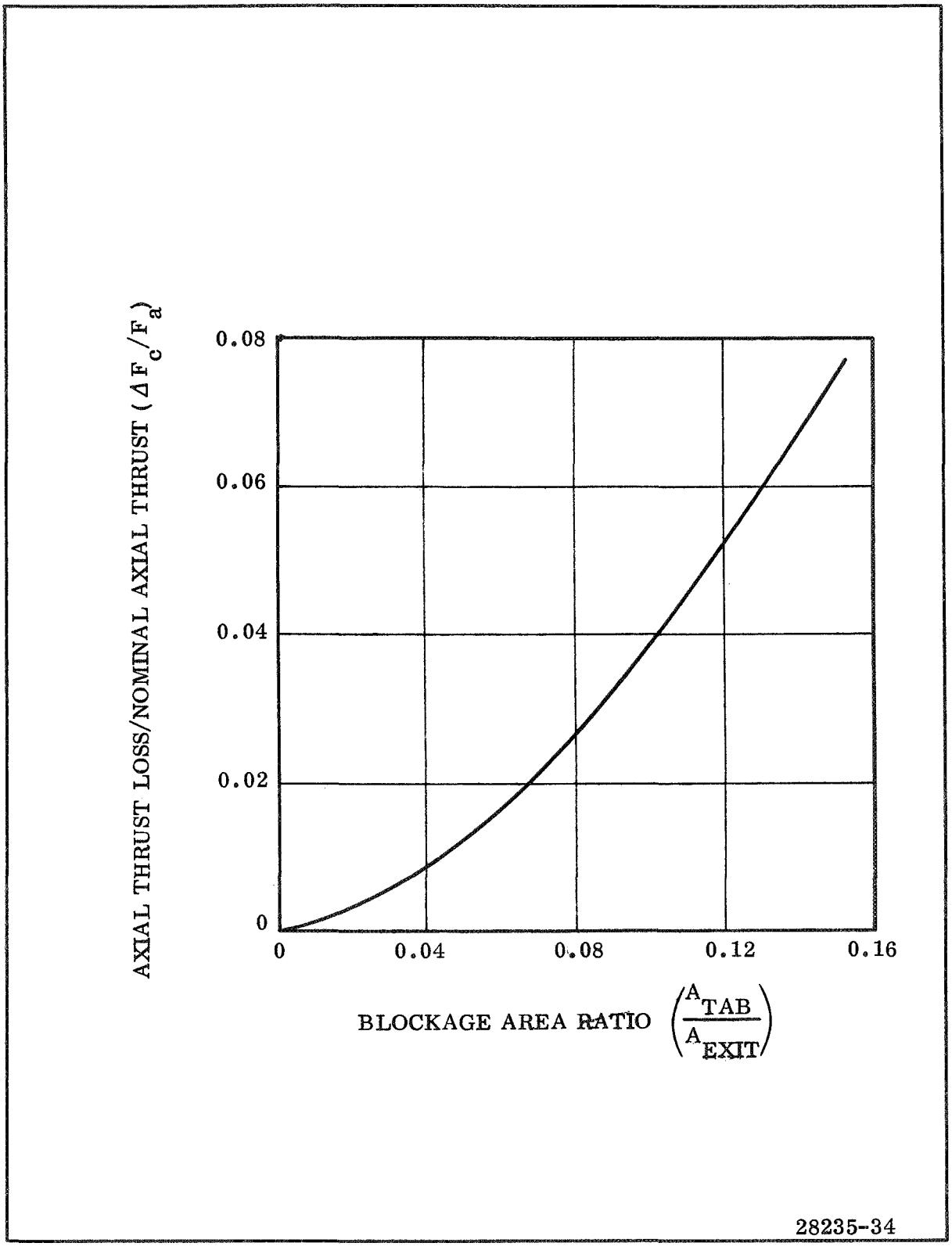

Figure 6-16. Typical Axial Thrust Loss vs Jet Tab Blockage Area Ratio

6.3 Preliminary Design and Screening

6.3.6 Jet Tabs

6.3.6.5 Results of Preliminary Design Review

MITVC SYSTEM INFERIOR TO LITVC AND MOVABLE NOZZLE SYSTEMS

It is clear that the MITVC system is inferior to both the movable nozzle and the LITVC systems from the standpoints of additional development risks and the additional propellant necessary to offset the performance loss of the jet tab system.

Following the recommendation of the most promising TVC system in each category (mechanical interference, liquid injection, and movable nozzle) it became clear that MITVC was inferior to the other two systems from many aspects.

Development risk was significantly greater with the MITVC system, primarily because of the severe materials problem. More than 9,000 lb (4,040 kg) of additional propellant are necessary to overcome the performance loss of the jet tab system. Performance loss of the movable nozzle is negligible and LITVC actually provides thrust augmentation. The total preliminary weight estimate of the jet tab TVC system, including the nozzle, was 86,475 lb (39,200 kg) compared to 57,300 lb (25,700 kg) for the movable nozzle and 82,900 lb (37,200 kg) for LITVC. Accordingly, completion of a detailed design of the jet tab TVC system was considered unnecessary and no further work was done on MITVC systems.

APPENDIX A
INDUSTRY LITVC BIBLIOGRAPHY

Saturn IB Improvement Study (Solid First Stage) Phase II: Final Summary Report. SM-51896, Vol I. Douglas Missile and Space Systems Division, Huntington Beach, Calif. Prepared under Contract No. NAS 8-20242, 30 Mar 1966.

Saturn IB Improvement Study (Solid First Stage) Phase II: Final Detailed Report. SM-51896, Vol II. Douglas Missile and Space Systems Division, Huntington Beach, Calif. Prepared under Contract No. NAS 8-20242, 30 Mar 1966.

Use of Large Solid Motors in Booster Applications; Thrust Vector Control Systems Comparison: Detailed Technical Report. DAC-58038, Vol III. Douglas Missile and Space Systems Division. Prepared under Contract No. NAS 8-21051, 30 Aug 1967.

A Partially Annotated Bibliography of Reports in the Field of Secondary Injection Thrust Vector Control, TM-54/01-27, LMSC Huntsville Research and Engineering Center, February 1964.

An Empirical Performance Model of Secondary Injection for Thrust Vector Control (U), LMSC Huntsville Research and Engineering Center, Contract NAS 8-11077, October 1964, CONFIDENTIAL, Downgrade Group 4.

TVC Candidate Fluid Study: Considerations in the Polaris B3 Pre-PDP Preliminary Design Study (U). LMSC-804360. Lockheed Missiles and Space Division, Sunnyvale, Calif. Contract No. NOw63-0050, July 1964, CONFIDENTIAL.

Curtis, D. D.: Advanced Polaris First Stage Motor Components Performance Summary Short Duration Static Tests (U). LMSC-804448. Lockheed Missiles and Space Company, 20 Oct 1964, CONFIDENTIAL, Downgrade Group 4.

Lockheed Missiles and Space Company: An Analysis of the Physical and Chemical Aspects of Liquid Injection. LMSC-A-24-65-1. Sunnyvale, Calif.: Lockheed Missiles and Space Company.

Lockheed Missiles and Space Company: Fluid Injection TVC Research. Report No. LMSC-803311. Sunnyvale, Calif.: Lockheed Missiles and Space Company, August 1964.

Lockheed Missiles and Space Company: Polaris B3 First and Second Stage $Sr(ClO_4)_2$ and $Pb(ClO_4)_2$ Secondary Injection Thrust Vector Control Data Report (U). TM 55-13-05, LMSC-804506. August 1964, CONFIDENTIAL, Downgrade Group 4.

Le Count, R. L.: Fluid Injection TVC Research. LMSC Report No. 53-42-BOW. Sunnyvale, Calif.: Lockheed Missiles and Space Company, July 1963.

Chapman, R. and Grunwald, G.: Experimental TVC Performance of Perchlorate Solutions. Page 671, Vol II, ICRPG/AIAA Solid Propulsion Conference, July 1966.

Subscale Thrust Vector Control During Motor Tailoff (U). ER-UTC 64-15, UTC: Sunnyvale, Calif., January 1964, CONFIDENTIAL, Downgrade Group 4.

Test Evaluation Report (Ground Test) XSR 47-UT-1 (UA 1205-8) (U). ER-UTC 64-265, UTC: Sunnyvale, Calif., December 1964, CONFIDENTIAL, Downgrade Group 4.

Test Evaluation Report 1201-2 (DVHW-1-2) (U). ER-UTC 63-116, UTC: Sunnyvale, Calif., July 1963, CONFIDENTIAL, Downgrade Group 4.

Green, C. J. and McCullough, F.: Liquid Injection Thrust Vector Control. NAVWEPS Report 7744, NOTS TP 2711. China Lake, Calif.: Naval Ordnance Testing Station, 16 Jun 1961.

Green, C. J. and McCullough, F.: SITVC with Storable Liquids as Injectants. Bulletin of the JANAF-LPG. China Lake, Calif.: Naval Ordnance Testing Station.

Motor Evaluation First Stage SDF Motor 7 (U). Report PME-548, Polaris Propulsion Development, Aerojet-General Corporation: 17 Apr 1964, CONFIDENTIAL, Downgrade Group 4.

Motor Evaluation Large Rocket, Preliminary Design Motor SDF-9 (U). Report PME-566, Aerojet-General Corporation: 20 Jul 1964, CONFIDENTIAL, Downgrade Group 4.

Motor Evaluation Large Rocket, Preliminary Design Motor SDF-10 (U). Report PME-571, LMSC Purchase Order 18-10277, Contract No. 2 63-0050C (FMB), Aerojet-General Corporation: 21 Jul 1964, CONFIDENTIAL, Downgrade Group 4.

Motor Evaluation Large Rocket, Preliminary Design Motor SDF-11 (U). Report PME-574, Aerojet-General Corporation: 13 Aug 1964, CONFIDENTIAL, Downgrade Group 4.

Motor Evaluation Large Rocket, Preliminary Design Motor SDF-12 (U). Report PME-577, Aerojet-General Corporation: 18 Sep 1964, CONFIDENTIAL, Downgrade Group 4.

Broadwell, J. E.: "Analysis of the Fluid Mechanics of Secondary Injection for Thrust Vector Control," AIAA Journal, Vol I, 1963: pages 1,067 thru 1,075.

Fox, J. J., et al.: Thrust Vector Control by Reactive Liquid Secondary Injection (U). Van Nuys, Calif.: Marquardt Corporation, CONFIDENTIAL, Downgrade Group 4.

Dahm, T. J.: The Development of an Analogy to Blast-Wave Theory for the Prediction of Interaction Forces Associated with Gaseous Secondary Injection into a Supersonic Stream. 9166-TN-3. Palo Alto, Calif.: Vidya Division of Itek Corporation, May 1964.

Dynamic Science Corporation: Chemical Aspects of Fluid Injection (U). Reports 1, 2, and 3, Lockheed Subcontract 18-2873. South Pasadena, Calif.: Dynamic Science Corporation, May, June, July 1961, CONFIDENTIAL, Downgrade Group 4.

Hsia, H., et al.: Shocks Induced by Secondary Fluid Injection. AIAA Preprint No. 64-111, 1964.

Hsia, H., et al.: Perturbation of Supersonic Flow by Secondary Injection. CPIA III, July 1966.

Karamcheti, K. and Hsia, H.: "Integral Approach to an Approximate Analysis of Thrust Vector Control by Secondary Injection," AIAA Journal, Vol I, 1963: pages 2,538 thru 2,544.

Lilich, L. S., and Dzhurinsky, B. F.: The Solubility of Perchlorates of Elements of the Second Group of the Periodic System. Journal of General Chemistry of the USSR, pages 1,733 thru 1,737, 1956.

Walker, R. E. and Shandor, M.: Influence of Injectant Properties for Fluid Injection Thrust Vector Control. AIAA Preprint No. 64-112, 1964.

Wu, J., et al.: An Approximate Analysis of Thrust Vector Control by Fluid Injection. ARS Paper No. 1609-61, 1961.

Wu, J., et al.: Polaris Thrust Vector Control Analysis. Final Report, Contract No. PO S-412707-OP. National Engineering Science Company, 1961.

Newton, Jr., et al.: Experiments on the Interaction of Secondary Injectants and Rocket Exhaust for Thrust Vector Control. Technical Report No. 32-203. Pasadena, Calif.: Jet Propulsion Laboratories, 12 Feb 1962.

Samsonov, A. E.: Candidate Liquid Selection for Improved MINUTEMAN TVC. Aerojet-General Corporation (date not known).

Sehgal, R. and Wu, J. M.: A Study of Thrust Vector Control by Liquid Injection Rocket Nozzles. Contract NAS T-100. Pasadena, Calif.: Jet Propulsion Laboratory.

APPENDIX B
THIOKOL LITVC BIBLIOGRAPHY

Thiokol Chemical Corporation: Proposal for Realigned MINUTEMAN III Stage III Rocket Motor (U): Volume VIII, LITVC Detail Design and Analysis - R & D, Thiokol Chemical Corporation, Brigham City, Utah, May 1966, CONFIDENTIAL.

Handzel, J. R. and Breslau, S. M.: Secondary Injection TVC for the Improved Stage I MINUTEMAN Motor.

Breslau, S. M. and Fuentes, M. N.: TVC System Analysis for Solid Space Booster Application (U). TW-177-2-62. Brigham City, Utah, Thiokol Chemical Corporation, Wasatch Division. February 1962, CONFIDENTIAL.

Thirkill, J. and Fuentes, M.: Evaluation of TVC Systems for Solid Propellant Motor Application. Brigham City, Utah: Thiokol Chemical Corporation, Wasatch Division, December 1963 (Prepared for the AIAA Solid Propellant Conference in Palo Alto, California, January 1964).

Thiokol Chemical Corporation: Final Design Report, Mobile Mid-Range Ballistic Missile Propulsion (U), Volumes V and VI. TW-256-2-63 and TW-257-2-63. Brigham City, Utah: Thiokol Chemical Corporation, Wasatch Division, March 1963, SECRET.

Thiokol Chemical Corporation: Phase IA Summary Progress Report, Addendum II, Detailed Technical Reports, Mobile Mid-Range Ballistic Missile Propulsion (U). TW-601-8-63. Brigham City, Utah: Thiokol Chemical Corporation, Wasatch Division, August 1963, CONFIDENTIAL.

Thiokol Chemical Corporation: Final Report, Pre-Phase II Carryon Effort, Appendix I, Staging Technical Impact Report, Mobile Mid-Range Ballistic Missile Propulsion (U). TW-244-6-64. Brigham City, Utah: Thiokol Chemical Corporation, Wasatch Division, July 1964, CONFIDENTIAL.

Erickson, L. H. and Bell, H. S., Jr.: Optimum Design Investigation of Secondary Injection Thrust Vector Control Systems (U), Technical Documentary Report of Contract AF 04(611)-7411, AFSC Project No. 3059, TW-965-12-61. Brigham City, Utah: Thiokol Chemical Corporation, Wasatch Division, March 1962, CONFIDENTIAL.

Fuentes, M. N. and Laramee, R. C.: Evaluation of a Secondary Freon Injection Thrust Vector Control Test. Brigham City, Utah: Thiokol Chemical Corporation, Wasatch Division, December 1961.

Thiokol Chemical Corporation: Test Results (Final) of Subscale Liquid Secondary Injection Using the TU-190.73 Rocket Motor LITVC-1 (U). TW-25-8-62.

Brigham City, Utah: Thiokol Chemical Corporation, Wasatch Division, August 1962, CONFIDENTIAL.

Thiokol Chemical Corporation: Test Results (Final) of Subscale Liquid Secondary Injection Using the TU-190.76 Rocket Motor LITVC-2 (U). TW-114-8-62. Brigham City, Utah: Thiokol Chemical Corporation, Wasatch Division, August 1962, CONFIDENTIAL.

Thiokol Chemical Corporation: Final Test Results of Subscale Liquid Secondary Injection Using the TU-190.77 Rocket Motor LITVC-3 (U). TW-269-8-62. Brigham City, Utah: Thiokol Chemical Corporation, Wasatch Division, August 1962, CONFIDENTIAL.

Thiokol Chemical Corporation: Proposal for Development of Large Solid Propellant Rocket Motors: Bid Package No. 15 (U). TW-8-10-64, TWP-0964-177, Brigham City, Utah: Thiokol Chemical Corporation, Wasatch Division, October 1964, CONFIDENTIAL.

Sparkman, D. M., et al.: TU-393 LITVC System Design Report. TWR-1319. Thiokol Chemical Corporation, August 1965.

Dyer, J. E. and Erickson, L. H.: LITVC System Performance - TU-393.01 (AF 156-7) Motor (U). TWR-2022. Thiokol Chemical Corporation, June 1966, CONFIDENTIAL.

Erickson, L. H.: Review and Analysis of Liquid Secondary Injection Thrust Vector Control Information (U). TW-641-10-62. Brigham City, Utah: Thiokol Chemical Corporation, Wasatch Division, October 1962, CONFIDENTIAL.

Yearsley, R., Muller, A., and Erickson, L. H.: Results of the Liquid Injection TVC Development Engineering Program Wing II-IV Stage I MINUTEMAN Motor. TWR-578, NTF 10098, Brigham City, Utah: Thiokol Chemical Corporation, February 1964.

Erickson, L. H.: Technical Note on Correlation and Comparison of Perchlorate Injection TVC Data. TWR-1242. Brigham City, Utah: Thiokol Chemical Corporation, July 1965.

Erickson, L. H.: Technical Note on Strontium and Lead Perchlorate SITVC Test Results for the Polaris Program (U). TC3-171-12-5. Brigham City, Utah: Thiokol Chemical Corporation, December 1965, CONFIDENTIAL.

Erickson, L. H.: Technical Note on Properties of Strontium Perchlorate Solutions. TWR-2120. Thiokol Chemical Corporation, September 1966.

Final Report - Advanced Thrust Vector Control Preliminary Design Computer Program (U). Volume I, Volume II, Book 1 and 2. AFRPL-TR-67-318, Contract AF 04(611)-11647, Thiokol Chemical Corporation, Brigham City, Utah, January 1968, CONFIDENTIAL.

APPENDIX C
SURVEY OF LITVC PERFORMANCE PREDICTION TECHNIQUES

The complex three dimensional interaction phenomenon between the secondary injectant and the primary flow has not been readily amenable to theoretical analyses.

Numerous analytical models have been proposed by various investigators to predict the performance of LITVC systems; these include (1) small perturbation analysis, (2) blast-wave analogy, (3) integral approach, and (4) a blunt body model.

Walker and Shandor[1] analyzed the fluid injection problem with the use of linearized supersonic flow theory. They stress in their analysis the importance of including thermochemistry. Karamcheti and Hsia[2] developed a theory utilizing the integral approach for a mixture of inert perfect gases. They neglect shock-boundary layer interaction and fluid mixing by analyzing flow conditions at the nozzle exit between the wall and bow shock. Wu, Chapkis, and Mager[3] assume that the injected fluid turns and flows parallel to the wall with no defined mixing. They include jet momentum boundary layer separation and separation induced shock effects. Reaction, however, is not included. Broadwell[4] presents a treatment of the fluid injection problem which has received considerable attention and which is applicable to liquid and gas injection. His study is concerned with the induced shock shape. Difficulty with this method arises in determining the energy transferred from any thermochemical effects occurring within the nozzle. In addition, Broadwell uses Sakurai's[5] first order solution of the shock wave equation, whereas, Karamcheti, Hsia and Seifert[6] show that the second order solution provides a better description of the shock shape. Dahm's[7] blast-wave theory was developed for Thiokol Chemical Corporation under Contract AF 04(611)-9075 and has made available

---

[1]Walker, R. E. and Shandor, M., "Influence of Injectant Properties for Fluid Injection Thrust Vector Control," AIAA Preprint No. 64-112, 1964.

[2]Karamcheti, K., and Hsia, H., "Integral Approach to an Approximate Analysis of Thrust Vector Control by Secondary Injection," AIAA Journal 1, 2538-2544 (1963).

[3]Wu, J., Chapkis, R. L., and Mager, A., "An Approximate Analysis of Thrust Vector Control by Fluid Injection," ARS Paper No. 1609-61, 1961.

[4]Broadwell, J. E., "Analysis of the Fluid Mechanics of Secondary Injection for Thrust Vector Control," AIAA Journal 1, 1067-1075 (1963).

[5]Sakurai, A., "On the Propagation and Structure of a Blast Wave," J. of the Physical Society of Japan, Part I, Vol. 8, 1953 and Part II, Vol. 9, 1954.

[6]Hsia, H., Seifert, H. S. and Karamcheti, K., "Shocks Induced by Secondary Fluid Injection," AIAA Preprint No. 64-111, 1964.

[7]Dahm, T. J., "The Development of an Analogy to Blast-Wave Theory for the Prediction of Interaction Forces Associated with Gaseous Secondary Injection into a Supersonic Stream," 9166-TN-3, Thiokol Contract No. 63-00558 (AF 04(611)-9075), Vidya Division of Itek Corporation, Palo Alto, California, May 1964.

analytical design techniques, which were experimentally verified, for use in design and selection of gas injection TVC systems for solid propellant rocket motors. The derived theory was partially developed for the general case of either liquid or gaseous injection, but completed only for the gaseous case. Sehgal and Wu[8] and the National Engineering Science Company[9] have each derived a model of liquid injection which is as near the actual case as has been studied to date. They analyze liquid droplet vaporization, trajectory, and vapor body formation, then study the flow interference effects. Although they neglect the chemistry involved, they do discuss the importance of liquid atomization, jet penetration, and the mixing of primary and secondary streams. Dynamic Science Corporation[10] has previously worked, under Lockheed subcontract, on an analytical model of liquid injection TVC to establish the important fluid parameters. The effects of an evaporating and reacting fluid on the primary exhaust stream were examined. The zone influenced by the injectant was treated as a solid body whose shape and dimensions depended on fluid properties. The parameters found to be important in the preliminary model were grouped into a correlating parameter called the "effective displacement." On this basis, the most effective fluid injection system would be one which provides the greatest effective displacement of the supersonic stream. This screening parameter was then used to compile a list of possible injectants which possess the desirable characteristics for SITVC.

Hsia, et al., [11] reported an analytical study carried out by treating the injectant mixing, vaporization and reaction process as if the process were a supersonic flow about a blunt body. The nose radius of an equivalent, spherical-nosed, axisymmetric body was obtained for various parameters of injection and primary flow conditions by considering the exchange of momentum and energy between the two fluids. In turn, explicit expressions for the separation distance, the shape of the induced bow shock, the shock detachment distance, and the pressure disturbance on the wall were obtained. Results given by the theory generally agree favorably with experimental data, except for the wall pressure distribution. The authors attribute this to the absence of a well-defined wall-shock intersection region and the exclusion from consideration of shock boundary-layer interaction along the shock front.

---

[8] Sehgal, R. and Wu, J. M., "A Study of Thrust Vector Control by Liquid Injection into Rocket Nozzles," Contract NAS T-100, Jet Propulsion Laboratory, Pasadena.

[9] Wu, J., Chapkis, R. L., Ai, D. K. and Rao, G. V. R., "Polaris Thrust Vector Control Analysis," Final Report, Contract No. PO S-412707-OP, Prepared for AGC by the National Engineering Science Company, 1961.

[10] "Chemical Aspects of Fluid Injection," (Reports 1, 2 and 3, Lockheed Subcontract 18-2873); Dynamic Science Corp., South Pasadena, Calif, May, June, July, 1961 (Confidential).

[11] Hsia, H., Karamcheti, K., Seifert, H. S., Perturbation of Supersonic Flow by Secondary Injection, CPIA III, July 1966.

Lockheed[12] has presented an analytical study which endeavors to describe liquid injection phenomena. Liquid breakup, fluid mixing, vaporization energy and mass exchange, reaction thermochemistry and kinetics, and shock generation are defined. The means are developed for predicting (1) the relative performance of injectants, and (2) the induced side force by integrating the pressure field on the nozzle wall after defining an effective vapor body and using the method of characteristics.

The models of JPL, NESCO, and LMSC appear promising for the calculation of side forces generated by secondary liquid injection. These models indicate rather thorough and painstaking analyses and are based on step-by-step approaches(ie, liquid jet breakup, vapor body formation, boundary layer separation, flow interference-shock fields, etc). For the prediction of side forces, however, the various models lack confident comparisons with various injectants and injection parameters.

The main approach to designing LITVC systems has been to establish empirical correlations from experimental data on various injectants and the related system variables during rocket motor static firings. These empirical correlations have permitted reasonable LITVC system tradeoff studies.

---

[12] "An Analysis of the Physical and Chemical Aspects of Liquid Injection," LMSC-A-24-65-1, Contract No. NOw 63-0050, Lockheed Missiles and Space Company, Sunnyvale, California.

APPENDIX D
STRUCTURAL ANALYSIS OF TOROIDAL TANK AND SUPPORT STRUCTURE

Structural analyses were conducted on the pressurant-injectant (GN_2-N_2O_4) toroidal tank and the tank support structure.

The basic thickness of the torus (0.175 in.) was calculated using membrane equations for a torus and a MEOP of 800 psi . A 7.2g load in the axial and radial directions was used to design the attachment pads and struts. The additional stresses induced into the membrane at the attachment points were relieved by adding to the basic thickness; the final wall thickness being 0.300 in. The loads induced into the torus and the pad size for attachment were found from equations and tables taken from "Stresses From Radial Loads in Cylindrical Pressure Vessels," by P. P. Bijlaard.

The g load was used to calculate the axial tensile or compressive loads in the struts. These struts were then designed for tensile load or compressive column buckling. The attachment bolts and brackets were designed for these same loads.

The following calculations were made during this analysis.

GN_2-N_2O_4 Tank Analysis

MEOP = 800 → 400 psi

Use 17-4 PH stainless steel
F_{tu} = 175,000 psi

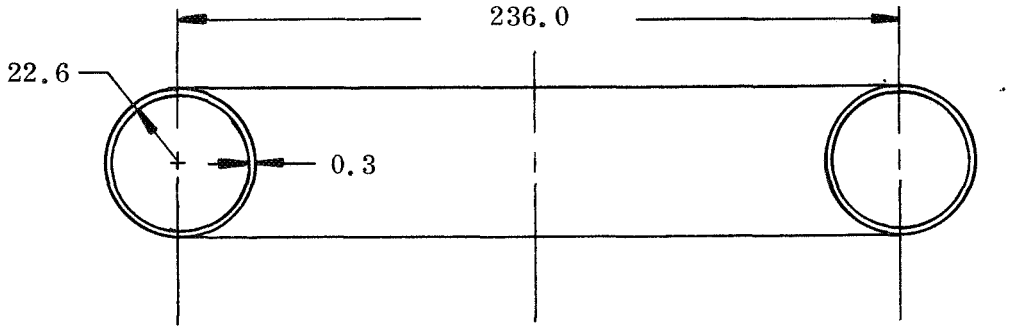

$$\text{(Inside)}\quad S_1 = \frac{Pb}{t}\left(\frac{2a-b}{2a-2b}\right) = 115,546$$

$$t = \frac{800(22.6)}{175,000}\left(\frac{2(118) - 22.6}{2 \times 118 - 2 \times 22.6}\right) \times 1.5$$

$$= 0.175 \text{ in.}$$

$$S_2 = \frac{Pb}{2t} = \frac{800 \times 22.6}{2(0.175)}$$

$$= 51,567 \text{ psi}$$

$$\text{(Outside) } S_1 = \frac{Pb}{t}\left(\frac{r+a}{2r}\right) = \frac{800 \times 22.6}{0.175}\left(\frac{140.6+118}{2(140.6)}\right)$$

$$= 95,008 \text{ psi}$$

$$V = \frac{1}{4}\pi^2 D(d_1^2 - d_2^2)$$

$$= \frac{1}{4}\pi^2 236(45.55^2 - 45.2^2)$$

$$= 18,496 \text{ cu in.}$$

$$W_t = 0.282 \times 18,496 = 5,216 \text{ lb}$$

Attachment Analysis

The following attachment pad analysis was taken from an article by P. P. Bijlaard on "Stresses From Radial Loads in Cylindrical Pressure Vessels." The attachment pads were sized and increased loads in the torus membrane found by utilizing this article. Tables in the article used the following parameters to obtain values for membrane loads and pad size.

$\alpha = \frac{l}{a}$

l = shell length

a = shell radius

$\gamma = \frac{a}{t}$

t = shell thickness

$\beta = \frac{c}{a}$

C = half pad width

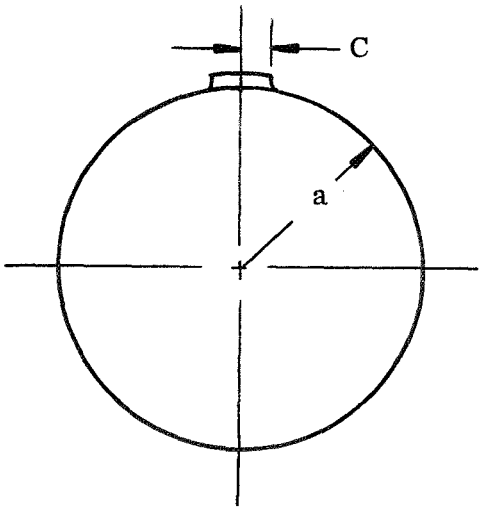

These stresses are added to the basic shell stresses which are calculated as previously described.

Using 0.175 wall

g load = 7.2

Wt N_2O_4 = 24,634 lb

GN_2 = 1,690

Tank = 5,216

Wt = 31,540 lb

$$\alpha = \frac{l}{a} = \frac{741.4}{22.7} = 32.6$$

$$\gamma = \frac{a}{t} = \frac{22.7}{0.175} = 129.7$$

$$\beta = \frac{c}{a} = \frac{6}{22.7} = 0.2643$$

g wt = 7.2 x 31,540 = 227,088 lb

$M_x = 0.01\ p$

$M_x = 0.004\ p$

$$p = \frac{227,088}{2 \times 8 \cos 54^\circ} = 24,146 \text{ lb}$$

M_x = 0.009 x 1.03 x 24,146 = 224 in.-lb

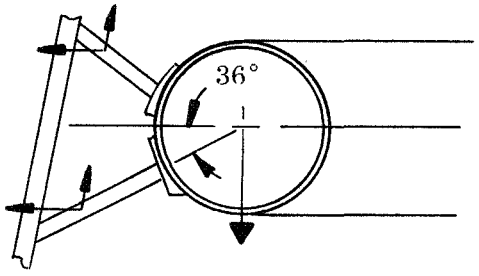

Stresses from radial loads in cylindrical pressure vessels - P. P. Bijlaard

$$N_x = 10\left(\frac{p}{a}\right)1.07 = 10 \times \frac{24,146}{22.7}(1.07) = 11,382 \text{ lb}$$

$$\sigma_1 = \frac{6 \times M}{t^2} + \frac{N_x}{t} = \frac{6 \times 224}{(0.175)^2} + \frac{11,382}{0.175}$$

43,921 + 65,040 = 108,961 psi

$S_1 + \sigma_1$ = 95,008 + 108,961 = 203,969 psi too high, try thicker wall

Assume 0.3 in. wall

$$\alpha = \frac{l}{a} = 32.6$$

$$\gamma = \frac{22.75}{0.3} = 75.8$$

V = 31.794 cu in.

Torus wt = 0.282 x 31.794 = 8,966 lb

$$\beta = \frac{6}{22.75} = 0.2637$$

N_2O_4 wt	24,634
GN_2 wt	1,690
	35,290 lb

$$P = \frac{7.2g \text{ load}}{\text{strut load}} = \frac{7.2 \times 35,290}{16 \cos 50°} = 27,017 \text{ lb}$$

$$M_x = 0.014p \times 1.03 \times 27,017 = 390 \text{ in.-lb}$$

$$N_x = (7.4)\frac{27,017}{22.75}\ 1.08 = 9,490 \text{ lb/in.}$$

*

Axial

$$\sigma_1 = \frac{6 \times 390}{(0.3)^2} + \frac{9,490}{0.3} =$$

$$26,000 + 31,633 = 57,633 \text{ psi}$$

Axial Membrane Stress

$$S_1 = \frac{800 \times 22.6}{0.3}\left(\frac{132 + 118}{2 \times 132}\right) = 57,067 \text{ psi}$$

Total Axial Stress = 57,633 + 57,067 = 114,700 psi

$$\text{F.S.} = \frac{175,000 \times 0.9}{114,700} = 1.37$$

Hoop

$$M\varphi = 0.036p \times 27,017 \times 1.07 = 1,041 \text{ in.-lb}$$

$$N\varphi = 3.6\frac{p}{a}\frac{27,017}{22.75} \times 0.99 = 4,232 \text{ lb/in.}$$

*Stresses From Radial Loads in Cylindrical Pressure Vessels - P. P. Bijlaard

Hoop

$$\sigma_2 = \frac{1,041 \times 6}{(0.3)^2} + \frac{4,232}{0.3}$$

$$= 69,400 + 14,106 = 83,506 \text{ psi}$$

Hoop Membrane

$$S_2 = \frac{800 \times 22.6}{2 \times 0.3} = 30,133 \text{ psi}$$

$$\text{Total Hoop Stress} = \underset{\sigma_2}{83,500} + \underset{S_2}{30,133} = 113,633 \text{ psi}$$

Use 3 in. pipe for strut

$$\text{Area} = \pi (1.75^2 - 1.534^2) = 8.9136 \text{ sq in.}$$

$$\sigma = \frac{27,017}{2.2283} = 12,124 \text{ psi}$$

Buckling

$$P_{cr} = \frac{\pi^2 EI}{L^2} \qquad I = \pi \frac{R_4 - r^4}{4} = 3.0174$$

$$= \frac{\pi^2 30 \times 10^6 \times 3.0174}{(34)^2}$$

$$= 772,855 \text{ lb}$$

$$\text{F.S.} = \frac{772,855}{27,017} = 28$$

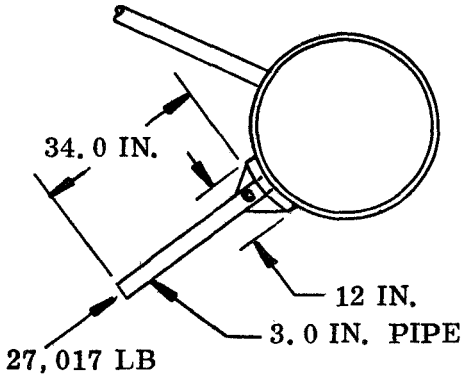

Assume 12 in. square pad with 0.25 fillet weld

$$M = 1,041 \text{ in.-lb/in.}$$

$$\text{Weld stress} = \frac{1,041 \times 12}{12 \times 2.12} + \frac{27,017}{8.48} = 3,677 \text{ psi}$$

Assume 3/4 pin

$$\tau = \frac{27,017 \times 4}{\pi (0.75)^2} = 22,932 \text{ psi}$$

Plate shearout assume 0.75 plate

$$\tau = \frac{27,017}{2 \times 0.75 \times 0.75} = 21,613 \text{ psi}$$

APPENDIX E
DEVELOPMENT AND QUALIFICATION PLAN FOR NASA 260 INCH LITVC SYSTEM

A. INTRODUCTION

This plan outlines the recommended plan for conducting development and qualification programs for the NASA 260 in. LITVC systems.

The TVC system development program will be initiated at the component level and will be concluded with seven preliminary flight rating tests (PFRT). It is assumed that the majority of component testing will be accomplished at the respective vendor facilities, that is, thermal cycling, leak tests, functional tests, pressure tests, cyclic limits, and structural and vibration tests.

Considerable LITVC system bench testing will be required to verify compatibility of components, structural integrity, and functioning of the system. The LITVC system bench testing effort will be followed by a series of three motor firings.

This firing program will consist of three development motor firings and seven PFRT firings. To make the development firing program more representative, all 10 motors will include the use of a prototype aft flare section and flightweight LITVC system components.

The seven PFRT firings will include flightweight LITVC hardware mounted within the aft flare section on the motor. Specific exception to the flight configuration will be the inversion and remanifolding of the N_2O_4 - GN_2 toroidal tank to conform to the "head-down" testing of large rocket motors. In this series of tests, emphasis will be placed on evaluating the acoustic and thermal environment for the flare-mounted components and the environment effect on TVC functioning.

Summaries of the planned component, bench and laboratory subsystem, development motor, and PFRT motor tests are discussed in the following subsections of this appendix.

B. COMPONENT TESTING

1. INTRODUCTION

The selected NASA 260 in. LITVC system incorporates the following available and proven hardware.

1. Electromechanical injector (16/system).
2. Burst disc (1/system)
3. Operational pressure transducer (1/system).

4. Pneumatic charge disconnect (1/system).
5. Relief vent valve (1/system).
6. Fill and drain disconnect (1/system).
7. Tank to injector ducts (16/system).

The remaining LITVC system components are new but represent straightforward design and fabrication techniques. These components consist of the following.

1. Injectant-pressurant toroidal tank (1/system).
2. Anti-vortexing device (16/system).
3. Injector plug seal (16/system).
4. Liquid level transmitter (1/system).
5. Pitch-yaw-dump electronic controller (1/system).

2. TESTING

a. Development and Qualification--Component testing will be conducted by the vendors who supply the items. Tests will include pressure proof, burst tests, flow tests, leakage tests, flow calibration, and functional checkout. The vendor will verify and qualify at the component level a minimum of three and a maximum of five units.

In addition to the vendor tests, further bench and laboratory LITVC system testing is planned.

b. Acceptance--The vendor will perform all acceptance testing, which will consist of functional, electrical, proof, visual and dynamics (as applicable). Each unit delivered will be subjected to this acceptance test program.

c. Receiving Inspection Tests--The TVC contractor will perform receiving inspection and confirmation tests on all components. These tests will consist of visual, master tool check, functional (where applicable) and electrical.

C. LITVC SYSTEM TESTING

1. INTRODUCTION

Three complete LITVC systems (designated within as A, B, and C) will be required for six test series. Each of the test series are discussed below.

2. TEST NO. 1 - TEST SERIES

Required LITVC test hardware consists of the following.

1. Dummy nozzle (cylindrical pipe).
2. Injectant receiver tank and weighing device.

3. LITVC system (A) tank modified to have only two adjacent quadrants operational. The remaining eight tank outlets will be capped.
4. Breadboard controller with auxiliary power source.
5. Substitute injectant with a density that approximates N_2O_4.
6. Facility GN_2 supply.

The tests conducted under test series No. 1 will use an injectant other than N_2O_4 to reduce handling, flushing, and corrosion problems through the test setup. A receiver tank will be provided to collect the injectant as it is expelled from the LITVC system. The injectant collected in the receiver tank will be weighed at the completion of each test run to determine the exact amount of liquid expelled. A signal to the injectors from a breadboard controller using an auxiliary power source will regulate the injectant flow in accordance with predetermined duty cycles.

The objectives of the LITVC Test No. 1 test series are to verify the following.

1. General functioning and flow characteristics of the LITVC system.
2. Injectant expulsion efficiency.
3. Injector cavity pressure as a function of injector activation and tank pressure.
4. Response time from command input to specified injector activation and cavity pressure.
5. Water hammer effects.
6. Leakage without injector plug seal.
7. Overpressurization effects.

A minimum of seven GN_2 pressurization and expulsion system tests will be required to define (1) injectant expulsion efficiency, (2) the pressurant-injectant tank blowdown characteristics, (3) the injector cavity pressures, (4) injector response time, and (5) overall functioning of the LITVC system. The injectant will be expelled in accordance with predetermined duty cycles. Three water hammer test runs will be conducted to check the maximum fluid hammer pressure, pressure rise rate, and total pressurization time.

An injector leakage test will be performed with the No. 1 LITVC bench test setup. Without the injector plug seals, the injector valves will be energized closed (tank pressure maintained at 1,000 psi) for a duration of 4 hr. At the end of the test, the leakage volume will be measured. The results of this test will determine whether it is to design injector valve plug seal apparatus.

Two overpressurization tests will be simulated to demonstrate the effects on the tank relief vent valve and burst disk.

Instrumentation requirements will be in accordance with Table I.

TABLE I

TEST NO. 1/INSTRUMENTATION REQUIREMENTS

Pickup Code	Priority	Accuracy (%)	Remarks
P001-010	M	±1.0	Pressure
V001-016	M	+5.0	Voltage
C001-016	M	±5.0	Current
M001-020		±5.0	Misc
F001-004	M	±5.0	Flow

3. TEST NO. 2 - TEST SERIES

The second LITVC test series hardware consists of the following.

1. Dummy nozzle + hemispherical closure.
2. Injectant receiver tank and weighing device.
3. Complete LITVC system A.
4. Flightweight controller.
5. Fluid level transmitter device.
6. Substitute injectant.
7. Facility GN_2 supply.

The objectives of the LITVC Test No. 2 test series are to verify the following.

1. The fluid level transmitter device.
2. Programed injectant dump concurrent with a selected duty cycle.
3. Injector plug seal apparatus (if required after analyzing prior leakage tests).
4. Full up LITVC system incorporating three different TVC cycles and programed dump.
5. Injection quadrant dynamics.

Instrumentation requirements will be in accordance with Table II.

TABLE II
TEST NO. 2 INSTRUMENTATION REQUIREMENTS

Pickup Code	Priority	Accuracy (%)	Remarks
V001-016	M	$\pm$5.0	Voltage
C001-016	M	$\pm$5.0	Current
M001-020		$\pm$5.0	Misc
F001-004	M	$\pm$5.0	Flow

4. TEST NO. 3 - TEST SERIES

The third LITVC test setup will use the same bench test setup as No. 1.

The objective of these tests will be to determine fatigue and water hammer effects on the LITVC system.

The LITVC system (no injectant) will be initially pressurized to the maximum tank design pressure from a facility GN_2 supply source. The system will then be run through approximately 100 cycles of degassing (through the tank relief vent valve) and pressurizing (from the facility GN_2 supply source). The system components will be inspected for fatigue effects.

A quadrant of injector valves will be cycled (about 20 cycles) from open (maximum flow) to close using the substitute injectant and a constant GN_2 pressure

(facility supplied). The LITVC system components will be monitored and inspected for water hammer and fatigue effects.

Instrumentation requirements will be in accordance with Table III.

TABLE III
TEST NO. 3 INSTRUMENTATION REQUIREMENTS

Pickup Code	Priority	Accuracy (%)	Remarks
P001	M	±1.0	Pressure
V001-008	M	±5.0	Voltage
C001-008	M	±5.0	Current
M001-4	M	±5.0	Misc
S001-050	75% M	±5.0	Strain gage

5. TEST NO. 4 - TEST SERIES

Environmental tests will be conducted to verify the capability of a complete LITVC system to function properly following exposure to various flight and transportation environmental conditions.

LITVC system B will be used for this test series. The tank will be filled with a substitute injectant and GN pressurant. Typical environmental tests include the following.

1. Vibrational.
2. Temperature cycling.
3. Relative humidity.
4. Salt spray, dust, etc.

Instrumentation requirements will be in accordance with Table IV.

TABLE IV
TEST NO. 4 INSTRUMENTATION REQUIREMENTS

Pickup Code	Priority	Accuracy (%)	Remarks
P001-2	M	±1.0	Pressure
D001-10	M	±5.0	Extensometer
T001-2	M	±5.0	Temperature
S001-100	M	±5.0	Strain gages
A001-10	M	±5.0	Acceleration
V001-4	M	±5.0	Voltage
C001-4	M	±5.0	Current
M001-25		±5.0	Misc
H001	M	±5.0	Humidity

6. TEST NO. 5 - TEST SERIES

Test series No. 5 will be conducted in the Test Area using LITVC system C, nitrogen tetroxide, as the injectant, and the test setup from the No. 2 test series.

The objectives of this test series are to verify the compatibility and functioning of the components and LITVC system with N_2O_4.

At the conclusion of this test series, further N_2O_4 compatibility tests will be conducted with LITVC system C.

Instrumentation requirements will be in accordance with Table V.

TABLE V
TEST NO. 5 INSTRUMENTATION REQUIREMENTS

Pickup Code	Priority	Accuracy (%)	Remarks
P001 & 2	M	$\pm$1.0	Pressure
T001-4	M	$\pm$5.0	Temperature
D001-2	M	$\pm$5.0	Extensometer
V001-4	M	$\pm$5.0	Voltage
C001-4	M	$\pm$5.0	Current
M001-020	--	$\pm$5.0	Misc

7. TEST NO. 6 - TEST SERIES

Lab tests will be run using one LITVC system for N_2O_4 compatibility testing, and two LITVC systems for hydroburst testing.

A N_2O_4 storage test of moderate duration will be conducted with the LITVC system used in the No. 2 test series.

Hydroburst testing will be performed on two of the LITVC systems to verify the structural capability of these units. Following failure of one component, the hydroburst testing will be conducted on the remaining components until all components of the LITVC system have failed.

Instrumentation requirements will be in accordance with Table VI.

TABLE VI
TEST NO. 6 INSTRUMENTATION REQUIREMENTS

Pickup Code	Priority	Accuracy (%)	Remarks
P001-010	M	$\pm$1.0	Pressure
M001-020	M	$\pm$5.0	Misc

8. STATIC FIRING TEST DEVELOPMENT

The development motor static firing LITVC tests will require support facilities and engineering effort greater than the LITVC subsystem test activity. A series of three development motor firings are planned.

The first developmental motor firing will include LITVC system functional operation with motor nozzle mounted electromechanical injector valves, manifolds, and facility mounted N_2O_4 supply, nitrogen pressurization supply, and control system. The second and third motor development firings will include a functioning LITVC system consisting of motor mounted prototype TVC components on a "battleship" structure.

Instrumentation requirements will be in accordance with Table VII.

TABLE VII
STATIC FIRING TEST INSTRUMENTATION REQUIREMENTS

Pickup Code	Priority	Accuracy (%)	Remarks
P001-2	M	$\pm$1.0	Pressure
D001-10	M	$\pm$5.0	Extensometer
T001-2	M	$\pm$5.0	Temperature
S001-100	M	$\pm$5.0	Strain gages
A001-10	M	$\pm$5.0	Acceleration
V001-020	M	$\pm$5.0	Voltage
C001-020	M	$\pm$5.0	Current
M001-25	--	$\pm$5.0	Misc
T001	M	$\pm$5.0	Thrust

9. PFRT TESTS

Because of the inverted position of the motor and the requirement of the aft flare or simulated structure for tank support, the test hardware support becomes fairly complex. Additional equipment is necessary to simulate the N_2O_4 injectant flow of flight conditions. For PFRT static tests, the tankage and manifolding will be specially designed and/or oriented to obtain satisfactory drainage of N_2O_4. The level sensor would also be reoriented and the tank pressure increased to compensate for the decrease in the injectant heat. A ground source of N_2O_4 could also be supplied to the injectant manifold, but this arrangement decreases flight simulation conditions and total system checkout verification confidence.

Instrumentation requirements will be in accordance with Table VII.

D. TEST EQUIPMENT

The following test equipment is required for development and qualification testing. All test equipment will be designed in conjunction with all testing to permit maximum flexibility in testing. The test matrix is shown in Table VIII.

Test No. 1	Requires a fixture that will hold the system and will provide a receiver tank to collect the injectant.
Test No. 2	Requires a fixture that will hold the system during testing.
Test No. 3	Same as above.
Test No. 4	Requires a vibration and shock fixture.
Test No. 5	Requires a fixture that will hold the system during testing.
Test No. 6	Requires a hydroburst test fixture.
Static firing test	Requires a static firing fixture.
PFRT test	Same as above.

TABLE VIII
TEST MATRIX

Para No.	Test	Development Test Unit A B C D E F	Qualification Test Unit A B C D E F G
C-2	Test No. 1 (7 tests)	X	
C-3	Test No. 2 (3 tests)	X	
C-4	Test No. 3 (3 tests)	X	
C-5	Test No. 4 (1 test)	X	
C-6	Test No. 5 (3 tests)	X	
C-7	Test No. 6		
	a. N_2O_4 compatibility (1 test)	X	
	b. Hydroburst (2 tests)	X X	
C-8	Static firing test development (3 tests)	X X X	
C-9	PFRT tests (7 tests)		X X X X X X X

LITVC SCHEDULE

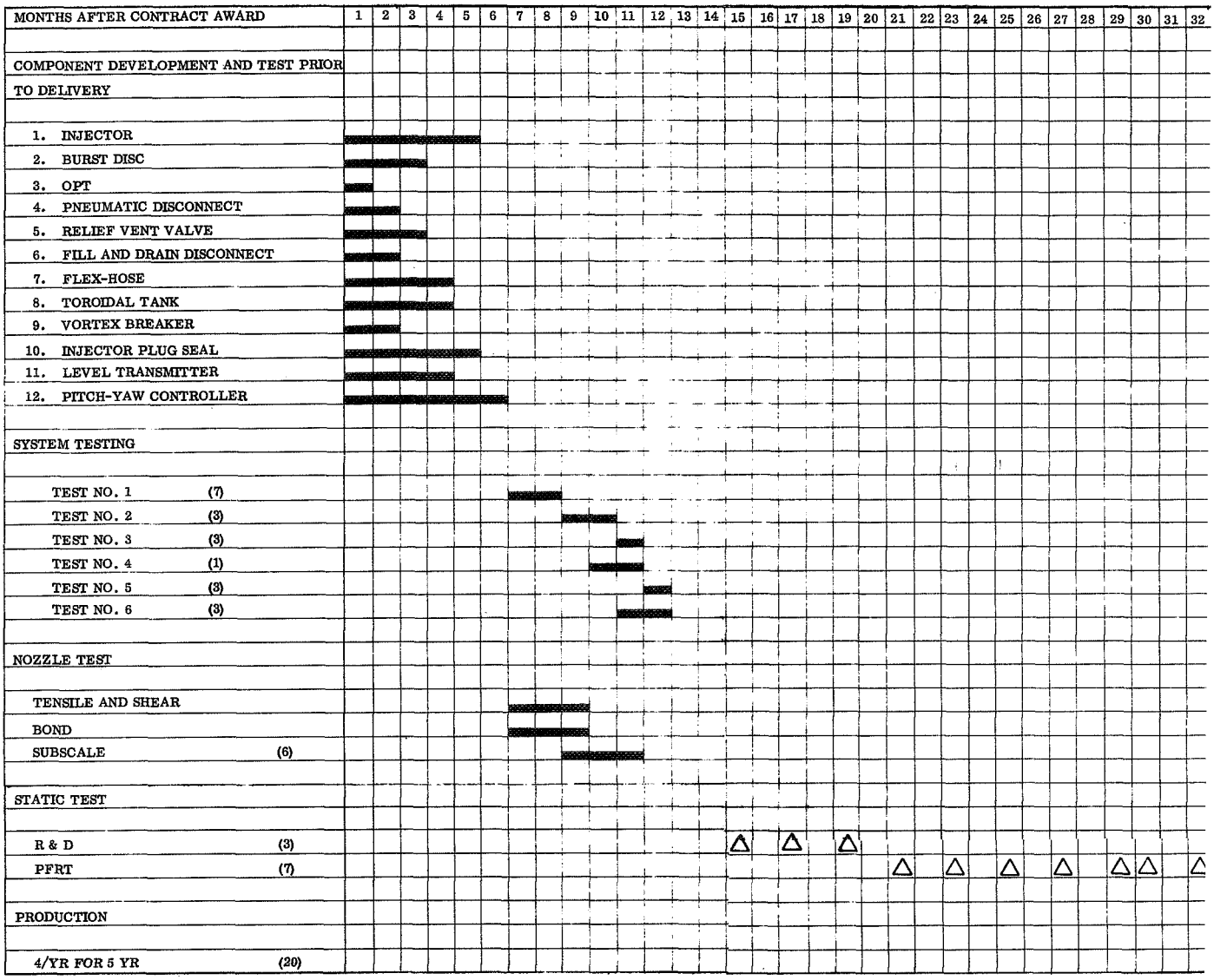

APPENDIX F
DEVELOPMENT AND QUALIFICATION PLAN FOR NASA 260 INCH AGC FLEXIBLE BEARING NOZZLE ASSEMBLY

A. INTRODUCTION

This document outlines the Thiokol Chemical Corporation plan for conducting a development and qualification program for the NASA 260 in. flex bearing nozzle TVC system.

Development testing of nozzle structural and insulative materials will be done prior to final nozzle design and fabrication.

Component testing of the flexible bearing assembly, nozzle actuators, actuation system accumulators, etc, will be done prior to static testing.

B. APPLICABLE DOCUMENTS

NASA Contract NAS 3-12040, Thiokol Chemical Corporation Proposal TWP 02369-05, Design, Fabrication, and Test of TVC Flexible Seals for 260-Inch Solid Rocket Motor.

C. COMPONENT/SUBSYSTEM TESTING

1. INTRODUCTION

The TVC system for the movable nozzle consists primarily of two subsystems.

1. Hydraulic expulsion system.
2. Actuation subsystem.

a. Hydraulic Expulsion Subsystem--The hydraulic expulsion subsystem consists of the following components:

1. Pressure tank.
*2. Solenoid valve.
*3. Operational pressure transducer.
*4. Fluid level indicator.
*5. Burst disc.
6. Vortex breaker.
*7. Charged vent valve.

*Currently developed units are available.

b. Actuation Subsystem--The actuation subsystem consists of the following components.

1. Actuator.
2. Servovalve.
3. Feedback device.
4. Filter.
5. Check valve.
6. Tubing, hose, disconnect, etc.
7. Pressure switch.

All the items with the exception of the actuator are currently developed items and can be obtained with either minor or no modification.

D. TESTING

1. DEVELOPMENT AND QUALIFICATION

Component testing will be conducted by the vendor who supply the item. Tests will include proof pressure, burst, flow, leakage, and functional checkouts. The vendor will verify and qualify at the component level a minimum of three and a maximum of five units. In addition to the vendor tests, further bench testing will be required at the TVC system contractor.

2. ACCEPTANCE TESTS

The vendor will perform all acceptance testing, which will consist of functional, electrical, proof, visual and dynamics as applicable. Each unit delivered will be subjected to the acceptance test program.

3. RECEIVING INSPECTION TEST

The TVC system contractor will perform receiving inspection and confirmation tests on all components. These will consist of visual, master tool check, functional (where applicable) and electrical.

4. COMPONENT TEST

a. Flexible Bearing Qualification Bench Test

(1) Objectives

1. To verify the design integrity of the bearing.
2. Determine the dynamic operating characteristics of the bearing
3. To determine the axial translation of the bearing.
4. To determine the pivot point movement of the bearing under simulated motor operating conditions.

5. To determine the damping coefficient of the bearing.

(2) Test No. 1 - Pivot Point Shift--The bearing will be installed into the test fixture (Figure F-1) without the load relieving assembly.

Subject the bearing to the required duty cycle at various loads until the axial load is equal to the nozzle load at 1.15 MEOP. The test fixture pressurizing media will be H_2O. The duty cycle will consist of sinusoidal events of magnitudes equal to $\pm 0.5°$, $\pm 1.0°$ and $\pm 1.0°$ at a slew rate of 4 °/sec, and a step function having holds at 0.5°, 1.0°, and 1.9°. The pivot point shift will be measured during this test.

(3) Test No. 2 - Axial Deflection--Disconnect the two actuators and install the four extensometers. Measure the axial deflection of the bearing at various pressure levels until the load equals the nozzle load at 1.15 MEOP.

(4) Test No. 3 - Twang Test--Deflect the bearing +1.0° and pressurize the test fixture until axial load is equal to nozzle load at 1.15 MEOP. Release bearing and measure bearing position as a function of time.

(5) Test No. 4 - Duty Cycle--Disassemble test fixture (Figure F-1) and install the load relieving assembly. Install the flex bearing into test fixture. Subject the bearing to the duty cycle shown at a fixture pressure of MEOP and 1.15 MEOP. Following duty cycle test, measure flange to flange null position concentricity and parallelism.

Gas leak test will be performed before and after each of the duty cycle tests.

(6) Test No. 5 - Destruct $\pm 1.9°$ --Destruct test with load relieving assembly with the bearing installed in the test fixture, increase the fixture pressure at 0.10 MEOP intervals and deflect the bearing $\pm 1.9°$ at each pressure level. Decrease fixture pressure and visually inspect bearing after each vector event. Continue pressure steps, vector events and visual inspection until failure or a test fixture pressure of 1,275 psi is reached.

(7) Test No. 6 - Destruct $\pm 2.5°$ --Destruct test at 2.5° vector angle. If bearing does not fail during Test No. 5, repeat Test No. 5 using a vector angle of $\pm 2.5°$.

(8) Test No. 7 - Destruct Test Without Load Relieving Assembly--If bearing does not fail during Test No. 6, disassemble test fixture and remove load relieving assembly.

Reassemble bearing into test fixture and deflect bearing +1.9° in one plane and increase test fixture pressure until bearing fails or project engineer stops test.

(9) Instrumentation--Instrumentation will be in accordance with Table I.

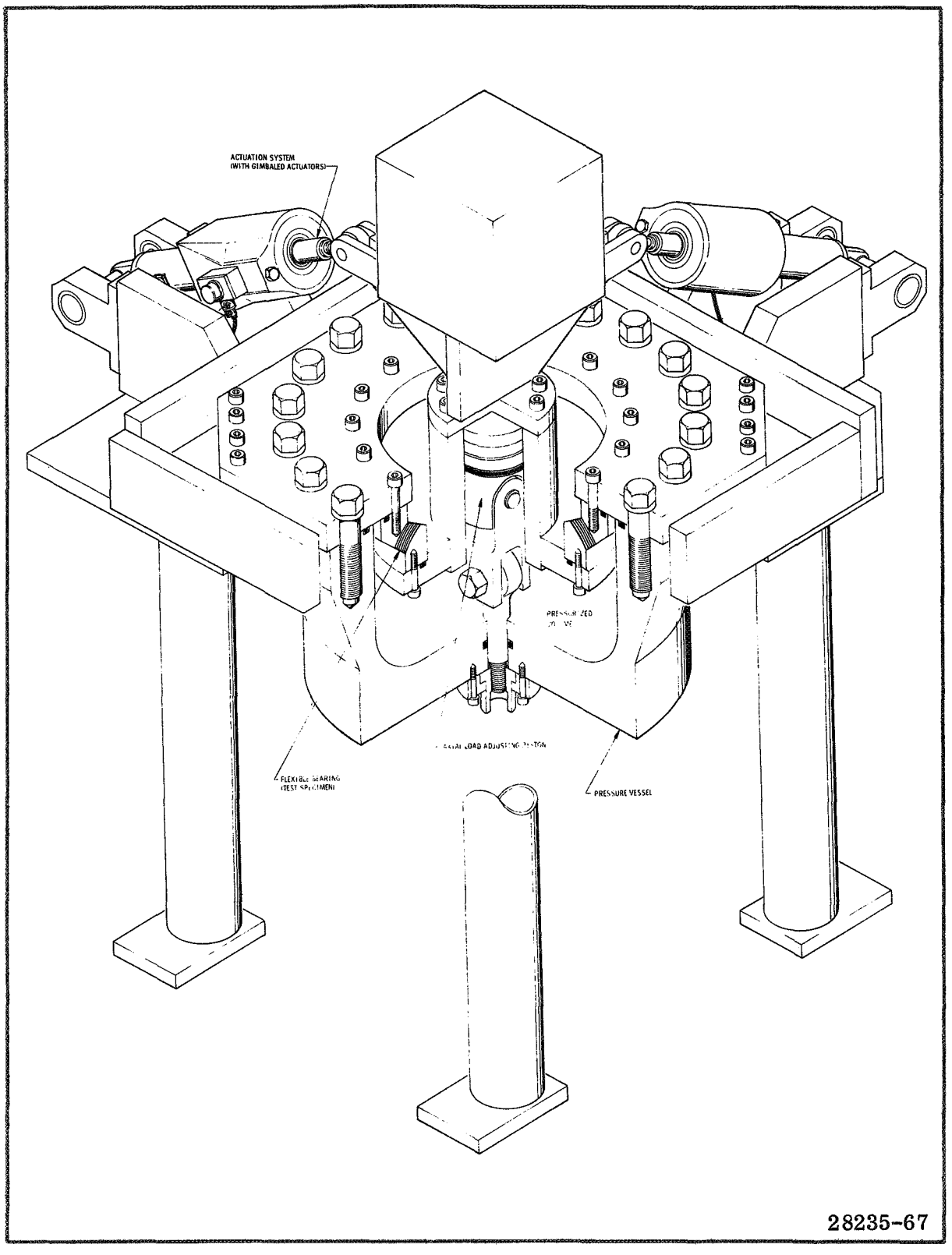

Figure F-1. Typical Test Fixture

TABLE I

FLEX BEARING TEST INSTRUMENTATION

Code No.	Accuracy (%)	Remarks
Displacement		
D001	5	Pitch displacement
D002	5	Yaw displacement
D003	5	Bearing compression
D004	5	Bearing compression
D005	5	Bearing compression
D006	5	Bearing compression
D007	5	Pitch plane displacement
D008	5	Yaw plane displacement
D009	5	45° plane displacement
D010	5	Pivot point fixture measurement
Pressure		
P001	5	Test fixture pressure
P002	5	Pitch actuator hydraulic AP
P003	5	Yaw actuator hydraulic AP
Strain		
S001-25	10	Strain gages

b. Flex Bearing Acceptance Test

(1) Objectives

1. Determine dynamic operating characteristics of the bearing.
2. Determine the axial translation of the bearing.
3. Determine pivot point movement under simulated motor operating conditions.
4. Determine bearing torque characteristics as a function of load and slew rate.
5. Determine the damping coefficient of the bearing.

(2) Test No. 1--Repeat D-4-a-(2)

(3) Test No. 2--Repeat D-4-a-(3)

(4) Test No. 3--Repeat D-4-a-(4)

(5) Test No. 4--Repeat D-4-a-(5)

(6) Instrumentation--Instrumentation will be in accordance with Table I.

c. Nozzle Component Materials Tests (Subscale Test)--(Applicable to LITVC Nozzle Development also)

(1) Objectives

1. Determine physical properties.
2. Determine material interface bond strengths.
3. Determine nozzle insulation erosion and char characteristics.

(2) Test No. 1 - Tensile and Shear Tests--Perform tensile tests of nozzle insulation and structural plastics and nozzle metal housing specimens to determine tensile strengths.

Perform shear tests of nozzle insulation and structural plastics to determine shear strengths with ply and cross-ply directions.

(3) Test No. 2 - Bond Tests--Perform double lap shear tests of candidate bonding materials and nozzle plastic components in a plastic-plastic combination and a plastic-metal combination.

(4) Test No. 3 - Subscale Fixed Nozzle Test Firings--Test fire subscale fixed nozzles with candidate nozzle plastics and full scale propellant formulation. Evaluate erosion and char to select best plastic component materials.

(5) Instrumentation--Instrumentation will be in accordance with Table II.

TABLE II

NOZZLE COMPONENT MATERIAL TEST INSTRUMENTATION

Test No.	Pickup Code	Accuracy (%)	Remarks
1	F001	5	Force
	T001	-	Time
	S001	-	Strain
2	F002	-	Force
	T002	-	Time
	S002	-	Strain
3	P001	5	Pressure
	T001	-	Time

d. TVC System Bench Test

(1) Objective--To determine the structural integrity and performance of the TVC system. To determine pressure decay in the accumulator.

(2) Test Configuration--The actual actuation system will be set up on a test fixture (Figure F-1) which will duplicate the actual motor geometry as much as possible. The system will be identical to the flight type system except for instrumentation. The actuators will be connected to the bearing with an additional mass added to the bearing to simulate nozzle inertia. Facility type electronics will be used on first bench tests.

(3) Structural and Leakage Test--The high pressure hydraulics with the exception of the tank will be subjected to a proof pressure test of 6,000 psi. The return lines will be proof pressure tested to 1,500 psi. No leaks will be allowed for either test.

(4) Response Test--The duty cycle supplied by NASA will be recorded on magnetic tape and input into the servoamplifier. Two channels will be used for pitch and yaw commands, and a third channel will be used as the firing signal. This signal will actuate the solenoid valve to pressurize the system. After the test, the system will be disassembled to determine the amount of hydraulic fluid remaining in the tank.

Additional tests will be run at three different constant supply pressures to determine the response to full scale steps and sinusoidal input.

Two above tests will be run with the test fixture pressurized and unpressurized.

An additional duty cycle tape will be created which will identify the maximum capabilities of the actuation system under load.

Instrumentation will be in accordance with Table III.

TABLE III
RESPONSE TEST INSTRUMENTATION

Pickup Code	Priority	Accuracy (%)	Remarks
D001-4	M	$\pm$5.0	Extensometer
D005-8	M	$\pm$5.0	LVDT (2)
S001-100	80M	$\pm$5.0	Strain gages
P001-2	M	$\pm$1.0	Supply pressure
V001 & 4	M	$\pm$3.0	Voltage (solenoid)
C001 & 4	M	$\pm$3.0	Current
I001-20	M	$\pm$3.0	Actuator input (2)
M001-010	M	$\pm$5.0	Misc
$P_1$003	M	$\pm$5.0	P_1 control pressure
$P_2$004	M	$\pm$5.0	P_2 control pressure
$P_3$005	M	$\pm$5.0	Return pressure

(5) Endurance Test--The entire actuation and expulsion system will be pressure-cycled 20 times between 4,000 psi and ambient. A repeat of the leakage test will be performed.

(6) Environmental Tests--Environmental tests will be conducted using system 2 to verify the capability of a complete TVC actuation system to function properly following exposure to various flight transportation and storage environmental conditions.

The following tests will be conducted.

1. Temperature cycling.
2. Salt spray.
3. Humidity.
4. Sand, dust, etc.
5. Vibration.
   a. Transportation.
   b. Handling.
   c. Flight.

All systems will be empty during the tests except for the flight vibration test. Following this test, the system will be subjected to the tests described in Sections D-4-d-(3) and D-4-d-(4) to verify the structural integrity and performance of the system.

Instrumentation will be in accordance with Table IV.

TABLE IV
ENVIRONMENTAL TEST INSTRUMENTATION

Pickup Code	Priority	Accuracy (%)	Remarks
S001-100	M80	±5.0	Strain gages
A001-20	M	±5.0	Acceleration
P001	M	±1.0	Pressure
T001-4	M	±5.0	Temperature
H001	M	±5.0	Humidity
E001	M	±5.0	Altitude

(7) Burst Tests--Both systems 1 and 2 will undergo hydroburst tests following completion of tests defined in D-4-d-(3), D-4-d-(4), D-4-d-(5), and D-4-d-(6). Following failure of one component, the test will be continued on the remaining components until all components have failed.

e. TVC System Static Firing - Development

(1) Objectives

1. Demonstrate the structural integrity of the flexible seal nozzle under actual operating conditions.
2. Determine the operating characteristics of this nozzle and TVC system under simulated flight conditions.

3. Determine the erosion and char profiles of the nozzle insulation materials under actual test conditions.
4. Demonstrate the integrity of the flexible seal thermal protective boot and its retention under actual firing conditions.

The development motor static firing movable nozzle test will require support facilities and engineering effort greater than the subsystem test activity. A series of three motor firings are planned.

The first developmental motor firing will demonstrate functional operation with flight type actuator and utilizing ground hydraulic supply. The second and third motor development firings will include a complete functioning flight type system. Because of the inverted position of the motor during static test (aft end up), the pressure tank will be inverted during all static test.

(2) Instrumentation--Instrumentation will be in accordance with Table V.

f. PFRT Test--The PFRT test will utilize a complete flight type actuation and pressurization system with the exception of the tank as described in D-4-c.

(1) Objective--Emphasis will be placed on evaluating the vibration and thermal environment of the flare mounted components and the environment effect on TVC functioning and all performance parameters.

(2) Instrumentation--Instrumentation will be in accordance with Table V.

TABLE V
STATIC FIRING AND PFRT INSTRUMENTATION

Pickup Code	Priority	Accuracy (%)	Remarks
C001-4	M	±5.0	Extensometer
D005-8	M	±5.0	Potentiometer
S001-100	80M	±5.0	Strain gages
P001-4	M	±1.0	Pressure
V001-4	M	±3.0	Voltage
C001-4	M	±3.0	Current
I001-20	M	±5.0	Actuator input
F001-4	M	±5.0	Flow
T001-4	M	±5.0	Temperature
TH001	M	±5.0	Thrust
L001-4	M	±5.0	Force
M001-010	M	±5.0	Misc

E. TEST EQUIPMENT

The following test equipment is required for development and qualification testing. All test equipment will be designed in conjunction with all testing to permit maximum flexibility in testing. The test matrix is shown in Table VI.

1. Flex bearing test - bench test fixture.
2. Actuator.
3. Environment test - requires a vibration and shock fixture.
4. Burst test - requires a holding and burst fixture.
5. TVC system static firing - requires a static firing fixture.

TABLE VI
TEST MATRIX

Paragraph Number	Test	Number of Development Test Units	Number of Qualification Test Units
D-4-a	Flexible bearing qualification bench test	2 tests	
D-4-a-(2)	Test No. 1 - pivot point shift	3 tests each bearing	
D-4-a-(3)	Test No. 2 - axial deflection	3 tests each bearing	
D-4-a-(4)	Test No. 3 - twang test	1 test each bearing	
D-4-a-(5)	Test No. 4 - duty cycle	3 tests each bearing	
D-4-a-(6)	Test No. 5 - destruct $\pm 1.0°$		
D-4-a-(7)	Test No. 6 - destruct $\pm 2.5°$	1 test	
D-4-a-(8)	Test No. 6 - destruct without load relieving assembly $\pm 1.9°$		
D-4-b	Flex bearing acceptance test		10 + 20 production
D-4-b-(2)	Test No. 1		
D-4-b-(3)	Test No. 2		
D-4-b-(4)	Test No. 3		
D-4-b-(5)	Test No. 4		
D-4-c	Nozzle component material test		
D-4-c-(2)	Test No. 1 - tensile and shear	4 specimens each material	
D-4-c-(3)	Test No. 2 - bond test	4 specimens each material	
D-4-c-(4)	Test No. 3 - subscale fixed nozzle test firings	6 tests	
D-4-d	TVC system bench test	2 tests	1 test
D-4-d-(3)	Structural and leakage test	2 tests each system	1 test
D-4-d-(4)	Response tests	2 tests each system	1 test
D-4-d-(5)	Endurance test	2 tests each system	1 test
D-4-d-(6)	Environment test	2 tests each system	
D-4-d-(7)	Burst test	1 test each system	
D-4-e	TVC system static firing - development	3 tests	
D-4-f	PFRT test		7 tests

FLEX-SEAL SCHEDULE

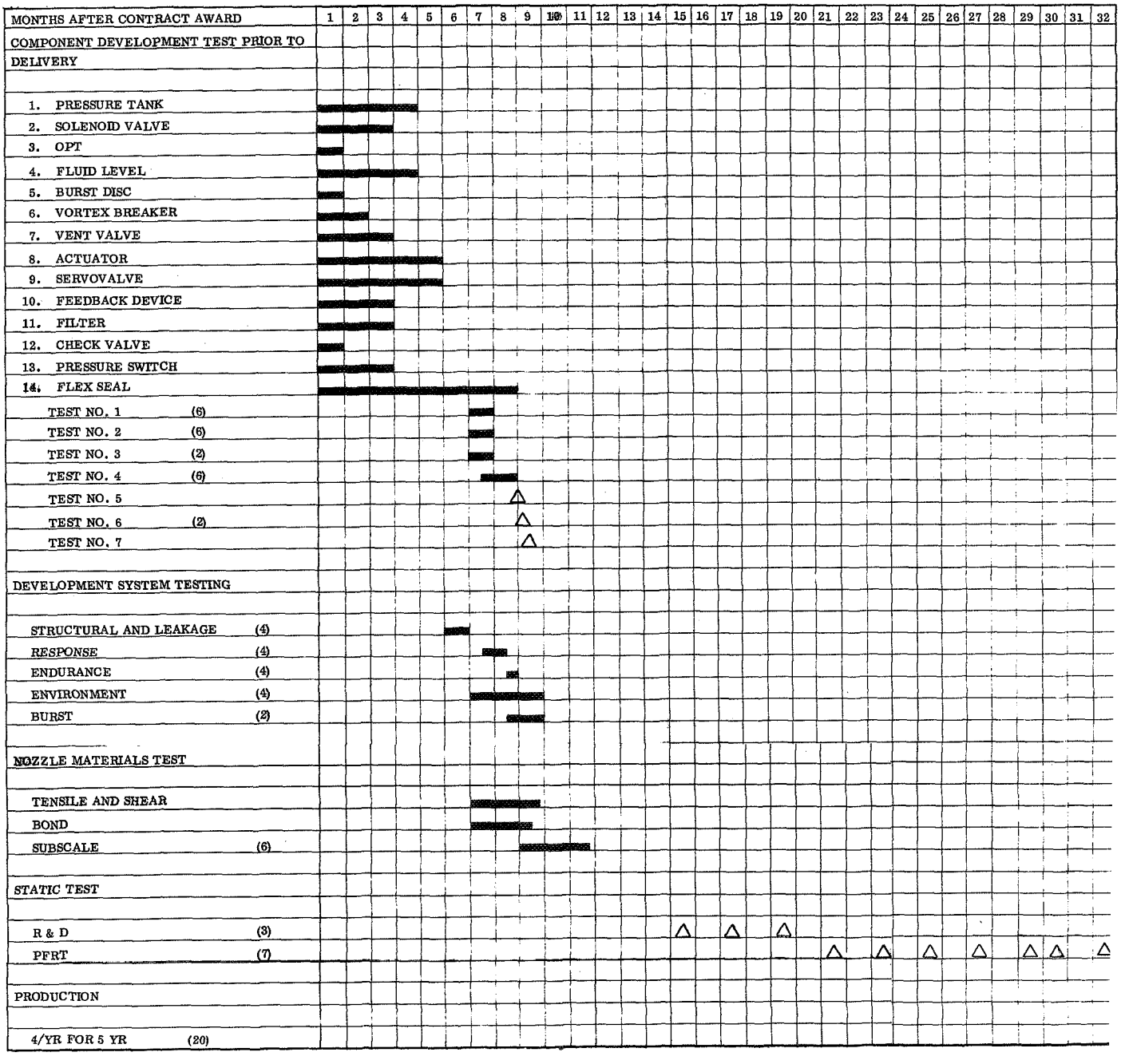

APPENDIX G

STRUCTURAL ANALYSIS OF TVC MOVABLE NOZZLE ACTUATOR AND BRACKETS

(See Nomenclature at End of Appendix)

Actuator Cylinder

MEOP = 4,000 psig

Proof = 6,000 psig

Burst = 10,000 psig

Use 4340 steel

F_{tu} = 180,000 psi

F_{su} = 105,000 psi

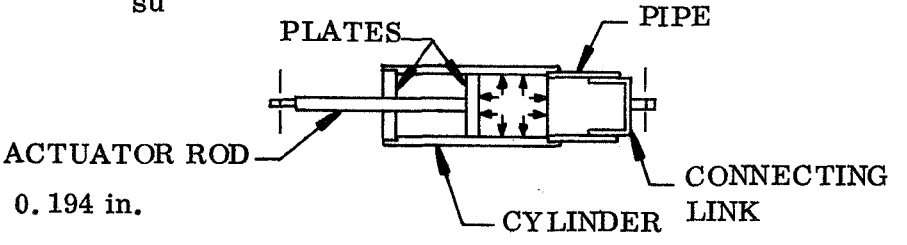

$$\sigma = \frac{PR}{t}$$

$$t = \frac{10,000 \times 3.5}{180,000} = 0.194 \text{ in.}$$

Use t = 0.3 per computer run

Actuator Rod

$$\text{Rod proof load} = \pi \left[(3.25)^2 - (0.75)^2\right] 6,000 = 188,496 \text{ lb}$$

$$\sigma = \frac{P}{A} = \frac{188,496}{\pi (0.75)^2} = 102,407 \text{ psi}$$

Buckling of Actuator Rod

$$\text{Critical load } P_{cr} = \frac{\pi^2 E I}{(L)^2} \qquad I = 0.2485$$

$$= \frac{\pi^2 \, 29 \times 10^6 \times 0.2485}{(14)^2} = 362,884 > 188,496 \text{ lb proof load}$$

Buckling of Pipe (Assume 0.3 in. wall thickness)

$$P_{cr} = \frac{\pi^2 \, 29 \times 10^6 \times 0.7539}{10^2} = 2,157,800 \text{ lb} > 188,496 \text{ lb proof}$$

Assume 0.25 wall at thread relief

$$\sigma_{pipe} = \frac{P}{A} = \frac{188,496}{\pi\,(1.7^2 - 1.45^2)} = 76,190 \text{ psi}$$

$$F.S. = \frac{180,000}{76,190} = 2.36 \text{ proof}$$

Pipe Thread Shear

$$\tau = \frac{P}{A} = \frac{188,496}{\pi\,(3)\,(0.5)\,(0.5)} = 80,000 \text{ psi proof}$$

$$F.S. = \frac{105,000}{80,000} = 1.31$$

Connecting Link Thread Shear

$$\tau = \frac{P}{A} = \frac{188,496}{\pi\,(3)\;2.4 \times 0.5} = 16,667 \text{ psi proof}$$

Piston Plate

Assume circular plate uniform load (Roark pg 200, case 21)

$$\sigma = \frac{3\,W}{4\,t^2}\left[\frac{4\,(a)^4\,(m+1)\log\frac{a}{b} - a^4\,(m+3) + b^4\,(m-1) + 4\,a^2b^2}{a^2\,(m+1) + b^2\,(m-1)}\right]$$

$$= \frac{3\,(6,000)}{4\,(1-2)^2}\left[\frac{4\,(3.25)^4\;(4.333)\;\;1.46633 - (3.25)^4\;6.333 + (0.15)^4\;2.333 + 4\,(3.25)^2\;0.75^2}{(3.25)^2\;4.333 + (0.75)^2\;2.333}\right]$$

$$= 142,929 \text{ psi proof}$$

$$F.S. = \frac{180,000}{142,929} = 1.25$$

End Plate

Assume circular plate uniform load (Roark pg 198, case 13)

$$\sigma = \frac{3\,W}{4\,mt^2(a^2-b^2)}\left[a^4(3\,m+1)+b^4(m-1)-4\,M\,a^2b^2-4\,(m+1)\,a^2b^2\log\frac{a}{b}\right]$$

$$= \frac{3\,(6,000)}{4\,(3.33)\,(0.1)^2\left[3.125^2-1^2\right]}\left[(3.125)^4(11)+(1)^4(2.333)-4(3.333)\right.$$

$$\left.(3.125)^2\,(1)^2-4\,(4.33)\,(3.125)^2\,(1)^2\,1.14\right]$$

$$\sigma = 112,150 \text{ psi proof}$$

$$\text{F.S.} = \frac{180,000}{112,150} = 1.60$$

Shear on End Plate Threads

$$\text{Load} = \left[(3.375)^2-(0.75)^2\right]\ 6,000 = 204,105 \text{ lb proof}$$

Assume 0.5 in. threads

$$\tau = \frac{204,105}{\pi\,(6.9)\ 0.5 \text{ x } 0.5} = 37,664 \text{ psi}$$

$$\text{F.S.} = \frac{105,000}{37,664} = 2.78$$

Actuator Load

$$\pi\left[(3.25)^2-(1)^2\right]\ 4,000 = 120,166 \text{ lb}$$

Proof load = 1.5 x 120,166 = 180,249 lb

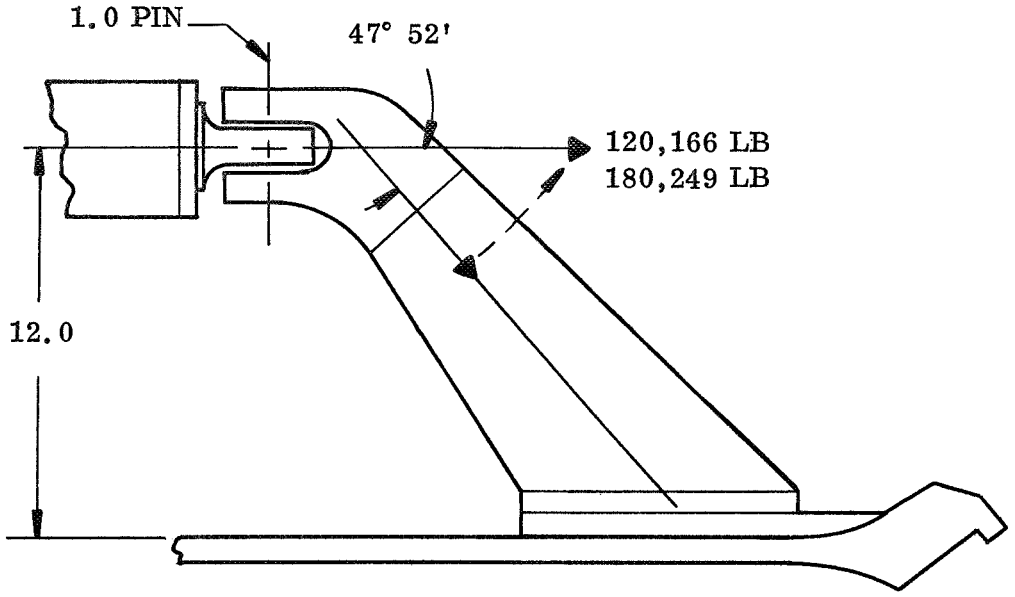

Pin Stress and Deflection

$$M = \frac{WL^2}{12} = 22,531 \text{ in.-lb}$$

$$\sigma = \frac{Mc}{I} = \frac{22,531 \times 0.5}{0.0491} = 229,440 \text{ psi}$$

$$\tau = \frac{4\ V}{3\ A} = \frac{4 \times 180,249 \text{ lb}}{2 \times 3 \times 0.7854} = 153,000 \text{ psi}$$

$$W = \frac{120,166}{1.5} = 80,110 \text{ lb/in.}$$

$$I = 0.0491 \text{ in.}^4$$

Pin Stress and Deflection

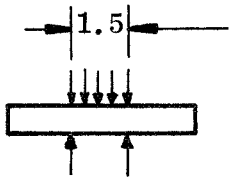

Deflection

$$\Delta = \frac{5\ WL^4}{384\ E\ 1} = \frac{5 \times 80,110\ (1-5)^4}{384\ (30 \times 10^6)\ 0.0491}$$

$$\Delta = 0.003585 \text{ in.}$$

Closure Actuator Bracket Stress and Deflection

$$\text{Shearout} = \frac{180,249}{4 \times 1.0 \times 1.0} = 45,062 \text{ psi}$$

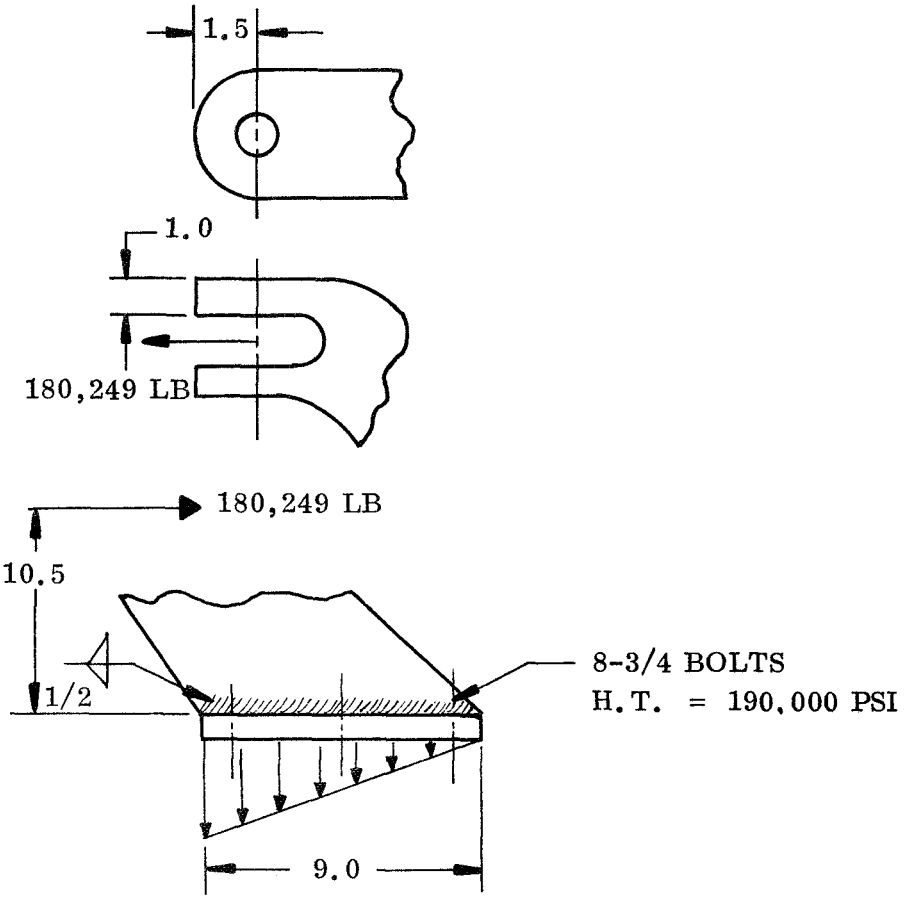

Bolt Load

$$10.5\ (180,249) = 8 \times B + \frac{5.5}{8}(5.5)\ B + \frac{1}{8}(1)\ B = 11.25\ B$$

$$B = 170,315 \text{ lb}$$

$$\text{Max load/bolt} = \frac{170,315}{3} = 56,771 \text{ lb/bolt}$$

$$\text{F.S.} = \frac{70,800}{56,771} = 1.25$$

$$\text{Weld load} = \frac{10.5 \times 180,249}{6} = 315,436 \text{ lb}$$

$$\text{Load/in.} = \frac{2 \times 315,436}{9} = 70,097 \text{ lb/in.}$$

$$\tau = \frac{70,097}{4 \times 0.707\ (0.5)} = 49,573 \text{ psi}$$

$$\text{F.S.} = \frac{109,000}{49,573} = 2.19$$

$$M = 10.5 \times 180,249 = 1,892,615 \text{ psi}$$

$$\sigma = \frac{Mc}{I} + \frac{P}{A} \qquad I = 91.1 \text{ in.}^4$$

$$= \frac{1,892,615 \times 4.5}{91.1} + \frac{120,921}{2 \times 9 \times 0.75} = 102,445$$

$$\text{F.S.} = \frac{180,000}{102,445} = 1.75$$

Deflection

$$\Delta = \frac{PL}{AE} = \frac{80,615 \times 14}{7 \times 0.75 \times 2 \times 29 \times 10^6}\ (0.67086) = 0.002486 \text{ in.}$$

$$\Delta_{\text{bolts}} = \frac{PL}{AE} = \frac{37,847 \times 0.75}{(0.4417)\ 30 \times 10^6} = 0.002142 \text{ in.}$$

$$\Delta = \frac{11.25}{8}\ (0.002142) = 0.003012 \text{ in.}$$

$$\Delta_{\text{cantilever}} = \frac{PL^3}{3\ E\ 1} = \frac{89,114\ (14)^3}{3 \times 29 \times 10^6 \times 20.8}\ (0.74159) = 0.1002 \text{ in.}$$

Nozzle Actuator Stress and Deflection

$$\Delta_{\text{pin}} = 0.003585 \text{ in.}$$

$$\Delta_{\text{bracket}} = \frac{PL}{AE}$$

$$= \frac{120,166 \times 7.5}{3.5 \times 4 \times 29 \times 10^6}$$

$$= 0.00222 \text{ in.}$$

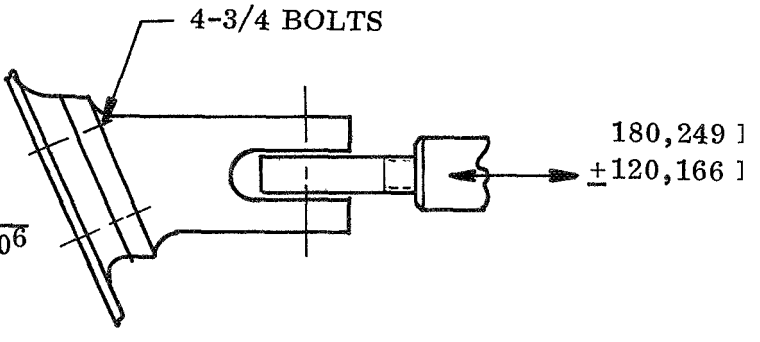

$$\text{Bolt load} = \frac{180,249}{4} = 45,062 \text{ lb}$$

$$\text{F.S.} = \frac{67,000}{45,062} = 1.48$$

$$\Delta_{\text{bolts}} = \frac{PL}{AE}$$

$$= \frac{120,166\ (0.75)}{4\ (0.4417)\ 30 \times 10^6}$$

$$= 0.0017 \text{ in.}$$

Nozzle total =	0.003585	pin
	0.00222	bracket
	0.0017	bolts
	0.007505	in.

Closure total =	0.003585	pin
	0.003012	bolts
	0.002486	bracket
	0.1002	bracket
	0.109283	in.

$$\text{Total} = 0.109283 + 0.007505 = 0.116788 \text{ in.}$$

Pressurization Tank

12 in. ID

2 to 1 elliptical dome

4340 steel $\qquad F_{tu} = 200,000$ psi

$$t = \frac{10,000\ (6.15)}{200,000} = 0.307$$

$$M = 0.75 \times 119,336 = 89,502 \text{ in.-lb}$$

$$\sigma = \frac{Mc}{I} = \frac{89,502 \times 0.375}{0.2812}$$

$$= 119,357 \text{ psi}$$

$$\text{F.S.} = \frac{180,000}{119,357} = 1.50$$

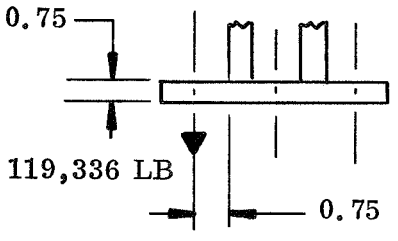

APPENDIX G

NOMENCLATURE

F_{tu}	=	Ultimate tensile strength
F_{su}	=	Ultimate shear strength
σ	=	Stress
P	=	Pressure (psi) or load (lb)
R	=	Radius
t	=	Thickness
E	=	Modulus of elasticity
I	=	Inertia
τ	=	Shear stress
A	=	Area
W	=	Pressure (psi) or load (lb)
a	=	Plate radius
b	=	Radius of plate opening
m	=	Reciprocal of Poisson's ratio
M	=	Bending moment
V	=	Shear load
L	=	Length
Δ	=	Deflection
B	=	Bolt load
c	=	Distance from centroid of item to extreme outside fiber

APPENDIX H

NOMENCLATURE

A_s	Servovalve orifice (in.^{4}/sec-lb$^{1/2}$)
A_p	Actuator area (sq in.)
F	Offset torque (in.-lb)
e_i	Input signal
I	Current from amplifier
I_n	Inertia of nozzle (lb sec^2 in.)
K_a	Compliance of nozzle (lb/in.)
F_{fb}	Feedback gain (volts/in.)
K_i	Amplifier gain (ma/volt)
K_n	Seal plus boot spring rate (in.-lb/rad)
K_2	Servovalve gain (in.^{4}/sec-lb$^{1/2}$-ma)
l	Moment arm (in.)
P_r	Dump pressure (psi)
P_s	Supply pressure (psi)
P_1	Control pressure (high) (psi)
P_2	Control pressure (low) (psi)
Q_1	Control flow to actuator (cu in./sec)
Q_2	Control flow to dump (cu in./sec)
s	Laplace operator (sec^{-1})

NOMENCLATURE (Cont)

T_c	Coulomb friction (in.-lb)
V_o	One-half volume of actuator cylinder (cu in.)
V_1	Volume of cylinder of P_1 side (cu in.)
V_2	Volume of cylinder of P_2 side (cu in.)
x	Travel of actuator (in.)
β	Bulk modulus of hydraulic oil (psi)
δ	Nozzle position (rad)
ϵ	Error signal to amplifier (ν)
ζ	Damping ratio of servovalve (dim)
ω	Natural frequency of servovalve (rad/sec)
I_{max}	Maximum current to servovalve (ma)
A_{max}	Maximum servovalve orifice ($in.^4/sec\text{-}lb^{1/2}$)
f_v	Viscous damping coefficient (in.-lb-sec/rad)
P_i	Initial gas pressure (psi)
V_i	Initial gas volume (cu in.)
V_T	Gas volume in tank at any time (cu in.)
t	Time (sec)
γ	Ratio of specific heat (dim)
hp	Pump output horsepower
hpp	Pump input horsepower
GHP	Gas horsepower

NOMENCLATURE (Cont)

$\dot{W}$	Warm gas flow rate (lb/sec)
H_{AD}	Adiabatic head (ft)
V_{03}	Volume of oil required for accumulator (cu in.)
V_{33}	Volume of Accumulator (cu in.)
P_{20}	Accumulator pressure after discharging V_o cu in. of oil (lb/sq in.)
P_{33}	Accumulator precharge pressure (lb/sq in.)
WGGP	Weight of warm gas generator grain (lb)
t_b	Motor burn time (sec)
GGW	Weight of gas generator (lb)
σ	Gas generator mass fraction (dim)
T	Total torque (in.-lb)
Q_m	Maximum hydraulic flow (gpm)
$\dot{x}$	Actuator velocity (in./sec)
$\dot{\delta}$	Nozzle slew rate (deg/sec)
ΔP	Pressure drop across actuator (lb/sq in.)
Q	Servovalve flow (gpm)
P_v	Pressure drop across servovalve (lb/sq in.)
V_x	Volume of oil expelled (warm gas blowdown) (cu in.)
$\dot{\delta}_y$, $\dot{\delta}_p$	Nozzle angular velocity (yaw and pitch) (deg/sec)

NOMENCLATURE (Cont)

V_{TB}	Total oil required for warm gas blowdown (cu in.)
Q_L	Servovalve leakage flow rate (cu in./sec)
ρ	Warm gas density (lb/cu in.)
V_{TH}	Total volume of fluid in tank (cu in.)
V_3	Gas volume at 60 sec (cu in.)
P_3	Gas pressure at 60 sec (lb/sq in.)
ΔL_P	Longitudinal growth of pressurization tank (in.)
ν	Poisson's Ratio
R	Radius of pressurization tank (in.)
tw	Tank wall thickness (in.)
E	Modulus of elasticity (lb/sq in.)
L	Length between supports of tank (in.)